THE JOURNAL
OF
CHEMICAL PHYSICS

VOLUME 12, NUMBER 6 JUNE, 1944

The Mechanism of Copolymerization

TURNER ALFREY, JR.,* *Springfield, Massachusetts*
AND
G. GOLDFINGER,** *Boston, Massachusetts*
(Received March 6, 1944)

The mechanism of catalytic copolymerization of two monomers A and B is treated with the the aid of steady state approximation. Two initiation and two termination rates are assumed, one for each monomer. Four propagation rates are considered, corresponding to the four possibilities of addition, namely, addition of monomer A to a chain ending in A^* or to a chain ending in B^* and addition of monomer B to a chain ending in A^* or to a chain ending in B^*. Over-all rate and number average molecular weight are calculated. The composition of the polymer and the number distribution curves of groups of submolecules a and of submolecules b are calculated as functions of the monomer composition and two rate constant ratios. These last results are of general character and independent of the nature of the initiation and termination processes provided that the average degree of polymerization is "high."

THE mechanism of polymerization reactions involving one single type of monomer has been treated extensively and successfully in the course of the last fifteen years. We have at our disposal a number of equations describing rate of polymerization, average degree of polymerization, and shape of size distribution curves as variables of reaction conditions for a wide variety of cases. Systems involving two or more monomers have also been investigated, but less thoroughly, in the past. F. T. Wall[1] treated, in a series of papers, the structure of vinyl copolymers. His results were compared to the experimental data of C. S. Marvel and co-workers.[2] More recently, H. Branson and R. Simha[3] attacked the problem. All these treatments involve one serious oversimplification: They assume only two distinct propagation processes—the addition of each type of monomer to the growing chain. Jenckel[4] recognizes the existence of four distinct propagation processes: addition of monomer A to active chain ending in A, addition of monomer A to chain ending in B, and addition of monomer B to each kind of active chain. However, Jenckel restricts his treatment by considering only those cases where certain simple relationships hold between the four propagation rate constants.

This paper is an attempt to handle the problem without restricting conditions as to the values of the rate constants of the elementary processes, and to give a general expression for the over-all rate and the number average molecular weight of a polymer obtained from the catalytic polymerization of two monomers. The structure and composition of the resulting polymer are also calculated—this, however, with the restriction

* At present with Monsanto Chemical Company, Springfield, Massachusetts.
** At present with Godfrey L. Cabot, Inc., Boston, Massachusetts.
[1] F. T. Wall, J. Am. Chem. Soc. **62**, 803 (1940); **63**, 821, 1862 (1941); **64**, 269 (1942).
[2] C. S. Marvel and co-workers, J. Am. Chem. Soc. **60**, 280 (1938); **61**, 3241, 3156 (1939); **62**, 3499 (1940); **64**, 92 (1942).
[3] H. Branson and R. Simha, J. Chem. Phys. **11**, 6, 297 (1943).
[4] E. Jenckel, Zeits. f. physik. Chemie **A170**, 24 (1941).

that the average molecular weight is "high." This restriction is not necessary from a mathematical point of view, but it makes the resulting equations much simpler and is applicable to all practical cases.

The treatment of the rate of polymerization is carried out in the customary manner, by means of a steady state approximation, as was used in many previous papers by Breitanbach, Mark, Schulz, Goldfinger, and others.[5] In the case of the copolymerization of two monomers, two different initiation rates must be assumed. Equations (1) and (2) give the rate of formation of active nuclei of the types A^* and B^* from the respective monomers A and B and catalyst c^* in a bimolecular process.

$$\frac{dA^*}{dt}=k_{1c}^{a}c^*A, \tag{1}$$

$$\frac{dB^*}{dt}=k_{1c}^{b}c^*B. \tag{2}$$

The constants k_{1c}^{a} and k_{1c}^{b} are written in this form in accordance with the constants used by Abere, Goldfinger, Mark, and Naidus.[5] The index 1 denotes that the constant refers to an initiation process, the subscript c that the process is catalytic, and the superscript a or b the nature of the monomer involved in the process. The constants which will be used later will be denoted similarly. The index 2 will stand for the growth process and the index 3 for the termination process.

The propagation reaction is governed by four differential equations. Their meaning can best be shown from a schematic table (Table I). Consequently, we will have to write for the rate of consumption of the monomer of the type A [(x) and (z)], Eq. (3).

$$-dA/dt=k_2^{aa}A^*A+k_2^{ba}B^*A, \tag{3}$$

and for the rate of consumption of the monomer of the type B [(y) and (u)], Eq. (4),

$$-dB/dt=k_2^{ab}A^*B+k_2^{bb}B^*B. \tag{4}$$

These four rates are to be considered since a chain ending in A^* can add another monomer of the type $A(x)$ and a chain ending in B^* can also add a monomer of the type $A(z)$. On the other hand, a chain ending in A^* can add a monomer of the type $B(y)$ or a chain ending in B^* can add a monomer of the type $B(u)$. Thus, four different propagation reactions occur. We assume two termination reactions.

$$-\frac{dA^*}{dt}=k_{3c}^{a}c^*A^*, \tag{5}$$

$$-\frac{dB^*}{dt}=k_{3c}^{b}c^*B^*. \tag{6}$$

In the first termination reaction a chain ending in A^* is deactivated by collision with a catalyst and in the second a chain ending in B^* is terminated by collision with a catalyst. By applying a steady state approximation it is easy to calculate the concentration of A^* and B^*. The approach is the same as that used in the case of polymerization of a single type of monomer. The only difference in the case of copolymerization is that not only the initiation and termination reactions influence the respective steady state concentrations of the two types of active nuclei, but their concentration is also changed by the propagation reaction. If, for example, reaction of type (y) and (u) is small as compared to the rate of the reaction of (x) and (z), then the concentration of active chain ends of the type A^* will be greater than that of chains ending in B^*.

Thus A^* is formed by reactions (1) and (3) and is consumed by reactions corresponding to the first terms of Eqs. (3) and (4), and also by Eq. (5). In the steady state, the rates of these reactions will be related by Eq. (7).

$$k_{1c}^{a}c^*A+k_2^{ba}B^*A=k_2^{ab}A^*B+k_{3c}^{a}c^*A^*. \tag{7}$$

TABLE I.

Growing chain	Monomer adding	Rate of process	Reaction product	
$\cdots\cdots A^*$	A	$k_2^{aa}A^*A$	$\cdots\cdots A-A^*$	(x)
	B	$k_2^{ab}A^*B$	$\cdots\cdots A-B^*$	(y)
$\cdots\cdots B^*$	A	$k_2^{ba}B^*A$	$\cdots\cdots B-A^*$	(z)
	B	$k_2^{bb}B^*B$	$\cdots\cdots B-B^*$	(u)

[5] Abere, Goldfinger, Mark, and Naidus, Ann. New York Acad. Sci. **44**, Art. 4, 267 (1943).

A similar steady state equation (8) can be written for the formation and destruction of B^*,

$$k_{1c}^{b}c^*B+k_2^{ab}A^*B=k_2^{ba}B^*A+k_{3c}^{b}c^*B^*. \quad (8)$$

Equations (7) and (8) can be directly solved to yield the steady state concentrations of A^* and B^*.

$$A^*=A\frac{k_{1c}^{a}k_{3c}^{b}c^*+k_2^{ba}A(k_{1c}^{a}A+k_{1c}^{b}B)}{k_2^{ab}k_{3c}^{b}B+k_{3c}^{a}(k_{3c}^{b}c^*+k_2^{ba}A)}, \quad (9)$$

$$B^*=B\frac{k_{1c}^{b}k_{3c}^{a}c^*+k_2^{ab}B(k_{1c}^{a}A+k_{1c}^{b}B)}{k_2^{ab}k_{3c}^{b}B+k_{3c}^{a}(k_{3c}^{b}c^*+k_2^{ba}A)}. \quad (10)$$

The over-all rate of polymerization is the rate of consumption of monomer A plus the rate of consumption of monomer B. Therefore, the over-all rate will be the sum of expressions (1), (2), (3), and (4). (1) and (2), however, must necessarily be negligibly small as compared to (3) and (4) if the resulting material is a "high" polymer. The over-all rate $-(dA+dB)/dt$ is given in Eq. (11) after neglecting (1) and (2),

$$-\frac{dA+dB}{dt}=\text{——(9)——}(k_2^{aa}A+k_2^{ab}B)+\text{——(10)——}(k_2^{ba}A+k_2^{bb}B). \quad (11)$$

By dividing the over-all rate of polymerization by the rate of nucleus formation the number average molecular weight is obtained. Since nuclei are formed only by reactions (1) and (2), and their number is not changed by the growth reactions, the rate of formation of growing chains is equal to the rate of nucleus formation. Therefore the number average molecular weight $\bar{P}_n$ is as given by Eq. (12).

$$\bar{P}_n=\frac{(9)(k_2^{aa}A+k_2^{ab}B)+(10)(k_2^{ba}A+k_2^{bb}B)}{k_{1c}^{a}c^*A+k_{1c}^{b}c^*B}. \quad (12)$$

If we do not distinguish between the two types of monomer and have therefore only one initiation, one growth, and one termination reaction, this expression reduces to

$$\bar{P}_n=k_2A/k_3c^*. \quad (13)$$

This result is of course identical with the number average molecular weight obtained for ordinary vinyl polymerization, on the basis of similar initiation and termination processes.

In the case of polymerization involving only one type of monomer, the resulting polymer is defined by the number average molecular weight as obtained above. In the case in which two different monomers are involved, however, it is necessary to know the relative concentrations of the constituents in the polymer resulting from the concentration ratios in the polymerizing mixture. Only for very special relations among the various rate constants will the composition of the resulting polymer be the same as the composition of the monomer mixture. In general the polymer will be richer in one or the other monomer than the polymerizing mixture. In order to obtain the composition of the polymer as a function of the concentration ratio in the polymerizing mixture, and the rate constants of the processes involved, it is necessary to solve separately for expressions (3) and (4) and compare the results. This calculation, while mathematically straightforward, results in an unwieldy expression. Furthermore, all eight rate constants are involved and, therefore, with the experimental means at our disposal, no satisfactory numerical calculations would be possible. If the solution is limited to the case where the resulting polymer is of reasonably high average molecular weight, then the contribution of the initiation reaction to the composition of the polymer can be neglected as compared to the contribution of the four growth reactions. In other words, if the rate $k_2^{ba}B^*A$ is large as compared to the rates $k_{1c}^{a}c^*A$, etc., the steady state concentration for A^* and B^* can be calculated from the four growth reactions alone. The result so obtained will be only slightly different from the result obtained from the unsimplified calculation.

The following treatment, involving only the four propagation processes, will give correct predictions for the chemical composition and distribution of monomeric units for any copolymerization reaction which results in a high average molecular weight, regardless of the mechanism of the initiation and termination processes. In this respect the following treatment is actually more general than our preceding rate considerations, which apply only for particular assumed mechanisms of initiation and termination. By consideration of propagation reactions only, a correct

evaluation is obtained of chemical composition and distribution of monomeric units within the interior of the chain. The statistical nature of the end groups, however, depends upon the nature of the initiation and termination processes. For a polymer of high molecular weight, neglect of the end groups is justifiable.

Using this approximation, and applying steady state considerations, we can write

$$k_2^{ab}A^*B = k_2^{ba}B^*A. \tag{14}$$

This indicates that in the steady state, the rate of reaction of polymers ending in A with monomer B must be equal to the rate of reaction of polymers ending in B with monomer A. It is now possible to express B^* in terms of A^*, although this approach cannot yield absolute values for A^* and B^*,

$$B^* = (k_2^{ab}/k_2^{ba})(B/A)A^*. \tag{15}$$

This value of B^* substituted in the rate of growth Eq. (3)

$$-dA/dt = k_2^{aa}A^*A + k_2^{ba}B^*A \tag{3}$$

gives

$$-dA/dt = A^*(k_2^{aa}A + k_2^{ab}B). \tag{16}$$

Similarly, the rate of addition of B to the polymer is

$$-dB/dt = k_2^{ab}A^*B + k_2^{bb}B^*B \tag{4}$$

and substituting the value from Eq. (15)

$$-\frac{dB}{dt} = A^*\left(k_2^{ab}B + \frac{k_2^{bb}k_2^{ab}}{k_2^{ba}}\frac{B^2}{A}\right). \tag{17}$$

Finally, the ratio between the rate of addition of B and the rate of addition of A is given by:

$$\frac{dB}{dA} = \frac{B}{A}\frac{k_2^{ab}}{k_2^{ba}}\frac{(k_2^{bb}B + k_2^{ba}A)}{(k_2^{ab}B + k_2^{aa}A)}. \tag{18}$$

Let us introduce two new variables α and β.

$$\alpha = k_2^{ab}/k_2^{aa}, \tag{19}$$

$$\beta = k_2^{bb}/k_2^{ba}. \tag{20}$$

Equation (21) can be rewritten in terms of α and β.

$$\frac{dB}{dA} = \frac{B}{A}\alpha\frac{\beta B + A}{\alpha B + A}. \tag{21}$$

The ratio of the rate of addition of the two monomers is, of course, also an expression for the ratio of those two monomers in the resulting polymer, a ratio which will be denoted in the future by b/a. In the particular case of an equimolecular mixture ($A = B$) the composition of the polymer is

$$\frac{b}{a} = \alpha\frac{\beta+1}{\alpha+1}. \tag{22}$$

It is clear that the initial polymer in general does not possess the same composition as the monomer mixture. This will be true only when A, B, α, and β are related by the following equation:

$$\alpha\frac{\beta B + A}{\alpha B + A} = 1. \tag{23}$$

Only in the still more special case where $\alpha = \beta = 1$ is the initial polymer of the same composition as the starting monomer mixture, *regardless of the concentrations of A and B*.

When Eq. (23) is not obeyed, the initial polymer is relatively richer in one component than in the other. The more reactive monomer is thus used up more rapidly, leaving the monomer mixture relatively poorer in this component. It necessarily follows that the last polymer to be formed is relatively richer in the less reactive constituent. The over-all polymerization product is thus a mixture of copolymer molecules of different chemical constitution. The variation of copolymer composition with extent of polymerization is a soluble mathematical problem, but the result is overly complicated. A more pertinent problem is the prevention of this variation in composition, as discussed in the next paragraphs.

If α and β are known for a given pair of monomers, it should be possible to prepare a copolymer of desired initial composition $b/a = x$ by starting with a monomer mixture in which the two components have the relative concentrations $B/A = y$, where y is determined by x, α, and β, as follows:

$$y = \frac{(x-1) + \left[(x-1)^2 + 4\frac{\beta}{\alpha}x\right]^{\frac{1}{2}}}{2\beta}. \tag{24}$$

This choice of initial monomer concentrations gives an initial copolymer of the desired composition, but as the polymerization proceeds, the polymer formed will become richer and richer in the less reactive component. If it is desired to produce a uniform polymer, all of the composition x, then not only must the starting monomers be present in the ratio y, but this monomer ratio

must be maintained throughout the course of the polymerization. This can be done by continuously adding additional quantities of the more reactive monomer.

Another question of equal importance as the composition of the polymer is the average length of sequences of monomer of the same type. It is obvious that, depending on the relative values of the propagation rate constants, groups of varying sizes of the same monomer will be found in the polymer. When the rate constants k_2^{aa} and k_2^{bb} are large as compared to the rate constants k_2^{ab} and k_2^{ba}, one can expect to find long sequences of A's followed by long sequences of B's, whereas if the relative values of those rate constants are reversed, then the polymer will contain short groups of A's followed by short groups of B's. This question is of very great importance since in the first case a copolymer might be truly a copolymer from a chemical point of view while exhibiting properties similar to the properties of a *mixture* of two polymers.

By defining four probabilites P_{aa}, P_{ab}, P_{ba}, P_{bb} for the probabilities of a monomer of the type A adding to a chain ending in A^*, a monomer of the type B adding to a chain ending in A^*, a monomer of the type A adding to a chain ending in B^*, and a monomer of the type B adding to a chain ending in B^*, it is easy to calculate the average length of segments of A's and B's.

To a chain ending in A^*, only one of two things can happen: (1) a monomer A or (2) a monomer B can add, therefore the probability P_{aa} will be the rate of addition of A over the rate of addition of A+the rate of addition of B, etc.

$$\begin{aligned} P_{aa} &= \frac{A}{A+\alpha B}, \\ P_{ab} &= \frac{\alpha B}{A+\alpha B}, \\ P_{ba} &= \frac{A}{A+\beta B}, \\ P_{bb} &= \frac{\beta B}{A+\beta B}. \end{aligned} \tag{25}$$

The average length (n) of groups of A's and the average length (m) of groups of B's can be determined by the following consideration: To the first constituent A of a group of A's picked at random, the addition reaction $k_2^{aa}A^*A$, whose probability is P_{aa}, has had to be repeated $(n-1)$ times, to yield a group of nA's. The probability of these $(n-1)$ consecutive additions is $(P_{aa})^{(n-1)}$. This sequence of reactions must then be followed by the addition of a B, which has the probability P_{ab}. The probability that a group of A's picked at random contains n members is thus:

$$N(n) = P_{aa}{}^{(n-1)}P_{ab}. \tag{26}$$

This is also the number distribution function for the lengths of A sequences.

Similarly, the number distribution function for sequences of B's is given by:

$$N(m) = P_{bb}{}^{(m-1)}P_{ba}, \tag{27}$$

where $N(m)$ represents the fraction of all B sequences which possess m members.

The *average* length of the A sequences must of course bear a very simple relationship to the average length of the B sequences, since there will be (neglecting end sequences) just as many A sequences as B sequences in the copolymer. If $\bar{n}$ and $\bar{m}$ are the number average lengths of A and B sequences, respectively, and a/b is the number ratio of A's to B's in the molecule, then $\bar{n}$ and $\bar{m}$ are related by the expression:

$$\bar{n}/\bar{m} = a/b. \tag{28}$$

SUMMARY

The catalytic copolymerization reaction of two monomers A and B is treated.

An expression is found for the over-all rate of polymerization (11) and the number average degree of polymerization (12). The composition of the copolymer is given as a function of the ratios of the four propagation rate constants, and the concentration of the reacting monomers (21) and (24). Finally, the arrangement of the constituents in this copolymer is calculated as a function of the same variables (26) and (27).

THE JOURNAL OF CHEMICAL PHYSICS VOLUME 12, NUMBER 6 JUNE, 1944

The Asymmetric Rotor

II. Calculation of Dipole Intensities and Line Classification*

PAUL C. CROSS AND R. M. HAINER, *Brown University, Providence, Rhode Island,*

AND

GILBERT W. KING, *Arthur D. Little, Inc., Cambridge, Massachusetts*

(Received February 15, 1944)

A table of line strengths for rigid asymmetric rotors is given, by means of which to this approximation the relative intensities of all important rotational lines up to $J<13$ for all bands of any molecule can be readily calculated, provided the asymmetry is roughly the same in the initial and final states. A classification of the irregularly spaced lines of the asymmetric rotor is made into "sub-branches" defined by the changes of the K values of the initial level in the limiting prolate and oblate symmetric rotors, and into "wings" which collect together lines of the sub-branches which have uniformly varying strength and Boltzmann factor, and fairly uniform spacing.

I. INTRODUCTION

IN a series of papers, of which this is the second, we propose to make a systematic approach to the analysis of the rotational structure of molecular spectra.[1] If the molecule is an asymmetric rotor, the stochastic method is the only one applicable. In the first paper a table was given from which the energy levels, and hence term values, for any molecule could be easily obtained from assumed values of interatomic angles and distances. Although line position is the primary tool used in the interpretation of spectra, it is not sufficient in complex spectra of asymmetric-rotor molecules with large moments of inertia, where the lines are neither regularly spaced nor completely resolved. In such bands intensities are equally important in analysis. In this paper we calculate the line strengths from the square of the elements of the direction-cosine matrices, covering, somewhat coarsely, the whole range of asymmetry possible for all levels up to $J<13$. Relative intensities can be easily calculated from the strengths.

No tables of line strengths or intensities have appeared hitherto in the literature. It has been customary to use the limiting prolate or oblate symmetric-rotor intensities for transitions from levels of high or low τ, respectively (τ being an ordinal index labelling the levels having the same quantum number J). The numerical results given here show that these can be in error by large factors, even with a low degree of asymmetry. The strengths of lines from intermediate τ levels are often of quite unexpected magnitudes.

A qualitative classification of the lines of the asymmetric rotor has been made. There are the usual P, Q, and R branches, determined by the change in total angular momentum J. As in the symmetric rotor these are divided into sub-branches, determined by changes in internal angular momentum around the symmetry axes, except that in the asymmetric rotor there are two pseudo-quantum numbers K_{-1} and K_1, introduced in our classification of energy levels.[1] Both of these K's obey the symmetric-rotor rules as far as parity goes. The principal sub-branches are those in which the magnitude of the change of both K's is the same as in the symmetric rotor $(0, \pm 1)$; next in importance are those for which only one ΔK is 0 or ± 1, and the other $|\Delta K|$ is greater than 1; and the least important are the "forbidden" sub-branches for which both $|\Delta K|$'s are greater than 1. Finally the lines of the sub-branches are classified into wings, in which one K or the other is held constant. This procedure groups together lines whose strength and Boltzmann factors vary uniformly and whose positions are as regular as can be expected.

* This paper is based on a portion of a thesis presented by R. M. Hainer in partial fulfillment of the requirements for the degree of Doctor of Philosophy in the Graduate School of Brown University.

[1] G. W. King, R. M. Hainer, and P. C. Cross, J.Chem. Phys. **11**, 27 (1943), the first of this series, which will hereafter be referred to as I.

This classification, coupled with the quantitative results which enable one to neglect various sub-branches and wings in appropriate ranges of asymmetry, clarifies the rotational structure of the bands of the asymmetric rotor.

II. ABSORPTION INTENSITY AND PROPERTIES OF THE DIRECTION-COSINE MATRICES

The intensity of a spectral line may, in principle, be evaluated by the application of the quantum theory of Einstein transition probabilities. Thus the intensity of absorption for the transition $n''\rightarrow n'$ is

$$I_{n'';n'}=\frac{8\pi^3\nu N g_{n''}(1-e^{-h\nu/kt})\exp(-E_{n''}/kt)}{3hc\Sigma g_n \exp(-E_n/kt)}\times|\mu_{n'';n'}|^2, \quad (1)$$

where n stands for all the quantum numbers describing the state, $E_{n''}$ is the energy of the lower state, $g_{n''}$ its weight factor. N is the number of molecules per cc and ν is the frequency of the absorption line. The last factor $|\mu_{n'';n'}|^2$, is to be taken as $|\int\psi^*_{n''}\mu\psi_{n'}dv|^2$, the square of the magnitude of the $n'';n'$ element in the matrix of the dipole vector μ. It can be expanded as $\Sigma_F|(\mu_F)_{n'';n'}|^2$, where F represents X, Y, Z, the axes of the space-fixed Cartesian system in terms of which the radiation field is described. In the absence of an external field (1) can be summed over the Zeeman components.

In molecular spectra for which the separation of the wave functions into a rotational part ψ_R and a vibrational-electronic part $\psi_{V,e}$ is a satisfactory approximation,

$$\int\psi^*_{n''}\mu_F\psi_{n'}dv=\Sigma_g\int\psi^*_{R''}\Phi_{Fg}\psi_{R'}dv\cdot\int\psi^*_{V'',e''}\mu_g\psi_{V',e'}dv, \quad (2)$$

where the μ_g's are the components of the electric moment associated with the vibrational-electronic selection rules along the x, y, z axes of a molecule-fixed Cartesian system in terms of which the shift of electron density due to changing vibrational and electronic wave functions may be described. The Φ_{Fg} are the direction cosines between the space-fixed F and rotating g axes. No loss of generality is incurred by identifying the x, y, z axes with the principal axes of inertia a, b, c of the molecule.[1] Thus except for the magnitude of the permanent and induced electric moments, $\int\psi^*_{V'',e''}\mu_g\psi_{V',e'}dv$, the intensities of the lines in the rotational structure of a band are readily evaluated from (1) and the elements of the matrices of the direction cosines in the representations which diagonalize the energy matrices for the upper and lower states.

The direction cosines are the elements of an orthogonal transformation from molecule-fixed to space-fixed coordinates, satisfying the relations

$$\mathcal{P}_F=\Sigma_g\Phi_{Fg}P_g, \quad P_g=\Sigma_F\Phi_{Fg}\mathcal{P}_F, \quad (3)$$

where P_g and $\mathcal{P}_F$ are the components of angular momentum in the molecule-fixed and in the space-fixed coordinate systems, respectively. Applying the laws of non-commuting vector analysis to the basic commutation rules of Heisenberg, or by expressing the P_g, $\mathcal{P}_F$, and Φ_{Fg} as functions of a set of Eulerian angles and obtaining the corresponding Schrödinger operators, one may derive the following commutation rules. These rules and the values of the matrix elements have been given before,[2] but as it is necessary in the symmetry classification of the lines to use a representation consistent with that used for the calculation of the energies and transformations, the commutation rules and direction-cosine matrices are given here for the phase relations chosen in I, footnote 10:

$$P_xP_y-P_yP_x=-ihP_z, \quad \text{etc.}, \quad (4)$$

$$\mathcal{P}_X\mathcal{P}_Y-\mathcal{P}_Y\mathcal{P}_X=ih\mathcal{P}_Z, \quad \text{etc.} \quad (5)$$

$$\mathcal{P}_X\Phi_{Yg}-\Phi_{Yg}\mathcal{P}_X=-\mathcal{P}_Y\Phi_{Xg}+\Phi_{Xg}\mathcal{P}_Y=ih\Phi_{Zg}, \text{ etc.}, \quad (6)$$

$$P_x\Phi_{Fy}-\Phi_{Fy}P_x=-P_y\Phi_{Fx}+\Phi_{Fx}P_y=-ih\Phi_{Fz}, \text{ etc.} \quad (7)$$

The other equations are obtained by a cyclic permutation of the indices.

$$\mathcal{P}_F\Phi_{Fg}-\Phi_{Fg}\mathcal{P}_F=P_g\Phi_{Fg}-\Phi_{Fg}P_g=0 \quad (8)$$

and

$$\Phi_{Fg}\Phi_{F'g'}-\Phi_{F'g'}\Phi_{Fg}=0. \quad (9)$$

[2] D. M. Dennison, in Rev. Mod. Phys. **3**, 280 (1931) and earlier papers published the square of the elements summed over the Zeeman components. H. B. G. Casimir, Zeits. f. Physik **59**, 623 (1929) gave in detail the commutation rules and matrix elements in the representation used by O. Klein, Zeits. f. Physik **58**, 730 (1929).

TABLE I. Values of the elements of all the direction-cosine matrices, separated into the three factors of (16). Note how the factor dependent on K changes with the internal axes $g=x, y, z$, and the factor dependent on M changes in the same way with the external axes $F=X, Y, Z$.

Matrix-element factor	Value of J': $J+1$	J	$J-1$
$(\Phi_{Fg})_{J,J'}$	$[4(J+1)\sqrt{(2J+1)(2J+3)}]^{-1}$	$[4J(J+1)]^{-1}$	$[4J\sqrt{4J^2-1}]^{-1}$
$(\Phi_{Fz})_{J,K;J'K}$	$2\sqrt{(J+K+1)(J-K+1)}$	$2K$	$-2\sqrt{J^2-K^2}$
$(\Phi_{Fy})_{J,K;J',K\pm1}$ $=\mp i(\Phi_{Fx})_{J,K;J',K\pm1}$	$\mp\sqrt{(J\pm K+1)(J\pm K+2)}$	$\sqrt{(J\mp K)(J\pm K+1)}$	$\mp\sqrt{(J\mp K)(J\mp K-1)}$
$(\Phi_{Zg})_{J,M;J',M}$	$2\sqrt{(J+M+1)(J-M+1)}$	$2M$	$-2\sqrt{J^2-M^2}$
$(\Phi_{Yg})_{J,M;J',M\pm1}$ $=\pm i(\Phi_{Xg})_{J,M;J',M\pm1}$	$\mp\sqrt{(J\pm M+1)(J\pm M+2)}$	$\sqrt{(J\mp M)(J\pm M+1)}$	$\mp\sqrt{(J\mp M)(J\mp M-1)}$

Since by definition

$$P^2=P_x^2+P_y^2+P_z^2=\mathcal{P}_X^2+\mathcal{P}_Y^2+\mathcal{P}_Z^2, \quad (10)$$

$$P^2P_g-P_gP^2=P^2\mathcal{P}_F-\mathcal{P}_FP^2=0. \quad (11)$$

Also

$$H=\tfrac{1}{2}(P_x^2/I_x+P_y^2/I_y+P_z^2/I_z) \quad (12)$$

(since x, y, z are identified with the principal axes of inertia) and

$$HP_g-P_gH=0, \quad H\mathcal{P}_F-\mathcal{P}_FH=0. \quad (13)$$

Choosing a representation which simultaneously diagonalizes P^2, P_z, and $\mathcal{P}_Z$, one may obtain the following solution of the above equations.

$$(P_y)_{J,K,M;\,J,K+1,M}=-i(P_x)_{J,K,M;\,J,K+1,M}$$
$$=(\hbar/2)[J(J+1)-K(K+1)]^{\frac{1}{2}},$$
$$(P_z)_{J,K,M;\,J,K,M}=\hbar K, \quad (14)$$

and

$$(\mathcal{P}_Y)_{J,K,M;\,J,K,M+1}=i(\mathcal{P}_X)_{J,K,M;\,J,K,M+1}$$
$$=(\hbar/2)[J(J+1)-M(M+1)]^{\frac{1}{2}},$$
$$(\mathcal{P}_Z)_{J,K,M;\,J,K,M}=\hbar M, \quad (15)$$

where the phase factors are such that P_y and $\mathcal{P}_Y$ are real and positive (see I-5 ff.), and where $|K|\leqslant J\geqslant|M|$.

From the above equations and choice of phases, the elements $(\Phi_{Fg})_{JKM;J'K'M'}$ of the direction-cosine matrices given in Table I were derived by the method outlined in Born and Jordan,[3] i.e., solving the above equations algebraically. Each element is composed of three factors: a J, J' component which is constant for a given ΔJ, i.e., for a given P, Q, or R block; a $JK, J'K'$ component which is independent of M, M'; and a $JM, J'M'$ component which is independent of K, K'. Thus an element has the structure

$$(\Phi_{Fg})_{J,K,M;J',K',M'}=(\Phi_{Fg})_{J;J'}\cdot(\Phi_{Fg})_{J,K;J',K'}\cdot(\Phi_{Fg})_{J,M;J',M'}. \quad (16)$$

III. CALCULATION OF DIRECTION-COSINE MATRICES

Symmetric-Rotor Direction Cosines in a Four-Group Representation

The symmetric-rotor basis functions employed in Table I belong to the group D_∞, whereas the asymmetric-rotor functions belong to the Four Group V. In order to calculate the asymmetric-rotor line strengths and to correlate them properly with the components of the degenerate pairs to which they converge in the symmetric-rotor limiting cases, it is necessary to transform to a set of symmetric-rotor basis functions, the Wang functions, which also belong to the Four Group. This transformation X, defined in (I-26) and (I-29), is easily applied by inspection to the direction-cosine matrices of the symmetric rotor in the representations of D_∞ as given in Table I, to give

$$\Phi_{Fg}{}^S=X'\Phi_{Fg}X. \quad (17)$$

The elements of the $\Phi_{Fg}{}^S$ yield the intensities of the limiting symmetric-rotor transitions in a somewhat unusual form in that the strengths of the two component transitions connecting two

[3] M. Born and P. Jordan, *Elementare Matrixmechanik* (Julius Springer, Berlin, 1930), Chapter IV, especially pp. 143. H. Rademacher and F. Reiche, Zeits. f. Physik **41**, 453 (1927), have evaluated the integrals $\int\psi_R\Phi_{Fg}\psi_{R'}^*dv$. Their results, which are not given in a form convenient for our purpose, may, however, be shown to agree with the elements in Table I.

doubly degenerate pairs of energy levels are given in terms of a species classification of the energy levels which applies over the entire range of asymmetry, including both the prolate- and oblate-symmetric limiting cases.

Asymmetric-Rotor Direction Cosines

An asymmetric-rotor wave function may be expressed as a linear combination of Wang functions of the same symmetry. Thus the direction-cosine matrices for the asymmetric rotor $\Phi_{F_g}{}^A$ can be calculated from the Φ_{F_g} given in Table I by

$$\Phi_{F_g}{}^A = T_1'\Phi_{F_g}{}^S T_2 = T_1'X'\Phi_{F_g}XT_2. \quad (18)$$

T_1 and T_2 are the transformation matrices for the lower and upper states, respectively. In this paper we shall consider only cases in which the asymmetry (defined uniquely by one parameter κ, I-11) is approximately the same in the two states, so that $T_1 \sim T_2 \sim T$.

The transformation matrix T is diagonal with respect to J. For each J it is split into four submatrices, one belonging to each of the four species of levels. The submatrices, given by (I-54), may be calculated by the procedure described in some detail in I—Section VI.

In the absence of external fields which remove the space degeneracy, X and T are both diagonal with respect to J and M, and the factors $(\Phi_{F_g})_{J;J'}$ and $(\Phi_{F_g})_{J,M;J',M'}$ of (16) are invariant under transformation by XT. Hence, in making our numerical computations, only the factor $(\Phi_{F_g})_{J,K;J'K'}$ was transformed.

Evaluation of Line Strengths

To include all the degenerate components contributing to a given transition, $J_\tau \rightarrow J'_{\tau'}$, the direction-cosine elements $(\Phi_{F_g}{}^A)_{J,\tau,M;J',\tau',M'}$ are squared and summed over M, M', and F. In the absence of external fields, X, Y, and Z are equivalent, and the summation of the squared elements over F may be accomplished by multiplying the squared elements for any given F by the factor three. Thus:

$$\sum_{F,M,M'} |\Phi_{F_g}|^2_{J,\tau,M;J',\tau',M'} = 3|\Phi_{Z_g}|^2_{J;J'} \cdot |\Phi_{Z_g}{}^A|^2_{J,\tau;J',\tau'} \cdot \sum_{M,M'} |\Phi_{Z_g}|^2_{J,M;J',M'} \quad (19)$$

(where Z on the right hand could be replaced by X or Y) and is called the *line strength* of the transition with the component of the electric moment μ_g, by analogy with the term used in atomic spectra.[4] The amount of calculation is minimized by transforming $(\Phi_{Z_z})_{J,K;J',K'}$ and $(\Phi_{Z\,y+iz})_{J,K;J',K'}$, from the latter of which the elements of $(\Phi_{Z_x}{}^A)_{J,\tau;J'\tau'}$ and $(\Phi_{Z_y}{}^A)_{J,\tau;J',\tau'}$ are obtained by inspection.

The orthogonal properties of the direction-cosine matrices aid in the calculation since they result in several kinds of stability[5] under unitary transformations. The following laws of "spectroscopic stability" were used to detect and eliminate errors in the matrix multiplications:

$$\sum_{J'=J-1}^{J} \sum_{\tau'} |\Phi_{F_g}{}^A|^2_{J,\tau;J'\tau'} = [2J]^2, \quad (20)$$

$$\sum_{J'=J}^{J+1} \sum_{\tau'} |\Phi_{F_g}{}^A|^2_{J,\tau;J'\tau'} = [2(J+1)]^2, \quad (21)$$

$$\sum_{F,J',\tau',M',M} |\Phi_{F_g}{}^A|^2_{J,\tau,M;J',\tau',M'} = 2J+1, \quad (22)$$

$$\sum_{F,g,\tau',M',M} |\Phi_{F_g}{}^A|^2_{J,\tau,M;J',\tau',M'} = 2J'+1, \quad (23)$$

$$\sum_{F,\tau,\tau',M',M} |\Phi_{F_g}{}^A|^2_{J,\tau,M;J',\tau',M'} = \tfrac{1}{3}(2J+1)(2J'+1). \quad (24)$$

The line strengths of all permitted asymmetric-rotor transitions involving levels of $J<13$, except for high order "forbidden" sub-branches of line strength no greater than 0.0030, are tabulated in a condensed form in the Appendix.[6]

All calculations were done to six decimal places and rounded off to four. A systematic application of the sum rules is believed to have eliminated all errors except inaccuracies due to rounding off. In taking sums by rule (22) the deviation from the exact value was found to be 0.0001 in many levels of low J's rising to 0.0003 in $J=6$, to 0.0004 in $J=11$, and to 0.0005 in $J=12$, where the sum involves seventeen levels each of which was rounded off to the fourth decimal.

---

[4] E. U. Condon and G. H. Shortley, *The Theory of Atomic Spectra* (Macmillan, Cambridge, England, 1935), p. 98.

[5] See, for atomic spectra, Condon and Shortley, reference 4, p. 71, and for Raman spectra, G. Placzek and E. Teller, Zeits. f. Physik **81**, 209 (1933).

[6] The various sum rules do not apply to the data of the Appendix because of these omissions.

TABLE II. Direction of the electric moment permitting transitions between states belonging to the representations of the Four Group.

Rep.		A	B_a	B_b	B_c
		ee	*eo*	*oo*	*oe*
A	*ee*	—	*a*	*b*	*c*
B_a	*eo*	*a*	—	*c*	*b*
B_b	*oo*	*b*	*c*	—	*a*
B_c	*oe*	*c*	*b*	*a*	—

TABLE III. Allowed changes in representation, labelled by the KK notation, for the three components of the electric moment, which show the selection rules in terms of parity changes in the K's.

Initial representation	Final representation for moment parallel to: *a* (least)	*b* (middle)	*c* (greatest)
ee	*eo*	*oo*	*oe*
eo	*ee*	*oe*	*oo*
oo	*oe*	*ee*	*eo*
oe	*oo*	*eo*	*ee*
Parity change is in	K_1	$K_{-1}K_1$	K_{-1}

IV. SELECTION RULES

The selection rules for the asymmetric rotor were given by Dennison[7] in terms of the + − notation. They can be stated quite simply in the KK notation, i.e., in terms of the symmetric-rotor selection rules, in a form which is valuable in unravelling the structure of the spectrum.

Since the transformation matrices are diagonal with respect to J, the selection rules for J in the asymmetric rotor are the same as in the symmetric rotor. Thus, $\Delta J=0, \pm1$, corresponding to Q, R, and P branches, respectively. The rules for K_{-1} and K_1 can be obtained very easily by means of group theory as follows. The components of the electric moment along the molecular a, b, c axes belong, respectively, to the representations B_a, B_b, B_c, of the Four Group (I—Table IV). The product of the characters of the representations of the initial and final wave functions and of the vector must be +1 for all group operators. Thus, if the representation of one is A, the other two must belong to the same representation, and if no representation is A, all must be different. Table II gives the permitted changes in representation for each component of the electric moment. These changes can now be interpreted in terms of the symmetric-rotor rules applied to each K index individually, except that the magnitude of ΔK, instead of being restricted to 0 and ±1 in the parallel and perpendicular directions of electric moment, respectively, is merely restricted to even and odd changes. (We shall see below, however, that the 0 and ±1 lines are of most significance in the asymmetric case.) If **o** and **e** are operators representing odd and even changes in K, the combined operators **eo**, **oo**, **oe**, to be applied to the double suffix, belong to the representations of the Four Group, *eo* (or B_a), *oo* (or B_b), and *oe* (or B_c), respectively, and in this way are directly related to the components of the electric moment a, b, c which also belong to these respective representations. The remaining operator **ee** belongs to representation *ee* (or A), but no branches of this type occur. The results for the asymmetric rotor can be summarized as follows (see also Table III).

For the electric moment parallel to the axis of least moment of inertia (a) the parity of the K_{-1} index does not change.

For the electric moment parallel to the axis of greatest moment of inertia (c) the parity of the K_1 index does not change.

For the electric moment parallel to the axis of intermediate moment of inertia (b) neither of the K indices does not change, i.e., both change.

These rules are independent of J or ΔJ values.

In the general case of the asymmetric rotor **e** can stand for $\Delta K=0, \pm2, \pm4$, etc., and the operator **o** can stand for $\Delta K=\pm1, \pm3$, etc. However, not all numerical combinations of ΔK_{-1} and ΔK_1 are possible because the sum $K_{-1}+K_1$ for any level is equal to J for even levels, and $J+1$ for odd levels.[8] The permitted values of $\Delta(K_{-1}+K_1)=\Delta K_{-1}+\Delta K_1=$ sum of the two operators **e** and **o** are given in Table IV.

Notation: In the symmetric rotor the branches of the spectrum are identified by a literal notation, i.e., for $\Delta J=0$, +1 and −1 by Q, R, and P,

[7] D. M. Dennison, Rev. Mod. Phys. **3**, 280 (1931).

[8] Odd and even levels are defined by the parity of γ in the definition of the Wang functions as positive and negative combinations of the symmetric-rotor functions (I-26). There are six different sets of γ (of which only two are distinct) corresponding to the six choices of symmetric-rotor functions. The γ used here, and in I—Table VIII, is that used with the functions which become the prolate and oblate functions in the limiting cases. The parity of γ, hence the level, can be readily found either from I—Table VIII or from the parity of the $J+K_{-1}+K_1$ or of $J+\tau$. See also reference 9.

respectively, and for $\Delta K=0$, $+1$ and -1 by q, r, and p, respectively, which define "sub-branches." Some authors have used such a notation for the asymmetric rotor near the limiting case of symmetry. However, half the sub-branches are not included in this notation, and some of them are among the strongest. It would be convenient to generalize these definitions so that the same concept of sub-branches could be used to describe the structure of the asymmetric-rotor spectrum, where the ΔK's can change by ± 2, ± 3, etc. Unfortunately, an extension of the literal notation becomes clumsy, so that we suggest a return to the numerical values of the ΔK's. For example, the asymmetric-rotor sub-branch R_{qr}, meaning $\Delta J=+1$, $\Delta K_{-1}=0$, and $\Delta K_1=1$, would be written $R_{0,1}$. Then a sub-branch such as $P_{\bar{2},1}$ would mean $\Delta J=-1$, $\Delta K_{-1}=-2$, $\Delta K_1=1$. Sometimes it may be simpler to identify transitions by $\Delta\tau=\Delta K_{-1}-\Delta K_1$. However, $\Delta\tau$ does not uniquely define a sub-branch, although with the direction of the electric moment specified, it is sufficient.

TABLE IV. Permitted changes in $\Delta(K_{-1}+K_1)=\Delta K_{-1}+\Delta K_1$. This table can also be used to find the parity of the levels from which the various transitions can arise. E.g., if $\Delta J=0$, $\Delta K_{-1}=1$, and $\Delta K_1=-1$, the sum $\Delta(K_{-1}+K_1)$ is 0, and the transitions can arise from even and odd levels to give both ${}^{b,c}Q_{1,\bar{1}}$ and ${}^{b,c}Q_{1,\bar{1}}$ sub-branches. If $\Delta J=-1$, $\Delta K_{-1}=1$, $\Delta K_1=-3$, then the sum is -2 and such transitions arise only from odd levels to give only ${}^{b,c}P_{1,\bar{3}}$.

Initial γ	P	Q	R
even	$-1, 0$	$0, 1$	$1, 2$
odd	$-1, -2$	$0, -1$	$1, 0$

In the identification of a sub-branch, the direction of the moment, as determined from the parities of the two ΔK's (Tables II and III), is indicated in a superscript, as is the parity of the initial level, e.g., ${}^{a,e}R_{0,1}$.

Branches of the Asymmetric Rotor

The distribution of sub-branches in the matrix of the line strengths between all states is shown in (25) where the non-zero elements have been indicated by inserting the values of ΔK_{-1} and ΔK_1.

	0_{00} *e*	1_{01} *e*	1_{11} *o*	1_{10} *e*	2_{02} *e*	2_{12} *o*	2_{11} *e*	2_{21} *o*	2_{20} *e*	3_{03} *e*	3_{13} *o*	3_{12} *e*	3_{22} *o*	3_{21} *e*	3_{31} *o*	3_{30} *e*
$0_{00}e$		01	11*	10†												
$1_{01}e$	$0\bar{1}$	—	10†	$1\bar{1}$*	01	11*	10†	—	$2\bar{1}$							
$1_{11}o$	$\bar{1}\bar{1}$*	$\bar{1}0$†	—	$0\bar{1}$	$\bar{1}1$*	01	—	10†	$1\bar{1}$*							
$1_{10}e$	$\bar{1}0$†	$\bar{1}1$*	01	—	$\bar{1}2$†	—	01	11*	10†							
$2_{02}e$		$0\bar{1}$	$1\bar{1}$*	$1\bar{2}$†	—	10†	$1\bar{1}$*	$2\bar{1}$	—	01	11*	10†	—	$2\bar{1}$	$3\bar{1}$*	$3\bar{2}$†
$2_{12}o$		$\bar{1}\bar{1}$*	$0\bar{1}$	—	$\bar{1}0$†	—	$0\bar{1}$	$1\bar{1}$*	$1\bar{2}$†	$\bar{1}1$*	01	—	10†	$1\bar{1}$*	$2\bar{1}$	—
$2_{11}e$		$\bar{1}0$†	—	$0\bar{1}$	$\bar{1}1$*	01	—	10†	$1\bar{1}$*	$\bar{1}2$†	—	01	11*	10†	—	$2\bar{1}$
$2_{21}o$		—	$\bar{1}0$†	$\bar{1}\bar{1}$*	$\bar{2}1$	$\bar{1}1$*	$\bar{1}0$†	—	$0\bar{1}$	—	$\bar{1}2$†	$\bar{1}1$*	01	—	10†	$1\bar{1}$*
$2_{20}e$		$\bar{2}1$	$\bar{1}1$*	$\bar{1}0$†	—	$\bar{1}2$†	$\bar{1}1$*	01	—	$\bar{2}3$	$\bar{1}3$*	$\bar{1}2$†	—	01	11*	10†
$3_{03}e$					$0\bar{1}$	$1\bar{1}$*	$1\bar{2}$†	—	$2\bar{3}$	—	10†	$1\bar{1}$*	$2\bar{1}$	—	$3\bar{2}$†	$3\bar{3}$*
$3_{13}o$					$\bar{1}\bar{1}$*	$0\bar{1}$	—	$1\bar{2}$†	$1\bar{3}$*	$\bar{1}0$†	—	$0\bar{1}$	$1\bar{1}$*	$1\bar{2}$†	—	$2\bar{3}$
$3_{12}e$					$\bar{1}0$†	—	$0\bar{1}$	$1\bar{1}$*	$1\bar{2}$†	$\bar{1}1$*	01	—	10†	$1\bar{1}$*	$2\bar{1}$	—
$3_{22}o$					—	$\bar{1}0$†	$\bar{1}\bar{1}$*	$0\bar{1}$	—	$\bar{2}1$	$\bar{1}1$*	$\bar{1}0$†	—	$0\bar{1}$	$1\bar{1}$*	$1\bar{2}$†
$3_{21}e$					$\bar{2}1$	$\bar{1}1$*	$\bar{1}0$†	—	$0\bar{1}$	—	$\bar{1}2$†	$\bar{1}1$*	01	—	10†	$1\bar{1}$*
$3_{31}o$					$\bar{3}1$*	$\bar{2}1$	—	$\bar{1}0$†	$\bar{1}\bar{1}$*	$\bar{3}2$†	—	$\bar{2}1$	$\bar{1}1$*	$\bar{1}0$†	—	$0\bar{1}$
$3_{30}e$					$\bar{3}2$†	—	$\bar{2}1$	$\bar{1}1$*	$\bar{1}0$†	$\bar{3}3$*	$\bar{2}3$	—	$\bar{1}2$†	$\bar{1}1$*	01	—

(25)

Plain numerals are used for branches appearing with a component along a, an asterisk the component along b, and a dagger the component along c. It is seen that the transitions of any

sub-branch appear only along diagonals of the blocks. Half the sub-branches arise from either odd or even levels. Examination of the numerical values of the others, which arise from both odd and even levels, shows that the strengths alternate in value. A smooth trend of numbers is obtained by separating the latter into "*e*" and "*o*" parts (arising from even and odd levels, respectively), each of which will henceforth be called a sub-branch,[9] e.g., ${}^{b,e}Q_{\bar{1},1}$ and ${}^{b,o}Q_{\bar{1},1}$. The *e* and *o* parts have now the same number of lines as the other sub-branches.

The values of the line strengths decrease away from the principal diagonal as ΔK_{-1}, ΔK_1 (and hence $\Delta\tau$) increase, i.e., as the departure from the selection rules of the symmetric rotor increases.

TABLE V. Summary of arrangement of sub-branches in the Table of Line Strengths in the Appendix. The reverse, inverse, and inverse-reverse (see Section VI) of any sub-branch are to be found in the same row of the table as is the primary. Sub-branches in columns 1 and 2 and columns 3 and 4 are reverses of each other and have the same strengths. Sub-branches in columns 3 and 4 are inverses of those in columns 1 and 2 and have the same strengths for opposite signs of κ. Column 5 summarizes the maximum line strengths found in any group of sub-branches by giving the number of digits in the strength $\times 10^4$, for five values of κ, ∓ 1, ∓ 0.5, 0, ± 0.5, and ± 1, where the upper sign applies to the sub-branches in columns 1 and 2, and the lower sign to those in columns 3 and 4.

"Symmetric-rotor" sub-branches *a* and *c* sub-branches				Strengths
Prolate and Oblate				
${}^{c,e}Q_{1,0}$	${}^{c,o}Q_{\bar{1},0}$	${}^{a,e}Q_{0,1}$	${}^{a,o}Q_{0,\bar{1}}$	6,6,6,6,6
${}^{c,e}R_{1,0}$	${}^{c,e}P_{\bar{1},0}$	${}^{a,e}R_{0,1}$	${}^{a,e}P_{0,\bar{1}}$	6,6,6,6,6
${}^{c,o}R_{1,0}$	${}^{c,o}P_{\bar{1},0}$	${}^{a,o}R_{0,1}$	${}^{a,o}P_{0,\bar{1}}$	6,6,6,6,6
Prolate only (*c*)		Oblate only (*a*)		
${}^{c,e}Q_{\bar{1},2}$	${}^{c,o}Q_{1,\bar{2}}$	${}^{a,e}Q_{2,\bar{1}}$	${}^{a,o}Q_{\bar{2},1}$	5,5,5,4,0
${}^{c,e}R_{\bar{1},2}$	${}^{c,e}P_{1,\bar{2}}$	${}^{a,e}R_{2,\bar{1}}$	${}^{a,e}P_{\bar{2},1}$	5,5,4,4,0
${}^{c,o}R_{\bar{1},2}$	${}^{c,o}P_{1,\bar{2}}$	${}^{a,o}R_{2,\bar{1}}$	${}^{a,o}P_{\bar{2},1}$	5,4,4,4,0
b sub-branches				
Prolate and Oblate				
${}^{b,e}Q_{\bar{1},1}$	${}^{b,e}Q_{1,\bar{1}}$	${}^{b,e}Q_{1,\bar{1}}$§	${}^{b,e}Q_{\bar{1},1}$§	6,5,5,5,6
${}^{b,o}Q_{\bar{1},1}$	${}^{b,o}Q_{1,\bar{1}}$	${}^{b,o}Q_{1,\bar{1}}$§	${}^{b,o}Q_{\bar{1},1}$§	5,5,5,5,5
${}^{b,e}R_{1,1}$	${}^{b,o}P_{\bar{1},\bar{1}}$	${}^{b,e}R_{1,1}$§	${}^{b,o}P_{\bar{1},\bar{1}}$§	6,6,6,6,6
${}^{b,o}R_{\bar{1},1}$	${}^{b,e}P_{1,\bar{1}}$	${}^{b,o}R_{1,\bar{1}}$	${}^{b,e}P_{\bar{1},1}$	5,6,6,6,6
Prolate only		Oblate only		
${}^{b,e}R_{\bar{1},3}$	${}^{b,o}P_{1,\bar{3}}$	${}^{b,e}R_{3,\bar{1}}$	${}^{b,o}P_{\bar{3},1}$	5,4,4,4,0
First-order forbidden sub-branches				
a and *c* sub-branches				
${}^{c,o}Q_{\bar{3},2}$	${}^{c,e}Q_{3,\bar{2}}$	${}^{a,e}Q_{2,\bar{3}}$	${}^{a,e}Q_{\bar{2},3}$	0,4,4,4,0
${}^{c,e}Q_{\bar{3},4}$	${}^{c,o}Q_{3,\bar{4}}$	${}^{a,e}Q_{4,\bar{3}}$	${}^{a,o}Q_{\bar{4},3}$	0,3,3,2,0
${}^{c,e}R_{3,\bar{2}}$	${}^{c,e}P_{\bar{3},2}$	${}^{a,e}R_{\bar{2},3}$	${}^{a,e}P_{2,\bar{3}}$	0,4,4,4,0
${}^{c,o}R_{3,\bar{2}}$	${}^{c,o}P_{\bar{3},2}$	${}^{a,o}R_{\bar{2},3}$	${}^{a,o}P_{2,\bar{3}}$	0,3,3,3,0
${}^{c,e}R_{\bar{3},4}$	${}^{c,e}P_{3,\bar{4}}$	${}^{a,e}R_{4,\bar{3}}$	${}^{a,e}P_{\bar{4},3}$	0,3,3,2,0
${}^{c,o}R_{\bar{3},4}$	${}^{c,o}P_{3,\bar{4}}$	${}^{a,o}R_{4,\bar{3}}$	${}^{a,o}P_{\bar{4},3}$	0,2,2,1,0
b sub-branches				
${}^{b,e}Q_{\bar{3},3}$	${}^{b,e}Q_{3,\bar{3}}$	${}^{b,e}Q_{3,\bar{3}}$§	${}^{b,e}Q_{\bar{3},3}$§	0,4,4,4,0
${}^{b,o}Q_{\bar{3},3}$	${}^{b,o}Q_{3,\bar{3}}$	${}^{b,o}Q_{3,\bar{3}}$§	${}^{b,o}Q_{\bar{3},3}$§	0,3,3,3,0
${}^{b,o}R_{\bar{3},3}$	${}^{b,e}P_{3,\bar{3}}$	${}^{b,o}R_{3,\bar{3}}$	${}^{b,e}P_{\bar{3},3}$	0,3,3,3,0
${}^{b,e}R_{\bar{3},5}$	${}^{b,o}P_{3,\bar{5}}$	${}^{b,e}R_{5,\bar{3}}$	${}^{b,o}P_{\bar{5},3}$	0,2,2,2,0

§ Same lines as in columns 1 and 2, but sorted on K_1.

[9] Since the parity of the initial levels with respect to γ has no direct significance in spectrum analysis, and since the representation of the Four Group to which the initial level belongs is of importance because differing nuclear-spin weight factors may have to be applied to each, one might expect a sub-division of the sub-branches on *ee*, *eo*, *oe*, and *oo*. The sorting of sub-branches into four parts arising from each of these species of the initial levels does not give smooth sequences of strengths. The parity of $J+\gamma$, not γ alone, is characteristic of each symmetry species (I—Table VIII); or, from the opposite point of view, each sub-branch, even when divided into γ-even and γ-odd components, arises from levels of all four species.

V. STRUCTURE OF THE SPECTRUM

The principal lines in the spectrum of the asymmetric rotor are those which occur in the symmetric rotor, if we first resolve the doubly degenerate levels of the latter into their Wang components, which retain their identity as the rotor becomes asymmetric. The resolution of this degeneracy, which splits the symmetric-rotor energy levels into those of the asymmetric rotor, also is responsible for a splitting of the *p*, *q*, and *r* sub-branches of the oblate- and prolate-rotor spectra into the sub-branches of the asymmetric-rotor spectra.

The principal sub-branches of the asymmetric rotor are those for which both K's change by 0 or ± 1, and so become *p*, *q*, or *r* branches in both the prolate- and the oblate-symmetric limiting cases. These sub-branches are listed first in the Table of Line Strengths found in the Appendix (of which Table V is a summary), and are shown diagrammatically by heavy lines in Fig. 1.

The next important sub-branches are those in which ΔK changes by 0, ± 1, i.e., which are *p*, *q*, or *r* sub-branches in either the prolate or oblate case, but for which the other index operator has an absolute value greater than 1, corresponding to forbidden transitions of zero intensity in the other symmetry case (oblate or prolate, respectively). These sub-branches, such as $P_{1,\bar{3}}$, are listed second in the tables, and are shown by light lines in Fig. 1. Note that in transitions of the symmetric rotor in the Wang resolution, changes in the K which is not the true quantum number can have an absolute value greater than unity.

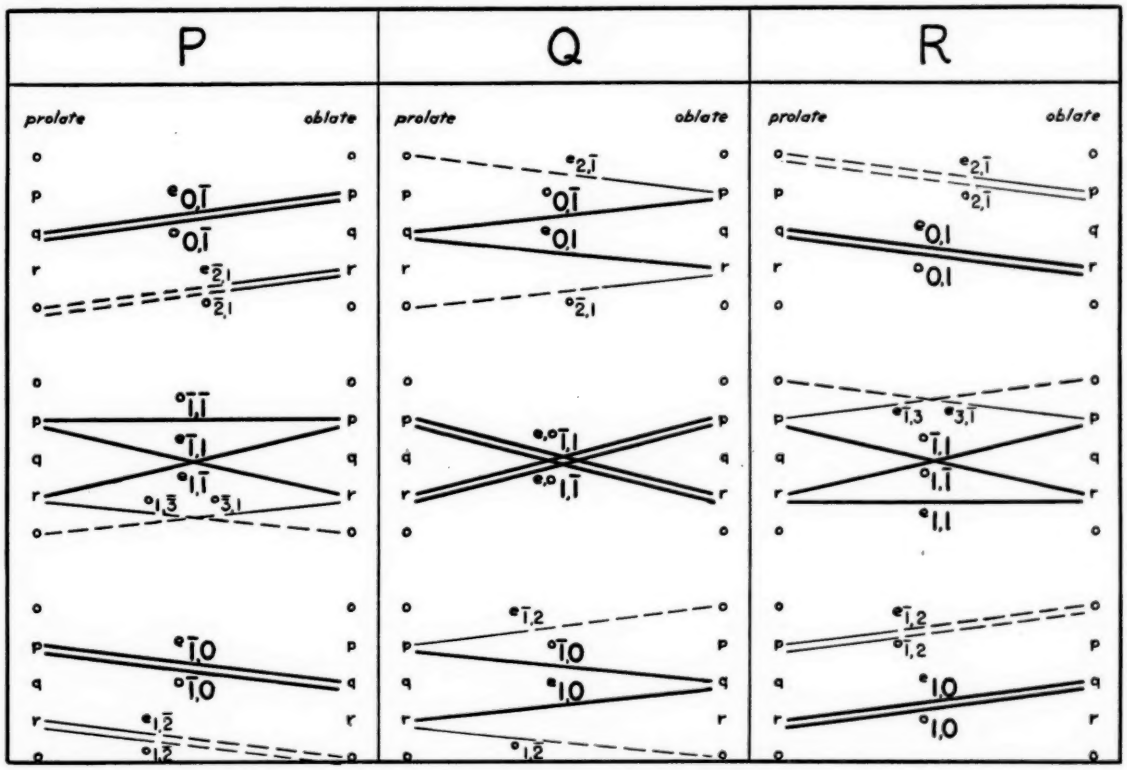

FIG. 1. A chart correlating the sub-branches of the asymmetric rotor with those of the symmetric-rotor limiting cases. Those permitted in both the prolate and oblate rotors, and hence of high strength throughout the whole range of asymmetry are indicated by heavy lines. Pairs of sub-branches arising from the same permitted sub-branch in one limiting case and going to the same or different sub-branches in the other case have about the same strengths. Sub-branches permitted in only one or the other limit are shown by fine lines. The strengths of the strong wings fall off very rapidly on moving away from the permitted limiting cases, and so can be neglected (as shown by dashed lines) except close to the limiting case where they are permitted.

Finally, in the last part of the tables we have listed sub-branches of the asymmetric rotor which are forbidden in both prolate and oblate limiting cases. These not only have very low intensities even for the most asymmetric rotor, but also do not occur below certain values of J. Even with a favorable Boltzmann factor these sub-branches can usually be disregarded in the structure of the rotational spectra of the asymmetric rotor. We have only tabulated the "first-order" forbidden sub-branches, $|\Delta\tau|=5$, 6, 7, 8, which appear first at $J\geqslant 3$. The highest strength of any forbidden line calculated ($J<13$) is 0.3100. Second-order forbidden transitions, $|\Delta\tau|=9$, 10, 11, 12, which appear first at $J\geqslant 5$, have strengths no greater than 0.0030; higher orders, $\Delta\tau>12$, which begin at $J\geqslant 7$, have strengths less than 0.0001.

VI. TABLES OF LINE STRENGTHS

Certain symmetrical relations in the matrices, based on the KK notation just discussed, enable us to condense the tabulation of the numerical material to one-quarter of the total number of transitions. Let us consider a transition from a level with $J=j$, $K_{-1}=k$, $K_1=l$, $\tau=t$, or $j_{kl,t}$, to another level $h_{mn,s}$; let this be called a "primary" transition. Related to this transition is the "reverse" transition $h_{mn,s}\rightarrow j_{kl,t}$. The term "reverse" is chosen because the spectral lines of the pure rotational emission spectra will suffer "line reversal" by the reverse transition, a well-known phenomenon in atomic spectra.[10] The strength for the reverse transition appears on the opposite

[10] In the pure rotational emission spectrum (1) would be replaced by an equation involving both Einstein coefficients.

side of the main diagonal of (25) from that on which the primary transition is located. When the asymmetry parameter is the same in the two states (the only case considered in this work), these two elements are numerically equal. In the Appendix a transition beginning on $j_{kl,t}$ is listed in column 1, the final level being read in column 2. The line strengths given in the next columns, 3–7 (with the upper sign of κ) are the same for another line, the reverse of the above, whose *initial* level is given in column 2 and *final* level in column 1. The columns in the Appendix are headed by the name of the sub-branch whose initial levels are given in that column, the final levels being found in the adjacent column.

The asymmetry parameter κ used in Part I simplified the study of the energy levels because the patterns for positive values of κ were inverted for negative κ, i.e.,

$$E(\kappa)j_{kl,t} = -E(-\kappa)j_{lk,-t}. \tag{26}$$

Therefore, the transformation matrices and hence (25) for negative values of κ will be numerically the same as for the positive values, but will have the row and column labelling inverted. Thus for a primary transition at κ there is an "inverse" transition $j_{lk,-t} \rightarrow h_{nm,-s}$ at $-\kappa$ which has the same strength as the primary. Finally, for a primary transition there is an inverse-reverse $h_{nm,-s} \rightarrow j_{lk,-t}$. The reverse and the inverse-reverse strengths are the same at opposite signs of κ. The lines which are inverses and inverse-reverses of the ones we chose as primary (column 1) in the Appendix are to be found by reading their initial levels in columns 8 and 9, respectively. The lower sign of κ in columns 3–7 is to be used for these lines.

As one would expect, the sub-branches appearing when the electric moment is parallel to the least axis are inverses of those appearing when the moment is parallel to the greatest, and vice versa. Inverses of *b* sub-branches are *b* sub-branches, and in some cases a *b* sub-branch is its own inverse, so that the same sub-branch reappears in columns 8 and 9 (see also Table V).

The sub-branches appearing in the four columns of the Appendix, or in the same row of Table V, form a group. The reverse, inverse, and inverse-reverse of any one of the group is also a member of the group (a consequence of the Four-Group symmetry). All members of the group have the same value of $|\Delta J|$ and $|\Delta\tau|$. In the following we shall identify a group by the sub-branch appearing in the first column. The discussion of the variation of line strength with J or κ is the same for all members of the group.

Arrangement of Lines Within Sub-Branches: Wings

As in the symmetric-rotor spectrum, a sub-branch of the asymmetric-rotor spectrum is composed of lines which can be classified either by J or a K. In order to list the lines in a way so that there is a continuous trend in the line strengths, one can hold K fixed and list by increasing J, or hold J fixed and list by K. The former is probably the most natural in spectrum analysis as it enables one to group together the dominant lines of a sub-branch, then the next most important, and so on. In the tables, then, we have sorted the lines of the sub-branches into "wings" of which there are two types: those in which K_{-1} is held constant, J varies (labelled wing $-K_{-1}$); and those in which K_1 is held constant (labelled wing $+K_1$). For any given sub-branch sorting on one of the two K's picks out the strongest lines starting from any J level and collects them into the first wing, then collects the second strongest into the second wing, etc. In the tables all sub-branches are sorted this way. Sorting on the other K usually picks out the weakest lines into the first wings, etc., an arrangement which is valuable for extrapolation to high J's, but not used here except by accident (see *b* branches). Wings also have the valuable properties that the Boltzmann factors and line positions vary uniformly for the lines standing in a wing. Lines in the same wing have like variation in strength with degree of asymmetry.

The strongest lines in the spectrum will be those which have a high transition probability and a favorable Boltzmann factor (low K_{-1} or τ). A sorting on K_{-1} would pick out lines with the most favorable Boltzmann factor. Unfortunately, for half the lines this is not compatible with high strength, and in most spectra the latter outweighs the Boltzmann factor at low J's. Thus, in the Appendix the sub-branches have been sorted for high strength on whichever K is necessary.

It is not always feasible to do this for all values of κ simultaneously.

For the sub-branches appearing with the moment parallel to c it is possible to sort the lines (on K_{-1}) whereby the first wing contains the strongest lines both on account of high transition probability and favorable Boltzmann factor, with two exceptions, ${}^cR_{1,0}$ and ${}^cP_{\bar{1},0}$, where it is impossible to sort for both simultaneously. In the table these sub-branches have been sorted (on K_1) for high strength. In a band associated with a moment parallel to c these two sub-branches will be much weaker than ${}^cQ_{\bar{1},0}$ and ${}^cQ_{1,0}$.

Except for ${}^aR_{0,1}$ and ${}^aP_{0,\bar{1}}$ (the inverses of the two exceptions just mentioned in c bands), the sub-branches appearing with moment parallel to a cannot be sorted for both influences favorable and are sorted (on K_{-1}) for high strength only. For many molecules, e.g., H_2S, this is more satisfactory than sorting for Boltzmann factor, and not for strength, because the latter usually outweighs the former. However, there may be some examples where the K_{-1} wings for the sub-branches listed on the right-hand side of the table are preferable. It is not at all difficult to pick them out from the tables. Since the two exceptions ${}^aR_{0,1}$ and ${}^aP_{0,\bar{1}}$ also have favorable Boltzmann factors, they will be the outstanding sub-branches of bands associated with a moment parallel to a, as is indeed the case in the 10,100A band of H_2S.[11]

The ${}^bQ$ branches can be sorted for both influences favorable only in one range of κ, namely, on K_{-1} for negative κ, and on K_1 for positive κ. Since these branches are their own inverses, the same numbers appear in both halves of the range of κ, so that K_{-1} wings can be found by reading from left to right and K_1 wings by reading from right to left. A similar situation exists with ${}^{b,e}R_{1,1}$ and ${}^{b,o}P_{\bar{1},\bar{1}}$.

The sub-branches ${}^bR_{\bar{1},1}$ and ${}^bP_{1,\bar{1}}$ can be sorted on K_{-1} for both high strength and favorable Boltzmann factor simultaneously whereas their inverses can be sorted only for one or the other, and the arrangement of the table has compelled their sorting to be on K_1, for high strength only.

The sorting of the prolate-or-oblate sub-branches is such that it favors high strength near $\kappa=-1$ (the commonest range of asymmetry), simultaneously favoring the Boltzmann factor for c branches and two b branches.

Variation of Line Strengths with Asymmetry

The double suffix notation for the lines and sub-branches shows qualitatively the way the asymmetric-rotor sub-branches resolve, in the limiting cases, into p, q, r, or forbidden symmetric-rotor sub-branches. (See Fig. 1.) Quantitatively this classification offers further simplifications because in some of the sub-branches the resolved pairs either have the same or very closely the same strengths, while other pairs diverge and the strength of one member dies out very rapidly with increasing asymmetry.

The best example is the ${}^cQ_{\bar{1},0}$ group. Here the prolate ${}^aQ_q$ sub-branch splits into ${}^{a,o}Q_{0,\bar{1}}$ and ${}^{a,e}Q_{0,1}$ which are their own reverses, and so are numerically the same. In the oblate limit, however, they show entirely different characteristics. Here they become one component of ${}^aQ_p$ and of ${}^aQ_r$, respectively. The other component of ${}^aQ_p$ is ${}^{a,e}Q_{2,\bar{1}}$, i.e., oblate ${}^aQ_p$ splits into the prolate-and-oblate ${}^{a,o}Q_{0,\bar{1}}$ and the oblate-only ${}^{a,e}Q_{2,\bar{1}}$. Numerically, these two sub-branches arising from ${}^aQ_p$ have nothing in common except the limiting oblate strength. The same applies to their reverses, which coalesce into ${}^aQ_r$ oblate. A similar situation applies, of course, to the other sub-branches of this group which appear with the c moment.

The prolate-and-oblate ${}^bQ_{\bar{1},1}$ group of sub-branches split from ${}^bQ_p$ or ${}^bQ_r$ into odd and even sub-branches with slightly different strength in the asymmetric region. Similarly, the prolate ${}^aR_q$ sub-branch splits into ${}^{a,e}R_{0,1}$ and ${}^{a,o}R_{0,1}$, which have very closely the same strengths over most of the range of κ.

The prolate-and-oblate ${}^bR_{1,1}$ group and the ${}^bR_{1,\bar{1}}$ group with which it coalesces in one or other of the limiting cases similarly differ only slightly in strength. But the ${}^bR_{1,\bar{1}}$ group in the other limiting case pairs up with the prolate-or-oblate decadent ${}^bR_{3,\bar{1}}$ group, with which it has nothing in common except the limiting value.

All the lines in ${}^bR_{1,1}$ (and ${}^bP_{\bar{1},\bar{1}}$) remain at

[11] P. C. Cross, Phys. Rev. **47**, 7 (1935) and J. Chem. Phys. **5**, 370 (1937).

practically the same strength for all values of κ, as one would expect from the unique symmetry of these sub-branches (degenerating to the ${}^bR_r$ and ${}^bP_p$ in both limits). The other prolate-and-oblate sub-branches contain several types of wings. Some have about the same strength at all values of κ. Others remain fairly constant throughout most of the range, then decrease very rapidly to a half or a tenth of their strength; e.g., in ${}^{a,o}Q_{0,\bar{1}}$ the transition $12_{12,1}\rightarrow 12_{12,0}$ stays at a value of 23 from $\kappa=-1$ to $+0.5$, then drops to 12.5 at $\kappa=+1.0$. The ${}^bR_{\bar{1},1}$ group of sub-branches contain certain wings which are as decadent as the prolate-or-oblate sub-branches; e.g., in ${}^{b,o}R_{1,\bar{1}}$ the transition $11_{1,11}\rightarrow 12_{2,10}$ changes from 3.7917 for the prolate rotor to 0.0967 at $\kappa=-0.5$, i.e., by a factor of 40 in the range where most triatomic molecules lie. Lines with similar decay characteristics are sometimes better grouped together by sorting on the K other than the one used in the tables.

All the wings of the prolate-or-oblate sub-branches decrease abruptly in strength at one end of the range of κ. The stronger wings drop in strength by a factor of 10 to 40 in the quarter next to their permitted symmetric rotor, while the weaker wings stay at a fairly constant strength over three-quarters of the range, then abruptly drop to zero strength in the quarter just before the forbidden limit.

The strengths of all the "forbidden" sub-branches have a characteristic similar to that of the prolate-or-oblate sub-branches. In one quarter of the range of κ the strengths rise abruptly from zero to the maximum value, then decrease more uniformly over the remaining three-quarters of the range.

It is evident that the rapid changes in strength with κ that occur in many strong lines can be very confusing in spectrum analysis, and can account for "missing" lines so often reported.

In any particular case the number of important sub-branches is considerably reduced from the number tabulated here in detail for all values of κ. Some of the prolate-or-oblate sub-branches and many wings of the others have negligible intensities for $-0.5<\kappa<+0.5$. Further, if one neglects the splitting of the prolate-and-oblate branches, the principal structure of the bands of the asymmetric rotor is made up of sub-branches characteristic of the prolate- or oblate-symmetric rotor, although the actual strengths of the lines will have changed, in most cases, by a large factor.

Interpolation for Intermediate Values of κ

The strengths of the transitions of the symmetric rotor from which those for the asymmetric rotor were calculated give us the values at the two ends of the range of κ. Naturally, the first calculations were done for the most asymmetric rotor with $\kappa=0$. The rapid changes in strength with asymmetry described above made it necessary to take an intermediate point, which we chose as $\kappa=-0.5$ (from which $\kappa=+0.5$ follows by symmetry). With five points we originally hoped to be able to use the recently published *Tables of the 5-Point Lagrangean Interpolation*.[12] Unfortunately, five-point Lagrangian interpolation gives a quite erroneous value when applied to the abruptly changing prolate-and-oblate lines, or to any prolate-or-oblate or forbidden lines, because the Lagrangian polynomial becomes oscillatory to accommodate the rapid changes in the functions, which characteristically take place over small ranges of κ. In extreme cases even negative strengths result. In general, three-point interpolation is preferable, or better, the average of two overlapping three-point interpolations.

For many strong lines, and in three-quarters of the range for all the others, linear interpolation is accurate enough to compare with most experimental data.

Variation of Line Strength with J and K

The arrangement of lines into wings allows a fairly straightforward extrapolation to higher J's when the strengths are increasing. Decreasing strengths, however, should be extrapolated with care. We hope at some later date to investigate high J transitions by means of the Correspondence Principle. It should be noted in extra-

[12] *Table of 5-Point Lagrangean Interpolation Coefficients (From 0 to 2, Argument 0.001, 7-Place)*. Mathematical Tables Project, Works Projects Administration for the City of New York sponsored by National Bureau of Standards.

polating that the two methods of sorting into wings complement each other. In this connection an irregularity of the wings $+0$ and -0 should be mentioned. These wings in the positive and negative range of κ, respectively, have about twice the strength of the others because they connect levels which are not degenerate ($K_{\pm 1}=0$) in the symmetric rotor. These lines take all the transition probability which is normally divided between two degenerate levels.

VII. CONCLUSION

The table of line strengths, when combined with Boltzmann and nuclear spin weight factors, gives a numerical value for the relative intensity of a line in the spectrum of the asymmetric rotor, and thus eliminates the troublesome uncertainty as to the strength with which a line is to be expected. This is particularly valuable for those lines whose intensities change rapidly with asymmetry.

With the energy level table of Part I and the strengths of this paper, one is in a position to draw up spectra of any molecule, given its dimensions of the upper and lower states, with one limitation. That is, if the asymmetries of the two states are appreciably different, the tables of line strengths may not be adequate, for in this case the direction-cosine matrices are no longer symmetrical, so that the reverse and primary sub-bands do not have identical strengths. Calculations for extreme changes in κ show there is a considerable redistribution of line strength among the transitions from a given level.

The results of the calculations reported in Parts I and II of this series have been applied to the calculation of pure rotation and vibration-rotation spectra of simple molecules, employing punched-card-machine methods. The ease with which representative spectra can be prepared in this manner makes the method of successive approximations more attractive in the analysis of rotational structure. When our present calculations have been extended by means of the Correspondence Principle to the energies and intensities for $J>12$, considerable information may be obtainable from unresolved band envelopes.

ACKNOWLEDGMENTS

In conclusion the authors express their appreciation of their many valuable discussions with Mr. Raymond R. Halverson; of the extensive and painstaking numerical work done by Messrs. Theodore P. Cotter, Norman R. Larson, Robert P. Larsen, Glenn H. Miller, Andrew D. Whitehead, and David G. Hedberg; and of the skill with which punched-card-machine methods were adapted to certain phases of this work by Dr. G. B. Thomas of the Center of Analysis, Massachusetts Institute of Technology.

APPENDIX. TABLE OF LINE STRENGTHS

The line strengths listed here (see Tables VI and VII) are the squares of the elements of the direction-cosine matrices in the representation which diagonalizes the energy matrix of the asymmetric rotor, summed over the Zeeman components and multiplied by 3 to account for the three equivalent space-fixed directions, i.e., line strength for the component of the electric moment μ_g, parallel to the molecule-fixed axes $g=a, b, c$ is

$$\sum_{F=X,Y,Z}\sum_{M''}\sum_{M'}|(\Phi_{Fg}{}^{A})_{J'',\tau'',M'';J',\tau',M'}|^2$$

$$=3\sum_{M''}\sum_{M'}\left|\int\psi^{*}_{J'',\tau'',M''}\Phi_{Fg}{}^{A}\psi_{J',\tau',M'}dv\right|^2$$

[where J, τ, M stand for R in (2)] and thus is the corresponding prefactor on the right-hand side of (2) summed over X, Y, Z, M', and M''. Actual intensities can then be obtained by substituting (2) in (1) provided the values of the integrals $\int\psi^{*}_{V'',e''}\mu_g\psi_{V',e'}dv$ are known. Relative intensities are obtained by putting such of these integrals that are non-vanishing equal to unity.

The entries have also been multiplied by 10^4 to eliminate decimal points. The parameter of asymmetry

$$\kappa=(2b-a-c)/(a-c)$$

where a, b, c equal $\hbar^2/2I_a$, $\hbar^2/2I_b$, $\hbar^2/2I_c$, respectively, and where the condition $I_a\leq I_b\leq I_c$ is applied in assigning the moments of inertia.

Transitions are classified by sub-branches which head the column in which the initial level can be found (identified by $JK_{-1},K_{1};\tau$) and whose final level is in the adjacent column on the same row.

The lines in each sub-branch are listed in wings which can be identified by K_{-1} or K_1, whichever is held constant, as can be determined by the subscripts of the initial levels.

Sub-branches in adjacent columns have identical strengths. Those in columns 1 and 2 apply to the upper sign of κ; those in columns 8 and 9 apply to the lower sign.

The strengths found in columns 3 and 7 are those occurring in the prolate- and oblate-symmetric rotor. When no entry is given, the transition is forbidden. "High order forbidden" branches for which $|\Delta\tau|\geq 9$ have been omitted. When the entry is 0, the strength is less than 0.0001.

TABLE VI. Symmetric-rotor sub-branches.

A. a and c prolate-and-oblate sub-branches.

Sub-branch		κ					Sub-branch	
$^{c,e}Q_{1,0}$	$^{c,o}Q_{\bar{1},0}$	∓ 1	∓ 0.5	0	± 0.5	± 1	$^{a,e}Q_{0,1}$	$^{a,o}Q_{0,\bar{1}}$
$1_{0,1;-1}$	$1_{1,1;0}$	15000	15000	15000	15000	15000	$1_{1,0;1}$	$1_{1,1;0}$
$2_{0,2;-2}$	$2_{1,2;-1}$	25000	28223	31100	32845	33333	$2_{2,0;2}$	$2_{2,1;1}$
$3_{0,3;-3}$	$3_{1,3;-2}$	35000	45104	50431	52155	52500	$3_{3,0;3}$	$3_{3,1;2}$
$4_{0,4;-4}$	$4_{1,4;-3}$	45000	64494	70244	71708	72000	$4_{4,0;4}$	$4_{4,1;3}$
$5_{0,5;-5}$	$5_{1,5;-4}$	55000	84696	90073	91399	91667	$5_{5,0;5}$	$5_{5,1;4}$
$6_{0,6;-6}$	$6_{1,6;-5}$	65000	104928	109923	111174	111429	$6_{6,0;6}$	$6_{6,1;5}$
$7_{0,7;-7}$	$7_{1,7;-6}$	75000	125065	129799	131004	131250	$7_{7,0;7}$	$7_{7,1;6}$
$8_{0,8;-8}$	$8_{1,8;-7}$	85000	145135	149698	150871	151111	$8_{8,0;8}$	$8_{8,1;7}$
$9_{0,9;-9}$	$9_{1,9;-8}$	95000	165170	169614	170764	171000	$9_{9,0;9}$	$9_{9,1;8}$
$10_{0,10;-10}$	$10_{1,10;-9}$	105000	185187	189544	190677	190909	$10_{10,0;10}$	$10_{10,1;9}$
$11_{0,11;-11}$	$11_{1,11;-10}$	115000	205194	209484	210603	210834	$11_{11,0;11}$	$11_{11,1;10}$
$12_{0,12;-12}$	$12_{1,12;-11}$	125000	225195	229434	230542	230769	$12_{12,0;12}$	$12_{12,1;11}$
$2_{1,1;0}$	$2_{2,1;1}$	8333	8333	8333	8333	8333	$2_{1,1;0}$	$2_{1,2;-1}$
$3_{1,2;-1}$	$3_{2,2;0}$	14583	16278	18811	21875	23333	$3_{2,1;1}$	$3_{2,2;0}$
$4_{1,3;-2}$	$4_{2,3;-1}$	20250	26168	34242	39363	40500	$4_{3,1;2}$	$4_{3,2;1}$
$5_{1,4;-3}$	$5_{2,4;-2}$	25667	39338	52949	57742	58667	$5_{4,1;3}$	$5_{4,2;2}$
$6_{1,5;-4}$	$6_{2,5;-3}$	30952	56179	72319	76548	77381	$6_{5,1;4}$	$6_{5,2;3}$
$7_{1,6;-5}$	$7_{2,6;-4}$	36161	75597	91744	95646	96429	$7_{6,1;5}$	$7_{6,2;4}$
$8_{1,7;-6}$	$8_{2,7;-5}$	41319	95950	111231	114943	115694	$8_{7,1;6}$	$8_{7,2;5}$
$9_{1,8;-7}$	$9_{2,8;-6}$	46444	116333	130792	134381	135111	$9_{8,1;7}$	$9_{8,2;6}$
$10_{1,9;-8}$	$10_{2,9;-7}$	51545	136551	150418	153921	154636	$10_{9,1;8}$	$10_{9,2;7}$
$11_{1,10;-9}$	$11_{2,10;-8}$	56629	156642	170100	173540	174242	$11_{10,1;9}$	$11_{10,2;8}$
$12_{1,11;-10}$	$12_{2,11;-9}$	61699	176660	189825	193216	193910	$12_{11,1;10}$	$12_{11,2;9}$
$3_{2,1;1}$	$3_{3,1;2}$	8750	7403	6406	5944	5833	$3_{1,2;-1}$	$3_{1,3;-2}$
$4_{2,2;0}$	$4_{3,2;1}$	15750	13221	13196	15598	18000	$4_{2,2;0}$	$4_{2,3;-1}$
$5_{2,3;-1}$	$5_{3,3;0}$	22000	19105	23397	30662	33000	$5_{3,2;1}$	$5_{3,3;0}$
$6_{2,4;-2}$	$6_{3,4;-1}$	27857	26374	38620	47709	49524	$6_{4,2;2}$	$6_{4,3;1}$
$7_{2,5;-3}$	$7_{3,5;-2}$	33482	36237	57062	65399	66964	$7_{5,2;3}$	$7_{5,3;2}$
$8_{2,6;-4}$	$8_{3,6;-3}$	38958	49682	76155	83565	85000	$8_{6,2;4}$	$8_{6,3;3}$
$9_{2,7;-5}$	$9_{3,7;-4}$	44333	66864	95251	102089	103444	$9_{7,2;5}$	$9_{7,3;4}$
$10_{2,8;-6}$	$10_{3,8;-5}$	49636	86630	114393	120880	122183	$10_{8,2;6}$	$10_{8,3;5}$
$11_{2,9;-7}$	$11_{3,9;-6}$	54886	107332	133621	139873	141136	$11_{9,2;7}$	$11_{9,3;6}$
$12_{2,10;-8}$	$12_{3,10;-7}$	60096	128002	152940	159022	160256	$12_{10,2;8}$	$12_{10,3;7}$
$4_{3,1;2}$	$4_{4,1;3}$	9000	7587	6026	4847	4500	$4_{1,3;-2}$	$4_{1,4;-3}$
$5_{3,2;1}$	$5_{4,2;2}$	16500	13464	11058	11750	14667	$5_{2,3;-1}$	$5_{2,4;-2}$
$6_{3,3;0}$	$6_{4,3;1}$	23214	18339	17488	23981	27857	$6_{3,3;0}$	$6_{3,4;-1}$
$7_{3,4;-1}$	$7_{4,4;0}$	29464	22914	27745	39794	42857	$7_{4,3;1}$	$7_{4,4;0}$
$8_{3,5;-2}$	$8_{4,5;-1}$	35417	28185	43063	56506	59028	$8_{5,3;2}$	$8_{5,4;1}$
$9_{3,6;-3}$	$9_{4,6;-2}$	41167	35293	61523	73754	76000	$9_{6,3;3}$	$9_{6,4;2}$
$10_{3,7;-4}$	$10_{4,7;-3}$	46773	45350	80547	91464	93546	$10_{7,3;4}$	$10_{7,4;3}$
$11_{3,8;-5}$	$11_{4,8;-4}$	52273	59213	99473	109542	111515	$11_{8,3;5}$	$11_{8,4;4}$
$12_{3,9;-6}$	$12_{4,9;-5}$	57692	76888	118383	127913	129808	$12_{9,3;6}$	$12_{9,4;5}$
$5_{4,1;3}$	$5_{5,1;4}$	9167	7777	6127	4374	3667	$5_{1,4;-3}$	$5_{1,5;-4}$
$6_{4,2;2}$	$6_{5,2;3}$	17024	14084	10758	9464	12381	$6_{2,4;-2}$	$6_{2,5;-3}$
$7_{4,3;1}$	$7_{5,3;2}$	24107	19340	15156	18769	24107	$7_{3,4;-1}$	$7_{3,5;-2}$
$8_{4,4;0}$	$8_{5,4;1}$	30694	23768	21441	33034	37778	$8_{4,4;0}$	$8_{4,5;-1}$
$9_{4,5;-1}$	$9_{5,5;0}$	36944	27638	31860	49002	52778	$9_{5,4;1}$	$9_{5,5;0}$
$10_{4,6;-2}$	$10_{5,6;-1}$	42955	31542	47402	65474	68727	$10_{6,4;2}$	$10_{6,5;1}$
$11_{4,7;-3}$	$11_{5,7;-2}$	48788	36457	66028	82425	85379	$11_{7,4;3}$	$11_{7,5;2}$
$12_{4,8;-4}$	$12_{5,8;-3}$	54487	43527	85120	99805	102564	$12_{8,4;4}$	$12_{8,5;3}$
$6_{5,1;4}$	$6_{6,1;5}$	9286	7913	6271	4244	3095	$6_{1,5;-4}$	$6_{1,6;-5}$
$7_{5,2;3}$	$7_{6,2;4}$	17411	14552	11116	8220	10714	$7_{2,5;-3}$	$7_{2,6;-4}$
$8_{5,3;2}$	$8_{6,3;3}$	24792	20246	14956	14996	21250	$8_{3,5;-2}$	$8_{3,6;-3}$
$9_{5,4;1}$	$9_{6,4;2}$	31667	25157	18940	27035	33778	$9_{4,5;-1}$	$9_{4,6;-2}$
$10_{5,5;0}$	$10_{6,5;1}$	38182	29364	25162	42308	47727	$10_{5,5;0}$	$10_{5,6;-1}$
$11_{5,6;-1}$	$11_{6,6;0}$	44432	32945	35783	58220	62727	$11_{6,5;1}$	$11_{6,6;0}$
$12_{5,7;-2}$	$12_{6,7;-1}$	50481	36135	51610	74526	78526	$12_{7,5;2}$	$12_{7,6;1}$

TABLE VI.—*Continued.*

Sub-branch				κ			Sub-branch	
$^{c,e}Q_{1,0}$	$^{c,o}Q_{\bar{1},0}$	∓ 1	∓ 0.5	0	± 0.5	± 1	$^{a,e}Q_{0,1}$	$^{a,o}Q_{0,\bar{1}}$
$7_{6,1;5}$	$7_{7,1;6}$	9375	8011	6383	4273	2679	$7_{1,6;-5}$	$7_{1,7;-6}$
$8_{6,2;4}$	$8_{7,2;5}$	17708	14899	11514	7682	9444	$8_{2,6;-4}$	$8_{2,7;-5}$
$9_{6,3;3}$	$9_{7,3;4}$	25333	20931	15562	12549	19000	$9_{3,6;-3}$	$9_{3,7;-4}$
$10_{6,4;2}$	$10_{7,4;3}$	32455	26254	18837	21925	30545	$10_{4,6;-2}$	$10_{4,7;-3}$
$11_{6,5;1}$	$11_{7,5;2}$	39205	30943	22510	36052	43561	$11_{5,6;-1}$	$11_{5,7;-2}$
$12_{6,6;0}$	$12_{7,6;1}$	45673	35027	28709	51607	57692	$12_{6,6;0}$	$12_{6,7;-1}$
$8_{7,1;6}$	$8_{8,1;7}$	9444	8087	6468	4346	2361	$8_{1,7;-6}$	$8_{1,8;-7}$
$9_{7,2;5}$	$9_{8,2;6}$	17944	15167	11832	7594	8444	$9_{2,7;-5}$	$9_{2,8;-6}$
$10_{7,3;4}$	$10_{8,3;5}$	25773	21462	16215	11172	17182	$10_{3,7;-4}$	$10_{3,8;-5}$
$11_{7,4;3}$	$11_{8,4;4}$	33106	27105	19675	18011	27879	$11_{4,7;-3}$	$11_{4,8;-4}$
$12_{7,5;2}$	$12_{8,5;3}$	40064	32174	22501	30163	40064	$12_{5,7;-2}$	$12_{5,8;-3}$
$9_{8,1;7}$	$9_{9,1;8}$	9500	8146	6535	4418	2111	$9_{1,8;-7}$	$9_{1,9;-8}$
$10_{8,2;6}$	$10_{9,2;7}$	18136	15380	12081	7731	7636	$10_{2,8;-6}$	$10_{2,9;-7}$
$11_{8,3;5}$	$11_{9,3;6}$	26136	21887	16748	10598	15682	$11_{3,8;-5}$	$11_{3,9;-6}$
$12_{8,4;4}$	$12_{9,4;5}$	33654	27788	20570	15383	25641	$12_{4,8;-4}$	$12_{4,9;-5}$
$10_{9,1;8}$	$10_{10,1;9}$	9545	8194	6588	4479	1909	$10_{1,9;-8}$	$10_{1,10;-9}$
$11_{9,2;7}$	$11_{10,2;8}$	18295	15554	12280	7933	6970	$11_{2,9;-7}$	$11_{2,10;-8}$
$12_{9,3;6}$	$12_{10,3;7}$	26442	22237	17176	10563	14423	$12_{3,9;-6}$	$12_{3,10;-7}$
$11_{10,1;9}$	$11_{11,1;10}$	9583	8234	6631	4530	1742	$11_{1,10;-9}$	$11_{1,11;-10}$
$12_{10,2;8}$	$12_{11,2;9}$	18429	15699	12443	8126	6410	$12_{2,10;-8}$	$12_{2,11;-9}$
$12_{11,1;10}$	$12_{12,1;11}$	9615	8268	6667	4571	1603	$12_{1,11;-10}$	$12_{1,12;-11}$
$^{c,e}R_{1,0}$	$^{c,e}P_{\bar{1},0}$	∓ 1	∓ 0.5	0	± 0.5	± 1	$^{a,e}R_{0,1}$	$^{a,e}P_{0,\bar{1}}$
$0_{0,0;0}$	$1_{1,0;1}$	10000	10000	10000	10000	10000	$0_{0,0;0}$	$1_{0,1;-1}$
$1_{1,0;1}$	$2_{2,0;2}$	15000	16934	18660	19707	20000	$1_{0,1;-1}$	$2_{0,2;-2}$
$2_{2,0;2}$	$3_{3,0;3}$	25000	25893	27201	29029	30000	$2_{0,2;-2}$	$3_{0,3;-3}$
$3_{3,0;3}$	$4_{4,0;4}$	35000	35773	36728	38312	40000	$3_{0,3;-3}$	$4_{0,4;-4}$
$4_{4,0;4}$	$5_{5,0;5}$	45000	45745	46619	47897	50000	$4_{0,4;-4}$	$5_{0,5;-5}$
$5_{5,0;5}$	$6_{6,0;6}$	55000	55730	56582	57727	60000	$5_{0,5;-5}$	$6_{0,6;-6}$
$6_{6,0;6}$	$7_{7,0;7}$	65000	65721	66562	67660	70000	$6_{0,6;-6}$	$7_{0,7;-7}$
$7_{7,0;7}$	$8_{8,0;8}$	75000	75714	76549	77628	80000	$7_{0,7;-7}$	$8_{0,8;-8}$
$8_{8,0;8}$	$9_{9,0;9}$	85000	85708	86539	87610	90000	$8_{0,8;-8}$	$9_{0,9;-9}$
$9_{9,0;9}$	$10_{10,0;10}$	95000	95704	96531	97597	100000	$9_{0,9;-9}$	$10_{0,10;-10}$
$10_{10,0;10}$	$11_{11,0;11}$	105000	105701	106525	107588	110000	$10_{0,10;-10}$	$11_{0,11;-11}$
$11_{11,0;11}$	$12_{12,0;12}$	115000	115698	116519	117580	120000	$11_{0,11;-11}$	$12_{0,12;-12}$
$1_{0,1;-1}$	$2_{1,1;0}$	15000	15000	15000	15000	15000	$1_{1,0;1}$	$2_{1,1;0}$
$2_{1,1;0}$	$3_{2,1;1}$	16667	22500	25581	26509	26667	$2_{1,1;0}$	$3_{1,2;-1}$
$3_{2,1;1}$	$4_{3,1;2}$	26250	29261	33801	36902	37500	$3_{1,2;-1}$	$4_{1,3;-2}$
$4_{3,1;2}$	$5_{4,1;3}$	36000	38400	41758	46530	48000	$4_{1,3;-2}$	$5_{1,4;-3}$
$5_{4,1;3}$	$6_{5,1;4}$	45833	48106	50867	55604	58333	$5_{1,4;-3}$	$6_{1,5;-4}$
$6_{5,1;4}$	$7_{6,1;5}$	55714	57930	60533	64605	68571	$6_{1,5;-4}$	$7_{1,6;-5}$
$7_{6,1;5}$	$8_{7,1;6}$	65625	67805	70356	73938	78750	$7_{1,6;-5}$	$8_{1,7;-6}$
$8_{7,1;6}$	$9_{8,1;7}$	75556	77710	80235	83593	88889	$8_{1,7;-6}$	$9_{1,8;-7}$
$9_{8,1;7}$	$10_{9,1;8}$	85500	87636	90142	93412	99000	$9_{1,8;-7}$	$10_{1,9;-8}$
$10_{9,1;8}$	$11_{10,1;9}$	95455	97576	100068	103301	109091	$10_{1,9;-8}$	$11_{1,10;-9}$
$11_{10,1;9}$	$12_{11,1;10}$	105416	107526	110008	113219	119166	$11_{1,10;-9}$	$12_{1,11;-10}$
$2_{0,2;-2}$	$3_{1,2;-1}$	20000	18636	17345	16724	16667	$2_{2,0;2}$	$3_{2,1;1}$
$3_{1,2;-1}$	$4_{2,2;0}$	18750	29055	30992	30230	30000	$3_{2,1;1}$	$4_{2,2;0}$
$4_{2,2;0}$	$5_{3,2;1}$	28000	34387	41441	42462	42000	$4_{2,2;0}$	$5_{2,3;-1}$
$5_{3,2;1}$	$6_{4,2;2}$	37500	41961	49227	53738	53333	$5_{2,3;-1}$	$6_{2,4;-2}$
$6_{4,2;2}$	$7_{5,2;3}$	47143	51182	56697	64087	64286	$6_{2,4;-2}$	$7_{2,5;-3}$
$7_{5,2;3}$	$8_{6,2;4}$	56875	60756	65450	73564	75000	$7_{2,5;-3}$	$8_{2,6;-4}$
$8_{6,2;4}$	$9_{7,2;5}$	66667	70451	74899	82413	85556	$8_{2,6;-4}$	$9_{2,7;-5}$
$9_{7,2;5}$	$10_{8,2;6}$	76500	80218	84567	91174	96000	$9_{2,7;-5}$	$10_{2,8;-6}$
$10_{8,2;6}$	$11_{9,2;7}$	86364	90031	94328	100297	106364	$10_{2,8;-6}$	$11_{2,9;-7}$
$11_{9,2;7}$	$12_{10,2;8}$	96250	99880	104134	109796	116666	$11_{2,9;-7}$	$12_{2,10;-8}$

TABLE VI.—*Continued.*

Sub-branch				κ			Sub-branch	
$^{c,e}R_{1,0}$	$^{c,e}P_{\bar{1},0}$	∓1	∓0.5	0	±0.5	±1	$^{a,e}R_{0,1}$	$^{a,e}P_{0,\bar{1}}$
$3_{0,3;-3}$	$4_{1,3;-2}$	25000	20331	18001	17567	17500	$3_{3,0;3}$	$4_{3,1;2}$
$4_{1,3;-2}$	$5_{2,3;-1}$	21000	34848	33475	32109	32000	$4_{3,1;2}$	$5_{3,2;1}$
$5_{2,3;-1}$	$6_{3,3;0}$	30000	41218	47032	45219	45000	$5_{3,2;1}$	$6_{3,3;0}$
$6_{3,3;0}$	$7_{4,3;1}$	39286	46575	57381	57683	57143	$6_{3,3;0}$	$7_{3,4;-1}$
$7_{4,3;1}$	$8_{5,3;2}$	48750	54876	64788	69691	68750	$7_{3,4;-1}$	$8_{3,5;-2}$
$8_{5,3;2}$	$9_{6,3;3}$	58333	64092	71834	80981	80000	$8_{3,5;-2}$	$9_{3,6;-3}$
$9_{6,3;3}$	$10_{7,3;4}$	68000	73557	80274	91312	91000	$9_{3,6;-3}$	$10_{3,7;-4}$
$10_{7,3;4}$	$11_{8,3;5}$	77727	83147	89526	100665	101818	$10_{3,7;-4}$	$11_{3,8;-5}$
$11_{8,3;5}$	$12_{9,3;6}$	87500	92819	90948	109320	112500	$11_{3,8;-5}$	$12_{3,9;-6}$
$4_{0,4;-4}$	$5_{1,4;-3}$	30000	20650	18478	18082	18000	$4_{4,0;4}$	$5_{4,1;3}$
$5_{1,4;-3}$	$6_{2,4;-2}$	23333	38686	34370	33475	33333	$5_{4,1;3}$	$6_{4,2;2}$
$6_{2,4;-2}$	$7_{3,4;-1}$	32143	48639	49439	47326	47143	$6_{4,2;2}$	$7_{4,3;1}$
$7_{3,4;-1}$	$8_{4,4;0}$	41250	52676	63082	60238	60000	$7_{4,3;1}$	$8_{4,4;0}$
$8_{4,4;0}$	$9_{5,4;1}$	50556	59229	73357	72645	72222	$8_{4,4;0}$	$9_{4,5;-1}$
$9_{5,4;1}$	$10_{6,4;2}$	60000	67888	80428	84877	84000	$9_{4,5;-1}$	$10_{4,6;-2}$
$10_{6,4;2}$	$11_{7,4;3}$	69546	77064	87093	96881	95455	$10_{4,6;-2}$	$11_{4,7;-3}$
$11_{7,4;3}$	$12_{8,4;4}$	79167	86444	95254	108226	106666	$11_{4,7;-3}$	$12_{4,8;-4}$
$5_{0,5;-5}$	$6_{1,5;-4}$	35000	20660	18847	18422	18333	$5_{5,0;5}$	$6_{5,1;4}$
$6_{1,5;-4}$	$7_{2,5;-3}$	25714	40254	35224	34447	34286	$6_{5,1;4}$	$7_{5,2;3}$
$7_{2,5;-3}$	$8_{3,5;-2}$	34375	54914	50352	48971	48750	$7_{5,2;3}$	$8_{5,3;2}$
$8_{3,5;-2}$	$9_{4,5;-1}$	43333	60334	65354	62490	62222	$8_{5,3;2}$	$9_{5,4;1}$
$9_{4,5;-1}$	$10_{5,5;0}$	52500	64543	79136	75309	75000	$9_{5,4;1}$	$10_{5,5;0}$
$10_{5,5;0}$	$11_{6,5;1}$	61818	72156	89354	87664	87273	$10_{5,5;0}$	$11_{5,6;-1}$
$11_{6,5;1}$	$12_{7,5;2}$	71250	80944	96120	99820	99167	$11_{5,6;-1}$	$12_{5,7;-2}$
$6_{0,6;-6}$	$7_{1,6;-5}$	40000	20793	19108	18664	18571	$6_{6,0;6}$	$7_{6,1;5}$
$7_{1,6;-5}$	$8_{2,6;-4}$	28125	40367	35988	35171	35000	$7_{6,1;5}$	$8_{6,2;4}$
$8_{2,6;-4}$	$9_{3,6;-3}$	36667	58807	51410	50241	50000	$8_{6,2;4}$	$9_{6,3;3}$
$9_{3,6;-3}$	$10_{4,6;-2}$	45500	68406	66193	64301	64000	$9_{6,3;3}$	$10_{6,4;2}$
$10_{4,6;-2}$	$11_{5,6;-1}$	54546	71334	81252	77627	77273	$10_{6,4;2}$	$11_{6,5;1}$
$11_{5,6;-1}$	$12_{6,6;0}$	63750	77023	95192	90399	90000	$11_{6,5;1}$	$12_{6,6;0}$
$7_{0,7;-7}$	$8_{1,7;-6}$	45000	20990	19300	18844	18750	$7_{7,0;7}$	$8_{7,1;6}$
$8_{1,7;-6}$	$9_{2,7;-5}$	30556	40255	36587	35733	35556	$8_{7,1;6}$	$9_{7,2;5}$
$9_{2,7;-5}$	$10_{3,7;-4}$	39000	60147	52457	51252	51000	$9_{7,2;5}$	$10_{7,3;4}$
$10_{3,7;-4}$	$11_{4,7;-3}$	47727	75043	67350	65775	65455	$10_{7,3;4}$	$11_{7,4;3}$
$11_{4,7;-3}$	$12_{5,7;-2}$	56667	79651	81971	79549	79167	$11_{7,4;3}$	$12_{7,5;2}$
$8_{0,8;-8}$	$9_{1,8;-7}$	50000	21170	19449	18985	18889	$8_{8,0;8}$	$9_{8,1;7}$
$9_{1,8;-7}$	$10_{2,8;-6}$	33000	40430	37059	36182	36000	$9_{8,1;7}$	$10_{8,2;6}$
$10_{2,8;-6}$	$11_{3,8;-5}$	41364	59963	53330	52078	51818	$10_{8,2;6}$	$11_{8,3;5}$
$11_{3,8;-5}$	$12_{4,8;-4}$	50000	78946	68596	66999	66667	$11_{8,3;5}$	$12_{8,4;4}$
$9_{0,9;-9}$	$10_{1,9;-8}$	55000	21315	19566	19097	19000	$9_{9,0;9}$	$10_{9,1;8}$
$10_{1,9;-8}$	$11_{2,9;-7}$	35454	40779	37443	36548	36364	$10_{9,1;8}$	$11_{9,2;7}$
$11_{2,9;-7}$	$12_{3,9;-6}$	43750	59640	54051	52766	52500	$11_{9,2;7}$	$12_{9,3;6}$
$10_{0,10;-10}$	$11_{1,10;-9}$	60000	21432	19662	19189	19091	$10_{10,0;10}$	$11_{10,1;9}$
$11_{1,10;-9}$	$12_{2,10;-8}$	37917	41138	37761	36854	36667	$11_{10,1;9}$	$12_{10,2;8}$
$11_{0,11;-11}$	$12_{1,11;-10}$	65000	21527	19742	19265	19167	$11_{11,0;11}$	$12_{11,1;10}$
$^{c,o}R_{1,0}$	$^{c,o}P_{\bar{1},0}$	∓1	∓0.5	0	±0.5	±1	$^{a,o}R_{0,1}$	$^{a,o}P_{0,\bar{1}}$
$1_{1,1;0}$	$2_{2,1;1}$	15000	15000	15000	15000	15000	$1_{1,1;0}$	$2_{1,2;-1}$
$2_{2,1;1}$	$3_{3,1;2}$	25000	25710	26243	26564	26667	$2_{1,2;-1}$	$3_{1,3;-2}$
$3_{3,1;2}$	$4_{4,1;3}$	35000	35758	36540	37210	37500	$3_{1,3;-2}$	$4_{1,4;-3}$
$4_{4,1;3}$	$5_{5,1;4}$	45000	45743	46583	47478	48000	$4_{1,4;-3}$	$5_{1,5;-4}$
$5_{5,1;4}$	$6_{6,1;5}$	55000	55730	56576	57578	58333	$5_{1,5;-4}$	$6_{1,6;-5}$
$6_{6,1;5}$	$7_{7,1;6}$	65000	65721	66561	67607	68571	$6_{1,6;-5}$	$7_{1,7;-6}$
$7_{7,1;6}$	$8_{8,1;7}$	75000	75714	76550	77609	78750	$7_{1,7;-6}$	$8_{1,8;-7}$
$8_{8,1;7}$	$9_{9,1;8}$	85000	85708	86539	87603	88889	$8_{1,8;-7}$	$9_{1,9;-8}$
$9_{9,1;8}$	$10_{10,1;9}$	95000	95704	96531	97595	99000	$9_{1,9;-8}$	$10_{1,10;-9}$
$10_{10,1;9}$	$11_{11,1;10}$	105000	105701	106525	107587	109091	$10_{1,10;-9}$	$11_{1,11;-10}$
$11_{11,1;10}$	$12_{12,1;11}$	115000	115698	116519	117580	119166	$11_{1,11;-10}$	$12_{1,12;-11}$

TABLE VI.—*Continued.*

Sub-branch $^{c,o}R_{1,0}$	Sub-branch $^{c,o}P_{\bar{1},0}$	κ ∓1	∓0.5	0	±0.5	±1	Sub-branch $^{a,o}R_{0,1}$	Sub-branch $^{a,o}P_{0,\bar{1}}$
$2_{1,2;-1}$	$3_{2,2;0}$	16667	16667	16667	16667	16667	$2_{2,1;1}$	$3_{2,2;0}$
$3_{2,2;0}$	$4_{3,2;1}$	26250	28258	29391	29882	30000	$3_{2,2;0}$	$4_{2,3;-1}$
$4_{3,2;1}$	$5_{4,2;2}$	36000	38290	40354	41637	42000	$4_{2,3;-1}$	$5_{2,4;-2}$
$5_{4,2;2}$	$6_{5,2;3}$	45833	48094	50537	52600	53333	$5_{2,4;-2}$	$6_{2,5;-3}$
$6_{5,2;3}$	$7_{6,2;4}$	55714	57929	60461	63088	64286	$6_{2,5;-3}$	$7_{2,6;-4}$
$7_{6,2;4}$	$8_{7,2;5}$	65625	67805	70340	73291	75000	$7_{2,6;-4}$	$8_{2,7;-5}$
$8_{7,2;5}$	$9_{8,2;6}$	75556	77710	80231	83338	85556	$8_{2,7;-5}$	$9_{2,8;-6}$
$9_{8,2;6}$	$10_{9,2;7}$	85500	87636	90142	93314	96000	$9_{2,8;-6}$	$10_{2,9;-7}$
$10_{9,2;7}$	$11_{10,2;8}$	95455	97576	100068	103262	106364	$10_{2,9;-7}$	$11_{2,10;-8}$
$11_{10,2;8}$	$12_{11,2;9}$	105416	107526	110008	113205	116666	$11_{2,10;-8}$	$12_{2,11;-9}$
$3_{1,3;-2}$	$4_{2,3;-1}$	18750	18207	17796	17564	17500	$3_{3,1;2}$	$4_{3,2;1}$
$4_{2,3;-1}$	$5_{3,3;0}$	28000	31148	32063	32074	32000	$4_{3,2;1}$	$5_{3,3;0}$
$5_{3,3;0}$	$6_{4,3;1}$	37500	41486	44187	45001	45000	$5_{3,3;0}$	$6_{3,4;-1}$
$6_{4,3;1}$	$7_{5,3;2}$	47143	51127	54949	56948	57143	$6_{3,4;-1}$	$7_{3,5;-2}$
$7_{5,3;2}$	$8_{6,3;3}$	56875	60749	64999	68208	68750	$7_{3,5;-2}$	$8_{3,6;-3}$
$8_{6,3;3}$	$9_{7,3;4}$	66667	70450	74791	78959	80000	$8_{3,6;-3}$	$9_{3,7;-4}$
$9_{7,3;4}$	$10_{8,3;5}$	76500	80217	84543	89339	91000	$9_{3,7;-4}$	$10_{3,8;-5}$
$10_{8,3;5}$	$11_{9,3;6}$	86364	90031	94320	99469	101818	$10_{3,8;-5}$	$11_{3,9;-6}$
$11_{9,3;6}$	$12_{10,3;7}$	96250	99880	104133	109453	112500	$11_{3,9;-6}$	$12_{3,10;-7}$
$4_{1,4;-3}$	$5_{2,4;-2}$	21000	19363	18449	18082	18000	$4_{4,1;3}$	$5_{4,2;2}$
$5_{2,4;-2}$	$6_{3,4;-1}$	30000	33887	33934	33473	33333	$5_{4,2;2}$	$6_{4,3;1}$
$6_{3,4;-1}$	$7_{4,4;0}$	39286	45000	47370	47311	47143	$6_{4,3;1}$	$7_{4,4;0}$
$7_{4,4;0}$	$8_{5,4;1}$	48750	54655	59178	60145	60000	$7_{4,4;0}$	$8_{4,5;-1}$
$8_{5,4;1}$	$9_{6,4;2}$	58333	64063	69788	72255	72222	$8_{4,5;-1}$	$9_{4,6;-2}$
$9_{6,4;2}$	$10_{7,4;3}$	68000	73554	79716	83787	84000	$9_{4,6;-2}$	$10_{4,7;-3}$
$10_{7,4;3}$	$11_{8,4;4}$	77727	83147	89384	94830	95455	$10_{4,7;-3}$	$11_{4,8;-4}$
$11_{8,4;4}$	$12_{9,4;5}$	87500	92819	99012	105459	106666	$11_{4,8;-4}$	$12_{4,9;-5}$
$5_{1,5;-4}$	$6_{2,5;-3}$	23333	20137	18843	18422	18333	$5_{5,1;4}$	$6_{5,2;3}$
$6_{2,5;-3}$	$7_{3,5;-2}$	32143	36189	35151	34447	34286	$6_{5,2;3}$	$7_{5,3;2}$
$7_{3,5;-2}$	$8_{4,5;-1}$	41250	48511	49684	48970	48750	$7_{5,3;2}$	$8_{5,4;1}$
$8_{4,5;-1}$	$9_{5,5;0}$	50556	58512	62686	62483	62222	$8_{5,4;1}$	$9_{5,5;0}$
$9_{5,5;0}$	$10_{6,5;1}$	60000	67785	74286	75273	75000	$9_{5,5;0}$	$10_{5,6;-1}$
$10_{6,5;1}$	$11_{7,5;2}$	69546	77050	84774	87504	87273	$10_{5,6;-1}$	$11_{5,7;-2}$
$11_{7,5;2}$	$12_{8,5;3}$	79167	86442	94594	99259	99167	$11_{5,7;-2}$	$12_{5,8;-3}$
$6_{1,6;-5}$	$7_{2,6;-4}$	25714	20629	19107	18664	18571	$6_{6,1;5}$	$7_{6,2;4}$
$7_{2,6;-4}$	$8_{3,6;-3}$	34375	37948	35978	35171	35000	$7_{6,2;4}$	$8_{6,3;3}$
$8_{3,6;-3}$	$9_{4,6;-2}$	43333	51721	51284	50241	50000	$8_{6,3;3}$	$9_{6,4;2}$
$9_{4,6;-2}$	$10_{5,6;-1}$	52500	62496	65297	64301	64000	$9_{6,4;2}$	$10_{6,5;1}$
$10_{5,6;-1}$	$11_{6,6;0}$	61818	71831	78026	77624	77273	$10_{6,5;1}$	$11_{6,6;0}$
$11_{6,6;0}$	$12_{7,6;1}$	71250	80896	89476	90385	90000	$11_{6,6;0}$	$12_{6,7;-1}$
$7_{1,7;-6}$	$8_{2,7;-5}$	28125	20944	19300	18844	18750	$7_{7,1;6}$	$8_{7,2;5}$
$8_{2,7;-5}$	$9_{3,7;-4}$	36667	39200	36585	35733	35556	$8_{7,2;5}$	$9_{7,3;4}$
$9_{3,7;-4}$	$10_{4,7;-3}$	45500	54420	52436	51252	51000	$9_{7,3;4}$	$10_{7,4;3}$
$10_{4,7;-3}$	$11_{5,7;-2}$	54546	66365	67167	65775	65455	$10_{7,4;3}$	$11_{7,5;2}$
$11_{5,7;-2}$	$12_{6,7;-1}$	63750	76087	80851	79549	79167	$11_{7,5;2}$	$12_{7,6;1}$
$8_{1,8;-7}$	$9_{2,8;-6}$	30556	21157	19449	18985	18889	$8_{8,1;7}$	$9_{8,2;6}$
$9_{2,8;-6}$	$10_{3,8;-5}$	39000	40063	37061	36182	36000	$9_{8,2;6}$	$10_{8,3;5}$
$10_{3,8;-5}$	$11_{4,8;-4}$	47727	56523	53327	52078	51818	$10_{8,3;5}$	$11_{8,4;4}$
$11_{4,8;-4}$	$12_{5,8;-3}$	56667	69870	68563	66999	66667	$11_{8,4;4}$	$12_{8,5;3}$
$9_{1,9;-8}$	$10_{2,9;-7}$	33000	21311	19566	19097	19000	$9_{9,1;8}$	$10_{9,2;7}$
$10_{2,9;-7}$	$11_{3,9;-6}$	41364	40664	37443	36548	36364	$10_{9,2;7}$	$11_{9,3;6}$
$11_{3,9;-6}$	$12_{4,9;-5}$	50000	58070	54050	52766	52500	$11_{9,3;6}$	$12_{9,4;5}$
$10_{1,10;-9}$	$11_{2,10;-8}$	35454	21431	19662	19189	19091	$10_{10,1;9}$	$11_{10,2;8}$
$11_{2,10;-8}$	$12_{3,10;-7}$	43750	41102	37761	36854	36667	$11_{10,2;8}$	$12_{10,3;7}$
$11_{1,11;-10}$	$12_{2,11;-9}$	37917	21526	19742	19265	19167	$11_{11,1;10}$	$12_{11,2;9}$

TABLE VI.—*Continued.*

B. *a* and *c* prolate-or-oblate sub-branches

Sub-branch				κ			Sub-branch	
$^{c,e}Q_{\bar{1},2}$	$^{c,o}Q_{1,\bar{2}}$	∓1	∓0.5	0	±0.5	±1	$^{a,e}Q_{2,\bar{1}}$	$^{a,o}Q_{\bar{2},1}$
$2_{2,0;2}$	$2_{1,2;-1}$	8333	5110	2233	488		$2_{0,2;-2}$	$2_{2,1;1}$
$3_{2,1;1}$	$3_{1,3;-2}$	14583	5722	1328	165		$3_{1,2;-1}$	$3_{3,1;2}$
$4_{2,2;0}$	$4_{1,4;-3}$	20250	4363	650	78		$4_{2,2;0}$	$4_{4,1;3}$
$5_{2,3;-1}$	$5_{1,5;-4}$	25667	2859	374	54		$5_{3,2;1}$	$5_{5,1;4}$
$6_{2,4;-2}$	$6_{1,6;-5}$	30952	1843	266	43		$6_{4,2;2}$	$6_{6,1;5}$
$7_{2,5;-3}$	$7_{1,7;-6}$	36161	1262	218	35		$7_{5,2;3}$	$7_{7,1;6}$
$8_{2,6;-4}$	$8_{1,8;-7}$	41319	945	183	30		$8_{6,2;4}$	$8_{8,1;7}$
$9_{2,7;-5}$	$9_{1,9;-8}$	46444	770	160	26		$9_{7,2;5}$	$9_{9,1;8}$
$10_{2,8;-6}$	$10_{1,10;-9}$	51545	664	141	23		$10_{8,2;6}$	$10_{10,1;9}$
$11_{2,9;-7}$	$11_{1,11;-10}$	56629	590	125	21		$11_{9,2;7}$	$11_{11,1;10}$
$12_{2,10;-8}$	$12_{1,12;-11}$	61699	533	115	19		$12_{10,2;8}$	$12_{12,1;11}$
$3_{3,0;3}$	$3_{2,2;0}$	8750	7055	4522	1458		$3_{0,3;-3}$	$3_{2,2;0}$
$4_{3,1;2}$	$4_{2,3;-1}$	15750	11214	4568	638		$4_{1,3;-2}$	$4_{3,2;1}$
$5_{3,2;1}$	$5_{2,4;-2}$	22000	12576	2754	274		$5_{2,3;-1}$	$5_{4,2;2}$
$6_{3,3;0}$	$6_{2,5;-3}$	27857	11283	1492	171		$6_{3,3;0}$	$6_{5,2;3}$
$7_{3,4;-1}$	$7_{2,6;-4}$	33482	8559	925	132		$7_{4,3;1}$	$7_{6,2;4}$
$8_{3,5;-2}$	$8_{2,7;-5}$	38958	5932	685	108		$8_{5,3;2}$	$8_{7,2;5}$
$9_{3,6;-3}$	$9_{2,8;-6}$	44333	4077	567	92		$9_{6,3;3}$	$9_{8,2;6}$
$10_{3,7;-4}$	$10_{2,9;-7}$	49636	2945	490	80		$10_{7,3;4}$	$10_{9,2;7}$
$11_{3,8;-5}$	$11_{2,10;-8}$	54886	2294	433	71		$11_{8,3;5}$	$11_{10,2;8}$
$12_{3,9;-6}$	$12_{2,11;-9}$	60096	1917	387	64		$12_{9,3;6}$	$12_{11,2;9}$
$4_{4,0;4}$	$4_{3,2;1}$	9000	7558	5617	2547		$4_{0,4;-4}$	$4_{2,3;-1}$
$5_{4,1;3}$	$5_{3,3;0}$	16500	13242	7983	1599		$5_{1,4;-3}$	$5_{3,3;0}$
$6_{4,2;2}$	$6_{3,4;-1}$	23214	17320	6820	681		$6_{2,4;-2}$	$6_{4,3;1}$
$7_{4,3;1}$	$7_{3,5;-2}$	29464	19464	4223	374		$7_{3,4;-1}$	$7_{5,3;2}$
$8_{4,4;0}$	$8_{3,6;-3}$	35417	19178	2433	273		$8_{4,4;0}$	$8_{6,3;3}$
$9_{4,5;-1}$	$9_{3,7;-4}$	41167	16526	1579	222		$9_{5,4;1}$	$9_{7,3;4}$
$10_{4,6;-2}$	$10_{3,8;-5}$	46773	12665	1205	188		$10_{6,4;2}$	$10_{8,3;5}$
$11_{4,7;-3}$	$11_{3,9;-6}$	52273	9080	1014	163		$11_{7,4;3}$	$11_{9,3;6}$
$12_{4,8;-4}$	$12_{3,10;-7}$	57692	6485	888	144		$12_{8,4;4}$	$12_{10,3;7}$
$5_{5,0;5}$	$5_{4,2;2}$	9167	7775	6052	3368		$5_{0,5;-5}$	$5_{2,4;-2}$
$6_{5,1;4}$	$6_{4,3;1}$	17024	14062	9982	3054		$6_{1,5;-4}$	$6_{3,4;-1}$
$7_{5,2;3}$	$7_{4,4;0}$	24107	19225	11103	1459		$7_{2,5;-3}$	$7_{4,4;0}$
$8_{5,3;2}$	$8_{4,5;-1}$	30694	23287	9000	720		$8_{3,5;-2}$	$8_{5,4;1}$
$9_{5,4;1}$	$9_{4,6;-2}$	36944	26001	5708	481		$9_{4,5;-1}$	$9_{6,4;2}$
$10_{5,5;0}$	$10_{4,7;-3}$	42955	26852	3433	382		$10_{5,5;0}$	$10_{7,4;3}$
$11_{5,6;-1}$	$11_{4,8;-4}$	48788	25327	2306	321		$11_{6,5;1}$	$11_{8,4;4}$
$12_{5,7;-2}$	$12_{4,9;-5}$	54487	21546	1796	277		$12_{7,5;2}$	$12_{9,4;5}$
$6_{6,0;6}$	$6_{5,2;3}$	9286	7912	6257	3863		$6_{0,6;-6}$	$6_{2,5;-3}$
$7_{6,1;5}$	$7_{5,3;2}$	17411	14550	10952	4657		$7_{1,6;-5}$	$7_{3,5;-2}$
$8_{6,2;4}$	$8_{5,4;1}$	24792	20233	13841	2772		$8_{2,6;-4}$	$8_{4,5;-1}$
$9_{6,3;3}$	$9_{5,5;0}$	31667	25098	14023	1322		$9_{3,6;-3}$	$9_{5,5;0}$
$10_{6,4;2}$	$10_{5,6;-1}$	38182	29140	11121	785		$10_{4,6;-2}$	$10_{6,5;1}$
$11_{6,5;1}$	$11_{5,7;-2}$	44432	32202	7197	595		$11_{5,6;-1}$	$11_{7,5;2}$
$12_{6,6;0}$	$12_{5,8;-3}$	50481	33921	4472	494		$12_{6,6;0}$	$12_{8,5;3}$
$7_{7,0;7}$	$7_{6,2;4}$	9375	8011	6381	4141		$7_{0,7;-7}$	$7_{2,6;-4}$
$8_{7,1;6}$	$8_{6,3;3}$	17708	14899	11480	5982		$8_{1,7;-6}$	$8_{3,6;-3}$
$9_{7,2;5}$	$9_{6,4;2}$	25333	20930	15306	4603		$9_{2,7;-5}$	$9_{4,6;-2}$
$10_{7,3;4}$	$10_{6,5;1}$	32455	26247	17406	2348		$10_{3,7;-4}$	$10_{5,6;-1}$
$11_{7,4;3}$	$11_{6,6;0}$	39205	30913	16805	1258		$11_{4,7;-3}$	$11_{6,6;0}$
$12_{7,5;2}$	$12_{6,7;-1}$	45673	34922	13192	878		$12_{5,7;-2}$	$12_{7,6;1}$
$8_{8,0;8}$	$8_{7,2;5}$	9444	8087	6468	4302		$8_{0,8;-8}$	$8_{2,7;-5}$
$9_{8,1;7}$	$9_{7,3;4}$	17944	15167	11825	6888		$9_{1,8;-7}$	$9_{3,7;-4}$
$10_{8,2;6}$	$10_{7,4;3}$	25773	21462	16158	6602		$10_{2,8;-6}$	$10_{4,7;-3}$
$11_{8,3;5}$	$11_{7,5;2}$	33106	27105	19325	3955		$11_{3,8;-5}$	$11_{5,7;-2}$
$12_{8,4;4}$	$12_{7,6;1}$	40064	32170	20771	2027		$12_{4,8;-4}$	$12_{6,7;-1}$
$9_{9,0;9}$	$9_{8,2;6}$	9500	8146	6535	4403		$9_{0,9;-9}$	$9_{2,8;-6}$
$10_{9,1;8}$	$10_{8,3;5}$	18136	15380	12079	7464		$10_{1,9;-8}$	$10_{3,8;-5}$
$11_{9,2;7}$	$11_{8,4;4}$	26136	21887	16736	8319		$11_{2,9;-7}$	$11_{4,8;-4}$
$12_{9,3;6}$	$12_{8,5;3}$	33654	27788	20487	6108		$12_{3,9;-6}$	$12_{5,8;-3}$

TABLE VI.—*Continued.*

Sub-branch				κ			Sub-branch	
$^{c,e}Q_{\bar{1},2}$	$^{c,o}Q_{1,\bar{2}}$	∓ 1	∓ 0.5	0	± 0.5	± 1	$^{a,e}Q_{2,\bar{1}}$	$^{a,o}Q_{\bar{2},1}$
$10_{10,0;10}$	$10_{9,2;7}$	9545	8194	6588	4474		$10_{0,10;-10}$	$10_{2,9;-7}$
$11_{10,1;9}$	$11_{9,3;6}$	18295	15554	12279	7835		$11_{1,10;-9}$	$11_{3,9;-6}$
$12_{10,2;8}$	$12_{9,4;5}$	26442	22237	17173	9567		$12_{2,10;-8}$	$12_{4,9;-5}$
$11_{11,0;11}$	$11_{10,2;8}$	9583	8234	6631	4528		$11_{0,11;-11}$	$11_{2,10;-8}$
$12_{11,1;10}$	$12_{10,3;7}$	18429	15699	12443	8090		$12_{1,11;-10}$	$12_{3,10;-7}$
$12_{12,0;12}$	$12_{11,2;9}$	9615	8268	6667	4571		$12_{0,12;-12}$	$12_{2,11;-9}$
$^{c,e}R_{\bar{1},2}$	$^{c,e}P_{1,\bar{2}}$	∓ 1	∓ 0.5	0	± 0.5	± 1	$^{a,e}R_{2,\bar{1}}$	$^{a,e}P_{\bar{2},1}$
$1_{1,0;1}$	$2_{0,2;-2}$	5000	3066	1340	293		$1_{0,1;-1}$	$2_{2,0;2}$
$2_{1,1;0}$	$3_{0,3;-3}$	10000	4167	1086	157		$2_{1,1;0}$	$3_{3,0;3}$
$3_{1,2;-1}$	$4_{0,4;-4}$	15000	3944	800	123		$3_{2,1;1}$	$4_{4,0;4}$
$4_{1,3;-2}$	$5_{0,5;-5}$	20000	3386	696	117		$4_{3,1;2}$	$5_{5,0;5}$
$5_{1,4;-3}$	$6_{0,6;-6}$	25000	2976	667	114		$5_{4,1;3}$	$6_{6,0;6}$
$6_{1,5;-4}$	$7_{0,7;-7}$	30000	2770	656	112		$6_{5,1;4}$	$7_{7,0;7}$
$7_{1,6;-5}$	$8_{0,8;-8}$	35000	2686	649	111		$7_{6,1;5}$	$8_{8,0;8}$
$8_{1,7;-6}$	$9_{0,9;-9}$	40000	2652	644	110		$8_{7,1;6}$	$9_{9,0;9}$
$9_{1,8;-7}$	$10_{0,10;-10}$	45000	2634	640	109		$9_{8,1;7}$	$10_{10,0;10}$
$10_{1,9;-8}$	$11_{0,11;-11}$	50000	2621	637	109		$10_{9,1;8}$	$11_{11,0;11}$
$11_{1,10;-9}$	$12_{0,12;-12}$	55000	2610	634	108		$11_{10,1;9}$	$12_{12,0;12}$
$2_{2,0;2}$	$3_{1,2;-1}$	1667	2062	1905	776		$2_{0,2;-2}$	$3_{2,1;1}$
$3_{2,1;1}$	$4_{1,3;-2}$	3750	5114	2884	480		$3_{1,2;-1}$	$4_{3,1;2}$
$4_{2,2;0}$	$5_{1,4;-3}$	6000	7788	2336	310		$4_{2,2;0}$	$5_{4,1;3}$
$5_{2,3;-1}$	$6_{1,5;-4}$	8333	8748	1768	268		$5_{3,2;1}$	$6_{5,1;4}$
$6_{2,4;-2}$	$7_{1,6;-5}$	10714	8172	1529	254		$6_{4,2;2}$	$7_{6,1;5}$
$7_{2,5;-3}$	$8_{1,7;-6}$	13125	7135	1445	246		$7_{5,2;3}$	$8_{7,1;6}$
$8_{2,6;-4}$	$9_{1,8;-7}$	15556	6332	1406	240		$8_{6,2;4}$	$9_{8,1;7}$
$9_{2,7;-5}$	$10_{1,9;-8}$	18000	5885	1380	235		$9_{7,2;5}$	$10_{9,1;8}$
$10_{2,8;-6}$	$11_{1,10;-9}$	20455	5673	1360	232		$10_{8,2;6}$	$11_{10,1;9}$
$11_{2,9;-7}$	$12_{1,11;-10}$	22917	5570	1344	229		$11_{9,2;7}$	$12_{11,1;10}$
$3_{3,0;3}$	$4_{2,2;0}$	1250	1176	1316	1061		$3_{0,3;-3}$	$4_{2,2;0}$
$4_{3,1;2}$	$5_{2,3;-1}$	3000	3166	3516	1032		$4_{1,3;-2}$	$5_{3,2;1}$
$5_{3,2;1}$	$6_{2,4;-2}$	5000	6089	4448	613		$5_{2,3;-1}$	$6_{4,2;2}$
$6_{3,3;0}$	$7_{2,5;-3}$	7143	9630	3653	469		$6_{3,3;0}$	$7_{5,2;3}$
$7_{3,4;-1}$	$8_{2,6;-4}$	9375	12493	2828	426		$7_{4,3;1}$	$8_{6,2;4}$
$8_{3,5;-2}$	$9_{2,7;-5}$	11667	13383	2447	404		$8_{5,3;2}$	$9_{7,2;5}$
$9_{3,6;-3}$	$10_{2,8;-6}$	14000	12500	2301	389		$9_{6,3;3}$	$10_{8,2;6}$
$10_{3,7;-4}$	$11_{2,9;-7}$	16364	11048	2226	378		$10_{7,3;4}$	$11_{9,2;7}$
$11_{3,8;-5}$	$12_{2,10;-8}$	18750	9884	2174	370		$11_{8,3;5}$	$12_{10,2;8}$
$4_{4,0;4}$	$5_{3,2;1}$	1000	882	849	963		$4_{0,4;-4}$	$5_{2,3;-1}$
$5_{4,1;3}$	$6_{3,3;0}$	2500	2272	2651	1677		$5_{1,4;-3}$	$6_{3,3;0}$
$6_{4,2;2}$	$7_{3,4;-1}$	4286	4145	5108	1110		$6_{2,4;-2}$	$7_{4,3;1}$
$7_{4,3;1}$	$8_{3,5;-2}$	6250	6720	6025	747		$7_{3,4;-1}$	$8_{5,3;2}$
$8_{4,4;0}$	$9_{3,6;-3}$	8333	10196	5011	636		$8_{4,4;0}$	$9_{6,3;3}$
$9_{4,5;-1}$	$10_{3,7;-4}$	10500	14160	3947	590		$9_{5,4;1}$	$10_{7,3;4}$
$10_{4,6;-2}$	$11_{3,8;-5}$	12727	17215	3427	561		$10_{6,4;2}$	$11_{8,3;5}$
$11_{4,7;-3}$	$12_{3,9;-6}$	15000	18047	3214	540		$11_{7,4;3}$	$12_{9,3;6}$
$5_{5,0;5}$	$6_{4,2;2}$	833	730	638	723		$5_{0,5;-5}$	$6_{2,4;-2}$
$6_{5,1;4}$	$7_{4,3;1}$	2143	1898	1863	2013		$6_{1,5;-4}$	$7_{3,4;-1}$
$7_{5,2;3}$	$8_{4,4;0}$	3750	3384	4016	1833		$7_{2,5;-3}$	$8_{4,4;0}$
$8_{5,3;2}$	$9_{4,5;-1}$	5556	5182	6701	1165		$8_{3,5;-2}$	$9_{5,4;1}$
$9_{5,4;1}$	$10_{4,6;-2}$	7500	7437	7610	901		$9_{4,5;-1}$	$10_{6,4;2}$
$10_{5,5;0}$	$11_{4,7;-3}$	9545	10443	6398	809		$10_{5,5;0}$	$11_{7,4;3}$
$11_{5,6;-1}$	$12_{4,8;-4}$	11667	14380	5109	758		$11_{6,5;1}$	$12_{8,4;4}$
$6_{6,0;6}$	$7_{5,2;3}$	714	625	533	530		$6_{0,6;-6}$	$7_{2,5;-3}$
$7_{6,1;5}$	$8_{5,3;2}$	1875	1652	1470	1860		$7_{1,6;-5}$	$8_{3,5;-2}$
$8_{6,2;4}$	$9_{5,4;1}$	3333	2968	2958	2593		$8_{2,6;-4}$	$9_{4,5;-1}$
$9_{6,3;3}$	$10_{5,5;0}$	5000	4516	5406	1801		$9_{3,6;-3}$	$10_{5,5;0}$
$10_{6,4;2}$	$11_{5,6;-1}$	6818	6288	8298	1256		$10_{4,6;-2}$	$11_{6,5;1}$
$11_{6,5;1}$	$12_{5,7;-2}$	8750	8348	9203	1069		$11_{5,6;-1}$	$12_{7,5;2}$

TABLE VI.—*Continued.*

Sub-branch				κ			Sub-branch	
${}^{c,e}R_{\bar{1},2}$	${}^{c,e}P_{1,\bar{2}}$	∓ 1	∓ 0.5	0	± 0.5	± 1	${}^{a,e}R_{2,\bar{1}}$	${}^{a,e}P_{\bar{2},1}$
$7_{7,0;7}$	$8_{6,2;4}$	625	546	463	411		$7_{0,7;-7}$	$8_{2,6;-4}$
$8_{7,1;6}$	$9_{6,3;3}$	1667	1465	1267	1486		$8_{1,7;-6}$	$9_{3,6;-3}$
$9_{7,2;5}$	$10_{6,4;2}$	3000	2656	2402	2962		$9_{2,7;-5}$	$10_{4,6;-2}$
$10_{7,3;4}$	$11_{6,5;1}$	4545	4065	4106	2664		$10_{3,7;-4}$	$11_{5,6;-1}$
$11_{7,4;3}$	$12_{6,6;0}$	6250	5659	6816	1772		$11_{4,7;-3}$	$12_{6,6;0}$
$8_{8,0;8}$	$9_{7,2;5}$	556	485	411	341		$8_{0,8;-8}$	$9_{2,7;-5}$
$9_{8,1;7}$	$10_{7,3;4}$	1500	1316	1129	1154		$9_{1,8;-7}$	$10_{3,7;-4}$
$10_{8,2;6}$	$11_{7,4;3}$	2727	2407	2110	2759		$10_{2,8;-6}$	$11_{4,7;-3}$
$11_{8,3;5}$	$12_{7,5;2}$	4167	3705	3398	3519		$11_{3,8;-5}$	$12_{5,7;-2}$
$9_{9,0;9}$	$10_{8,2;6}$	500	436	369	298		$9_{0,9;-9}$	$10_{2,8;-6}$
$10_{9,1;8}$	$11_{8,3;5}$	1364	1195	1021	932		$10_{1,9;-8}$	$11_{3,8;-5}$
$11_{9,2;7}$	$12_{8,4;4}$	2500	2201	1910	2276		$11_{2,9;-7}$	$12_{4,8;-4}$
$10_{10,0;10}$	$11_{9,2;7}$	455	397	335	268		$10_{0,10;-10}$	$11_{2,9;-7}$
$11_{10,1;9}$	$12_{9,3;6}$	1250	1094	933	797		$11_{1,10;-9}$	$12_{3,9;-6}$
$11_{11,0;11}$	$12_{10,2;8}$	417	363	307	244		$11_{0,11;-11}$	$12_{2,10;-8}$
${}^{c,o}R_{\bar{1},2}$	${}^{c,o}P_{1,\bar{2}}$	∓ 1	∓ 0.5	0	± 0.5	± 1	${}^{a,o}R_{2,\bar{1}}$	${}^{a,o}P_{\bar{2},1}$
$2_{2,1;1}$	$3_{1,3;-2}$	1667	956	423	103		$2_{1,2;-1}$	$3_{3,1;2}$
$3_{2,2;0}$	$4_{1,4;-3}$	3750	1742	609	118		$3_{2,2;0}$	$4_{4,1;3}$
$4_{2,3;-1}$	$5_{1,5;-4}$	6000	2228	657	116		$4_{3,2;1}$	$5_{5,1;4}$
$5_{2,4;-2}$	$6_{1,6;-5}$	8333	2480	661	114		$5_{4,2;2}$	$6_{6,1;5}$
$6_{2,5;-3}$	$7_{1,7;-6}$	10714	2590	655	112		$6_{5,2;3}$	$7_{7,1;6}$
$7_{2,6;-4}$	$8_{1,8;-7}$	13125	2627	649	111		$7_{6,2;4}$	$8_{8,1;7}$
$8_{2,7;-5}$	$9_{1,9;-8}$	15556	2633	644	110		$8_{7,2;5}$	$9_{9,1;8}$
$9_{2,8;-6}$	$10_{1,10;-9}$	18000	2627	640	109		$9_{8,2;6}$	$10_{10,1;9}$
$10_{2,9;-7}$	$11_{1,11;-10}$	20455	2619	637	109		$10_{9,2;7}$	$11_{11,1;10}$
$11_{2,10;-8}$	$12_{1,12;-11}$	22917	2610	634	108		$11_{10,2;8}$	$12_{12,1;11}$
$3_{3,1;2}$	$4_{2,3;-1}$	1250	1025	643	213		$3_{1,3;-2}$	$4_{3,2;1}$
$4_{3,2;1}$	$5_{2,4;-2}$	3000	2317	1159	269		$4_{2,3;-1}$	$5_{4,2;2}$
$5_{3,3;0}$	$6_{2,5;-3}$	5000	3522	1389	265		$5_{3,3;0}$	$6_{5,2;3}$
$6_{3,4;-1}$	$7_{2,6;-4}$	7143	4450	1442	254		$6_{4,3;1}$	$7_{6,2;4}$
$7_{3,5;-2}$	$8_{2,7;-5}$	9375	5049	1429	246		$7_{5,3;2}$	$8_{7,2;5}$
$8_{3,6;-3}$	$9_{2,8;-6}$	11667	5372	1403	240		$8_{6,3;3}$	$9_{8,2;6}$
$9_{3,7;-4}$	$10_{2,9;-7}$	14000	5507	1379	235		$9_{7,3;4}$	$10_{9,2;7}$
$10_{3,8;-5}$	$11_{2,10;-8}$	16364	5539	1360	232		$10_{8,3;5}$	$11_{10,2;8}$
$11_{3,9;-6}$	$12_{2,11;-9}$	18750	5523	1344	229		$11_{9,3;6}$	$12_{11,2;9}$
$4_{4,1;3}$	$5_{3,3;0}$	1000	869	664	300		$4_{1,4;-3}$	$5_{3,3;0}$
$5_{4,2;2}$	$6_{3,4;-1}$	2500	2168	1455	440		$5_{2,4;-2}$	$6_{4,3;1}$
$6_{4,3;1}$	$7_{3,5;-2}$	4286	3662	2018	447		$6_{3,4;-1}$	$7_{5,3;2}$
$7_{4,4;0}$	$8_{3,6;-3}$	6250	5157	2266	424		$7_{4,4;0}$	$8_{6,3;3}$
$8_{4,5;-1}$	$9_{3,7;-4}$	8333	6471	2309	404		$8_{5,4;1}$	$9_{7,3;4}$
$9_{4,6;-2}$	$10_{3,8;-5}$	10500	7475	2272	389		$9_{6,4;2}$	$10_{8,3;5}$
$10_{4,7;-3}$	$11_{3,9;-6}$	12727	8130	2220	378		$10_{7,4;3}$	$11_{9,3;6}$
$11_{4,8;-4}$	$12_{3,10;-7}$	15000	8481	2173	370		$11_{8,4;4}$	$12_{10,3;7}$
$5_{5,1;4}$	$6_{4,3;1}$	833	729	601	346		$5_{1,5;-4}$	$6_{3,4;-1}$
$6_{5,2;3}$	$7_{4,4;0}$	2143	1889	1489	603		$6_{2,5;-3}$	$7_{4,4;0}$
$7_{5,3;2}$	$8_{4,5;-1}$	3750	3329	2360	656		$7_{3,5;-2}$	$8_{5,4;1}$
$8_{5,4;1}$	$9_{4,6;-2}$	5556	4947	2953	626		$8_{4,5;-1}$	$9_{6,4;2}$
$9_{5,5;0}$	$10_{4,7;-3}$	7500	6629	3209	589		$9_{5,5;0}$	$10_{7,4;3}$
$10_{5,6;-1}$	$11_{4,8;-4}$	9545	8239	3235	561		$10_{6,5;1}$	$11_{8,4;4}$
$11_{5,7;-2}$	$12_{4,9;-5}$	11667	9627	3171	540		$11_{7,5;2}$	$12_{9,4;5}$
$6_{6,1;5}$	$7_{5,3;2}$	714	625	527	357		$6_{1,6;-5}$	$7_{3,5;-2}$
$7_{6,2;4}$	$8_{5,4;1}$	1875	1651	1386	726		$7_{2,6;-4}$	$8_{4,5;-1}$
$8_{6,3;3}$	$9_{5,5;0}$	3333	2962	2400	873		$8_{3,6;-3}$	$9_{5,5;0}$
$9_{6,4;2}$	$10_{5,6;-1}$	5000	4489	3326	858		$9_{4,6;-2}$	$10_{6,5;1}$
$10_{6,5;1}$	$11_{5,7;-2}$	6818	6181	3940	804		$10_{5,6;-1}$	$11_{7,5;2}$
$11_{6,6;0}$	$12_{5,8;-3}$	8750	7975	4195	758		$11_{6,6;0}$	$12_{8,5;3}$

TABLE VI.—*Continued.*

Sub-branch $^{c,o}R_{\bar{1},2}$	$^{c,o}P_{1,\bar{2}}$	∓ 1	∓ 0.5	κ 0	± 0.5	± 1	Sub-branch $^{a,o}R_{2,\bar{1}}$	$^{a,o}P_{\bar{2},1}$
$7_{7,1;6}$	$8_{6,3;3}$	625	546	462	341		$7_{1,7;-6}$	$8_{3,6;-3}$
$8_{7,2;5}$	$9_{6,4;2}$	1667	1465	1251	793		$8_{2,7;-5}$	$9_{4,6;-2}$
$9_{7,3;4}$	$10_{6,5;1}$	3000	2656	2267	1069		$9_{3,7;-4}$	$10_{5,6;-1}$
$10_{7,4;3}$	$11_{6,6;0}$	4545	4062	3368	1110		$10_{4,7;-3}$	$11_{6,6;0}$
$11_{7,5;2}$	$12_{6,7;-1}$	6250	5646	4336	1050		$11_{5,7;-2}$	$12_{7,6;1}$
$8_{8,1;7}$	$9_{7,3;4}$	556	485	411	317		$8_{1,8;-7}$	$9_{3,7;-4}$
$9_{8,2;6}$	$10_{7,4;3}$	1500	1316	1126	808		$9_{2,8;-6}$	$10_{4,7;-3}$
$10_{8,3;5}$	$11_{7,5;2}$	2727	2407	2082	1216		$10_{3,8;-5}$	$11_{5,7;-2}$
$11_{8,4;4}$	$12_{7,6;1}$	4167	3704	3209	1361		$11_{4,8;-4}$	$12_{6,7;-1}$
$9_{9,1;8}$	$10_{8,3;5}$	500	436	369	290		$9_{1,9;-8}$	$10_{3,8;-5}$
$10_{9,2;7}$	$11_{8,4;4}$	1364	1195	1021	786		$10_{2,9;-7}$	$11_{4,8;-4}$
$11_{9,3;6}$	$12_{8,5;3}$	2500	2201	1904	1296		$11_{3,9;-6}$	$12_{5,8;-3}$
$10_{10,1;9}$	$11_{9,3;6}$	455	397	335	265		$10_{1,10;-9}$	$11_{3,9;-6}$
$11_{10,2;8}$	$12_{9,4;5}$	1250	1094	931	741		$11_{2,10;-8}$	$12_{4,9;-5}$
$11_{11,1;10}$	$12_{10,3;7}$	417	363	307	243		$11_{1,11;-10}$	$12_{3,10;-7}$

C. *b* prolate-and-oblate sub-branches

$^{b,e}Q_{\bar{1},1}$	$^{b,e}Q_{1,\bar{1}}$	∓ 1	∓ 0.5	0	± 0.5	± 1	$^{b,e}Q_{1,\bar{1}}$	$^{b,e}Q_{\bar{1},1}$
$1_{1,0;1}$	$1_{0,1;-1}$	15000	15000	15000	15000	15000	$1_{0,1;-1}$	$1_{1,0;1}$
$2_{1,1;0}$	$2_{0,2;-2}$	25000	21289	16667	12044	8333	$2_{1,1;0}$	$2_{2,0;2}$
$3_{1,2;-1}$	$3_{0,3;-3}$	35000	23196	14583	10583	8750	$3_{2,1;1}$	$3_{3,0;3}$
$4_{1,3;-2}$	$4_{0,4;-4}$	45000	22157	13527	10617	9000	$4_{3,1;2}$	$4_{4,0;4}$
$5_{1,4;-3}$	$5_{0,5;-5}$	55000	20634	13413	10753	9167	$5_{4,1;3}$	$5_{5,0;5}$
$6_{1,5;-4}$	$6_{0,6;-6}$	65000	19779	13484	10861	9286	$6_{5,1;4}$	$6_{6,0;6}$
$7_{1,6;-5}$	$7_{0,7;-7}$	75000	19511	13559	10943	9375	$7_{6,1;5}$	$7_{7,0;7}$
$8_{1,7;-6}$	$8_{0,8;-8}$	85000	19487	13620	11008	9444	$8_{7,1;6}$	$8_{8,0;8}$
$9_{1,8;-7}$	$9_{0,9;-9}$	95000	19524	13669	11060	9500	$9_{8,1;7}$	$9_{9,0;9}$
$10_{1,9;-8}$	$10_{0,10;-10}$	105000	19565	13710	11103	9545	$10_{9,1;8}$	$10_{10,0;10}$
$11_{1,10;-9}$	$11_{0,11;-11}$	115000	19604	13744	11139	9583	$11_{10,1;9}$	$11_{11,0;11}$
$12_{1,11;-10}$	$12_{0,12;-12}$	125000	19633	13774	11170	9615	$12_{11,1;10}$	$12_{12,0;12}$
$2_{2,0;2}$	$2_{1,1;0}$	8333	12044	16667	21289	25000	$2_{0,2;-2}$	$2_{1,1;0}$
$3_{2,1;1}$	$3_{1,2;-1}$	14583	24417	28872	24417	14583	$3_{1,2;-1}$	$3_{2,1;1}$
$4_{2,2;0}$	$4_{1,3;-2}$	20250	36119	31154	20622	15750	$4_{2,2;0}$	$4_{3,1;2}$
$5_{2,3;-1}$	$5_{1,4;-3}$	25667	43650	28164	20038	16500	$5_{3,2;1}$	$5_{4,1;3}$
$6_{2,4;-2}$	$6_{1,5;-4}$	30952	45529	26402	20356	17024	$6_{4,2;2}$	$6_{5,1;4}$
$7_{2,5;-3}$	$7_{1,6;-5}$	36161	43602	26163	20670	17411	$7_{5,2;3}$	$7_{6,1;5}$
$8_{2,6;-4}$	$8_{1,7;-6}$	41319	41002	26300	20926	17708	$8_{6,2;4}$	$8_{7,1;6}$
$9_{2,7;-5}$	$9_{1,8;-7}$	46444	39408	26465	21134	17944	$9_{7,2;5}$	$9_{8,1;7}$
$10_{2,8;-6}$	$10_{1,9;-8}$	51545	38815	26611	21307	18136	$10_{8,2;6}$	$10_{9,1;8}$
$11_{2,9;-7}$	$11_{1,10;-9}$	56629	38701	26737	21452	18295	$11_{9,2;7}$	$11_{10,1;9}$
$12_{2,10;-8}$	$12_{1,11;-10}$	61699	38736	26846	21576	18429	$12_{10,2;8}$	$12_{11,1;10}$
$3_{3,0;3}$	$3_{2,1;1}$	8750	10583	14583	23196	35000	$3_{0,3;-3}$	$3_{1,2;-1}$
$4_{3,1;2}$	$4_{2,2;0}$	15750	20622	31154	36119	20250	$4_{1,3;-2}$	$4_{2,2;0}$
$5_{3,2;1}$	$5_{2,3;-1}$	22000	32340	44017	32340	22000	$5_{2,3;-1}$	$5_{3,2;1}$
$6_{3,3;0}$	$6_{2,4;-2}$	27857	45986	45920	29422	23214	$6_{3,3;0}$	$6_{4,2;2}$
$7_{3,4;-1}$	$7_{2,5;-3}$	33482	58783	41862	29481	24107	$7_{4,3;1}$	$7_{5,2;3}$
$8_{3,5;-2}$	$8_{2,6;-4}$	38953	66715	39333	29932	24792	$8_{5,3;2}$	$8_{6,2;4}$
$9_{3,6;-3}$	$9_{2,7;-5}$	44333	68174	38859	30348	25333	$9_{6,3;3}$	$9_{7,2;5}$
$10_{3,7;-4}$	$10_{2,8;-6}$	49636	65282	38980	30705	25773	$10_{7,3;4}$	$10_{8,2;6}$
$11_{3,8;-5}$	$11_{2,9;-7}$	54886	61636	39182	31011	26136	$11_{8,3;5}$	$11_{9,2;7}$
$12_{3,9;-6}$	$12_{2,10;-8}$	60096	59285	39377	31275	26442	$12_{9,3;6}$	$12_{10,2;8}$
$4_{4,0;4}$	$4_{3,1;2}$	9000	10617	13527	22157	45000	$4_{0,4;-4}$	$4_{1,3;-2}$
$5_{4,1;3}$	$5_{3,2;1}$	16500	20038	28164	43650	25667	$5_{1,4;-3}$	$5_{2,3;-1}$
$6_{4,2;2}$	$6_{3,3;0}$	23214	29422	45920	45986	27857	$6_{2,4;-2}$	$6_{3,3;0}$
$7_{4,3;1}$	$7_{3,4;-1}$	29464	39987	59402	39987	29464	$7_{3,4;-1}$	$7_{4,3;1}$
$8_{4,4;0}$	$8_{3,5;-2}$	35417	52950	60829	38601	30694	$8_{4,4;0}$	$8_{5,3;2}$
$9_{4,5;-1}$	$9_{3,6;-3}$	41167	67954	55712	38960	31667	$9_{5,4;1}$	$9_{6,3;3}$
$10_{4,6;-2}$	$10_{3,7;-4}$	46773	81732	52398	39466	32455	$10_{6,4;2}$	$10_{7,3;4}$
$11_{4,7;-3}$	$11_{3,8;-5}$	52273	89952	51626	39938	33106	$11_{7,4;3}$	$11_{8,3;5}$
$12_{4,8;-4}$	$12_{3,9;-6}$	57692	90961	51673	40360	33654	$12_{8,4;4}$	$12_{9,3;6}$

TABLE VI.—*Continued.*

Sub-branch $^{b,e}Q_{\bar{1},1}$	Sub-branch $^{b,e}Q_{1,\bar{1}}$	κ ∓ 1	∓ 0.5	0	± 0.5	± 1	Sub-branch $^{b,e}Q_{1,\bar{1}}$	Sub-branch $^{b,e}Q_{\bar{1},1}$
$5_{5,0;5}$	$5_{4,1;3}$	9167	10753	13413	20634	55000	$5_{0,5;-5}$	$5_{1,4;-3}$
$6_{5,1;4}$	$6_{4,2;2}$	17024	20356	26402	45529	30952	$6_{1,5;-4}$	$6_{2,4;-2}$
$7_{5,2;3}$	$7_{4,3;1}$	24107	29481	41862	58783	33482	$7_{2,5;-3}$	$7_{3,4;-1}$
$8_{5,3;2}$	$8_{4,4;0}$	30694	38601	60829	52950	35417	$8_{3,5;-2}$	$8_{4,4;0}$
$9_{5,4;1}$	$9_{4,5;-1}$	36944	48332	74882	48332	36944	$9_{4,5;-1}$	$9_{5,4;1}$
$10_{5,5;0}$	$10_{4,6;-2}$	42955	59745	75829	47998	38182	$10_{5,5;0}$	$10_{6,4;2}$
$11_{5,6;-1}$	$11_{4,7;-3}$	48788	73909	69690	48463	39205	$11_{6,5;1}$	$11_{7,4;3}$
$12_{5,7;-2}$	$12_{4,8;-4}$	54487	90148	65598	48989	40064	$12_{7,5;2}$	$12_{8,4;4}$
$6_{6,0;6}$	$6_{5,1;4}$	9286	10861	13484	19779	65000	$6_{0,6;-6}$	$6_{1,5;-4}$
$7_{6,1;5}$	$7_{5,2;3}$	17411	20670	26163	43602	36161	$7_{1,6;-5}$	$7_{2,5;-3}$
$8_{6,2;4}$	$8_{5,3;2}$	24792	29932	39333	66715	38958	$8_{2,6;-4}$	$8_{3,5;-2}$
$9_{6,3;3}$	$9_{5,4;1}$	31667	38960	55712	67954	41167	$9_{3,6;-3}$	$9_{4,5;-1}$
$10_{6,4;2}$	$10_{5,5;0}$	38182	47998	75829	59745	42955	$10_{4,6;-2}$	$10_{5,5;0}$
$11_{6,5;1}$	$11_{5,6;-1}$	44432	57343	90410	57343	44432	$11_{5,6;-1}$	$11_{6,5;1}$
$12_{6,6;0}$	$12_{5,7;-2}$	50481	67590	90893	57486	45673	$12_{6,6;-0}$	$12_{7,5;2}$
$7_{7,0;7}$	$7_{6,1;5}$	9375	10943	13559	19511	75000	$7_{0,7;-7}$	$7_{1,6;-5}$
$8_{7,1;6}$	$8_{6,2;4}$	17708	20926	26300	41002	41319	$8_{1,7;-6}$	$8_{2,6;-4}$
$9_{7,2;5}$	$9_{6,3;3}$	25333	30348	38859	68174	44333	$9_{2,7;-5}$	$9_{3,6;-3}$
$10_{7,3;4}$	$10_{6,4;2}$	32455	39466	52398	81732	46773	$10_{3,7;-4}$	$10_{4,6;-2}$
$11_{7,4;3}$	$11_{6,5;1}$	39205	48463	69690	73909	48788	$11_{4,7;-3}$	$11_{5,6;-1}$
$12_{7,5;2}$	$12_{6,6;0}$	45673	57486	90893	67590	50481	$12_{5,7;-2}$	$12_{6,6;0}$
$8_{8,0;8}$	$8_{7,1;6}$	9444	11008	13620	19487	85000	$8_{0,8;-8}$	$8_{1,7;-6}$
$9_{8,1;7}$	$9_{7,2;5}$	17944	21134	26465	39408	46444	$9_{1,8;-7}$	$9_{2,7;-5}$
$10_{8,2;6}$	$10_{7,3;4}$	25773	30705	38980	65282	49636	$10_{2,8;-6}$	$10_{3,7;-4}$
$11_{8,3;5}$	$11_{7,4;3}$	33106	39938	51626	89952	52273	$11_{3,8;-5}$	$11_{4,7;-3}$
$12_{8,4;4}$	$12_{7,5;2}$	40064	48989	65598	90148	54487	$12_{4,8;-4}$	$12_{5,7;-2}$
$9_{9,0;9}$	$9_{8,1;7}$	9500	11060	13669	19524	95000	$9_{0,9;-9}$	$9_{1,8;-7}$
$10_{9,1;8}$	$10_{8,2;6}$	18136	21307	26611	38815	51545	$10_{1,9;-8}$	$10_{2,8;-6}$
$11_{9,2;7}$	$11_{8,3;5}$	26136	31011	39182	61636	54886	$11_{2,9;-7}$	$11_{3,8;-5}$
$12_{9,3;6}$	$12_{8,4;4}$	33654	40360	51673	90961	57692	$12_{3,9;-6}$	$12_{4,8;-4}$
$10_{10,0;10}$	$10_{9,1;8}$	9545	11103	13710	19565	105000	$10_{0,10;-10}$	$10_{1,9;-8}$
$11_{10,1;9}$	$11_{9,2;7}$	18295	21452	26737	38701	56629	$11_{1,10;-9}$	$11_{2,9;-7}$
$12_{10,2;8}$	$12_{9,3;6}$	26442	31275	39377	59285	60096	$12_{2,10;-8}$	$12_{3,9;-6}$
$11_{11,0;11}$	$11_{10,1;9}$	9583	11139	13744	19604	115000	$11_{0,11;-11}$	$11_{1,10;-9}$
$12_{11,1;10}$	$12_{10,2;8}$	18429	21576	26846	38736	61699	$12_{1,11;-10}$	$12_{2,10;-8}$
$12_{12,0;12}$	$12_{11,1;10}$	9615	11170	13774	19633	125000	$12_{0,12;-12}$	$12_{1,11;-10}$
$^{b,a}Q_{\bar{1},1}$	$^{b,a}Q_{1,\bar{1}}$	∓ 1	∓ 0.5	0	± 0.5	± 1	$^{b,a}Q_{1,\bar{1}}$	$^{b,a}Q_{\bar{1},1}$
$2_{2,1;1}$	$2_{1,2;-1}$	8333	8333	8333	8333	8333	$2_{1,2;-1}$	$2_{2,1;1}$
$3_{2,2;0}$	$3_{1,3;-2}$	14583	13160	11667	10173	8750	$3_{2,2;0}$	$3_{3,1;2}$
$4_{2,3;-1}$	$4_{1,4;-3}$	20250	16126	12886	10584	9000	$4_{3,2;1}$	$4_{4,1;3}$
$5_{2,4;-2}$	$5_{1,5;-4}$	25667	17823	13300	10751	9167	$5_{4,2;2}$	$5_{5,1;4}$
$6_{2,5;-3}$	$6_{1,6;-5}$	30952	18716	13464	10860	9286	$6_{5,2;3}$	$6_{6,1;5}$
$7_{2,6;-4}$	$7_{1,7;-6}$	36161	19158	13555	10943	9375	$7_{6,2;4}$	$7_{7,1;6}$
$8_{2,7;-5}$	$8_{1,8;-7}$	41319	19374	13619	11008	9444	$8_{7,2;5}$	$8_{8,1;7}$
$9_{2,8;-6}$	$9_{1,9;-8}$	46444	19487	13669	11060	9500	$9_{8,2;6}$	$9_{9,1;8}$
$10_{2,9;-7}$	$10_{1,10;-9}$	51545	19553	13710	11103	9545	$10_{9,2;7}$	$10_{10,1;9}$
$11_{2,10;-8}$	$11_{1,11;-10}$	56629	19598	13744	11139	9583	$11_{10,2;8}$	$11_{11,1;10}$
$12_{2,11;-9}$	$12_{1,12;-11}$	61699	19632	13774	11170	9615	$12_{11,2;9}$	$12_{12,1;11}$
$3_{3,1;2}$	$3_{2,2;0}$	8750	10173	11667	13160	14583	$3_{1,3;-2}$	$3_{2,2;0}$
$4_{3,2;1}$	$4_{2,3;-1}$	15750	18280	19208	18280	15750	$4_{2,3;-1}$	$4_{3,2;1}$
$5_{3,3;0}$	$5_{2,4;-2}$	22000	24936	23333	19781	16500	$5_{3,3;0}$	$5_{4,2;2}$
$6_{3,4;-1}$	$6_{2,5;-3}$	27857	30089	25173	20331	17024	$6_{4,3;1}$	$6_{5,2;3}$
$7_{3,5;-2}$	$7_{2,6;-4}$	33482	33722	25914	20668	17411	$7_{5,3;2}$	$7_{6,2;4}$
$8_{3,6;-3}$	$8_{2,7;-5}$	38958	36030	26251	20926	17708	$8_{6,3;3}$	$8_{7,2;5}$
$9_{3,7;-4}$	$9_{2,8;-6}$	44333	37360	26455	21134	17944	$9_{7,3;4}$	$9_{8,2;6}$
$10_{3,8;-5}$	$10_{2,9;-7}$	49636	38072	26609	21307	18136	$10_{8,3;5}$	$10_{9,2;7}$
$11_{3,9;-6}$	$11_{2,10;-8}$	54886	38443	26737	21452	18295	$11_{9,3;6}$	$11_{10,2;8}$
$12_{3,10;-7}$	$12_{2,11;-9}$	60096	38646	26846	21576	18429	$12_{10,3;7}$	$12_{11,2;9}$

TABLE VI.—*Continued.*

Sub-branch				κ			Sub-branch	
$^{b,a}Q_{\bar{1},1}$	$^{b,a}Q_{1,\bar{1}}$	∓1	∓0.5	0	±0.5	±1	$^{b,a}Q_{1,\bar{1}}$	$^{b,a}Q_{\bar{1},1}$
$4_{4,1;3}$	$4_{3,2;1}$	9000	10584	12886	16126	20250	$4_{1,4;-3}$	$4_{2,3;-1}$
$5_{4,2;2}$	$5_{3,3;0}$	16500	19781	23333	24936	22000	$5_{2,4;-2}$	$5_{3,3;0}$
$6_{4,3;1}$	$6_{3,4;-1}$	23214	28237	30910	28237	23214	$6_{3,4;-1}$	$6_{4,3;1}$
$7_{4,4;0}$	$7_{3,5;-2}$	29464	35974	35396	29347	24107	$7_{4,4;0}$	$7_{5,3;2}$
$8_{4,5;-1}$	$8_{3,6;-3}$	35417	42717	37550	29917	24792	$8_{5,4;1}$	$8_{6,3;3}$
$9_{4,6;-2}$	$9_{3,7;-4}$	41167	48149	38467	30347	25333	$9_{6,4;2}$	$9_{7,3;4}$
$10_{4,7;-3}$	$10_{3,8;-5}$	46773	52121	38896	30705	25773	$10_{7,4;3}$	$10_{8,3;5}$
$11_{4,8;-4}$	$11_{3,9;-6}$	52273	54738	39163	31011	26136	$11_{8,4;4}$	$11_{9,3;6}$
$12_{4,9;-5}$	$12_{3,10;-7}$	57692	56299	39373	31275	26442	$12_{9,4;5}$	$12_{10,3;7}$
$5_{5,1;4}$	$5_{4,2;2}$	9167	10751	13300	17823	25667	$5_{1,5;-4}$	$5_{2,4;-2}$
$6_{5,2;3}$	$6_{4,3;1}$	17024	20331	25173	30089	27857	$6_{2,5;-3}$	$6_{3,4;-1}$
$7_{5,3;2}$	$7_{4,4;0}$	24107	29347	35396	35974	29464	$7_{3,5;-2}$	$7_{4,4;0}$
$8_{5,4;1}$	$8_{4,5;-1}$	30694	38050	43064	38050	30694	$8_{4,5;-1}$	$8_{5,4;1}$
$9_{5,5;0}$	$9_{4,6;-2}$	36944	46432	47757	38893	31667	$9_{5,5;0}$	$9_{6,4;2}$
$10_{5,6;-1}$	$10_{4,7;-3}$	42955	54266	50083	39458	32455	$10_{6,5;1}$	$10_{7,4;3}$
$11_{5,7;-2}$	$11_{4,8;-4}$	48788	61181	51087	39937	33106	$11_{7,5;2}$	$11_{8,4;4}$
$12_{5,8;-3}$	$12_{4,9;-5}$	54487	66823	51551	40360	33654	$12_{8,5;3}$	$12_{9,4;5}$
$6_{6,1;5}$	$6_{5,2;3}$	9286	10860	13464	18716	30952	$6_{1,6;-5}$	$6_{2,5;-3}$
$7_{6,2;4}$	$7_{5,3;2}$	17411	20668	25914	33722	33482	$7_{2,6;-4}$	$7_{3,5;-2}$
$8_{6,3;3}$	$8_{5,4;1}$	24792	29917	37550	42717	35417	$8_{3,6;-3}$	$8_{4,5;-1}$
$9_{6,4;2}$	$9_{5,5;0}$	31667	38893	47757	46432	36944	$9_{4,6;-2}$	$9_{5,5;0}$
$10_{6,5;1}$	$10_{5,6;-1}$	38182	47745	55515	47745	38182	$10_{5,6;-1}$	$10_{6,5;1}$
$11_{6,6;0}$	$11_{5,7;-2}$	44432	56495	60341	48430	39205	$11_{6,6;0}$	$11_{7,5;2}$
$12_{6,7;-1}$	$12_{5,8;-3}$	50481	65013	62764	48985	40064	$12_{7,6;1}$	$12_{8,5;3}$
$7_{7,1;6}$	$7_{6,2;4}$	9375	10943	13555	19158	36161	$7_{1,7;-6}$	$7_{2,6;-4}$
$8_{7,2;5}$	$8_{6,3;3}$	17708	20926	26251	36030	38958	$8_{2,7;-5}$	$8_{3,6;-3}$
$9_{7,3;4}$	$9_{6,4;2}$	25333	30347	38467	48149	41167	$9_{3,7;-4}$	$9_{4,6;-2}$
$10_{7,4;3}$	$10_{6,5;1}$	32455	39458	50083	54266	42955	$10_{4,7;-3}$	$10_{5,6;-1}$
$11_{7,5;2}$	$11_{6,6;0}$	39205	48430	60341	56495	44432	$11_{5,7;-2}$	$11_{6,6;0}$
$12_{7,6;1}$	$12_{6,7;-1}$	45673	57370	68182	57370	45673	$12_{6,7;-1}$	$12_{7,6;1}$
$8_{8,1;7}$	$8_{7,2;5}$	9444	11008	13619	19374	41319	$8_{1,8;-7}$	$8_{2,7;-5}$
$9_{8,2;6}$	$9_{7,3;4}$	17944	21134	26455	37360	44333	$9_{2,8;-6}$	$9_{3,7;-4}$
$10_{8,3;5}$	$10_{7,4;3}$	25773	30705	38896	52121	46773	$10_{3,8;-5}$	$10_{4,7;-3}$
$11_{8,4;4}$	$11_{7,5;2}$	33106	39937	51087	61181	48788	$11_{4,8;-4}$	$11_{5,7;-2}$
$12_{8,5;3}$	$12_{7,6;1}$	40064	48985	62764	65013	50481	$12_{5,8;-3}$	$12_{6,7;-1}$
$9_{9,1;8}$	$9_{8,2;6}$	9500	11060	13669	19487	46444	$9_{1,9;-8}$	$9_{2,8;-6}$
$10_{9,2;7}$	$10_{8,3;5}$	18136	21307	26609	38072	49636	$10_{2,9;-7}$	$10_{3,8;-5}$
$11_{9,3;6}$	$11_{8,4;4}$	26136	31011	39163	54738	52273	$11_{3,9;-6}$	$11_{4,8;-4}$
$12_{9,4;5}$	$12_{8,5;3}$	33654	40360	51551	66823	54487	$12_{4,9;-5}$	$12_{5,8;-3}$
$10_{10,1;9}$	$10_{9,2;7}$	9545	11103	13710	19553	51545	$10_{1,10;-9}$	$10_{2,9;-7}$
$11_{10,2;8}$	$11_{9,3;6}$	18295	21452	26737	38443	54886	$11_{2,10;-8}$	$11_{3,9;-6}$
$12_{10,3;7}$	$12_{9,4;5}$	26442	31275	39373	56299	57692	$12_{3,10;-7}$	$12_{4,9;-5}$
$11_{11,1;10}$	$11_{10,2;8}$	9583	11139	13744	19598	56629	$11_{1,11;-10}$	$11_{2,10;-8}$
$12_{11,2;9}$	$12_{10,3;7}$	18429	21576	26846	38646	60096	$12_{2,11;-9}$	$12_{3,10;-7}$
$12_{12,1;11}$	$12_{11,2;9}$	9615	11170	13774	19632	61699	$12_{1,12;-11}$	$12_{2,11;-9}$
$^{b,c}R_{1,1}$	$^{b,a}P_{\bar{1},\bar{1}}$	∓1	∓0.5	0	±0.5	±1	$^{b,c}R_{1,1}$	$^{b,a}P_{\bar{1},\bar{1}}$
$0_{0,0;0}$	$1_{1,1;0}$	10000	10000	10000	10000	10000	$0_{0,0;0}$	$1_{1,1;0}$
$1_{1,0;1}$	$2_{2,1;1}$	15000	15000	15000	15000	15000	$1_{0,1;-1}$	$2_{1,2;-1}$
$2_{2,0;2}$	$3_{3,1;2}$	25000	24086	22847	21383	20000	$2_{0,2;-2}$	$3_{1,3;-2}$
$3_{3,0;3}$	$4_{4,1;3}$	35000	34083	32533	29584	25000	$3_{0,3;-3}$	$4_{1,4;-3}$
$4_{4,0;4}$	$5_{5,1;4}$	45000	44117	42585	39100	30000	$4_{0,4;-4}$	$5_{1,5;-4}$
$5_{5,0;5}$	$6_{6,1;5}$	55000	54140	52653	49126	35000	$5_{0,5;-5}$	$6_{1,6;-5}$
$6_{6,0;6}$	$7_{7,1;6}$	65000	64155	62702	59250	40000	$6_{0,6;-6}$	$7_{1,7;-6}$
$7_{7,0;7}$	$8_{8,1;7}$	75000	74165	72737	69364	45000	$7_{0,7;-7}$	$8_{1,8;-7}$
$8_{8,0;8}$	$9_{9,1;8}$	85000	84173	82763	79453	50000	$8_{0,8;-8}$	$9_{1,9;-8}$
$9_{9,0;9}$	$10_{10,1;9}$	95000	94179	92782	89522	55000	$9_{0,9;-9}$	$10_{1,10;-9}$
$10_{10,0;10}$	$11_{11,1;10}$	105000	104184	102798	99576	60000	$10_{0,10;-10}$	$11_{1,11;-10}$
$11_{11,0;11}$	$12_{12,1;11}$	115000	114188	112810	109620	65000	$11_{0,11;-11}$	$12_{1,12;-11}$

TABLE VI.—*Continued.*

Sub-branch				κ			Sub-branch	
${}^{b,a}R_{1,1}$	${}^{b,a}P_{\bar{1},\bar{1}}$	∓ 1	∓ 0.5	0	± 0.5	± 1	${}^{b,c}R_{1,1}$	${}^{b,a}P_{\bar{1},\bar{1}}$
$1_{0,1;-1}$	$2_{1,2;-1}$	15000	15000	15000	15000	15000	$1_{1,0;1}$	$2_{2,1;1}$
$2_{1,1;0}$	$3_{2,2;0}$	16667	16667	16667	16667	16667	$2_{1,1;0}$	$3_{2,2;0}$
$3_{2,1;1}$	$4_{3,2;1}$	26250	23549	21079	19563	18750	$3_{1,2;-1}$	$4_{2,3;-1}$
$4_{3,1;2}$	$5_{4,2;2}$	36000	33165	28748	23919	21000	$4_{1,3;-2}$	$5_{2,4;-2}$
$5_{4,1;3}$	$6_{5,2;3}$	45833	43122	38409	30161	23333	$5_{1,4;-3}$	$6_{2,5;-3}$
$6_{5,1;4}$	$7_{6,2;4}$	55714	53091	48508	38383	25714	$6_{1,5;-4}$	$7_{2,6;-4}$
$7_{6,1;5}$	$8_{7,2;5}$	65625	63059	58609	48001	28125	$7_{1,6;-5}$	$8_{2,7;-5}$
$8_{7,1;6}$	$9_{8,2;6}$	75556	73030	68678	58192	30556	$8_{1,7;-6}$	$9_{2,8;-6}$
$9_{8,1;7}$	$10_{9,2;7}$	85500	83002	78720	68479	33000	$9_{1,8;-7}$	$10_{2,9;-7}$
$10_{9,1;8}$	$11_{10,2;8}$	95455	92979	88749	78723	35454	$10_{1,9;-8}$	$11_{2,10;-8}$
$11_{10,1;9}$	$12_{11,2;9}$	105416	102958	98767	88911	37917	$11_{1,10;-9}$	$12_{2,11;-9}$
$2_{0,2;-2}$	$3_{1,3;-2}$	20000	21383	22847	24086	25000	$2_{2,0;2}$	$3_{3,1;2}$
$3_{1,2;-1}$	$4_{2,3;-1}$	18750	19563	21079	23549	26250	$3_{2,1;1}$	$4_{3,2;1}$
$4_{2,2;0}$	$5_{3,3;0}$	28000	23609	22028	23609	28000	$4_{2,2;0}$	$5_{3,3;0}$
$5_{3,2;1}$	$6_{4,3;1}$	37500	32338	26305	24633	30000	$5_{2,3;-1}$	$6_{3,4;-1}$
$6_{4,2;2}$	$7_{5,3;2}$	47143	42259	34093	27060	32143	$6_{2,4;-2}$	$7_{3,5;-2}$
$7_{5,2;3}$	$8_{6,3;3}$	56875	52226	43935	31293	34375	$7_{2,5;-3}$	$8_{3,6;-3}$
$8_{6,2;4}$	$9_{7,3;4}$	66667	62172	54199	37664	36667	$8_{2,6;-4}$	$9_{3,7;-4}$
$9_{7,2;5}$	$10_{8,3;5}$	76500	72110	64411	46127	39000	$9_{2,7;-5}$	$10_{3,8;-5}$
$10_{8,2;6}$	$11_{9,3;6}$	86364	82050	74550	56030	41364	$10_{2,8;-6}$	$11_{3,9;-6}$
$11_{9,2;7}$	$12_{10,3;7}$	96250	91993	84638	66512	43750	$11_{2,9;-7}$	$12_{3,10;-7}$
$3_{0,3;-3}$	$4_{1,4;-3}$	25000	29584	32533	34083	35000	$3_{3,0;3}$	$4_{4,1;3}$
$4_{1,3;-2}$	$5_{2,4;-2}$	21000	23919	28748	33165	36000	$4_{3,1;2}$	$5_{4,2;2}$
$5_{2,3;-1}$	$6_{3,4;-1}$	30000	24633	26305	32338	37500	$5_{3,2;1}$	$6_{4,3;1}$
$6_{3,3;0}$	$7_{4,4;0}$	39286	31500	26801	31500	39286	$6_{3,3;0}$	$7_{4,4;0}$
$7_{4,3;1}$	$8_{5,4;1}$	48750	41277	31054	31018	41250	$7_{3,4;-1}$	$8_{4,5;-1}$
$8_{5,3;2}$	$9_{6,4;2}$	58333	51336	39046	31553	43333	$8_{3,5;-2}$	$9_{4,6;-2}$
$9_{6,3;3}$	$10_{7,4;3}$	68000	61325	49147	33704	45500	$9_{3,6;-3}$	$10_{4,7;-3}$
$10_{7,3;4}$	$11_{8,4;4}$	77727	71271	59638	37919	47727	$10_{3,7;-4}$	$11_{4,8;-4}$
$11_{8,3;5}$	$12_{9,4;5}$	87500	81200	70013	44472	50000	$11_{3,8;-5}$	$12_{4,9;-5}$
$4_{0,4;-4}$	$5_{1,5;-4}$	30000	39100	42585	44117	45000	$4_{4,0;4}$	$5_{5,1;4}$
$5_{1,4;-3}$	$6_{2,5;-3}$	23333	30161	38409	43122	45833	$5_{4,1;3}$	$6_{5,2;3}$
$6_{2,4;-2}$	$7_{3,5;-2}$	32143	27060	34093	42259	47143	$6_{4,2;2}$	$7_{5,3;2}$
$7_{3,4;-1}$	$8_{4,5;-1}$	41250	31018	31054	41277	48750	$7_{4,3;1}$	$8_{5,4;1}$
$8_{4,4;0}$	$9_{5,5;0}$	50556	40057	31211	40057	50556	$8_{4,4;0}$	$9_{5,5;0}$
$9_{5,4;1}$	$10_{6,5;1}$	60000	50269	35484	38709	52500	$9_{4,5;-1}$	$10_{5,6;-1}$
$10_{6,4;2}$	$11_{7,5;2}$	69546	60393	43709	37729	54546	$10_{4,6;-2}$	$11_{5,7;-2}$
$11_{7,4;3}$	$12_{8,5;3}$	79167	70407	54102	37878	56667	$11_{4,7;-3}$	$12_{5,8;-3}$
$5_{0,5;-5}$	$6_{1,6;-5}$	35000	49126	52653	54140	55000	$5_{5,0;5}$	$6_{6,1;5}$
$6_{1,5;-4}$	$7_{2,6;-4}$	25714	38383	48508	53091	55714	$6_{5,1;4}$	$7_{6,2;4}$
$7_{2,5;-3}$	$8_{3,6;-3}$	34375	31293	43935	52226	56875	$7_{5,2;3}$	$8_{6,3;3}$
$8_{3,5;-2}$	$9_{4,6;-2}$	43333	31553	39046	51336	58333	$8_{5,3;2}$	$9_{6,4;2}$
$9_{4,5;-1}$	$10_{5,6;-1}$	52500	38709	35484	50269	60000	$9_{5,4;1}$	$10_{6,5;1}$
$10_{5,5;0}$	$11_{6,6;0}$	61818	48913	35365	48913	61818	$10_{5,5;0}$	$11_{6,6;0}$
$11_{6,5;1}$	$12_{7,6;1}$	71250	59273	39679	47228	63750	$11_{5,6;-1}$	$12_{6,7;-1}$
$6_{0,6;-6}$	$7_{1,7;-6}$	40000	59250	62702	64155	65000	$6_{6,0;6}$	$7_{7,1;6}$
$7_{1,6;-5}$	$8_{2,7;-5}$	28125	48001	58609	63059	65625	$7_{6,1;5}$	$8_{7,2;5}$
$8_{2,6;-4}$	$9_{3,7;-4}$	36667	37664	54199	62172	66667	$8_{6,2;4}$	$9_{7,3;4}$
$9_{3,6;-3}$	$10_{4,7;-3}$	45500	33704	49147	61325	68000	$9_{6,3;3}$	$10_{7,4;3}$
$10_{4,6;-2}$	$11_{5,7;-2}$	54546	37729	43709	60393	69546	$10_{6,4;2}$	$11_{7,5;2}$
$11_{5,6;-1}$	$12_{6,7;-1}$	63750	47228	39679	59273	71250	$11_{6,5;1}$	$12_{7,6;1}$
$7_{0,7;-7}$	$8_{1,8;-7}$	45000	69364	72737	74165	75000	$7_{7,0;7}$	$8_{8,1;7}$
$8_{1,7;-6}$	$9_{2,8;-6}$	30556	58192	68678	73030	75556	$8_{7,1;6}$	$9_{8,2;6}$
$9_{2,7;-5}$	$10_{3,8;-5}$	39000	46127	64411	72110	76500	$9_{7,2;5}$	$10_{8,3;5}$
$10_{3,7;-4}$	$11_{4,8;-4}$	47727	37919	59638	71271	77727	$10_{7,3;4}$	$11_{8,4;4}$
$11_{4,7;-3}$	$12_{5,8;-3}$	56667	37878	54102	70407	79167	$11_{7,4;3}$	$12_{8,5;3}$
$8_{0,8;-8}$	$9_{1,9;-8}$	50000	79453	82763	84173	85000	$8_{8,0;8}$	$9_{9,1;8}$
$9_{1,8;-7}$	$10_{2,9;-7}$	33000	68479	78720	83002	85500	$9_{8,1;7}$	$10_{9,2;7}$
$10_{2,8;-6}$	$11_{3,9;-6}$	41364	56030	74550	82050	86364	$10_{8,2;6}$	$11_{9,3;6}$
$11_{3,8;-5}$	$12_{4,9;-5}$	50000	44472	70013	81200	87500	$11_{8,3;5}$	$12_{9,4;5}$

TABLE VI.—*Continued.*

Sub-branch $^{b,e}R_{1,1}$	Sub-branch $^{b,o}P_{\bar{1},\bar{1}}$	κ ∓1	∓0.5	0	±0.5	±1	Sub-branch $^{b,e}R_{1,1}$	Sub-branch $^{b,o}P_{\bar{1},\bar{1}}$
$9_{0,9;-9}$	$10_{1,10;-9}$	55000	89522	92782	94179	95000	$9_{9,0;9}$	$10_{10,1;9}$
$10_{1,9;-8}$	$11_{2,10;-8}$	35454	78723	88749	92979	95455	$10_{9,1;8}$	$11_{10,2;8}$
$11_{2,9;-7}$	$12_{3,10;-7}$	43750	66512	84638	91993	96250	$11_{9,2;7}$	$12_{10,3;7}$
$10_{0,10;-10}$	$11_{1,11;-10}$	60000	99576	102798	104184	105000	$10_{10,0;10}$	$11_{11,1;10}$
$11_{1,10;-9}$	$12_{2,11;-9}$	37917	88911	98767	102958	105416	$11_{10,1;9}$	$12_{11,2;9}$
$11_{0,11;-11}$	$12_{1,12;-11}$	65000	109620	112810	114188	115000	$11_{11,0;11}$	$12_{12,1;11}$
$^{b,o}R_{\bar{1},1}$	$^{b,e}P_{1,\bar{1}}$	∓1	∓0.5	0	±0.5	±1	$^{b,o}R_{1,\bar{1}}$	$^{b,e}P_{\bar{1},1}$
$1_{1,1;0}$	$2_{0,2;-2}$	5000	7226	10000	12774	15000	$1_{1,1;0}$	$2_{2,0;2}$
$2_{1,2;-1}$	$3_{0,3;-3}$	10000	16667	21498	23874	25000	$2_{2,1;1}$	$3_{3,0;3}$
$3_{1,3;-2}$	$4_{0,4;-4}$	15000	27406	32266	34065	35000	$3_{3,1;2}$	$4_{4,0;4}$
$4_{1,4;-3}$	$5_{0,5;-5}$	20000	38266	42535	44115	45000	$4_{4,1;3}$	$5_{5,0;5}$
$5_{1,5;-4}$	$6_{0,6;-6}$	25000	48829	52643	54140	55000	$5_{5,1;4}$	$6_{6,0;6}$
$6_{1,6;-5}$	$7_{0,7;-7}$	30000	59146	62700	64155	65000	$6_{6,1;5}$	$7_{7,0;7}$
$7_{1,7;-6}$	$8_{0,8;-8}$	35000	69327	72736	74165	75000	$7_{7,1;6}$	$8_{8,0;8}$
$8_{1,8;-7}$	$9_{0,9;-9}$	40000	79440	82762	84173	85000	$8_{8,1;7}$	$9_{9,0;9}$
$9_{1,9;-8}$	$10_{0,10;-10}$	45000	89517	92782	94179	95000	$9_{9,1;8}$	$10_{10,0;10}$
$10_{1,10;-9}$	$11_{0,11;-11}$	50000	99574	102798	104184	105000	$10_{10,1;9}$	$11_{11,0;11}$
$11_{1,11;-10}$	$12_{0,12;-12}$	55000	109619	112810	114188	115000	$11_{11,1;10}$	$12_{12,0;12}$
$2_{2,1;1}$	$3_{1,2;-1}$	1667	2792	5168	10000	16667	$2_{1,2;-1}$	$3_{2,1;1}$
$3_{2,2;0}$	$4_{1,3;-2}$	3750	7602	15000	22398	26250	$3_{2,2;0}$	$4_{3,1;2}$
$4_{2,3;-1}$	$5_{1,4;-3}$	6000	14796	26797	33039	36000	$4_{3,2;1}$	$5_{4,1;3}$
$5_{2,4;-2}$	$6_{1,5;-4}$	8333	24389	37946	43109	45833	$5_{4,2;2}$	$6_{5,1;4}$
$6_{2,5;-3}$	$7_{1,6;-5}$	10714	35443	48405	53090	55714	$6_{5,2;3}$	$7_{6,1;5}$
$7_{2,6;-4}$	$8_{1,7;-6}$	13125	46736	58587	63059	65625	$7_{6,2;4}$	$8_{7,1;6}$
$8_{2,7;-5}$	$9_{1,8;-7}$	15556	57689	68672	73029	75556	$8_{7,2;5}$	$9_{8,1;7}$
$9_{2,8;-6}$	$10_{1,9;-8}$	18000	68283	78719	83002	85500	$9_{8,2;6}$	$10_{9,1;8}$
$10_{2,9;-7}$	$11_{1,10;-9}$	20455	78648	88749	92979	95455	$10_{9,2;7}$	$11_{10,1;9}$
$11_{2,10;-8}$	$12_{1,11;-10}$	22917	88882	98767	102958	105416	$11_{10,2;8}$	$12_{11,1;10}$
$3_{3,1;2}$	$4_{2,2;0}$	1250	1537	2692	6941	18750	$3_{1,3;-2}$	$4_{2,2;0}$
$4_{3,2;1}$	$5_{2,3;-1}$	3000	4022	8877	19900	28000	$4_{2,3;-1}$	$5_{3,2;1}$
$5_{3,3;0}$	$6_{2,4;-2}$	5000	7698	19335	31792	37500	$5_{3,3;0}$	$6_{4,2;2}$
$6_{3,4;-1}$	$7_{2,5;-3}$	7143	13138	31685	42193	47143	$6_{4,3;1}$	$7_{5,2;3}$
$7_{3,5;-2}$	$8_{2,6;-4}$	9375	20912	43306	52219	56875	$7_{5,3;2}$	$8_{6,2;4}$
$8_{3,6;-3}$	$9_{2,7;-5}$	11667	31041	54046	62172	66667	$8_{6,3;3}$	$9_{7,2;5}$
$9_{3,7;-4}$	$10_{2,8;-6}$	14000	42620	64375	72111	76500	$9_{7,3;4}$	$10_{8,2;6}$
$10_{3,8;-5}$	$11_{2,9;-7}$	16364	54434	74542	82050	86364	$10_{8,3;5}$	$11_{9,2;7}$
$11_{3,9;-6}$	$12_{2,10;-8}$	18750	65840	84638	91993	96250	$11_{9,3;6}$	$12_{10,2;8}$
$4_{4,1;3}$	$5_{3,2;1}$	1000	1162	1666	4522	21000	$4_{1,4;-3}$	$5_{2,3;-1}$
$5_{4,2;2}$	$6_{3,3;0}$	2500	2920	5238	16127	30000	$5_{2,4;-2}$	$6_{3,3;0}$
$6_{4,3;1}$	$7_{3,4;-1}$	4286	5148	12183	29700	39286	$6_{3,4;-1}$	$7_{4,3;1}$
$7_{4,4;0}$	$8_{3,5;-2}$	6250	8062	23299	41022	48750	$7_{4,4;0}$	$8_{5,3;2}$
$8_{4,5;-1}$	$9_{3,6;-3}$	8333	12161	36249	51302	58333	$8_{5,4;1}$	$9_{6,3;3}$
$9_{4,6;-2}$	$10_{3,7;-4}$	10500	18094	48371	61321	68000	$9_{6,4;2}$	$10_{7,3;4}$
$10_{4,7;-3}$	$11_{3,8;-5}$	12727	26418	59438	71271	77727	$10_{7,4;3}$	$11_{8,3;5}$
$11_{4,8;-4}$	$12_{3,9;-6}$	15000	37104	69962	81200	87500	$11_{8,4;4}$	$12_{9,3;6}$
$5_{5,1;4}$	$6_{4,2;2}$	833	966	1253	2984	23333	$5_{1,5;-4}$	$6_{2,4;-2}$
$6_{5,2;3}$	$7_{4,3;1}$	2143	2475	3549	11918	32143	$6_{2,5;-3}$	$7_{3,4;-1}$
$7_{5,3;2}$	$8_{4,4;0}$	3750	4309	7685	26263	41250	$7_{3,5;-2}$	$8_{4,4;0}$
$8_{5,4;1}$	$9_{4,5;-1}$	5556	6389	15266	39231	50556	$8_{4,5;-1}$	$9_{5,4;1}$
$9_{5,5;0}$	$10_{4,6;-2}$	7500	8819	27015	50150	60000	$9_{5,5;0}$	$10_{6,4;2}$
$10_{5,6;-1}$	$11_{4,7;-3}$	9545	11954	40562	60377	69546	$10_{6,5;1}$	$11_{7,4;3}$
$11_{5,7;-2}$	$12_{4,8;-4}$	11667	16365	53190	70405	79167	$11_{7,5;2}$	$12_{8,4;4}$
$6_{6,1;5}$	$7_{5,2;3}$	714	829	1052	2102	25714	$6_{1,6;-5}$	$7_{2,5;-3}$
$7_{6,2;4}$	$8_{5,3;2}$	1875	2170	2825	8386	34375	$7_{2,6;-4}$	$8_{3,5;-2}$
$8_{6,3;3}$	$9_{5,4;1}$	3333	3839	5485	21522	43333	$8_{3,6;-3}$	$9_{4,5;-1}$
$9_{6,4;2}$	$10_{5,5;0}$	5000	5717	10057	36378	52500	$9_{4,6;-2}$	$10_{5,5;0}$
$10_{6,5;1}$	$11_{5,6;-1}$	6818	7736	18198	48537	61818	$10_{5,6;-1}$	$11_{6,5;1}$
$11_{6,6;0}$	$12_{5,7;-2}$	8750	9912	30549	59217	71250	$11_{6,6;0}$	$12_{7,5;2}$

TABLE VI.—*Continued.*

Sub-branch $^{b,e}R_{\bar{1},1}$	$^{b,e}P_{1,\bar{1}}$	∓ 1	∓ 0.5	K 0	± 0.5	± 1	Sub-branch $^{b,e}R_{1,\bar{1}}$	$^{b,e}P_{\bar{1},1}$
$7_{7,1;6}$	$8_{6,2;4}$	625	726	918	1615	28125	$7_{1,7;-6}$	$8_{2,6;-4}$
$8_{7,2;5}$	$9_{6,3;3}$	1667	1932	2461	5953	36667	$8_{2,7;-5}$	$9_{3,6;-3}$
$9_{7,3;4}$	$10_{6,4;2}$	3000	3467	4517	16387	45500	$9_{3,7;-4}$	$10_{4,6;-2}$
$10_{7,4;3}$	$11_{6,5;1}$	4545	5226	7432	32088	54546	$10_{4,7;-3}$	$11_{5,6;-1}$
$11_{7,5;2}$	$12_{6,6;0}$	6250	7134	12369	46152	63750	$11_{5,7;-2}$	$12_{6,6;0}$
$8_{8,1;7}$	$9_{7,2;5}$	556	645	816	1342	30556	$8_{1,8;-7}$	$9_{2,7;-5}$
$9_{8,2;6}$	$10_{7,3;4}$	1500	1741	2210	4454	39000	$9_{2,8;-6}$	$10_{3,7;-4}$
$10_{8,3;5}$	$11_{7,4;3}$	2727	3158	4030	12003	47727	$10_{3,8;-5}$	$11_{4,7;-3}$
$11_{8,4;4}$	$12_{7,5;2}$	4167	4808	6264	26503	56667	$11_{4,8;-4}$	$12_{5,7;-2}$
$9_{9,1;8}$	$10_{8,2;6}$	500	581	734	1176	33000	$9_{1,9;-8}$	$10_{2,8;-6}$
$10_{9,2;7}$	$11_{8,3;5}$	1364	1583	2009	3581	41364	$10_{2,9;-7}$	$11_{3,8;-5}$
$11_{9,3;6}$	$12_{8,4;4}$	2500	2898	3688	8874	50000	$11_{3,9;-6}$	$12_{4,8;-4}$
$10_{10,1;9}$	$11_{9,2;7}$	455	528	667	1059	35454	$10_{1,10;-9}$	$11_{2,9;-7}$
$11_{10,2;8}$	$12_{9,3;6}$	1250	1452	1841	3076	43750	$11_{2,10;-8}$	$12_{3,9;-6}$
$11_{11,1;10}$	$12_{10,2;8}$	417	484	611	967	37917	$11_{1,11;-10}$	$12_{2,10;-8}$

D. *b* prolate-or-oblate sub-branches.

$^{b,e}R_{\bar{1},3}$	$^{b,e}P_{1,\bar{3}}$	∓ 1	∓ 0.5	0	± 0.5	± 1	$^{b,e}R_{3,\bar{1}}$	$^{b,e}P_{\bar{3},1}$
$2_{2,0;2}$	$3_{1,3;-2}$	1667	1097	486	101		$2_{0,2;-2}$	$3_{3,1;2}$
$3_{2,1;1}$	$4_{1,4;-3}$	3750	1452	297	32		$3_{1,2;-1}$	$4_{4,1;3}$
$4_{2,2;0}$	$5_{1,5;-4}$	6000	1159	140	14		$4_{2,2;0}$	$5_{5,1;4}$
$5_{2,3;-1}$	$6_{1,6;-5}$	8333	758	77	9		$5_{3,2;1}$	$6_{6,1;5}$
$6_{2,4;-2}$	$7_{1,7;-6}$	10714	481	54	7		$6_{4,2;2}$	$7_{7,1;6}$
$7_{2,5;-3}$	$8_{1,8;-7}$	13125	323	42	6		$7_{5,2;3}$	$8_{8,1;7}$
$8_{2,6;-4}$	$9_{1,9;-8}$	15556	238	35	5		$8_{6,2;4}$	$9_{9,1;8}$
$9_{2,7;-5}$	$10_{1,10;-9}$	18000	191	30	4		$9_{7,2;5}$	$10_{10,1;9}$
$10_{2,8;-6}$	$11_{1,11;-10}$	20455	163	27	4		$10_{8,2;6}$	$11_{11,1;10}$
$11_{2,9;-7}$	$12_{1,12;-11}$	22917	144	24	3		$11_{9,2;7}$	$12_{12,1;11}$
$3_{3,0;3}$	$4_{2,3;-1}$	1250	1323	1091	416		$3_{0,3;-3}$	$4_{3,2;1}$
$4_{3,1;2}$	$5_{2,4;-2}$	3000	2753	1252	163		$4_{1,3;-2}$	$5_{4,2;2}$
$5_{3,2;1}$	$6_{2,5;-3}$	5000	3538	737	62		$5_{2,3;-1}$	$6_{5,2;3}$
$6_{3,3;0}$	$7_{2,6;-4}$	7143	3362	375	35		$6_{3,3;0}$	$7_{6,2;4}$
$7_{3,4;-1}$	$8_{2,7;-5}$	9375	2573	219	26		$7_{4,3;1}$	$8_{7,2;5}$
$8_{3,5;-2}$	$9_{2,8;-6}$	11667	1754	155	20		$8_{5,3;2}$	$9_{8,2;6}$
$9_{3,6;-3}$	$10_{2,9;-7}$	14000	1174	124	17		$9_{6,3;3}$	$10_{9,2;7}$
$10_{3,7;-4}$	$11_{2,10;-8}$	16364	826	104	14		$10_{7,3;4}$	$11_{10,2;8}$
$11_{3,8;-5}$	$12_{2,11;-9}$	18750	628	90	12		$11_{8,3;5}$	$12_{11,2;9}$
$4_{4,0;4}$	$5_{3,3;0}$	1000	1144	1259	855		$4_{0,4;-4}$	$5_{3,3;0}$
$5_{4,1;3}$	$6_{3,4;-1}$	2500	2771	2305	514		$5_{1,4;-3}$	$6_{4,3;1}$
$6_{4,2;2}$	$7_{3,5;-2}$	4286	4433	2107	189		$6_{2,4;-2}$	$7_{5,3;2}$
$7_{4,3;1}$	$8_{3,6;-3}$	6250	5663	1258	92		$7_{3,4;-1}$	$8_{6,3;3}$
$8_{4,4;0}$	$9_{3,7;-4}$	8333	6007	676	62		$8_{4,4;0}$	$9_{7,3;4}$
$9_{4,5;-1}$	$10_{3,8;-5}$	10500	5335	411	47		$9_{5,4;1}$	$10_{8,3;5}$
$10_{4,6;-2}$	$11_{3,9;-6}$	12727	4082	298	38		$10_{6,4;2}$	$11_{9,3;6}$
$11_{4,7;-3}$	$12_{3,10;-7}$	15000	2866	241	32		$11_{7,4;3}$	$12_{10,3;7}$
$5_{5,0;5}$	$6_{4,3;1}$	833	965	1174	1186		$5_{0,5;-5}$	$6_{3,4;-1}$
$6_{5,1;4}$	$7_{4,4;0}$	2143	2461	2707	1158		$6_{1,5;-4}$	$7_{4,4;0}$
$7_{5,2;3}$	$8_{4,5;-1}$	3750	4229	3560	488		$7_{2,5;-3}$	$8_{5,4;1}$
$8_{5,3;2}$	$9_{4,6;-2}$	5556	6040	3008	209		$8_{3,5;-2}$	$9_{6,4;2}$
$9_{5,4;1}$	$10_{4,7;-3}$	7500	7603	1831	125		$9_{4,5;-1}$	$10_{7,4;3}$
$10_{5,5;0}$	$11_{4,8;-4}$	9545	8531	1026	92		$10_{5,5;0}$	$11_{8,4;4}$
$11_{5,6;-1}$	$12_{4,9;-5}$	11667	8452	644	73		$11_{6,5;1}$	$12_{9,4;5}$
$6_{6,0;6}$	$7_{5,3;2}$	714	829	1039	1321		$6_{0,6;-6}$	$7_{3,5;-2}$
$7_{6,1;5}$	$8_{5,4;1}$	1875	2169	2640	1942		$7_{1,6;-5}$	$8_{4,5;-1}$
$8_{6,2;4}$	$9_{5,5;0}$	3333	3830	4213	1086		$8_{2,6;-4}$	$9_{5,5;0}$
$9_{6,3;3}$	$10_{5,6;-1}$	5000	5676	4833	447		$9_{3,6;-3}$	$10_{6,5;1}$
$10_{6,4;2}$	$11_{5,7;-2}$	6818	7575	3937	234		$10_{4,6;-2}$	$11_{7,5;2}$
$11_{6,5;1}$	$12_{5,8;-3}$	8750	9349	2441	161		$11_{5,6;-1}$	$12_{8,5;3}$

TABLE VI.—*Continued.*

Sub-branch $^{b,e}R_{\bar{1},3}$	Sub-branch $^{b,o}P_{1,\bar{3}}$	∓ 1	∓ 0.5	κ 0	± 0.5	± 1	Sub-branch $^{b,e}R_{3,\bar{1}}$	Sub-branch $^{b,o}P_{\bar{3},1}$
$7_{7,0;7}$	$8_{6,3;3}$	625	726	916	1313		$7_{0,7;-7}$	$8_{3,6;-3}$
$8_{7,1;6}$	$9_{6,4;2}$	1667	1932	2426	2561		$8_{1,7;-6}$	$9_{4,6;-2}$
$9_{7,2;5}$	$10_{6,5;1}$	3000	3466	4214	2032		$9_{2,7;-5}$	$10_{5,6;-1}$
$10_{7,3;4}$	$11_{6,6;0}$	4545	5221	5738	917		$10_{3,7;-4}$	$11_{6,6;0}$
$11_{7,4;3}$	$12_{6,7;-1}$	6250	7114	6113	427		$11_{4,7;-3}$	$12_{7,6;1}$
$8_{8,0;8}$	$9_{7,3;4}$	556	645	816	1238		$8_{0,8;-8}$	$9_{3,7;-4}$
$9_{8,1;7}$	$10_{7,4;3}$	1500	1741	2204	2870		$9_{1,8;-7}$	$10_{4,7;-3}$
$10_{8,2;6}$	$11_{7,5;2}$	2727	3158	3967	3126		$10_{2,8;-6}$	$11_{5,7;-2}$
$11_{8,3;5}$	$12_{7,6;1}$	4167	4807	5836	1752		$11_{3,8;-5}$	$12_{6,7;-1}$
$9_{9,0;9}$	$10_{8,3;5}$	500	581	734	1143		$9_{0,9;-9}$	$10_{3,8;-5}$
$10_{9,1;8}$	$11_{8,4;4}$	1364	1583	2008	2924		$10_{1,9;-8}$	$11_{4,8;-4}$
$11_{9,2;7}$	$12_{8,5;3}$	2500	2898	3676	4014		$11_{2,9;-7}$	$12_{5,8;-3}$
$10_{10,0;10}$	$11_{9,3;6}$	455	528	667	1049		$10_{0,10;-10}$	$11_{3,9;-6}$
$11_{10,1;9}$	$12_{9,4;5}$	1250	1452	1841	2831		$11_{1,10;-9}$	$12_{4,9;-5}$
$11_{11,0;11}$	$12_{10,3;7}$	417	484	611	964		$11_{0,11;-11}$	$12_{3,10;-7}$

TABLE VII. Forbidden sub-branches.

A. *a* and *c* sub-branches.

Sub-branch $^{c,o}Q_{\bar{3},2}$	Sub-branch $^{c,e}Q_{3,\bar{2}}$	∓ 1	∓ 0.5	κ 0	± 0.5	± 1	Sub-branch $^{a,o}Q_{2,\bar{3}}$	Sub-branch $^{a,e}Q_{\bar{2},3}$
$3_{3,1;2}$	$3_{0,3;-3}$		104	169	69		$3_{1,3;-2}$	$3_{3,0;3}$
$4_{3,2;1}$	$4_{0,4;-4}$		356	283	68		$4_{2,3;-1}$	$4_{4,0;4}$
$5_{3,3;0}$	$5_{0,5;-5}$		621	286	53		$5_{3,3;0}$	$5_{5,0;5}$
$6_{3,4;-1}$	$6_{0,6;-6}$		773	250	43		$6_{4,3;1}$	$6_{6,0;6}$
$7_{3,5;-2}$	$7_{0,7;-7}$		809	213	35		$7_{5,3;2}$	$7_{7,0;7}$
$8_{3,6;-3}$	$8_{0,8;-8}$		774	183	30		$8_{6,3;3}$	$8_{8,0;8}$
$9_{3,7;-4}$	$9_{0,9;-9}$		712	160	26		$9_{7,3;4}$	$9_{9,0;9}$
$10_{3,8;-5}$	$10_{0,10;-10}$		645	141	23		$10_{8,3;5}$	$10_{10,0;10}$
$11_{3,9;-6}$	$11_{0,11;-11}$		584	127	21		$11_{9,3;6}$	$11_{11,0;11}$
$12_{3,10;-7}$	$12_{0,12;-12}$		531	115	19		$12_{10,3;7}$	$12_{12,0;12}$
$4_{4,1;3}$	$4_{1,3;-2}$		31	164	153		$4_{1,4;-3}$	$4_{3,1;2}$
$5_{4,2;2}$	$5_{1,4;-3}$		174	504	193		$5_{2,4;-2}$	$5_{4,1;3}$
$6_{4,3;1}$	$6_{1,5;-4}$		527	708	163		$6_{3,4;-1}$	$6_{5,1;4}$
$7_{4,4;0}$	$7_{1,6;-5}$		1057	716	131		$7_{4,4;0}$	$7_{6,1;5}$
$8_{4,5;-1}$	$8_{1,7;-6}$		1557	642	108		$8_{5,4;1}$	$8_{7,1;6}$
$9_{4,6;-2}$	$9_{1,8;-7}$		1855	559	92		$9_{6,4;2}$	$9_{8,1;7}$
$10_{4,7;-3}$	$10_{1,9;-8}$		1940	489	80		$10_{7,4;3}$	$10_{9,1;8}$
$11_{4,8;-4}$	$11_{1,10;-9}$		1888	432	71		$11_{8,4;4}$	$11_{10,1;9}$
$12_{4,9;-5}$	$12_{1,11;-10}$		1770	387	64		$12_{9,4;5}$	$12_{11,1;10}$
$5_{5,1;4}$	$5_{2,3;-1}$		9	79	191		$5_{1,5;-4}$	$5_{3,2;1}$
$6_{5,2;3}$	$6_{2,4;-2}$		52	413	342		$6_{2,5;-3}$	$6_{4,2;2}$
$7_{5,3;2}$	$7_{2,5;-3}$		187	919	325		$7_{3,5;-2}$	$7_{5,2;3}$
$8_{5,4;1}$	$8_{2,6;-4}$		515	1216	268		$8_{4,5;-1}$	$8_{6,2;4}$
$9_{5,5;0}$	$9_{2,7;-5}$		1123	1236	222		$9_{5,5;0}$	$9_{7,2;5}$
$10_{5,6;-1}$	$10_{2,8;-6}$		1924	1128	188		$10_{6,5;1}$	$10_{8,2;6}$
$11_{5,7;-2}$	$11_{2,9;-7}$		2650	999	163		$11_{7,5;2}$	$11_{9,2;7}$
$12_{5,8,-3}$	$12_{2,10;-8}$		3098	885	144		$12_{8,5;3}$	$12_{10,2;8}$
$6_{6,1;5}$	$6_{3,3;0}$		4	33	168		$6_{1,6;-5}$	$6_{3,3;0}$
$7_{6,2;4}$	$7_{3,4;-1}$		22	212	457		$7_{2,6;-4}$	$7_{4,3;1}$
$8_{6,3;3}$	$8_{3,5;-2}$		68	714	524		$8_{3,6;-3}$	$8_{5,3;2}$
$9_{6,4;2}$	$9_{3,6;-3}$		184	1385	456		$9_{4,6;-2}$	$9_{6,3;3}$
$10_{6,5;1}$	$10_{3,7;-4}$		445	1777	379		$10_{5,6;-1}$	$10_{7,3;4}$
$11_{6,6;0}$	$11_{3,8;-5}$		971	1816	320		$11_{6,6;0}$	$11_{8,3;5}$
$12_{6,7;-1}$	$12_{3,9;-6}$		1829	1681	277		$12_{7,6;1}$	$12_{9,3;6}$

TABLE VII.—*Continued.*

Sub-branch				κ			Sub-branch	
$^{c,e}Q\bar{3},2$	$^{c,e}Q3,\bar{2}$	∓1	∓0.5	0	±0.5	±1	$^{a,e}Q2,\bar{3}$	$^{a,e}Q\bar{2},3$
$7_{7,1;6}$	$7_{4,3;1}$		3	17	114		$7_{1,7;-6}$	$7_{3,4;-1}$
$8_{7,2;5}$	$8_{4,4;0}$		13	98	480		$8_{2,7;-5}$	$8_{4,4;0}$
$9_{7,3;4}$	$9_{4,5;-1}$		36	385	714		$9_{3,7;-4}$	$9_{5,4;1}$
$10_{7,4;3}$	$10_{4,6;-2}$		84	1053	686		$10_{4,7;-3}$	$10_{6,4;2}$
$11_{7,5;2}$	$11_{4,7;-3}$		183	1885	584		$11_{5,7;-2}$	$11_{7,4;3}$
$12_{7,6;1}$	$12_{4,8;-4}$		384	2375	493		$12_{6,7;-1}$	$12_{8,4;4}$
$8_{8,1;7}$	$8_{5,3;2}$		2	10	69		$8_{1,8;-7}$	$8_{3,5;-2}$
$9_{8,2;6}$	$9_{5,4;1}$		8	52	403		$9_{2,8;-6}$	$9_{4,5;-1}$
$10_{8,3;5}$	$10_{5,5;0}$		23	190	830		$10_{3,8;-5}$	$10_{5,5;0}$
$11_{8,4;4}$	$11_{5,6;-1}$		52	588	931		$11_{4,8;-4}$	$11_{6,5;1}$
$12_{8,5;3}$	$12_{5,7;-2}$		102	1419	832		$12_{5,8;-3}$	$12_{7,5;2}$
$9_{9,1;8}$	$9_{6,3;3}$		1	7	41		$9_{1,9;-8}$	$9_{3,6;-3}$
$10_{9,2;7}$	$10_{6,4;2}$		6	34	282		$10_{2,9;-7}$	$10_{4,6;-2}$
$11_{9,3;6}$	$11_{6,5;1}$		17	106	817		$11_{3,9;-6}$	$11_{5,6;-1}$
$12_{9,4;5}$	$12_{6,6;0}$		36	304	1141		$12_{4,9;-5}$	$12_{6,6;0}$
$10_{10,1;9}$	$10_{7,3;4}$		1	5	25		$10_{1,10;-9}$	$10_{3,7;-4}$
$11_{10,2;8}$	$11_{7,4;3}$		5	24	180		$11_{2,10;-8}$	$11_{4,7;-3}$
$12_{10,3;7}$	$12_{7,5;2}$		12	70	677		$12_{3,10;-7}$	$12_{5,7;-2}$
$11_{11,1;10}$	$11_{8,3;5}$		1	4	17		$11_{1,11;-10}$	$11_{3,8;-5}$
$12_{11,2;9}$	$12_{8,4;4}$		4	19	112		$12_{2,11;-9}$	$12_{4,8;-4}$
$12_{12,1;11}$	$12_{9,3;6}$		0	3	13		$12_{1,12;-11}$	$12_{3,9;-6}$
$^{c,e}Q\bar{3},4$	$^{c,e}Q3,\bar{4}$	∓1	∓0.5	0	±0.5	±1	$^{a,e}Q4,\bar{3}$	$^{a,e}Q\bar{4},3$
$4_{4,0;4}$	$4_{1,4;-3}$		8	10	2		$4_{0,4;-4}$	$4_{4,1;3}$
$5_{4,1;3}$	$5_{1,5;-4}$		24	14	1		$5_{1,4;-3}$	$5_{5,1;4}$
$6_{4,2;2}$	$6_{1,6;-5}$		42	9	0		$6_{2,4;-2}$	$6_{6,1;5}$
$7_{4,3;1}$	$7_{1,7;-6}$		51	2	0		$7_{3,4;-1}$	$7_{7,1;6}$
$8_{4,4;0}$	$8_{1,8;-7}$		48	1	0		$8_{4,4;0}$	$8_{8,1;7}$
$9_{4,5;-1}$	$9_{1,9;-8}$		35	1	0		$9_{5,4;1}$	$9_{9,1;8}$
$10_{4,6;-2}$	$10_{1,10;-9}$		22	0	0		$10_{6,4;2}$	$10_{10,1;9}$
$11_{4,7;-3}$	$11_{1,11;-10}$		12	0	0		$11_{7,4;3}$	$11_{11,1;10}$
$12_{4,8;-4}$	$12_{1,12;-11}$		7	0	0		$12_{8,4;4}$	$12_{12,1;11}$
$5_{5,0;5}$	$5_{2,4;-2}$		7	17	7		$5_{0,5;-5}$	$5_{4,2;2}$
$6_{5,1;4}$	$6_{2,5;-3}$		27	39	4		$6_{1,5;-4}$	$6_{5,2;3}$
$7_{5,2;3}$	$7_{2,6;-4}$		62	44	1		$7_{2,5;-3}$	$7_{6,2;4}$
$8_{5,3;2}$	$8_{2,7;-5}$		106	28	0		$8_{3,5;-2}$	$8_{7,2;5}$
$9_{5,4;1}$	$9_{2,8;-6}$		142	13	0		$9_{4,5;-1}$	$9_{8,2;6}$
$10_{5,5;0}$	$10_{2,9;-7}$		154	5	0		$10_{5,5;0}$	$10_{9,2;7}$
$11_{5,6;-1}$	$11_{2,10;-8}$		137	3	0		$11_{6,5;1}$	$11_{10,2;8}$
$12_{5,7;-2}$	$12_{2,11;-9}$		102	1	0		$12_{7,5;2}$	$12_{11,2;9}$
$6_{6,0;6}$	$6_{3,4;-1}$		4	16	14		$6_{0,6;-6}$	$6_{4,3;1}$
$7_{6,1;5}$	$7_{3,5;-2}$		19	53	15		$7_{1,6;-5}$	$7_{5,3;2}$
$8_{6,2;4}$	$8_{3,6;-3}$		50	88	5		$8_{2,6;-4}$	$8_{6,3;3}$
$9_{6,3;3}$	$9_{3,7;-4}$		102	88	2		$9_{3,6;-3}$	$9_{7,3;4}$
$10_{6,4;2}$	$10_{3,8;-5}$		170	56	1		$10_{4,6;-2}$	$10_{8,3;5}$
$11_{6,5;1}$	$11_{3,9;-6}$		240	27	0		$11_{5,6;-1}$	$11_{9,3;6}$
$12_{6,6;0}$	$12_{3,10;-7}$		289	12	0		$12_{6,6;0}$	$12_{10,3;7}$
$7_{7,0;7}$	$7_{4,4;0}$		3	13	19		$7_{0,7;-7}$	$7_{4,4;0}$
$8_{7,1;6}$	$8_{4,5;-1}$		12	51	30		$8_{1,7;-6}$	$8_{5,4;1}$
$9_{7,2;5}$	$9_{4,6;-2}$		34	108	17		$9_{2,7;-5}$	$9_{6,4;2}$
$10_{7,3;4}$	$10_{4,7;-3}$		74	152	5		$10_{3,7;-4}$	$10_{7,4;3}$
$11_{7,4;3}$	$11_{4,8;-4}$		137	144	2		$11_{4,7;-3}$	$11_{8,4;4}$
$12_{7,5;2}$	$12_{4,9;-5}$		223	93	1		$12_{5,7;-2}$	$12_{9,4;5}$
$8_{8,0;8}$	$8_{5,4;1}$		2	10	20		$8_{0,8;-8}$	$8_{4,5;-1}$
$9_{8,1;7}$	$9_{5,5;0}$		8	41	46		$9_{1,8;-7}$	$9_{5,5;0}$
$10_{8,2;6}$	$10_{5,6;-1}$		23	102	39		$10_{2,8;-6}$	$10_{6,5;1}$
$11_{8,3;5}$	$11_{5,7;-2}$		51	179	15		$11_{3,8;-5}$	$11_{7,5;2}$
$12_{8,4;4}$	$12_{5,8;-3}$		97	229	5		$12_{4,8;-4}$	$12_{8,5;3}$

TABLE VII.—*Continued.*

Sub-branch				κ			Sub-branch	
$^{c,e}Q_{3,4}$	$^{c,e}Q_{3,\bar{4}}$	∓ 1	∓ 0.5	0	± 0.5	± 1	$^{a,e}Q_{4,\bar{3}}$	$^{a,e}Q_{\bar{4},3}$
$9_{9,0;9}$	$9_{6,4;2}$		1	7	19		$9_{0,9;-9}$	$9_{4,6;-2}$
$10_{9,1;8}$	$10_{6,5;1}$		6	32	56		$10_{1,9;-8}$	$10_{5,6;-1}$
$11_{9,2;7}$	$11_{6,6;0}$		17	84	67		$11_{2,9;-7}$	$11_{6,6;0}$
$12_{9,3;6}$	$12_{6,7;-1}$		36	169	37		$12_{3,9;-6}$	$12_{7,6;1}$
$10_{10,0;10}$	$10_{7,4;3}$		1	5	17		$10_{0,10;-10}$	$10_{4,7;-3}$
$11_{10,1;9}$	$11_{7,5;2}$		5	24	59		$11_{1,10;-9}$	$11_{5,7;-2}$
$12_{10,2;8}$	$12_{7,6;1}$		12	66	93		$12_{2,10;-8}$	$12_{6,7;-1}$
$11_{11,0;11}$	$11_{8,4;4}$		1	4	14		$11_{0,11;-11}$	$11_{4,8;-4}$
$12_{11,1;10}$	$12_{8,5;3}$		4	19	57		$12_{1,11;-10}$	$12_{5,8;-3}$
$12_{12,0;12}$	$12_{9,4;5}$		0	3	12		$12_{0,12;-12}$	$12_{4,9;-5}$
$^{c,e}R_{3,\bar{2}}$	$^{c,e}P_{\bar{3},2}$	∓ 1	∓ 0.5	0	± 0.5	± 1	$^{a,e}R_{\bar{2},3}$	$^{a,e}P_{2,\bar{3}}$
$2_{0,2;-2}$	$3_{3,0;3}$		75	215	138		$2_{2,0;2}$	$3_{0,3,-3}$
$3_{0,3;-3}$	$4_{3,1;2}$		294	313	51		$3_{3,0;3}$	$4_{1,3;-2}$
$4_{0,4;-4}$	$5_{3,2;1}$		528	176	17		$4_{4,0;4}$	$5_{2,3;-1}$
$5_{0,5,-5}$	$6_{3,3;0}$		558	79	9		$5_{5,0;5}$	$6_{3,3;0}$
$6_{0,6;-6}$	$7_{3,4;-1}$		418	41	5		$6_{6,0;6}$	$7_{4,3;1}$
$7_{0,7;-7}$	$8_{3,5;-2}$		263	26	4		$7_{7,0;7}$	$8_{5,3;2}$
$8_{0,8;-8}$	$9_{3,6;-3}$		159	19	3		$8_{8,0;8}$	$9_{6,3;3}$
$9_{0,9;-9}$	$10_{3,7;-4}$		102	14	2		$9_{9,0;9}$	$10_{7,3;4}$
$10_{0,10;-10}$	$11_{3,8;-5}$		70	11	2		$10_{10,0;10}$	$11_{8,3;5}$
$11_{0,11;-11}$	$12_{3,9;-6}$		53	9	1		$11_{11,0;11}$	$12_{9,3;6}$
$3_{1,2;-1}$	$4_{4,0;4}$		24	146	272		$3_{2,1;1}$	$4_{0,4;-4}$
$4_{1,3;-2}$	$5_{4,1;3}$		122	538	212		$4_{3,1;2}$	$5_{1,4;-3}$
$5_{1,4;-3}$	$6_{4,2;2}$		377	665	76		$5_{4,1;3}$	$6_{2,4;-2}$
$6_{1,5;-4}$	$7_{4,3;1}$		803	409	34		$6_{5,1;4}$	$7_{3,4;-1}$
$7_{1,6;-5}$	$8_{4,4;0}$		1171	206	21		$7_{6,1;5}$	$8_{4,4;0}$
$8_{1,7;-6}$	$9_{4,5;-1}$		1200	115	15		$8_{7,1;6}$	$9_{5,4;1}$
$9_{1,8;-7}$	$10_{4,6;-2}$		938	76	11		$9_{8,1;7}$	$10_{6,4;2}$
$10_{1,9;-8}$	$11_{4,7;-3}$		631	57	9		$10_{9,1;8}$	$11_{7,4;3}$
$11_{1,10;-9}$	$12_{4,8;-4}$		409	45	7		$11_{10,1;9}$	$12_{8,4;4}$
$4_{2,2;0}$	$5_{5,0;5}$		11	70	262		$4_{2,2;0}$	$5_{0,5;-5}$
$5_{2,3;-1}$	$6_{5,1;4}$		46	359	464		$5_{3,2;1}$	$6_{1,5;-4}$
$6_{2,4;-2}$	$7_{5,2;3}$		142	894	220		$6_{4,2;2}$	$7_{2,5;-3}$
$7_{2,5;-3}$	$8_{5,3;2}$		364	1038	92		$7_{5,2;3}$	$8_{3,5;-2}$
$8_{2,6;-4}$	$9_{5,4;1}$		793	675	52		$8_{6,2;4}$	$9_{4,5;-1}$
$9_{2,7;-5}$	$10_{5,5;0}$		1395	365	36		$9_{7,2;5}$	$10_{5,5;0}$
$10_{2,8;-6}$	$11_{5,6;-1}$		1869	215	27		$10_{8,2;6}$	$11_{6,5;1}$
$11_{2,9;-7}$	$12_{5,7;-2}$		1887	148	21		$11_{9,2;7}$	$12_{7,5;2}$
$5_{3,2;1}$	$6_{6,0;6}$		7	39	184		$5_{2,3;-1}$	$6_{0,6;-6}$
$6_{3,3;0}$	$7_{6,1;5}$		27	187	624		$6_{3,3;0}$	$7_{1,6;-5}$
$7_{3,4;-1}$	$8_{6,2;4}$		69	610	487		$7_{4,3;1}$	$8_{2,6;-4}$
$8_{3,5;-2}$	$9_{6,3;3}$		157	1272	210		$8_{5,3;2}$	$9_{3,6;-3}$
$9_{3,6;-3}$	$10_{6,4;2}$		336	1426	108		$9_{6,3;3}$	$10_{4,6;-2}$
$10_{3,7;-4}$	$11_{6,5;1}$		684	963	71		$10_{7,3;4}$	$11_{5,6;-1}$
$11_{3,8;-5}$	$12_{6,6;0}$		1276	548	53		$11_{8,3;5}$	$12_{6,6;0}$
$6_{4,2;2}$	$7_{7,0;7}$		5	27	119		$6_{2,4;-2}$	$7_{0,7;-7}$
$7_{4,3;1}$	$8_{7,1;6}$		19	110	574		$7_{3,4;-1}$	$8_{1,7;-6}$
$8_{4,4;0}$	$9_{7,2;5}$		46	338	816		$8_{4,4;0}$	$9_{2,7;-5}$
$9_{4,5;-1}$	$10_{7,3;4}$		94	887	435		$9_{5,4;1}$	$10_{3,7;-4}$
$10_{4,6;-2}$	$11_{7,4;3}$		176	1662	205		$10_{6,4;2}$	$11_{4,7;-3}$
$11_{4,7;-3}$	$12_{7,5;2}$		321	1825	126		$11_{7,4;3}$	$12_{5,7;-2}$
$7_{5,2;3}$	$8_{8,0;8}$		4	21	81		$7_{2,5;-3}$	$8_{0,8;-8}$
$8_{5,3;2}$	$9_{8,1;7}$		15	78	424		$8_{3,5;-2}$	$9_{1,8;-7}$
$9_{5,4;1}$	$10_{8,2;6}$		36	206	995		$9_{4,5;-1}$	$10_{2,8;-6}$
$10_{5,5;0}$	$11_{8,3;5}$		69	514	790		$10_{5,5;0}$	$11_{3,8;-5}$
$11_{5,6;-1}$	$12_{8,4;4}$		121	1183	381		$11_{6,5;1}$	$12_{4,8;-4}$

TABLE VII.—*Continued.*

Sub-branch				κ			Sub-branch	
$^{c,e}R_{3,\bar{2}}$	$^{c,e}P_{\bar{3},2}$	∓ 1	∓ 0.5	0	± 0.5	± 1	$^{a,e}R_{\bar{2},3}$	$^{a,e}P_{2,\bar{3}}$
$8_{6,2;4}$	$9_{9,0;9}$		4	18	60		$8_{2,6;-4}$	$9_{0,9;-9}$
$9_{6,3;3}$	$10_{9,1;8}$		13	62	292		$9_{3,6;-3}$	$10_{1,9;-8}$
$10_{6,4;2}$	$11_{9,2;7}$		29	149	910		$10_{4,6;-2}$	$11_{2,9;-7}$
$11_{6,5;1}$	$12_{9,3;6}$		55	324	1182		$11_{5,6;-1}$	$12_{3,9;-6}$
$9_{7,2;5}$	$10_{10,0;10}$		3	15	48		$9_{2,7;-5}$	$10_{0,10;-10}$
$10_{7,3;4}$	$11_{10,1;9}$		11	52	207		$10_{3,7;-4}$	$11_{1,10;-9}$
$11_{7,4;3}$	$12_{10,2;8}$		24	121	694		$11_{4,7;-3}$	$12_{2,10;-8}$
$10_{8,2;6}$	$11_{11,0;11}$		3	13	41		$10_{2,8;-6}$	$11_{0,11;-11}$
$11_{8,3;5}$	$12_{11,1;10}$		9	45	158		$11_{3,8;-5}$	$12_{1,11;-10}$
$11_{9,2;7}$	$12_{12,0;12}$		2	12	36		$11_{2,9;-7}$	$12_{0,12;-12}$
$^{c,e}R_{3,\bar{2}}$	$^{c,e}P_{\bar{3},2}$	∓ 1	∓ 0.5	0	± 0.5	± 1	$^{a,e}R_{\bar{2},3}$	$^{a,e}P_{2,\bar{3}}$
$3_{1,3;-2}$	$4_{4,1;3}$		10	21	13		$3_{3,1;2}$	$4_{1,4;-3}$
$4_{1,4;-3}$	$5_{4,2;2}$		31	38	12		$4_{4,1;3}$	$5_{2,4;-2}$
$5_{1,5;-4}$	$6_{4,3;1}$		56	39	8		$5_{5,1;4}$	$6_{3,4;-1}$
$6_{1,6;-5}$	$7_{4,4;0}$		73	32	5		$6_{6,1;5}$	$7_{4,4;0}$
$7_{1,7;-6}$	$8_{4,5;-1}$		80	24	4		$7_{7,1;6}$	$8_{5,4;1}$
$8_{1,8;-7}$	$9_{4,6;-2}$		77	18	3		$8_{8,1;7}$	$9_{6,4;2}$
$9_{1,9;-8}$	$10_{4,7;-3}$		68	14	2		$9_{9,1;8}$	$10_{7,4;3}$
$10_{1,10;-9}$	$11_{4,8;-4}$		58	11	2		$10_{10,1;9}$	$11_{8,4;4}$
$11_{1,11;-10}$	$12_{4,9;-5}$		49	9	1		$11_{11,1;10}$	$12_{9,4;5}$
$4_{2,3;-1}$	$5_{5,1;4}$		9	31	32		$4_{3,2;1}$	$5_{1,5;-4}$
$5_{2,4;-2}$	$6_{5,2;3}$		33	79	39		$5_{4,2;2}$	$6_{2,5;-3}$
$6_{2,5;-3}$	$7_{5,3;2}$		73	108	30		$6_{5,2;3}$	$7_{3,5;-2}$
$7_{2,6;-4}$	$8_{5,4;1}$		124	108	21		$7_{6,2;4}$	$8_{4,5;-1}$
$8_{2,7;-5}$	$9_{5,5;0}$		172	91	15		$8_{7,2;5}$	$9_{5,5;0}$
$9_{2,8;-6}$	$10_{5,6;-1}$		205	72	11		$9_{8,2;6}$	$10_{6,5;1}$
$10_{2,9;-7}$	$11_{5,7;-2}$		216	56	9		$10_{9,2;7}$	$11_{7,5;2}$
$11_{2,10;-8}$	$12_{5,8;-3}$		209	45	7		$11_{10,2;8}$	$12_{8,5;3}$
$5_{3,3;0}$	$6_{6,1;5}$		7	30	46		$5_{3,3;0}$	$6_{1,6;-5}$
$6_{3,4;-1}$	$7_{6,2;4}$		25	92	76		$6_{4,3;1}$	$7_{2,6;-4}$
$7_{3,5;-2}$	$8_{6,3;3}$		60	163	67		$7_{5,3;2}$	$8_{3,6;-3}$
$8_{3,6;-3}$	$9_{6,4;2}$		115	202	50		$8_{6,3;3}$	$9_{4,6;-2}$
$9_{3,7;-4}$	$10_{6,5;1}$		187	199	36		$9_{7,3;4}$	$10_{5,6;-1}$
$10_{3,8;-5}$	$11_{6,6;0}$		267	171	27		$10_{8,3;5}$	$11_{6,6;0}$
$11_{3,9;-6}$	$12_{6,7;-1}$		337	139	21		$11_{9,3;6}$	$12_{7,6;1}$
$6_{4,3;1}$	$7_{7,1;6}$		5	25	53		$6_{3,4;-1}$	$7_{1,7;-6}$
$7_{4,4;0}$	$8_{7,2;5}$		19	86	110		$7_{4,4;0}$	$8_{2,7;-5}$
$8_{4,5;-1}$	$9_{7,3;4}$		46	177	118		$8_{5,4;1}$	$9_{3,7;-4}$
$9_{4,6;-2}$	$10_{7,4;3}$		89	268	94		$9_{6,4;2}$	$10_{4,7;-3}$
$10_{4,7;-3}$	$11_{7,5;2}$		154	316	70		$10_{7,4;3}$	$11_{5,7;-2}$
$11_{4,8;-4}$	$12_{7,6;1}$		241	309	53		$11_{8,4;4}$	$12_{6,7;-1}$
$7_{5,3;2}$	$8_{8,1;7}$		4	21	53		$7_{3,5;-2}$	$8_{1,8;-7}$
$8_{5,4;1}$	$9_{8,2;6}$		15	73	134		$8_{4,5;-1}$	$9_{2,8;-6}$
$9_{5,5;0}$	$10_{8,3;5}$		35	163	173		$9_{5,5;0}$	$10_{3,8;-5}$
$10_{5,6;-1}$	$11_{8,4;4}$		69	281	155		$10_{6,5;1}$	$11_{4,8;-4}$
$11_{5,7;-2}$	$12_{8,5;3}$		119	390	120		$11_{7,5;2}$	$12_{5,8;-3}$
$8_{6,3;3}$	$9_{9,1;8}$		4	18	49		$8_{3,6;-3}$	$9_{1,9;-8}$
$9_{6,4;2}$	$10_{9,2;7}$		13	61	143		$9_{4,6;-2}$	$10_{2,9;-7}$
$10_{6,5;1}$	$11_{9,3;6}$		29	140	219		$10_{5,6;-1}$	$11_{3,9;-6}$
$11_{6,6;0}$	$12_{9,4;5}$		54	258	224		$11_{6,6;0}$	$12_{4,9;-5}$
$9_{7,3;4}$	$10_{10,1;9}$		3	15	44		$9_{3,7;-4}$	$10_{1,10;-9}$
$10_{7,4;3}$	$11_{10,2;8}$		11	52	140		$10_{4,7;-3}$	$11_{2,10;-8}$
$11_{7,5;2}$	$12_{10,3;7}$		24	119	249		$11_{5,7;-2}$	$12_{3,10;-7}$
$10_{8,3;5}$	$11_{11,1;10}$		3	13	40		$10_{3,8;-5}$	$11_{1,11;-10}$
$11_{8,4;4}$	$12_{11,2;9}$		9	45	131		$11_{4,8;-4}$	$12_{2,11;-9}$
$11_{9,3;6}$	$12_{12,1;11}$		2	12	36		$11_{3,9;-6}$	$12_{1,12;-11}$

TABLE VII.—*Continued.*

Sub-branch				κ			Sub-branch	
$^{c,e}R_{3,4}^{\bar{3}}$	$^{c,e}P_{3,\bar{4}}$	∓1	∓0.5	0	±0.5	±1	$^{a,e}R_{4,\bar{3}}$	$^{a,e}P_{\bar{4},3}$
$3_{3,0;3}$	$4_{0,4;-4}$		28	18	2		$3_{0,3;-3}$	$4_{4,0;4}$
$4_{3,1;2}$	$5_{0,5;-5}$		78	17	0		$4_{1,3;-2}$	$5_{5,0;5}$
$5_{3,2;1}$	$6_{0,6;-6}$		107	8	0		$5_{2,3;-1}$	$6_{6,0;6}$
$6_{3,3;0}$	$7_{0,7;-7}$		96	3	0		$6_{3,3;0}$	$7_{7,0;7}$
$7_{3,4;-1}$	$8_{0,8;-8}$		65	2	0		$7_{4,3;1}$	$8_{8,0;8}$
$8_{3,5;-2}$	$9_{0,9;-9}$		39	1	0		$8_{5,3;2}$	$9_{9,0;9}$
$9_{3,6;-3}$	$10_{0,10;-10}$		23	1	0		$9_{6,3;3}$	$10_{10,0;10}$
$10_{3,7;-4}$	$11_{0,11,-11}$		14	1	0		$10_{7,3;4}$	$11_{11,0;11}$
$11_{3,8;-5}$	$12_{0,12,-12}$		9	0	0		$11_{8,3;5}$	$12_{12,0;12}$
$4_{4,0;4}$	$5_{1,4;-3}$		11	31	7		$4_{0,4;-4}$	$5_{4,1;3}$
$5_{4,1;3}$	$6_{1,5;-4}$		58	62	3		$5_{1,4;-3}$	$6_{5,1;4}$
$6_{4,2;2}$	$7_{1,6;-5}$		152	51	1		$6_{2,4;-2}$	$7_{6,1;5}$
$7_{4,3;1}$	$8_{1,7;-6}$		252	25	0		$7_{3,4;-1}$	$8_{7,1;6}$
$8_{4,4;0}$	$9_{1,8;-7}$		290	11	0		$8_{4,4;0}$	$9_{8,1;7}$
$9_{4,5;-1}$	$10_{1,9;-8}$		250	6	0		$9_{5,4;1}$	$10_{9,1;8}$
$10_{4,6;-2}$	$11_{1,10;-9}$		175	4	0		$10_{6,4;2}$	$11_{10,1;9}$
$11_{4,7;-3}$	$12_{1,11;-10}$		109	3	0		$11_{7,4;3}$	$12_{11,1;10}$
$5_{5,0;5}$	$6_{2,4;-2}$		3	21	15		$5_{0;5;-5}$	$6_{4,2;2}$
$6_{5,1;4}$	$7_{2,5;-3}$		17	83	12		$6_{1,5;-4}$	$7_{5,2;3}$
$7_{5,2;3}$	$8_{2,6;-4}$		65	124	4		$7_{2,5;-3}$	$8_{6,2;4}$
$8_{5,3;2}$	$9_{2,7;-5}$		173	96	1		$8_{3,5;-2}$	$9_{7,2;5}$
$9_{5,4;1}$	$10_{2,8;-6}$		335	50	1		$9_{4,5;-1}$	$10_{8,2;6}$
$10_{5,5;0}$	$11_{2,9;-7}$		477	23	0		$10_{5,5;0}$	$11_{9,2;7}$
$11_{5,6;-1}$	$12_{2,10;-8}$		517	13	0		$11_{6,5;1}$	$12_{10,2;8}$
$6_{6,0;6}$	$7_{3,4;-1}$		1	9	21		$6_{0,6;-6}$	$7_{4,3;1}$
$7_{6,1;5}$	$8_{3,5;-2}$		5	59	28		$7_{1,6;-5}$	$8_{5,3;2}$
$8_{6,2;4}$	$9_{3,6;-3}$		20	151	12		$8_{2,6;-4}$	$9_{6,3;3}$
$9_{6,3;3}$	$10_{3,7;-4}$		60	198	4		$9_{3,6;-3}$	$10_{7,3;4}$
$10_{6,4;2}$	$11_{3,8;-5}$		155	151	2		$10_{4,6;-2}$	$11_{8,3;5}$
$11_{6,5;1}$	$12_{3,9;-6}$		329	81	1		$11_{5,6;-1}$	$12_{9,3;6}$
$7_{7,0;7}$	$8_{4,4;0}$		0	4	20		$7_{0,7;-7}$	$8_{4,4;0}$
$8_{7,1;6}$	$9_{4,5;-1}$		2	26	46		$8_{1,7;-6}$	$9_{5,4;1}$
$9_{7,2;5}$	$10_{4,6;-2}$		8	107	31		$9_{2,7;-5}$	$10_{6,4;2}$
$10_{7,3;4}$	$11_{4,7;-3}$		22	230	11		$10_{3,7;-4}$	$11_{7,4;3}$
$11_{7,4;3}$	$12_{4,8;-4}$		55	282	4		$11_{4,7;-3}$	$12_{8,4;4}$
$8_{8,0;8}$	$9_{5,4;1}$		0	2	15		$8_{0,8;-8}$	$9_{4,5;-1}$
$9_{8,1;7}$	$10_{5,5;0}$		1	12	56		$9_{1,8;-7}$	$10_{5,5;0}$
$10_{8,2;6}$	$11_{5,6;-1}$		4	54	59		$10_{2,8;-6}$	$11_{6,5;1}$
$11_{8,3;5}$	$12_{5,7;-2}$		11	165	27		$11_{3,8;-5}$	$12_{7,5;2}$
$9_{9,0;9}$	$10_{6,4;2}$		0	1	10		$9_{0,9;-9}$	$10_{4,6;-2}$
$10_{9,1;8}$	$11_{6,5;1}$		1	6	53		$10_{1,9;-8}$	$11_{5,6;-1}$
$11_{9,2;7}$	$12_{6,6;0}$		3	25	87		$11_{2,9;-7}$	$12_{6,6;0}$
$10_{10,0;10}$	$11_{7,4;3}$		0	1	5		$10_{0,10;-10}$	$11_{4,7;-3}$
$11_{10,1;9}$	$12_{7,5;2}$		1	4	41		$11_{1,10;-9}$	$12_{5,7;-2}$
$11_{11,0;11}$	$12_{8,4;4}$		0	0	3		$11_{0,11;-11}$	$12_{4,8;-4}$
$^{c,o}R_{3,4}^{\bar{3}}$	$^{c,o}P_{3,\bar{4}}$	∓1	∓0.5	0	±0.5	±1	$^{a,o}R_{4,\bar{3}}$	$^{a,o}P_{\bar{4},3}$
$4_{4,1;3}$	$5_{1,5;-4}$		2	1	0		$4_{1,4;-3}$	$5_{5,1;4}$
$5_{4,2;2}$	$6_{1,6;-5}$		5	2	0		$5_{2,4;-2}$	$6_{6,1;5}$
$6_{4,3;1}$	$7_{1,7;-6}$		8	2	0		$6_{3,4;-1}$	$7_{7,1;6}$
$7_{4,4;0}$	$8_{1,8;-7}$		11	1	0		$7_{4,4;0}$	$8_{8,1;7}$
$8_{4,5;-1}$	$9_{1,9;-8}$		12	1	0		$8_{5,4;1}$	$9_{9,1;8}$
$9_{4,6;-2}$	$10_{1,10;-9}$		11	1	0		$9_{6,4;2}$	$10_{10,1;9}$
$10_{4,7;-3}$	$11_{1,11;-10}$		9	1	0		$10_{7,4;3}$	$11_{11,1;10}$
$11_{4,8;-4}$	$12_{1,12;-11}$		8	0	0		$11_{8,4;4}$	$12_{12,1;11}$

TABLE VII.—*Continued.*

Sub-branch				κ			Sub-branch	
$^{c,o}R\bar{3},4$	$^{c,o}P3,\bar{4}$	∓1	∓0.5	0	±0.5	±1	$^{a,o}R4,\bar{3}$	$^{a,o}P\bar{4},3$
$5_{5,1;4}$	$6_{2,5;-3}$		1	2	0		$5_{1,5;-4}$	$6_{5,2;3}$
$6_{5,2;3}$	$7_{2,6;-4}$		6	5	0		$6_{2,5;-3}$	$7_{6,2;4}$
$7_{5,3;2}$	$8_{2,7;-5}$		14	6	0		$7_{3,5;-2}$	$8_{7,2;5}$
$8_{5,4;1}$	$9_{2,8;-6}$		23	6	0		$8_{4,5;-1}$	$9_{8,2;6}$
$9_{5,5;0}$	$10_{2,9;-7}$		32	4	0		$9_{5,5;0}$	$10_{9,2;7}$
$10_{5,6;-1}$	$11_{2,10;-8}$		36	3	0		$10_{6,5;1}$	$11_{10,2;8}$
$11_{5,7;-2}$	$12_{2,11;-9}$		37	3	0		$11_{7,5;2}$	$12_{11,2;9}$
$6_{6,1;5}$	$7_{3,5;-2}$		1	2	1		$6_{1,6;-5}$	$7_{5,3;2}$
$7_{6,2;4}$	$8_{3,6;-3}$		4	8	1		$7_{2,6;-4}$	$8_{6,3;3}$
$8_{6,3;3}$	$9_{3,7;-4}$		11	13	1		$8_{3,6;-3}$	$9_{7,3;4}$
$9_{6,4;2}$	$10_{3,8,-5}$		23	14	1		$9_{4,6;-2}$	$10_{8,3;5}$
$10_{6,5;1}$	$11_{3,9;-6}$		39	13	0		$10_{5,6;-1}$	$11_{9,3;6}$
$11_{6,6;0}$	$12_{3,10;-7}$		56	10	0		$11_{6,6;0}$	$12_{10,3;7}$
$7_{7,1;6}$	$8_{4,5;-1}$		0	2	2		$7_{1,7;-6}$	$8_{5,4;1}$
$8_{7,2;5}$	$9_{4,6;-2}$		2	8	3		$8_{2,7;-5}$	$9_{6,4;2}$
$9_{7,3;4}$	$10_{4,7;-3}$		7	17	2		$9_{3,7;-4}$	$10_{7,4;3}$
$10_{7,4;3}$	$11_{4,8;-4}$		16	24	1		$10_{4,7;-3}$	$11_{8,4;4}$
$11_{7,5;2}$	$12_{4,9;-5}$		32	25	1		$11_{5,7;-2}$	$12_{9,4;5}$
$8_{8,1;7}$	$9_{5,5;0}$		0	1	2		$8_{1,8;-7}$	$9_{5,5;0}$
$9_{8,2;6}$	$10_{5,6;-1}$		1	6	4		$9_{2,8;-6}$	$10_{6,5;1}$
$10_{8,3;5}$	$11_{5,7;-2}$		4	17	4		$10_{3,8;-5}$	$11_{7,5;2}$
$11_{8,4;4}$	$12_{5,8;-3}$		10	29	3		$11_{4,8;-4}$	$12_{8,5;3}$
$9_{9,1;8}$	$10_{6,5;1}$		0	1	2		$9_{1,9;-8}$	$10_{5,6;-1}$
$10_{9,2;7}$	$11_{6,6;0}$		1	5	5		$10_{2,9;-7}$	$11_{6,6;0}$
$11_{9,3;6}$	$12_{6,7;-1}$		3	14	7		$11_{3,9;-6}$	$12_{7,6;1}$
$10_{10,1;9}$	$11_{7,5;2}$		0	1	2		$10_{1,10;-9}$	$11_{5,7;-2}$
$11_{10,2;8}$	$12_{7,6;1}$		1	3	6		$11_{2,10;-8}$	$12_{6,7;-1}$
$11_{11,1;10}$	$12_{8,5;3}$		0	0	2		$11_{1,11;-10}$	$12_{5,8;-3}$

B. *b* sub-branches.

$^{b,e}Q\bar{3},3$	$^{b,e}Q3,\bar{3}$	∓1	∓0.5	0	±0.5	±1	$^{b,e}Q3,\bar{3}$	$^{b,e}Q\bar{3},3$
$3_{3,0;3}$	$3_{0,3;-3}$		138	297	138		$3_{0,3;-3}$	$3_{3,0;3}$
$4_{3,1;2}$	$4_{0,4;-4}$		445	319	41		$4_{1,3;-2}$	$4_{4,0;4}$
$5_{3,2;1}$	$5_{0,5;-5}$		674	158	13		$5_{2,3;-1}$	$5_{5,0;5}$
$6_{3,3;0}$	$6_{0,6;-6}$		640	67	6		$6_{3,3;0}$	$6_{6,0;6}$
$7_{3,4;-1}$	$7_{0,7;-7}$		450	33	4		$7_{4,3;1}$	$7_{7,0;7}$
$8_{3,5;-2}$	$8_{0,8;-8}$		273	21	3		$8_{5,3;2}$	$8_{8,0;8}$
$9_{3,6;-3}$	$9_{0,9;-9}$		162	15	2		$9_{6,3;3}$	$9_{9,0;9}$
$10_{3,7;-4}$	$10_{0,10;-10}$		101	11	1		$10_{7,3;4}$	$10_{10,0;10}$
$11_{3,8;-5}$	$11_{0,11;-11}$		69	9	1		$11_{8,3;5}$	$11_{11,0;11}$
$12_{3,9;-6}$	$12_{0,12;-12}$		52	7	1		$12_{9,3;6}$	$12_{12,0;12}$
$4_{4,0;4}$	$4_{1,3;-2}$		41	319	445		$4_{0,4;-4}$	$4_{3,1;2}$
$5_{4,1;3}$	$5_{1,4;-3}$		230	846	230		$5_{1,4;-3}$	$5_{4,1;3}$
$6_{4,2;2}$	$6_{1,5;-4}$		684	793	70		$6_{2,4;-2}$	$6_{5,1;4}$
$7_{4,3;1}$	$7_{1,6;-5}$		1287	422	29		$7_{3,4;-1}$	$7_{6,1;5}$
$8_{4,4;0}$	$8_{1,7;-6}$		1640	197	17		$8_{4,4;0}$	$8_{7,1;6}$
$9_{4,5;-1}$	$9_{1,8;-7}$		1513	105	11		$9_{5,4;1}$	$9_{8,1;7}$
$10_{4,6;-2}$	$10_{1,9;-8}$		1105	67	8		$10_{6,4;2}$	$10_{9,1;8}$
$11_{4,7;-3}$	$11_{1,10;-9}$		713	49	6		$11_{7,4;3}$	$11_{10,1;9}$
$12_{4,8;-4}$	$12_{1,11;-10}$		449	38	5		$12_{8,4;4}$	$12_{11,1;10}$
$5_{5,0;5}$	$5_{2,3;-1}$		13	158	674		$5_{0,5;-5}$	$5_{3,2;1}$
$6_{5,1;4}$	$6_{2,4;-2}$		70	793	684		$6_{1,5;-4}$	$6_{4,2;2}$
$7_{5,2;3}$	$7_{2,5;-3}$		248	1513	248		$7_{2,5;-3}$	$7_{5,2;3}$
$8_{5,3;2}$	$8_{2,6;-4}$		681	1360	91		$8_{3,5;-2}$	$8_{6,2;4}$
$9_{5,4;1}$	$9_{2,7;-5}$		1444	763	48		$9_{4,5;-1}$	$9_{7,2;5}$
$10_{5,5;0}$	$10_{2,8;-6}$		2306	380	31		$10_{5,5;0}$	$10_{8,2;6}$
$11_{5,6;-1}$	$11_{2,9;-7}$		2749	212	22		$11_{6,5;1}$	$11_{9,2;7}$
$12_{5,7;-2}$	$12_{2,10;-8}$		2519	141	16		$12_{7,5;2}$	$12_{10,2;8}$

TABLE VII.—*Continued.*

Sub-branch				κ			Sub-branch	
$^{b,a}Q_{3,3}$	$^{b,a}Q_{3,\bar{3}}$	∓1	∓0.5	0	±0.5	±1	$^{b,a}Q_{3,\bar{3}}$	$^{b,a}Q_{\bar{3},3}$
$6_{6,0;6}$	$6_{3,3;0}$		6	67	640		$6_{0,6;-6}$	$6_{3,3;0}$
$7_{6,1;5}$	$7_{3,4;-1}$		29	422	1287		$7_{1,6;-5}$	$7_{4,3;1}$
$8_{6,2;4}$	$8_{3,5;-2}$		91	1360	681		$8_{2,6;-4}$	$8_{5,3;2}$
$9_{6,3;3}$	$9_{3,6;-3}$		245	2252	245		$9_{3,6;-3}$	$9_{6,3;3}$
$10_{6,4;2}$	$10_{3,7;-4}$		592	1993	112		$10_{4,6;-2}$	$10_{7,3;4}$
$11_{6,5;1}$	$11_{3,8;-5}$		1278	1165	69		$11_{5,6;-1}$	$11_{8,3;5}$
$12_{6,6;0}$	$12_{3,9;-6}$		2337	609	48		$12_{6,6;0}$	$12_{9,3;6}$
$7_{7,0;7}$	$7_{4,3;1}$		4	33	450		$7_{0,7;-7}$	$7_{3,4;-1}$
$8_{7,1;6}$	$8_{4,4;0}$		17	197	1640		$8_{1,7;-6}$	$8_{4,4;0}$
$9_{7,2;5}$	$9_{4,5;-1}$		48	763	1444		$9_{2,7;-5}$	$9_{5,4;1}$
$10_{7,3;4}$	$10_{4,6;-2}$		112	1993	592		$10_{3,7;-4}$	$10_{6,4;2}$
$11_{7,4;3}$	$11_{4,7;-3}$		244	3040	244		$11_{4,7;-3}$	$11_{7,4;3}$
$12_{7,5;2}$	$12_{4,8;-4}$		512	2675	136		$12_{5,7;-2}$	$12_{8,4;4}$
$8_{8,0;8}$	$8_{5,3;2}$		3	21	273		$8_{0,8;-8}$	$8_{3,5;-2}$
$9_{8,1;7}$	$9_{5,4;1}$		11	105	1513		$9_{1,8;-7}$	$9_{4,5;-1}$
$10_{8,2;6}$	$10_{5,5;0}$		31	380	2306		$10_{2,8;-6}$	$10_{5,5;0}$
$11_{8,3;5}$	$11_{5,6;-1}$		69	1165	1278		$11_{3,8;-5}$	$11_{6,5;1}$
$12_{8,4;4}$	$12_{5,7;-2}$		136	2675	512		$12_{4,8;-4}$	$12_{7,5;2}$
$9_{9,0;9}$	$9_{6,3;3}$		2	15	162		$9_{0,9;-9}$	$9_{3,6;-3}$
$10_{9,1;8}$	$10_{6,4;2}$		8	67	1105		$10_{1,9;-8}$	$10_{4,6;-2}$
$11_{9,2;7}$	$11_{6,5;1}$		22	212	2749		$11_{2,9;-7}$	$11_{5,6;-1}$
$12_{9,3;6}$	$12_{6,6;0}$		48	609	2337		$12_{3,9;-6}$	$12_{6,6;-0}$
$10_{10,0;10}$	$10_{7,3;4}$		1	11	101		$10_{0,10;-10}$	$10_{3,7;-4}$
$11_{10,1;9}$	$11_{7,4;3}$		6	49	713		$11_{1,10;-9}$	$11_{4,7;-3}$
$12_{10,2;8}$	$12_{7,5;2}$		16	141	2519		$12_{2,10;-8}$	$12_{5,7;-2}$
$11_{11,0;11}$	$11_{8,3;5}$		1	9	69		$11_{0,11;-11}$	$11_{3,8;-5}$
$12_{11,1;10}$	$12_{8,4,4}$		5	38	449		$12_{1,11;-10}$	$12_{4,8;-4}$
$12_{12,0;12}$	$12_{9,3;6}$		1	7	52		$12_{0,12;-12}$	$12_{3,9;-6}$
$^{b,a}Q_{3,3}$	$^{b,a}Q_{3,\bar{3}}$	∓1	∓0.5	0	±0.5	±1	$^{b,a}Q_{3,\bar{3}}$	$^{b,a}Q_{\bar{3},3}$
$4_{4,1;3}$	$4_{1,4;-3}$		10	20	10		$4_{1,4;-3}$	$4_{4,1;3}$
$5_{4,2;2}$	$5_{1,5;-4}$		34	33	9		$5_{2,4;-2}$	$5_{5,1;4}$
$6_{4,3;1}$	$6_{1,6;-5}$		58	33	6		$6_{3,4;-1}$	$6_{6,1;5}$
$7_{4,4;0}$	$7_{1,7;-6}$		76	26	4		$7_{4,4;0}$	$7_{7,1;6}$
$8_{4,5;-1}$	$8_{1,8;-7}$		82	19	3		$8_{5,4;1}$	$8_{8,1;7}$
$9_{4,6;-2}$	$9_{1,9;-8}$		77	14	2		$9_{6,4;2}$	$9_{9,1;8}$
$10_{4,7;-3}$	$10_{1,10;-9}$		68	11	1		$10_{7,4;3}$	$10_{10,1;9}$
$11_{4,8;-4}$	$11_{1,11;-10}$		58	9	1		$11_{8,4;4}$	$11_{11,1;10}$
$12_{4,9;-5}$	$12_{1,12;-11}$		48	7	1		$12_{9,4;5}$	$12_{12,1;11}$
$5_{5,1;4}$	$5_{2,4;-2}$		9	33	34		$5_{1,5;-4}$	$5_{4,2;2}$
$6_{5,2;3}$	$6_{2,5;-3}$		36	83	36		$6_{2,5;-3}$	$6_{5,2;3}$
$7_{5,3;2}$	$7_{2,6;-4}$		84	108	25		$7_{3,5;-2}$	$7_{6,2;4}$
$8_{5,4;1}$	$8_{2,7;-5}$		144	102	16		$8_{4,5;-1}$	$8_{7,2;5}$
$9_{5,5;0}$	$9_{2,8;-6}$		199	83	11		$9_{5,5;0}$	$9_{8,2;6}$
$10_{5,6;-1}$	$10_{2,9;-7}$		233	63	8		$10_{6,5;1}$	$10_{9,2;7}$
$11_{5,7;-2}$	$11_{2,10;-8}$		241	48	6		$11_{7,5;2}$	$11_{10,2;8}$
$12_{5,8;-3}$	$12_{2,11;-9}$		228	38	5		$12_{8,5;3}$	$12_{11,2;9}$
$6_{6,1;5}$	$6_{3,4;-1}$		6	33	58		$6_{1,6;-5}$	$6_{4,3;1}$
$7_{6,2;4}$	$7_{3,5;-2}$		25	108	84		$7_{2,6;-4}$	$7_{5,3;2}$
$8_{6,3;3}$	$8_{3,6;-3}$		67	187	67		$8_{3,6;-3}$	$8_{6,3;3}$
$9_{6,4;2}$	$9_{3,7;-4}$		136	221	45		$9_{4,6;-2}$	$9_{7,3;4}$
$10_{6,5;1}$	$10_{3,8;-5}$		228	206	31		$10_{5,6;-1}$	$10_{8,3;5}$
$11_{6,6;0}$	$11_{3,9;-6}$		328	169	22		$11_{6,6;0}$	$11_{9,3;6}$
$12_{6,7;-1}$	$12_{3,10;-7}$		410	132	16		$12_{7,6;1}$	$12_{10,3;7}$

TABLE VII.—*Continued.*

Sub-branch				κ			Sub-branch	
$^{b,o}Q_{3,3}$	$^{b,o}Q_{3,\bar{3}}$	∓1	∓0.5	0	±0.5	±1	$^{b,o}Q_{3,\bar{3}}$	$^{b,o}Q_{\bar{3},3}$
$7_{7,1;6}$	$7_{4,4;0}$		4	26	76		$7_{1,7;-6}$	$7_{4,4;0}$
$8_{7,2;5}$	$8_{4,5;-1}$		16	102	144		$8_{2,7;-5}$	$8_{5,4;1}$
$9_{7,3;4}$	$9_{4,6;-2}$		45	221	136		$9_{3,7;-4}$	$9_{6,4;2}$
$10_{7,4;3}$	$10_{4,7;-3}$		98	327	98		$10_{4,7;-3}$	$10_{7,4;3}$
$11_{7,5;2}$	$11_{4,8;-4}$		183	367	68		$11_{5,7;-2}$	$11_{8,4;4}$
$12_{7,6;1}$	$12_{4,9;-5}$		299	340	48		$12_{6,7;-1}$	$12_{9,4;5}$
$8_{8,1;7}$	$8_{5,4;1}$		3	19	82		$8_{1,8;-7}$	$8_{4,5;-1}$
$9_{8,2;6}$	$9_{5,5;0}$		11	83	199		$9_{2,8;-6}$	$9_{5,5;0}$
$10_{8,3;5}$	$10_{5,6;-1}$		31	206	228		$10_{3,8;-5}$	$10_{6,5;1}$
$11_{8,4;4}$	$11_{5,7;-2}$		68	367	183		$11_{4,8;-4}$	$11_{7,5;2}$
$12_{8,5;3}$	$12_{5,8;-3}$		129	498	129		$12_{5,8;-3}$	$12_{8,5;3}$
$9_{9,1;8}$	$9_{6,4;2}$		2	14	77		$9_{1,9;-8}$	$9_{4,6;-2}$
$10_{9,2;7}$	$10_{6,5;1}$		8	63	233		$10_{2,9;-7}$	$10_{5,6;-1}$
$11_{9,3;6}$	$11_{6,6;0}$		22	169	328		$11_{3,9;-6}$	$11_{6,6;0}$
$12_{9,4;5}$	$12_{6,7;-1}$		48	340	299		$12_{4,9;-5}$	$12_{7,6;1}$
$10_{10,1;9}$	$10_{7,4;3}$		1	11	68		$10_{1,10;-9}$	$10_{4,7;-3}$
$11_{10,2;8}$	$11_{7,5;2}$		6	48	241		$11_{2,10;-8}$	$11_{5,7;-2}$
$12_{10,3;7}$	$12_{7,6;1}$		16	132	410		$12_{3,10;-7}$	$12_{6,7;-1}$
$11_{11,1;10}$	$11_{8,4;4}$		1	9	58		$11_{1,11;-10}$	$11_{4,8;-4}$
$12_{11,2;9}$	$12_{8,5;3}$		5	38	228		$12_{2,11;-9}$	$12_{5,8;-3}$
$12_{12,1;11}$	$12_{9,4;5}$		1	7	48		$12_{1,12;-11}$	$12_{4,9;-5}$
$^{b,o}R_{\bar{3},3}$	$^{b,e}P_{3,\bar{3}}$	∓1	∓0.5	0	±0.5	±1	$^{b,o}R_{3,\bar{3}}$	$^{b,e}P_{\bar{3},3}$
$3_{3,1;2}$	$4_{0,4;-4}$		38	41	13		$3_{1,3;-2}$	$4_{4,0;4}$
$4_{3,2;1}$	$5_{0,5;-5}$		111	62	12		$4_{2,3;-1}$	$5_{5,0;5}$
$5_{3,3;0}$	$6_{0,6;-6}$		175	59	9		$5_{3,3;0}$	$6_{6,0;6}$
$6_{3,4;-1}$	$7_{0,7;-7}$		206	50	7		$6_{4,3;1}$	$7_{7,0;7}$
$7_{3,5;-2}$	$8_{0,8;-8}$		209	42	6		$7_{5,3;2}$	$8_{8,0;8}$
$8_{3,6;-3}$	$9_{0,9;-9}$		195	35	5		$8_{6,3;3}$	$9_{9,0;9}$
$9_{3,7;-4}$	$10_{0,10;-10}$		177	30	4		$9_{7,3;4}$	$10_{10,0;10}$
$10_{3,8;-5}$	$11_{0,11;-11}$		158	27	4		$10_{8,3;5}$	$11_{11,0;11}$
$11_{3,9;-6}$	$12_{0,12;-12}$		142	24	3		$11_{9,3;6}$	$12_{12,0;12}$
$4_{4,1;3}$	$5_{1,4;-3}$		14	63	41		$4_{1,4;-3}$	$5_{4,1;3}$
$5_{4,2;2}$	$6_{1,5;-4}$		77	149	44		$5_{2,4;-2}$	$6_{5,1;4}$
$6_{4,3;1}$	$7_{1,6;-5}$		209	182	34		$6_{3,4;-1}$	$7_{6,1;5}$
$7_{4,4;0}$	$8_{1,7;-6}$		370	170	26		$7_{4,4;0}$	$8_{7,1;6}$
$8_{4,5;-1}$	$9_{1,8;-7}$		493	146	20		$8_{5,4;1}$	$9_{8,1;7}$
$9_{4,6;-2}$	$10_{1,9;-8}$		549	122	17		$9_{6,4;2}$	$10_{9,1;8}$
$10_{4,7;-3}$	$11_{1,10;-9}$		550	104	14		$10_{7,4;3}$	$11_{10,1;9}$
$11_{4,8;-4}$	$12_{1,11;-10}$		519	90	12		$11_{8,4;4}$	$12_{11,1;10}$
$5_{5,1;4}$	$6_{2,4;-2}$		3	43	71		$5_{1,5;-4}$	$6_{4,2;2}$
$6_{5,2;3}$	$7_{2,5;-3}$		23	175	97		$6_{2,5;-3}$	$7_{5,2;3}$
$7_{5,3;2}$	$8_{2,6;-4}$		87	305	80		$7_{3,5;-2}$	$8_{6,2;4}$
$8_{5,4;1}$	$9_{2,7;-5}$		234	347	61		$8_{4,5;-1}$	$9_{7,2;5}$
$9_{5,5;0}$	$10_{2,8;-6}$		466	324	47		$9_{5,5;0}$	$10_{8,2;6}$
$10_{5,6;-1}$	$11_{2,9;-7}$		715	279	38		$10_{6,5;1}$	$11_{9,2;7}$
$11_{5,7;-2}$	$12_{2,10;-8}$		896	237	32		$11_{7,5;2}$	$12_{10,2;8}$
$6_{6,1;5}$	$7_{3,4;-1}$		1	19	87		$6_{1,6;-5}$	$7_{4,3;1}$
$7_{6,2;4}$	$8_{3,5;-2}$		7	118	162		$7_{2,6;-4}$	$8_{5,3;2}$
$8_{6,3;3}$	$9_{3,6;-3}$		26	321	153		$8_{3,6;-3}$	$9_{6,3;3}$
$9_{6,4;2}$	$10_{3,7;-4}$		80	495	119		$9_{4,6;-2}$	$10_{7,3;4}$
$10_{6,5;1}$	$11_{3,8;-5}$		208	547	91		$10_{5,6;-1}$	$11_{8,3;5}$
$11_{6,6;0}$	$12_{3,9;-6}$		446	511	73		$11_{6,6;0}$	$12_{9,3;6}$
$7_{7,1;6}$	$8_{4,4;0}$		1	7	82		$7_{1,7;-6}$	$8_{4,4;0}$
$8_{7,2;5}$	$9_{4,5;-1}$		3	55	218		$8_{2,7;-5}$	$9_{5,4;1}$
$9_{7,3;4}$	$10_{4,6;-2}$		11	218	247		$9_{3,7;-4}$	$10_{6,4;2}$
$10_{7,4;3}$	$11_{4,7;-3}$		29	492	205		$10_{4,7;-3}$	$11_{7,4;3}$
$11_{7,5;2}$	$12_{4,8;-4}$		73	711	158		$11_{5,7;-2}$	$12_{8,4;4}$

TABLE VII.—*Continued.*

Sub-branch				κ			Sub-branch	
$^{b,o}R^{\bar{3}}_{3,3}$	$^{b,e}P_{3,\bar{3}}$	∓ 1	∓ 0.5	0	± 0.5	± 1	$^{b,o}R_{3,\bar{3}}$	$^{b,e}P^{\bar{3}}_{3,3}$
$8_{8,1;7}$	$9_{5,4;1}$		0	4	62		$8_{1,8;-7}$	$9_{4,5;-1}$
$9_{8,2;6}$	$10_{5,5;0}$		2	24	241		$9_{2,8;-6}$	$10_{5,5;0}$
$10_{8,3;5}$	$11_{5,6;-1}$		6	108	346		$10_{3,8;-5}$	$11_{6,5;1}$
$11_{8,4;4}$	$12_{5,7;-2}$		14	336	319		$11_{4,8;-4}$	$12_{7,5;2}$
$9_{9,1;8}$	$10_{6,4;2}$		0	2	38		$9_{1,9;-8}$	$10_{4,6;-2}$
$10_{9,2;7}$	$11_{6,5;1}$		1	12	219		$10_{2,9;-7}$	$11_{5,6;-1}$
$11_{9,3;6}$	$12_{6,6;0}$		4	50	420		$11_{3,9;-6}$	$12_{6,6;0}$
$10_{10,1;9}$	$11_{7,4;3}$		0	1	22		$10_{1,10;-9}$	$11_{4,7;-3}$
$11_{10,2;8}$	$12_{7,5;2}$		1	7	165		$11_{2,10;-8}$	$12_{5,7;-2}$
$11_{11,1;10}$	$12_{8,4;4}$		0	1	12		$11_{1,11;-10}$	$12_{4,8;-4}$
$^{b,e}R^{\bar{3}}_{3,5}$	$^{b,o}P_{3,\bar{5}}$	∓ 1	∓ 0.5	0	± 0.5	± 1	$^{b,e}R_{5,\bar{3}}$	$^{b,o}P^{\bar{5}}_{3,3}$
$4_{4,0;4}$	$5_{1,5;-4}$		2	2	0		$4_{0,4;-4}$	$5_{5,1;4}$
$5_{4,1;3}$	$6_{1,6;-5}$		6	3	0		$5_{1,4;-3}$	$6_{6,1;5}$
$6_{4,2;2}$	$7_{1,7;-6}$		11	2	0		$6_{2,4;-2}$	$7_{7,1;6}$
$7_{4,3;1}$	$8_{1,8;-7}$		13	1	0		$7_{3,4;-1}$	$8_{8,1;7}$
$8_{4,4;0}$	$9_{1,9;-8}$		12	0	0		$8_{4,4;0}$	$9_{9,1;8}$
$9_{4,5;-1}$	$10_{1,10;-9}$		9	0	0		$9_{5,4;1}$	$10_{10,1;9}$
$10_{4,6;-2}$	$11_{1,11;-10}$		5	0	0		$10_{6,4;2}$	$11_{11,1;10}$
$11_{4,7;-3}$	$12_{1,12;-11}$		3	0	0		$11_{7,4;3}$	$12_{12,1;11}$
$5_{5,0;5}$	$6_{2,5;-3}$		2	4	2		$5_{0,5;-5}$	$6_{5,2;3}$
$6_{5,1;4}$	$7_{2,6;-4}$		8	9	1		$6_{1,5;-4}$	$7_{6,2;4}$
$7_{5,2;3}$	$8_{2,7;-5}$		18	10	0		$7_{2,5;-3}$	$8_{7,2;5}$
$8_{5,3;2}$	$9_{2,8;-6}$		30	6	0		$8_{3,5;-2}$	$9_{8,2;6}$
$9_{5,4;1}$	$10_{2,9;-7}$		40	3	0		$9_{4,5;-1}$	$10_{9,2;7}$
$10_{5,5;0}$	$11_{2,10;-8}$		43	1	0		$10_{5,5;0}$	$11_{10,2;8}$
$11_{5,6;-1}$	$12_{2,11;-9}$		37	1	0		$11_{6,5;1}$	$12_{11,2;9}$
$6_{6,0;6}$	$7_{3,5;-2}$		1	5	4		$6_{0,6;-6}$	$7_{5,3;2}$
$7_{6,1;5}$	$8_{3,6;-3}$		5	15	4		$7_{1,6;-5}$	$8_{6,3;3}$
$8_{6,2;4}$	$9_{3,7;-4}$		15	24	1		$8_{2,6;-4}$	$9_{7,3;4}$
$9_{6,3;3}$	$10_{3,8;-5}$		31	23	0		$9_{3,6;-3}$	$10_{8,3;5}$
$10_{6,4;2}$	$11_{3,9;-6}$		52	14	0		$10_{4,6;-2}$	$11_{9,3;6}$
$11_{6,5;1}$	$12_{3,10;-7}$		73	6	0		$11_{5,6;-1}$	$12_{10,3;7}$
$7_{7,0;7}$	$8_{4,5;-1}$		1	4	6		$7_{0,7;-7}$	$8_{5,4;1}$
$8_{7,1;6}$	$9_{4,6;-2}$		3	16	9		$8_{1,7;-6}$	$9_{6,4;2}$
$9_{7,2;5}$	$10_{4,7;-3}$		9	33	4		$9_{2,7;-5}$	$10_{7,4;3}$
$10_{7,3;4}$	$11_{4,8;-4}$		22	44	1		$10_{3,7;-4}$	$11_{8,4;4}$
$11_{7,4;3}$	$12_{4,9;-5}$		42	39	0		$11_{4,7;-3}$	$12_{9,4;5}$
$8_{8,0;8}$	$9_{5,5;0}$		0	3	7		$8_{0,8;-8}$	$9_{5,5;0}$
$9_{8,1;7}$	$10_{5,6;-1}$		2	13	15		$9_{1,8;-7}$	$10_{6,5;1}$
$10_{8,2;6}$	$11_{5,7;-2}$		6	33	11		$10_{2,8;-6}$	$11_{7,5;2}$
$11_{8,3;5}$	$12_{5,8;-3}$		14	57	4		$11_{3,8;-5}$	$12_{8,5;3}$
$9_{9,0;9}$	$10_{6,5;1}$		0	2	8		$9_{0,9;-9}$	$10_{5,6;-1}$
$10_{9,1;8}$	$11_{6,6;0}$		1	9	21		$10_{1,9;-8}$	$11_{6,6;0}$
$11_{9,2;7}$	$12_{6,7;-1}$		4	28	22		$11_{2,9;-7}$	$12_{7,6;1}$
$10_{10,0;10}$	$11_{7,5;2}$		0	1	7		$10_{0,10;-10}$	$11_{5,7;-2}$
$11_{10,1;9}$	$12_{7,6;1}$		1	7	24		$11_{1,10;-9}$	$12_{6,7;-1}$
$11_{11,0;11}$	$12_{8,5;3}$		0	1	6		$11_{0,11;-11}$	$12_{5,8;-3}$

THE JOURNAL OF CHEMICAL PHYSICS VOLUME 12, NUMBER 6 JUNE, 1944

Electrical Anisotropy of Xerogels of Hydrophile Colloids

Part I*

S. E. SHEPPARD AND P. T. NEWSOME
Kodak Research Laboratories, Eastman Kodak Company, Rochester, New York

(Received April 3, 1944)

A number of colloid materials—proteins, plastics, and the like—have been coated in sheet form and "fibered" internally by stretching to 100 percent or more elongation. Circular disks were cut from the fibered sheets, and their degree of orientation measured in an (alternating) electric field. Account is given of the relation of the orientation measured to field strength, thickness, humidity, and moisture content. It was observed that induced electrical anisotropy is not shown by all kinds of natural and synthetic colloids; thus it is not shown by organophile xerogels, but only by the hydrophile ones. With most of these the electrical response depends upon the relative humidity and the absorbed water content, but with polyvinyl alcohol the effect was independent of the absorbed water.

INTRODUCTION

IT is well known that elongated particles in an electric field, if free to rotate, become oriented with their long axes parallel to the electric force. H. J. Woods[1] observed that wool cells exhibit the effect in high degree, being about 100μ in length, and only a few microns thick. When suspended in water they are readily pulled into alignment by an alternating field—used in place of a direct field to prevent drift of the cells.

Woods made the further observation that *circular* pieces, cylinders, or disks, of finger nail and of cow's horn, when suspended horizontally by a silk thread in an alternating field, tended to orient so that the direction of the protein chain was parallel to the electric force. Randomly oriented films of myosin and of denatured proteins showed no such electrical anistropy unless previously stretched. Such orientation was explained as due to a difference of dielectric constant for fields parallel and perpendicular, respectively, to the protein chains. However, the orienting effect caused by internal anisotropy was much less than that dependent on external shape. If the eccentricity exceeded about 0.4, the effect of fiber orientation could no longer be detected.

It appeared to us that the electrical orientation of disks might furnish interesting information on the direction and extent of molecular or micellar orientation, and we decided to apply it to various proteins, cellulose derivatives, and synthetic resins. Conversely, it appeared possible, from previous observations[2] on the influence of molecular or micellar orientation in cellulosic films upon static electrification, that the production of temporary electrets might throw light upon this problem also.

APPARATUS AND OPERATIONS

The sheet material was usually prepared in the form of disks 1.50 cm in diameter, but in some cases (for investigating the form factor) as oblong rectangles 1.50 cm long and 0.25 cm wide. In measurements they were suspended from a torsion head by a pure nickel wire 50.5 cm long and 0.00432 cm in diameter (cf. Fig. 1). The specimens were not attached directly to the wire, but to an intermediate short length of glass rod surmounted by a mirror 0.5 cm square which, in turn, was cemented to the wire. The section of glass rod prevents arcing between the electrodes and the wire. The electrodes consisted of pieces of brass rod 1.905 cm in diameter mounted 2 cm apart in Bakelite blocks. The image of a single-wire filament lamp was reflected from the small mirror and focused on the circular scale to permit measurement of the electric orientation. The measurement consisted in determining the

* Communication No. 970 from the Kodak Research Laboratories.

[1] H. J. Woods, Proc. Roy. Soc. London **A166**, 76 (1938).

[2] Unpublished observations of J. G. McNally of these Laboratories.

rotation of the torsion head necessary to bring the image of the lamp filament back to its zero position prior to application of the electric field.

The entire suspension, excluding the torsion head itself, was enclosed in a glass case firmly closed in front by a glass door. This eliminated disturbance by air currents and allowed control of humidity and temperature. The torsion wire extended through a very small hole drilled in the top of the enclosure.

RELEVANT QUANTITATIVE FACTORS

The voltage applied could be varied from 0 to 25,000 volts a.c. by the use of a transformer and a Variac (General Radio Company). The couple G required to twist the wire through an angle ϕ is given by the equation

$$G = na^4\phi/2l, \qquad (1)$$

where a = radius of wire in cm, l = length of wire in cm, and n = rigidity of wire in dynes per cm². The rigidity n was determined by measuring the period of oscillation of a thin brass disk having about the same weight as that of the suspended system actually used, *viz.*, 0.6 gram, and attached to the end of the wire. The value obtained was 6.44×10^{11} dynes per cm², whence the calculated value of G is 0.439 dyne per radian.

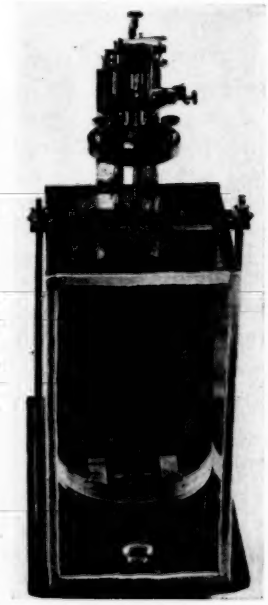

FIG. 1. Apparatus for determining the electrical anisotropy.

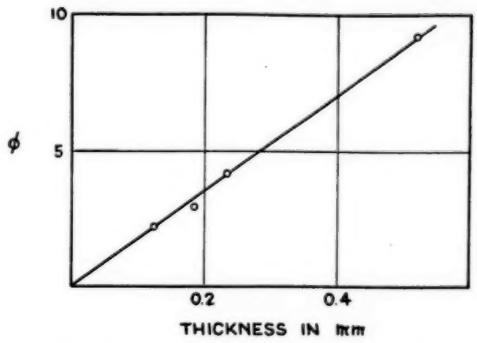

FIG. 2. Effect of thickness of specimen (cellulose acetate, 40 percent acetyl) on electrical anisotropy.

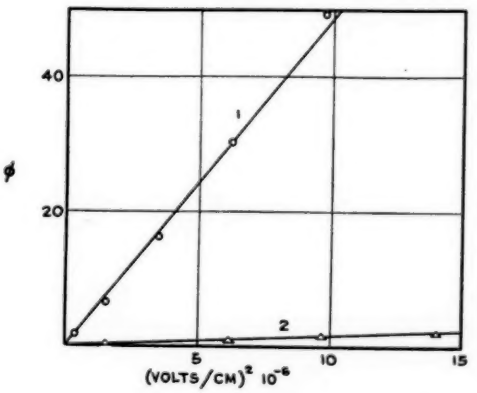

FIG. 3. Relation of E. A. to applied potential for polyvinyl alcohol and a polyvinyl (butal) (Vinylite X).

The electrical anisotropy, measured as ϕ, the angle of rotation, is expressible in reduced measure per unit volume as follows: It is a volume or mass property, proportional, therefore, to the thickness t of the specimen, as shown in Fig. 2. Further, the flux density of electrification will be proportional to V^2, where V is the applied potential difference between the electrodes,[3] experimentally demonstrated in Fig. 3. With circular, i.e., cylindrical reactors, there would be no electrical response for isotropic material. Otherwise, we have an axis of anisotropy, and the electrical response will be a function of the angle θ between this axis and that of the applied field. Functionally, then, ϕ is proportional to $\sin\theta\cos\theta$, that is, to $\sin 2\theta$. By setting θ at 45°, this factor becomes unity, and may be omitted. In our case, the *anisotropy* was enforced by

[3] Cf. J. S. Donal, Jr., and D. B. Langmuir, Proc. I. R. E. **31**, 208 (1943).

TABLE I. Electrical anisotropy of various colloids in disk form.

Material	Percent water absorption at 50% R. H.	Percent elongation	Hydroxyl content percent	E. A. ϕ/V^2l at 50% R. H.	Birefringence $n_\gamma - n_\beta$	X-ray evidence of orientation
Polyvinyl alcohol	6.7	250	38.6	$195 \cdot 10^{-6}$	$2350 \cdot 10^{-5}$	Yes
Gelatin	16.0	200		141	293	Yes
Cellulose acetate, 24.5% acetyl	8.1	100	14.8	23	1200	Yes
Polyvinyl acetal	3.8	350	6.4	10	544	Yes
Hydrolyzed polyvinyl acetate	2.5	550	5.5	9	12*	No
Vinylite X	1.9	220	9.1**	8	1120	Yes
Cellulose acetate, 40% acetyl	3.5	100	3.2	0	460	Yes
Cellulose nitrate	1.5	100	4.7	0	364	Yes
Polyvinyl acetate, R. H. 361	1.0	250	0	0	2*	No
Polyvinyl acetal	2.4	250	3.0	0	1250	Yes
Polystyrene	0.03	300	0	0	12*	No

* Maximum index n_γ is perpendicular to plane of the sheet in these cases. See J. Spence, J. Phys. Chem. **43**, 865 (1939); **45**, 401 (1941).
** Calculated on the assumption of one hydroxyl group to one divinylbutal group.
Note: Dependence of E. A. and the electrical conductance on water content is noted in the text.

stretching the original samples; on cutting out circular disks, the axis of anisotropy was parallel to the direction of (pre-)stretching. This conclusion, and the presence of anisotropy produced by stretching were confirmed by measurement of the optical birefringence (for material sufficiently transparent) and by x-ray diffraction investigation. Confirmation of the $\phi \propto \sin 2\theta$ relation is afforded by the results shown in Fig. 4. In our experiments, however, θ was generally set at 45°, when $\sin 2\theta = 1$ and does not appear in the expression.

OPERATING CONTROLS

The materials tested (cf. Table I) were usually coated from solution in sheet form on glass, and

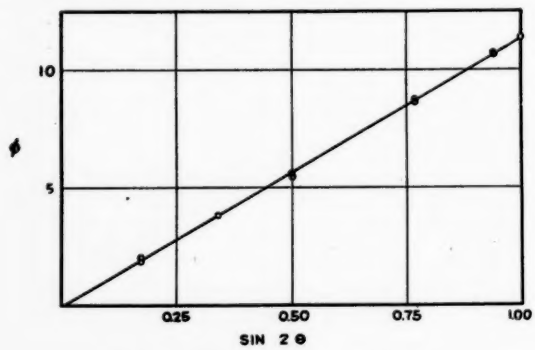

FIG. 4. Relation of E. A. to sin 2θ.

after drying and stripping were stretched under conditions giving high internal orientation, as indicated by birefringence, x-ray diffraction, and practically complete elastic recovery at or near the initial (high) temperature and contents of water and solvent. Certain particulars of this are discussed later.

Relative humidity inside the apparatus chamber was adjusted by solutions of sulfuric acid of suitable concentration.[4] Measurements of electrical conductivity of certain materials were made by the procedure described by Sheppard, Houck, and Dittmar.[5] Measurements of optical birefringence and examination of x-ray diffraction were made on practically all of the sheet materials.

EXPERIMENTAL RESULTS

The relative magnitude of the electrical anisotropy can be expressed by the quantity ϕ/V^2l (disposing of θ as previously noticed). A more explicit measure, involving the torque or couple G corresponding to the angle ϕ [cf. Eq. (1)] in dynes per radian, and other factors is under consideration.

Table I lists a number of materials in descending order of the relative E. A. Also given are such factors as the percentage elongation, the hydroxyl content of the molecule, where known, the actual water content at 50 percent relative humidity, etc.

It is apparent from the table that the property of induced electrical anisotropy—induced by stretching—is not shown by all kinds of natural and synthetic colloids, but is limited (a) to

[4] R. E. Wilson, Ind. Eng. Chem. **13**, 326 (1921).
[5] S. E. Sheppard, R. C. Houck, and C. Dittmar, J. Phys. Chem. **44**, 185 (1940).

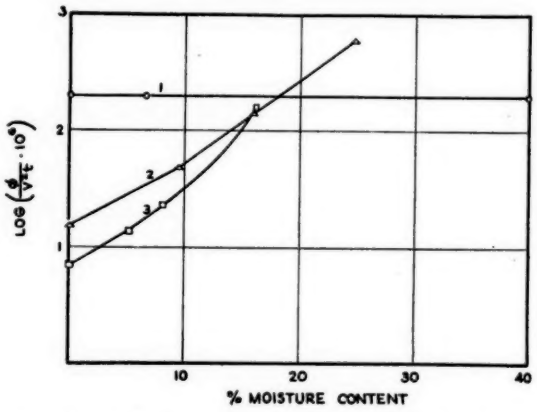

FIG. 5. Relation of E. A. to moisture content for: 1. Polyvinyl alcohol, 2. Gelatin, 3. Cellulose acetate (24.5 percent acetyl).

those containing an appreciable amount of fixed hydroxyl and/or absorbed water, and (b) those capable of absorbing considerable water. A further differentiation is noted in Table II and Fig. 5.

TABLE II. Dependence of electrical anisotropy and conductivity on water adsorption.

Material	Electrical anisotropy	Electrical conductivity
Polyvinyl alcohol	No	Yes
Gelatin	Yes	Yes
Cellulose acetate, 24.5% acetyl	Yes	Yes

INFLUENCE OF HUMIDITY AND ABSORBED WATER

It will be seen that whereas with gelatin and hydrolyzed cellulose acetate, the E. A. varies sharply with absorbed water content, in the case of *polyvinyl alcohol* it is independent of the water content, although this material strongly absorbs water—becoming indeed soluble therein.

Although the E. A. of polyvinyl alcohol is independent of absorbed water, its electrical conductance is dependent. Within certain limits, the logarithm of the conductance is a linear function of the logarithm of the water content (cf. Fig. 6). It had been previously observed by Sheppard, Houck, and Dittmar[5] that the logarithm of the conductance of gelatin is directly proportional to the water content. Combining this result with present observations, we find that the logarithm of the E. A. for gelatin varies linearly with the logarithm of the conductance (cf. Fig. 7).

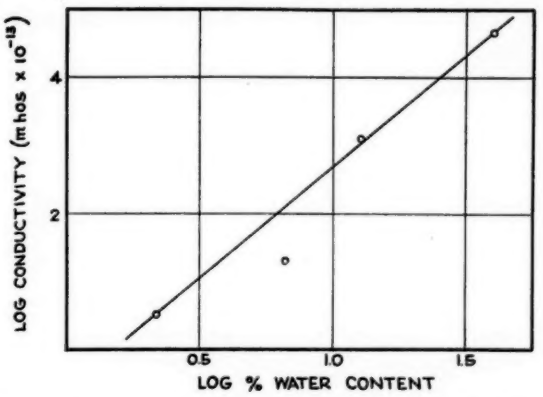

FIG. 6. Relation of conductance of polyvinyl alcohol to water content.

DISCUSSION

One principal result from this survey is that electrical anisotropy in colloids as xerogels[6] is limited to hydrophile or hydroxylated substances, which further have an axis of physical (structural) anisotropy. It is not solely a matter of an (induced) structural anisotropy (with varying dielectric capacity along and across) as suggested by Woods.[1] This is shown by the inactivity of the hydrophobe colloids, such as vinylite, polyvinyl acetate, etc.

A further notable result is the contrast between polyvinyl alcohol, on the one hand, and the hydrophile cellulose acetate and gelatin (and presumably cellulose and proteins in general).

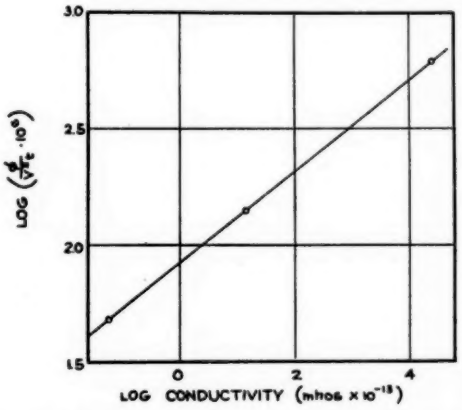

FIG. 7. Relation of log (E. A.) to long conductivity with gelatin.

[6] Term used for dried colloid gels. Cf. S. E. Sheppard, Trans. Faraday Soc. **29**, 77 (1933).

Whereas the former shows electrical anisotropy independent of moisture content (although hygroscopic), the latter are only electrically anisotropic on taking up water, and increase proportionately. This indicates a preponderant role of −OH groups—in the case of polyvinyl alcohol, a preemptive role of the structural hydroxyls, which in the cellulosic and protein bodies, can be assumed by adsorbed water.

It appears probable that the phenomenon is connected with the formation of oriented −OH or H-bridge chains. However, certain questions persist, e.g., why the −OH groups of cellulose cannot function *per se* but require adsorbed water. This may be a matter of spacing or contiguity. Next, why the effect with polyvinyl alcohol does not increase with adsorption of water. Perhaps this indicates a species of "saturation" already achieved by the molecular hydroxyls. Before more explicit answers can be given, or a definite mechanism be proposed, it is desirable that more and fuller data be obtained. We are examining *amylose*[7] and various protein substances, as well as specific modifications of polyvinyl alcohol and polyamides, and will report on these later. From the further experiments now planned it should be possible to indicate the mechanism of E. A. more clearly, and to relate it to the structure of these colloids.

ACKNOWLEDGMENT

Our thanks are due to Dr. W. Vanselow of these Laboratories for the measurements of electrical conductivity, and to Dr. R. L. Griffith, also of these Laboratories, who made the optical birefringence measurements and the x-ray diffraction studies.

[7] R. E. Rundle, L. Daasch, and D. French, J. Am. Chem. Soc. **66**, 130 (1944).

Raman Spectra of Hexachloroethane and Hexabromoethane[1]

DWIGHT T. HAMILTON[2] AND FORREST F. CLEVELAND
Department of Physics, Illinois Institute of Technology, Chicago, Illinois

(Received February 10, 1944)

Raman frequencies, relative intensities, and depolarization factors are reported for hexachloroethane and hexabromoethane. The relative intensities and depolarization factors were obtained by use of a Gaertner microdensitometer. The fundamental frequencies of hexachloroethane were used to calculate force constants from the equations used by Stitt for ethane. The Raman data indicate that the equilibrium configuration for hexachloroethane is that corresponding to the point group D_{3d}. The force constants so obtained were then used to calculate the values of the frequencies that are allowed by the selection rules in the infra-red spectrum. Selection rules for the fundamentals, binary combinations, overtones of non-degenerate frequencies, and overtones of degenerate frequencies up to the fourth overtone for any molecule whose symmetry is D_{3h}, D'_{3h}, or D_{3d} were worked out and are discussed.

INTRODUCTION

ETHANE-LIKE molecules are especially interesting in view of the many investigations[3-6] of the ethane molecule during the last few years. These studies have been concerned particularly with the orientation of the methyl groups and the potential barrier restricting internal rotation about the carbon-carbon single bond. Karweil and Schäfer[6] concluded that the stable equilibrium configuration for ethane was that corresponding to the point group D_{3h}, but Stitt[4] in his paper on C_2D_6 regarded the evidence for this conclusion as insufficient and decided after analyzing the data for both the symmetries D_{3h} and D_{3d} that the equilibrium configuration could not be reliably determined from the data then available for C_2H_6 and C_2D_6.

It appeared that it might be interesting to extend the above studies to include molecules of the ethane type, with larger atoms substituted for the hydrogen atoms. For such molecules the potential barrier restricting the internal rotation would be expected to be greater than in ethane and it could be expected that a more definite decision in regard to the equilibrium configuration might be obtained.

The molecules chosen for this investigation were hexachloroethane and hexabromoethane. Raman frequencies, relative intensities, and depolarization factors were obtained (in solution) for these molecules. The more complete spectrum of hexachloroethane seems to indicate clearly that the equilibrium configuration for this molecule is D_{3d}, in agreement with the conclusion of Mizushima and Morino.[7] Force constants were calculated for hexachloroethane, using the Raman fundamental frequencies, and the fundamental frequencies allowed in the infra-red spectrum by the selection rules were then obtained by use of these force constants. Considerable previous data[7-12] were available for hexachloroethane, but there was some uncertainty in regard to three of the frequencies, the depolarization data were incomplete, and the relative intensities were only visual estimates. Hexabromoethane had been investigated only once[13] and the Raman frequencies and relative intensities obtained in that

[1] Presented at the Chicago meeting of the American Physical Society, November, 1942; Phys. Rev. **63**, 64 (1943). Communication No. 38 from the Spectroscopy Laboratory.

[2] This paper is a report on an investigation carried out in partial fulfillment of the requirements for the degree of Master of Science by Mr. Dwight T. Hamilton whose present address is: Department of Physics, Denison University, Granville, Ohio.

[3] W. H. Avery and C. F. Ellis, J. Chem. Phys. **10**, 10 (1942).

[4] F. Stitt, J. Chem. Phys. **7**, 297 (1939).

[5] B. L. Crawford, Jr., W. H. Avery, and J. W. Linnett, J. Chem. Phys. **6**, 682 (1938).

[6] J. Karweil and C. Schäfer, Zeits. f. physik. Chemie **B40**, 382 (1938).

[7] S. Mizushima and Y. Morino, Sci. Papers Inst. Phys. Chem. Research (Tokyo) **29**, 188 (1936).

[8] A. Dadieu and K. W. F. Kohlrausch, Sitz. Akad. Wiss. Wien [IIa] **138**, 635 (1929).

[9] P. Krishnamurti, Ind. J. Phys. **6**, 309 (1931).

[10] S. Bhagavantam and S. Venkateswaran, Proc. Roy. Soc. **A127**, 360 (1930).

[11] F. Heidenreich, Zeits. f. Physik **97**, 277 (1935).

[12] R. Ananthakrishnan, Proc. Ind. Acad. Sci. **A5**, 285 (1937).

[13] H. Gockel, Zeits. f. physik. Chemie **B29**, 79 (1935).

investigation are not in satisfactory agreement with those obtained in the present study. No previous polarization data seem to exist for this molecule.

EXPERIMENTAL

The spectrograms were obtained with apparatus previously described.[14–16] The relative intensities and depolarization factors were obtained with the aid of a Gaertner microdensitometer, calibrated by methods described in recent papers.[17] Excitation was by Hg 4358A.

Exposures of from ten to thirty-five hours were made for the following solutions: C_2Cl_6 dissolved in carbon tetrachloride, chloroform, and carbon disulfide; C_2Br_6 dissolved in dioxane, ethylene bromide, and ethyl bromide. The hexachloroethane and hexabromoethane were Eastman grade chemicals obtained from the Eastman Kodak Company. A portion of the solvent used in preparing each solution was used to obtain an exposure equal to that of the longest exposure made on the solution in order to be sure that no solvent lines were attributed to the hexachloroethane or hexabromoethane.

RESULTS

The results obtained for hexachloroethane are compared with the previous data in Table I.

TABLE I. Comparison of the present Raman data for hexachloroethane with that of previous investigators.*

	Previous data			Present results		
N	$\Delta\nu$	I_e	ρ	$\Delta\nu$	I	ρ
3	144	1	r	162	vw	P
9	220	4	v	±223	450	0.80
12	340	4	v	±340	370	0.86
12	432	7	r	±431	1000	0.15
1	673	0				
9	858	3	v	859	220	0.81
3	978	1		975	33	0.35

* N is the number of times the line has been observed previously in different investigations, $\Delta\nu$ is the Raman frequency in cm^{-1}, I_e is the estimated relative intensity, I is the relative intensity obtained with the aid of the microdensitometer, r or v indicates right or left circularly polarized, respectively, ρ is the depolarization factor, P indicates a polarized line that was too weak to permit a quantitative determination of ρ, vw (very weak) designates a line that was too weak to measure with the microdensitometer, and the ± sign means that the line was observed both as a Stokes and as an anti-Stokes line.

[14] Forrest F. Cleveland and M. J. Murray, J. Chem. Phys. **7**, 396 (1939).
[15] Forrest F. Cleveland, M. J. Murray, H. H. Haney, and Julia Shackelford, J. Chem. Phys. **8**, 153 (1940).
[16] Forrest F. Cleveland, M. J. Murray, J. R. Coley, and V. I. Komarewsky, J. Chem. Phys. **10**, 18 (1942).
[17] Forrest F. Cleveland, J. Chem. Phys. **11**, 1, 227 (1943).

Several independent measurements made on three different spectrograms consistently locate a very weak line at about 162 cm^{-1}, which is somewhat higher than the average of the values previously reported. Since this line was very weak and in some cases difficult to measure due to overlapping by the Rayleigh wing, its exact location is not readily established. The line at 975 cm^{-1} appeared as a polarized line and was strong enough to be easily observed and measured. The line previously reported by one investigator at 673 cm^{-1} was not found in the present investigation.

TABLE II. Comparison of the present Raman data for hexabromoethane with previous data.

Gockel Solid C_2Br_6		Present results C_2Br_6 in solution		
$\Delta\nu$	I_e	$\Delta\nu$	I	ρ
154	3	139	530	0.47
177	1			
211	½	±204	780	0.83
264	1	±255	1000	0.13
		768	460	0.70

The results obtained for hexabromoethane are compared with the previous results of Gockel[13] in Table II. The present $\Delta\nu$ values are somewhat lower than the corresponding values obtained by Gockel and the intensities show very poor agreement. Furthermore, no line corresponding to the 177 cm^{-1} frequency could be observed on the several spectrograms of hexabromoethane obtained in this laboratory, although these spectrograms did show a line at 768 cm^{-1}, strong enough to be readily observed, that was not reported in the previous investigation.

In comparing the Raman data for hexachloroethane and hexabromoethane, one notices that the frequencies of the hexabromoethane lie somewhat lower than the corresponding frequencies of hexachloroethane; this is what one would expect in view of the larger masses of the bromine atoms and of the inferior strength of the C−Br bonds. Had a better solvent been known for hexabromoethane, lines corresponding to the weak lines at 162 and 975 cm^{-1} in the hexachloroethane spectrum might have appeared. Since these two lines could not be observed for hexabromoethane, it was not possible to calculate force constants for this molecule. It is to be hoped that later in-

vestigations may succeed in obtaining the complete Raman spectrum.

CALCULATIONS

The six Raman frequencies observed for hexachloroethane were used to calculate force constants for this molecule from the equations used by Stitt[4] for C_2H_6 and C_2D_6. The particular equations used were those obtained by Stitt from a six-constant potential function of the modified valence force type.* Two cubic equations were involved, one for the three A_{1g} frequencies, another for the three E_g frequencies. Substitution of the observed values of the A_{1g} and E_g frequencies thus would give six equations with six unknown force constants. However, it did not seem practicable to solve these equations directly for the force constants since such complicated expressions were involved. Consequently the procedure followed was to establish relations[18] between the roots (observed $\Delta\nu$ values) and the coefficients for each cubic equation. These relations were simplified by omitting certain terms, but in spite of this omission one could obtain good approximations of the force constants by use of the simplified relations.

Since the analysis of the two cubic equations yielded two sets of approximate values for the force constants, subsequent adjustment of the values was necessary in order to establish a single set which would best satisfy both cubic equations, i.e., would yield the best "test values" for the frequencies (see Table IV).

TABLE III. Force constants in 10^5 dynes/cm for ethane and hexachloroethane.

Force constant	C_2Cl_6	C_2H_6
K_C	4.00	4.60
K_{Cl}	2.00	
K_H		4.79
K_α	0.75	0.46
K_β	0.35	0.46
$K_{\alpha\beta}$	−0.65	−0.015
$K_{C\gamma}$	−1.36	−0.47

* See Eq. (2) of reference 4, page 303.

[18] Relations between the roots and coefficients of an equation: If $a_1, a_2, a_3, \cdots, a_n$ are the n roots of the equation $x^n+p_1x^{n-1}+p_2x^{n-2}+\cdots+p_{n-1}x+p_n=0$, then

$$p_1=-(a_1+a_2+a_3+\cdots+a_n),$$
$$p_2=(a_1a_2+a_1a_3+\cdots),$$
$$p_3=-(a_1a_2a_3+a_1a_2a_4+\cdots),$$
$$\cdots \qquad \cdots$$
$$p_n=(-1)^n a_1a_2a_3\cdots a_n.$$

The best set of force constants resulting from these calculations is given in Table III, along with the corresponding constants calculated by Stitt for ethane. K_C is the carbon-carbon force constant, K_{Cl} and K_H are, respectively, the carbon-chlorine and carbon-hydrogen force constants, K_α and K_β are, respectively, the bond angle force constants for the Cl−C−Cl and Cl−C−C angles, and $K_{\alpha\beta}$ and $K_{C\gamma}$ are associated with interactions within a CCl_3 or CH_3 group, respectively. The bond distances used in the calculations were obtained from electron diffraction data for similar molecules; they were C−Cl=1.76A and C−C=1.54A.

TABLE IV. Calculated and observed frequencies for hexachloroethane.

Type	Raman observed	Test values	Type	Infra-red Calculated
	162	282		310
A_{1g}	431	313	A_{2u}	1001
	975	972		
	223	209		100
E_g	340	341	E_u	325
	859	869		869

As a test of the accuracy and reliability of the above set of force constants and as a safeguard against errors of calculation, the calculations were repeated in reverse order, the frequencies being obtained from the force constants. The extent to which the force constants reproduce the six observed Raman frequencies may be seen in Table IV in which the so-called "test values" are the values calculated from the A_{1g} and E_g equations by use of the force constants listed in Table III.

Having now more or less reliably established the force constants, the A_{2u} and E_u frequencies, allowed only in the infra-red spectrum, were calculated. The calculated A_{2u} and E_u frequencies, as yet unmeasured, are of interest in that they give the neighborhood in which the infra-red bands may be expected to appear.

DISCUSSION

There are three possibilities in regard to the orientation of the two CCl_3 groups: (1) *free rotation*, in which there is no potential restricting rotation about the C−C bond, symmetry $\mathbf{D}'_{3h}$;

(2) *eclipsed*, the orientation in which the Cl atoms are as close together as possible, symmetry $\mathbf{D}_{3h}$; and (3) *staggered*, the orientation in which the Cl atoms are as far apart as possible, symmetry $\mathbf{D}_{3d}$. The selection rules for fundamentals, binary combinations, non-degenerate overtones, and doubly degenerate overtones up to the fourth overtone have been worked out for each of the three cases by methods described elsewhere,[19] but will not be listed here since they have been published in a condensed form already.[20]

The selection rules show that three polarized Raman lines are allowed for each of the three configurations, but that the number of depolarized Raman lines allowed is smaller for the $\mathbf{D}_{3d}$ than for the $\mathbf{D}_{3h}$ or the $\mathbf{D}'_{3h}$ configurations. For $\mathbf{D}_{3d}$ only *three* depolarized lines are allowed, while for $\mathbf{D}_{3h}$ or $\mathbf{D}'_{3h}$ *six* depolarized lines are permitted. Since only three depolarized lines were observed, the Raman spectra data thus establish the equilibrium configuration as $\mathbf{D}_{3d}$, unless one makes the improbable assumption that three of the depolarized lines were so weak as to escape observation. This conclusion could be tested further if the infra-red data were available since the selection rules for combinations and overtones for $\mathbf{D}_{3d}$ are quite different from those for the other two configurations.

TABLE V. Comparison of the Raman data and assignments for hexachloroethane and hexabromoethane.

Hexachloroethane					Hexabromoethane				
$\Delta\nu$	I	ρ	Type	D*	$\Delta\nu$	I	ρ	Type	D
162	vw	P	A_{1g}	1	—	—	—	—	—
431	1000	0.15	A_{1g}	1	255	1000	0.13	A_{1g}	1
975	33	0.35	A_{1g}	1	—	—	—	—	—
223	450	0.80	E_g	2	139	530	0.47	E_g	2
340	370	0.86	E_g	2	204	780	0.83	E_g	2
859	220	0.81	E_g	2	768	460	0.70	E_g	2

* D is the degeneracy.

The $\mathbf{D}_{3d}$ configuration seems probable on other grounds as well, for the potential barrier restricting internal rotation in ethane is about 3000 calories per mole and since the chlorine atoms are larger and the interactions therefore presumably larger, it seems quite reasonable to suppose that the orientation of the CCl_3 groups should be that in which the Cl atoms in different CCl_3 groups are as far apart as possible. Mizushima and Morino[7] have discussed this point.

Using the calculated infra-red frequencies given in Table IV in conjunction with the selection rules for $\mathbf{D}_{3d}$, one can predict the regions in which infra-red absorption should occur. The numerical values of these expected infra-red frequencies are not written down here since it is not known just how reliable the calculated infra-red frequencies may be. The three lowest infra-red frequencies fall in a region where their observation would be difficult, but it is possible that they may be established by observation of overtone or combination frequencies. Only the second, fourth, sixth, etc., overtones of the A_{2u} and E_u frequencies are permitted in the infra-red spectrum, but six combinations, $A_{1g}\times A_{2u}$, $A_{1g}\times E_u$, $A_{1u}\times E_g$, $A_{2g}\times E_u$, $A_{2u}\times E_g$, and $E_g\times E_u$, are allowed. Especially interesting are those combinations of the torsional A_{1u} frequency, which is forbidden in both the Raman and infra-red spectra, with the three frequencies of the E_g type. From these three combination frequencies, if they could be observed and identified in the infra-red spectrum, one might be able to get a value for the torsional A_{1u} frequency. If this frequency and the A_{2u} and E_u fundamentals could be established by an infra-red investigation, it would then be possible to calculate thermodynamical quantities for hexachloroethane.

With the results for hexachloroethane as a guide, one can make tentative assignments of the observed frequencies for hexabromoethane, assuming that its equilibrium configuration is likewise $\mathbf{D}_{3d}$. The spectra of the two compounds and the assignments are compared in Table V.

ACKNOWLEDGMENT

The microdensitometer used in this investigation was secured with a grant to one of us (F. F. C.) from the Penrose Fund of the American Philosophical Society. The authors wish to express their appreciation for this assistance.

[19] A. G. Meister, F. F. Cleveland, and M. J. Murray, Am. J. Phys. **11**, 239 (1943).

[20] T. Y. Wu, *Vibrational Spectra and Structure of Polyatomic Molecules* (National University of Peking, Kunming, China, 1939), page 296.

THE JOURNAL OF CHEMICAL PHYSICS VOLUME 12, NUMBER 6 JUNE, 1944

Theory of Chain Copolymerization Reactions*

ROBERT SIMHA, *Department of Chemistry,*

AND

HERMAN BRANSON, *Department of Physics, Howard University, Washington, D. C.*

(Received February 25, 1944)

The kinetics of chain copolymerizations is developed for reactions consisting of three steps: first, an activation of stable monomer; second, a growth of activated polymer radical by means of monomer addition; third, a stabilization of the growing chains by (a) monomer addition, (b) by means of growing polymer [Eq. (1)]. The existence of a steady state in respect to the concentration of growing chains beyond the induction period is assumed. The rate constants of growth and termination will in general depend upon the individual composition and upon the nature of the activated chain end. Equations for the rate of change of mole ratio z of the two monomer species are developed in terms of mean rates of growth and termination obtained by averaging the actual rates over the distribution of growing polymer [(4), (4a), (4′)]. The equilibrium conditions lead to a set of difference equations for this distribution [(5), (5′)]. It is investigated whether the solution and results derived therefrom are of a form which permits a determination of the dependence of the rate constants for growth and termination upon the composition of the polymer molecule (6). In addition, the influence of the type of active chain end involved on over-all rate and size distribution is considered by introducing four constants for propagation and termination, respectively, according to the four possibilities $A-A$, $A-B$, $B-A$, $B-B$ [(6a), (7), (4b), (4b′)], but independent of chain composition. Various special cases according to the relative magnitude of the rates for the two reactants are presented. Experimentally it is difficult to distinguish on the basis of kinetic data between the foregoing mechanism and one in which the rates of growth (and termination) for each of the two kinds of monomer depend solely upon the nature of the monomer molecule added and are independent of the nature of the active chain end [(4c), (4c′), (4c″)]. Relations are derived for the molecular size distribution, the inhomogeneity of the copolymer mixture in regard to composition, the average molecular weight, and the average composition of copolymer as function of the composition of the monomer residue [(8a), (8a′), (9a), (10)]. The importance of these results for soluble and insoluble copolymers and for the theory of gel formation in vinyl-divinyl type polymers is pointed out.

THE kinetics of chain polymerization reactions has been extensively treated.[1] Starting with the main elementary processes of chain initiation, propagation, and termination, it is possible to derive expressions for the over-all consumption of monomer, for the average chain length of the polymer formed during the various stages of the process and for the distribution of molecular weights. This in turn permits an analysis of the elementary rate constants, and therefore of energies of activation and frequency factors.

If two monomer species copolymerize, additional questions arise, e.g., the composition distribution of polymer, the molecular arrangement of the two types within a chain, particularly if one of the two species acts as cross-linking agent, as in the vinyl-divinyl copolymerization.

The kinetics of copolymer formation has received much less attention than that of one-component systems. Norrish and Brookman[2] have considered the over-all rate of the chain process. Jenckel[3] was the first to specify the special types of copolymers obtainable, depending upon the relative values of the rate constants for the two species. However, since he did not introduce the initiation and termination, as pointed out by himself, his method is limited and the results obtained represent rather special cases, as will become evident in the following. Wall[4] has considered this question, however, without treating the process as a chain reaction governed by the above elementary processes. Instead, he starts with the assumption of a first-order over-all rate of disappearance for each of the two kinds of monomer. His equations, therefore, also refer to special cases and are in part identical with those of Jenckel. Recently the present authors approached this problem from the point

* Publication assisted by The Graduate School of Howard University.

[1] Compare the symposium on "High Polymers" held by the New York Academy of Sciences, Ann. N. Y. Acad. Sci. **44**, 263 (1943).

[2] R. G. W. Norrish and E. F. Brookman, Proc. Roy. Soc. **A171**, 147 (1939).

[3] E. Jenckel, Zeits. f. physik. Chemie **A190**, 24 (1941).

[4] F. T. Wall, J. Am. Chem. Soc. **63**, 1862 (1941).

of view of a chain reaction governed by an activation, propagation, and cessation.[5] Expressions for the over-all rate and for the size and composition distribution were given. In the following the previous short account of this work is presented in full and a more complete analysis is undertaken.

The treatment is based upon the steady state method. It is valid if the mean lifetime of the growing polymer is small compared with the half-life of the over-all consumption of monomer. This implies essentially a vanishingly small rate of initiation. In polymerization reactions which lead to the formation of high molecular weight products, this steady state approximation appears satisfactory.[6] The mechanism underlying the mathematical derivations is somewhat simplified by neglecting the possibility of chain transfer[1] between polymer radical and monomer or solvent and by representing the initiation in terms of constant parameters without considering in detail the catalyst action.[1] At the present stage of experimental investigation, considerations of this kind, necessary for a more complete analysis of the data available on simple polymerization processes and on molecular distribution curves, are hardly possible.

The rates of growth and termination will, in general, depend upon the individual compositions of the chains and upon the nature of their active ends, formed by either of the two monomer species 1 and 2. In the following the rate constants will be designated by symbols $k_{ij}(r, s, A)$ and $k_{ij}(r, s, B)$. r, s indicate the composition of the chain in question, r being the number of type one groups and s of type two groups in the chain. A and B refer to the two kinds of active ends of the growing polymer molecules. i runs from 1 to 3 according to whether the k constant designates initiation, growth, or termination, j assumes the values of one or two, characterizing the type of monomer involved in the kinetic act. In this notation, $k_{21}(r, s, A)$, for instance, signifies the rate of growth of a polymer radical of indicated composition and active end by addition of a monomer of type 1, $k_{22}(r, s, A)$ by addition of type 2. The following reaction schemes are considered:

Initiation:

$$N_1 \xrightarrow{I_1} n_{10}; \quad N_2 \xrightarrow{I_2} n_{01}.$$

Propagation:

$$n_{rs}(A)+N_1 \xrightarrow{k_{21}(r,s,A)} n_{r+1s}(A);$$

$$n_{rs}(A)+N_2 \xrightarrow{k_{22}(r,s,A)} n_{rs+1}(B),$$

$$n_{rs}(B)+N_1 \xrightarrow{k_{21}(r,s,B)} n_{r+1s}(A);$$

$$n_{rs}(B)+N_2 \xrightarrow{k_{22}(r,s,B)} n_{rs+1}(B).$$

Termination:

$$\text{(a)}\quad n_{rs}(A)+N_1 \xrightarrow{k_{31}(r,s,A)} N_{r+1s};$$

$$n_{rs}(A)+N_2 \xrightarrow{k_{32}(r,s,A)} N_{rs+1},$$

$$n_{rs}(B)+N_1 \xrightarrow{k_{31}(r,s,B)} N_{r+1s};$$

$$n_{rs}(B)+N_2 \xrightarrow{k_{32}(r,s,B)} N_{rs+1}.$$

$$\text{(b)}\quad n_{rs}(A)+n_{ik}(A) \xrightarrow{k_3(r,s,i,k,A,A)} N_{r+is+k} \qquad (1)$$

$$\text{or } N_{rs}+N_{ik},$$

$$n_{rs}(A)+n_{ik}(B) \xrightarrow{k_3(r,s,i,k,A,B)} N_{r+is+k}$$

$$\text{or } N_{rs}+N_{ik},$$

$$n_{rs}(B)+n_{ik}(B) \xrightarrow{k_3(r,s,i,k,B,B)} N_{r+is+k}$$

$$\text{or } N_{rs}+N_{ik}.$$

$n_{rs}(A)$ are growing radicals with a reacting end formed by type 1 monomer and similarly for $n_{rs}(B)$. N_{rs} indicates the mole fraction of stable polymer with given composition r, s. I_1 and I_2 indicate the velocities of the initiation act, $I_1=k_{11}N_1^{n-i-1}N_2^{i}$; $I_2=k_{12}N_1^{n-j-1}N_2^{j}$ for an nth-order process. Two possibilities of breaking the growing polymer or monomer are considered, monomer termination and radical-radical termination. The radical mechanism of polymerization makes the latter process the more probable one.[1] However, in order to establish the connection with the special results previously mentioned and with certain results on molecular weight distributions of simple polymer, monomer termination is included. Besides, the mathematical treatment

[5] H. Branson and R. Simha, J. Chem. Phys. **11**, 297 (1943).

[6] R. Ginell and R. Simha, J. Am. Chem. Soc. **65**, 706, 715 (1943).

is closely connected for both cases. It has been suggested[1] that termination occurs by a first-order process when activation proceeds by means of an ionic mechanism. This case can easily be treated on the basis of the following results for the radical distribution.

I. THE GENERAL OVER-ALL REACTION

In terms of the above scheme the consumption of monomer is given for monomer termination by:

$$\frac{1}{N_l}\frac{dN_l}{dt}=I_l+\sum_{r,s}\{[k_{2l}(r,s,A)+k_{3l}(r,s,A)]n_{rs}(A)+[k_{2l}(r,s,B)+k_{3l}(r,s,B)]n_{rs}(B)\}, \quad (2)$$

with $l=1, 2$.

We introduce the mean values of the rates of growth and termination by averaging over the radical distribution.

$$\bar{k}_{ml}\sum_{r,s}[n_{rs}(A)+n_{rs}(B)]=\sum_{r,s}[k_{ml}(r,s,A)n_{rs}(A)+k_{ml}(r,s,B)n_{rs}(B)].$$

Equation (2) then becomes:

$$\frac{1}{N_l}\frac{dN_l}{dt}=I_l+(k_{2l}+k_{3l})\sum_{r,s}[n_{rs}(A)+n_{rs}(B)]. \quad (2a)$$

Since a steady state is assumed to exist, the rate of production equals the rate of destruction of active chains. This leads at once to an equation for the total concentration of these chains, which assumes the following form:

$$\sum_{r,s}[n_{rs}(A)+n_{rs}(B)]=\frac{I_1N_1+I_2N_2}{k_{31}N_1+k_{32}N_2}. \quad (3)$$

Equations (2a) and (3) together determine the over-all rate in terms of the average rates $\bar{k}_{ml}$ and the initiations I_1 and I_2. The over-all rate is best expressed by introducing the mole ratio of monomer residue:

$$z=N_1/N_2.$$

The above results then lead to

$$\frac{dN_1}{dN_2}=z\frac{R_1z+R_2}{R_3z+R_4}$$

and

$$\frac{d\ln z}{dt}=\frac{(R_3-R_1)z+R_4-R_2}{\bar{k}_{31}z+\bar{k}_{32}}, \quad (4)$$

with

$$R_1=I_1(k_{21}+2k_{31}); \quad R_2=I_1k_{32}+I_2(k_{21}+k_{31});$$
$$R_3=I_2\bar{k}_{31}+I_1(\bar{k}_{22}+\bar{k}_{32}); \quad R_4=I_2(\bar{k}_{22}+2\bar{k}_{32}).$$

In the following species two will be assumed to be the more rapidly reacting, such that for $t\to\infty$, $z\to\infty$. It may be noted that (3) cannot be integrated directly, since the average values of the rates depend, in general, upon the instantaneous monomer composition z. However, it can be simplified, since the rate of initiation under our assumption is very small and furthermore the velocity of growth much larger than that of termination. Equation (4) then reduces to

$$\frac{d\ln z}{dt}=(k_{22}-\bar{k}_{21})\frac{I_1z+I_2}{\bar{k}_{31}z+\bar{k}_{32}}. \quad (4a)$$

In the case of radical termination one has:

$$-\frac{dN_l}{dt}=I_l+N_lk_{21}\sum_{r,s}[n_{rs}(A)+n_{rs}(B)]; \quad l=1, 2. \quad (2')$$

The average value of the termination is defined as follows:

$$\bar{k}_3\{\sum_{r,s,i,j}[n_{rs}(A)+n_{ij}(B)]\}^2=\sum_{r,s,i,j}\{k_3(r,s,i,j,A,A)n_{rs}(A)n_{ij}(A)+2k_3(r,s,i,j,A,B)n_{rs}(A)n_{ij}(B)+k_3(r,s,i,j,B,B)n_{rs}(B)n_{ij}(B)\}.$$

The radical concentration is found from the equation:

$$\bar{k}_3[\sum_{r,s}n_{rs}(A)+n_{rs}(B)]^2=I_1N_1+I_2N_2.$$

Therefore:

$$\frac{dN_1}{dN_2}=\frac{I_1+k_{21}N_2^{\frac{1}{2}}k_3^{-\frac{1}{2}}(I_1z+I_2)^{\frac{1}{2}}}{I_2+\bar{k}_{22}N_2^{\frac{1}{2}}k_3^{-\frac{1}{2}}(I_1z+I_2)^{\frac{1}{2}}},$$
$$\frac{d\ln z}{dt}=I_2-I_1+(k_{22}-k_{21})\bar{k}_3^{-\frac{1}{2}}N_2^{\frac{1}{2}}(I_1z+I_2)^{\frac{1}{2}}. \quad (4')$$

Equations (4) and (4'), containing mean rate constants, are of general validity. The specific dependence of the individual rates upon com-

position and chain end determines the radical distribution and therefore the variation of the average rates with z.

II. DETERMINATION OF RADICAL DISTRIBUTION

Because of the existence of a steady state

$$\frac{dn_{rs}(A)}{dt}=\frac{dn_{rs}(B)}{dt}=0.$$

Scheme (1) then leads to the following set of difference equations for the concentration of growing polymer of indicated type:

$$\begin{aligned}\alpha_{rs}(A)n_{rs}(A)&=\beta_{r-1s}(A)n_{r-1s}(A)\\&\quad+\beta_{r-1s}(B)n_{r-1s}(B),\\\alpha_{rs}(B)n_{rs}(B)&=\gamma_{rs-1}(A)n_{rs-1}(A)\\&\quad+\gamma_{rs-1}(B)n_{rs-1}(B),\\\alpha_{10}(A)n_{10}&=I_1N_1;\quad\alpha_{01}(B)n_{01}=I_2N_2.\end{aligned}\tag{5}$$

For monomer termination:

$$\begin{aligned}\alpha_{rs}(L)&=[k_{21}(r,s,L)+k_{31}(r,s,L)]N_1\\&\quad+[k_{22}(r,s,L)+k_{32}(r,s,L)]N_2,\\\beta_{rs}(L)&=k_{21}(r,s,L)N_1;\quad\gamma_{rs}(L)=k_{22}(r,s,L)N_2,\end{aligned}$$

with $L=A$ or B. For radical termination:

$$\begin{aligned}\alpha_{rs}(L)&=k_{21}(r,s,L)N_1+k_{22}(r,s,L)N_2\\&\quad+\sum_{i,j}[k_3(r,s,i,j,L,A)n_{ij}(A)\\&\quad+k_3(r,s,i,j,L,B)n_{ij}(B)]\\&=k_{21}(r,s,L)N_1+k_{22}(r,s,L)N_2\\&\quad+\bar{k}_3(r,s,L,A)\sum_{i,j}n_{ij}(A)\\&\quad+\bar{k}_3(r,s,L,B)\sum_{i,j}n_{ij}(B).\end{aligned}\tag{5'}$$

$\bar{k}_3(r,s,L,A)$ and $\bar{k}_3(r,s,L,B)$ with $\bar{k}_3(A,B)=\bar{k}_3(B,A)$ are suitably defined average rates.

The general solution of system (5) leads to complex expressions, depending upon the specific nature of the rates as function of the individual chain composition r, s. Herington and Robertson[7] have developed equations for simple polymerization processes permitting in principle to deduce the dependence of the growth to termination ratio upon individual molecular size from determinations of the instantaneous distribution curve. One may think of a similar procedure here. To investigate this, the complexity of (5) is reduced first by disregarding the dependence of growth and cessation upon the type of active end involved. This will be nearly correct, if no further steric conditions remain to be satisfied once an active end has been formed. The only important contribution of the growing chain to the rate constant then depends upon its size and composition only. In this case one has:

$$n_{rs}(A)+n_{rs}(B)=2n_{rs}(A)=n_{rs}$$

and (5) reduces to:

$$\alpha_{rs}n_{rs}=\beta_{r-1s}n_{r-1s}+\gamma_{rs-1}n_{rs-1};\quad r,s\geqq 1.\tag{5a}$$

This set may be solved by induction, as shown in Appendix I. The solution is:

$$n_{rs}=\frac{\alpha_{0s}}{\beta_{rs}}\prod_{l=0}^{r}\left(\frac{\beta_{ls}}{\alpha_{ls}}\right)n_{0s}+\sum_{j=1}^{r}n_{js-1}\frac{\gamma_{js-1}}{\beta_{rs}}\prod_{l=j}^{r}\frac{\beta_{ls}}{\alpha_{ls}}.$$

For the pure polymers, n_{r0} and n_{0s}, we have:

$$\beta_{r-10}n_{r-10}=\alpha_{r0}n_{r0};\quad\gamma_{0s-1}n_{0s-1}=\alpha_{0s}n_{0s}.$$

Therefore:

$$I_1N_1=\beta_{r0}n_{r0}\prod_{l=1}^{r}\frac{\alpha_{l0}}{\beta_{l0}};\quad I_2N_2=\gamma_{0s}n_{0s}\prod_{l=1}^{s}\frac{\alpha_{0l}}{\gamma_{0l}}.$$

Whereupon:

$$n_{rs}=\frac{I_2N_2}{\alpha_{rs}}\prod_{l=0}^{r-1}\frac{\beta_{ls}}{\alpha_{ls}}\prod_{l=1}^{s-1}\frac{\gamma_{0l}}{\alpha_{0l}}+\frac{1}{\alpha_{rs}}\sum_{j=1}^{r}\gamma_{js-1}n_{js-1}\prod_{l=j}^{r-1}\frac{\beta_{ls}}{\alpha_{ls}}.$$

Defining:

$$\frac{\beta_{ij}}{\alpha_{ij}}=\omega_{ij}\quad\text{and}\quad\frac{\gamma_{ij}}{\alpha_{ij}}=\omega'_{ij},$$

the probabilities for growth by means of monomer 1 and 2, respectively, n_{rs} becomes finally:

$$\begin{aligned}n_{rs}&=\frac{I_1N_1}{\alpha_{rs}}\sum_{i_1=1}^{r}\sum_{i_2=1}^{i_1}\cdots\sum_{i_s=1}^{i_{s-1}}\prod_{l=1}^{i_s-1}\omega_{l0}\omega'_{i_s0}\prod_{l=i_s}^{i_{s-1}-1}\omega_{l1}\omega'_{i_{s-1}1}\\&\quad\times\prod_{l=i_{s-1}}^{i_{s-2}-1}\omega_{l2}\cdots+\frac{I_2N_2}{\alpha_{rs}}\sum_{i=0}^{s-1}\sum_{i_1=1}^{r}\cdots\sum_{i_i=1}^{i_{i-1}}\prod_{l=1}^{s-i-1}\omega'_{0l}\\&\quad\times\prod_{l=0}^{i_i-1}\omega_{ls-i}\omega'_{i_is-i}\prod_{l=j_i}^{i_{i-1}-1}\omega_{ls-i+1}\cdots\omega'_{i_1s-1}\prod_{l=i_1}^{r-1}\omega_{ls}.\end{aligned}\tag{6}$$

The term on the right multiplied by I_1N_1 gives the n_{rs} initiated by monomer species 1. The first product gives the probability that the chain

[7] E. F. G. Herington and A. Robertson, Trans. Faraday Soc. **38**, 490 (1942).

so initiated adds (j_s-1) monomers of species 1 before a species 2 is added, as represented by the factor $\omega'_{j_s 0}$. The second product describes the further growth of the polymer by addition of more 1's until there are $(j_{s-1}-1)$ of the first species. At this stage a monomer of the second type is added. The remaining factors express the further growth. Finally, the summations over the j's give the total number of possible intramolecular arrangements consistent with the composition r, s and initiated by the first species. The second term is interpreted similarly.

In the case of radical termination, the same solution is obtained with the α's defined as in (5') after suitable specialization.

We may investigate the specific effect of different growing ends upon the reaction by neglecting the dependence upon chain composition. Equation (5) becomes upon division by $\alpha(A)$ and $\alpha(B)$, respectively:

$$\begin{aligned} n_{rs}(A) &= \omega(A)n_{r-1s}(A)+\omega(B)n_{r-1s}(B), \\ n_{rs}(B) &= \omega'(A)n_{rs-1}(A)+\omega'(B)n_{rs-1}(B), \end{aligned} \tag{5b}$$

where the ω's are defined as:

$$\omega(A)=\frac{\beta(A)}{\alpha(A)}; \quad \omega(B)=\frac{\beta(B)}{\alpha(A)};$$

$$\omega'(A)=\frac{\gamma(A)}{\alpha(B)}; \quad \omega'(B)=\frac{\gamma(B)}{\alpha(B)}.$$

They represent probabilities for $-A-A, -B-A, -A-B, -B-B$ addition, respectively. The solutions of (5b) are, as shown in Appendix II:

$$\begin{aligned} n_{rs}(A) &= [\omega(A)]^{r-1}[\omega'(B)]^{s} \\ &\quad \times\left\{\frac{I_1N_1}{\alpha(A)}[F(1-r,\,-s,\,1,\,x) \right. \\ &\quad -F(1-r,\,1-s,\,1,\,x)] \\ &\quad \left.+\frac{I_2N_2}{\alpha(B)}\frac{\omega(A)}{\omega'(A)}F(1-r,\,1-s,\,1,\,x)\right\}; \\ n_{rs}(B) &= [\omega(A)]^{r}[\omega'(B)]^{s-1} \\ &\quad \times\left\{\frac{I_1N_1}{\alpha(A)}\frac{\omega'(A)}{\omega(A)}F(1-r,\,1-s,\,1,\,x) \right. \\ &\quad \left.+\frac{I_2N_2}{\alpha(B)}[F(-r,\,1-s,\,1,\,x) \right. \\ &\quad \left.\left.-F(1-r,\,1-s,\,1,\,x)]\right\}, \end{aligned} \tag{6a}$$

where the F's are hypergeometric functions with

$$x=\frac{\omega'(A)\omega(B)}{\omega(A)\omega'(B)}=\frac{\gamma(A)}{\beta(A)}\frac{\beta(B)}{\gamma(B)},$$

corresponding to $\dfrac{-A-B}{-A-A}\dfrac{-B-A}{-B-B}$ addition.

The interpretation of (6a) is analogous to that of (6). The first term always gives the total number of active chains of stated composition initiated by the first species. In the case of radical termination (6a) remains valid with the α's defined as in (5'), but independent of r and s. For the developments in the next section we need the total number of radicals of specified ends (see Appendix II):

$$\begin{aligned} \sum_{r,s\geq 1} n_{rs}(A) &= \frac{\omega(A)\omega(B)x}{[(1-\omega(A))(1-\omega(B))-x\omega(A)\omega'(B)]}\left[\frac{I_1N_1}{\alpha(A)(1-\omega(A))}+\frac{I_2N_2}{\alpha(B)\omega'(A)}\right], \\ \sum_{r} n_{r0}(A) &= \frac{I_1N_1}{\alpha(A)}\frac{1}{1-\omega(A)}, \\ \sum_{r,s\geq 1} n_{rs}(B) &= \frac{\omega(A)\omega'(B)x}{[(1-\omega(A))(1-\omega'(B))-x\omega(A)\omega'(B)]}\left[\frac{I_1N_1}{\alpha(A)\omega(B)}+\frac{I_2N_2}{\alpha(B)(1-\omega'(B))}\right], \\ \sum_{s} n_{0s}(B) &= \frac{I_2N_2}{\alpha(B)}\frac{1}{1-\omega'(B)}. \end{aligned} \tag{7}$$

III. SPECIAL RATE EQUATIONS

From the results obtained for the radical distribution, it is possible to determine the average rates $\bar{k}_{21}, \bar{k}_{22}, \bar{k}_{31}, \bar{k}_{32}$ and introduce them into the general equations (2) and (4'). The mean rates, obtained

by averaging over the rates for A and B ends, respectively, according to the general equation previously given, are:

$$\bar{k}\sum_{r,s}[n_{rs}(A)+n_{rs}(B)]=\sum_{r,s}[k(A)n_{rs}(A)+k(B)n_{rs}(B)],$$

where, as before, the $\bar{k}$'s are independent of r, s. Substituting for the sums, one has:

$$\bar{k}=\frac{k(A)[I_1N_1(\alpha(B)-\gamma(B))+I_2N_2\beta(B)]+k(B)[I_1N_1\gamma(A)+I_2N_2(\alpha(A)-\beta(A)]}{I_1N_1[\alpha(B)+\gamma(A)-\gamma(B)]+I_2N_2[\alpha(A)+\beta(B)-\beta(A)]}.$$

Therefrom:

$$-\frac{1}{N_l}\frac{dN_l}{dt}=I_l+(\bar{k}_{2l}+\bar{k}_{3l})[\sum_{r,s}n_{rs}(A)+\sum_{r,s}n_{rs}(B)]$$

with $l=1, 2$. Equation (4a) then yields:

$$\frac{d}{dt}\ln z=(I_1z+I_2)\frac{c_1z^2+c_2z+c_3}{c_4z^3+c_5z^2+c_6z+c_7}, \tag{4b}$$

where

$$c_1=I_1[k_{22}(A)-k_{21}(A)][k_{21}(B)+k_{31}(B)]\doteq I_1k_{21}(B)[k_{22}(A)-k_{21}(A)],$$

$$c_2\doteq I_2k_{21}(B)[k_{22}(A)-k_{21}(A)]+I_1k_{22}(A)[k_{22}(B)-k_{21}(B)],$$

$$c_3\doteq I_2k_{22}(A)[k_{22}(B)-k_{21}(B)],$$

$$c_4\doteq I_1k_{21}(B)k_{31}(A),$$

$$c_5\doteq I_2k_{21}(B)k_{31}(A)+I_1[k_{22}(A)k_{31}(B)+k_{21}(B)k_{32}(A)],$$

$$c_6\doteq I_2[k_{22}(A)k_{31}(B)+k_{21}(B)k_{32}(A)]+I_1k_{22}(A)k_{32}(B),$$

$$c_7\doteq I_2k_{22}(A)k_{32}(B),$$

in which we neglected k_3's with respect to k_2's. It should be noted that for a first-order initiation process I_1 and I_2 are independent of N_1 and N_2, the c's are constants, and the right-hand side of (4b) depends solely upon z. For higher order initiation, $d\ln z/dt$ depends explicitly upon z, the mole ratio, and upon N_2, the number of moles of the second species present.

During the last stages of the reaction, $z\to\infty$, the slope of the $\ln z$ curve becomes $I_1/k_{31}(A)[k_{22}(A)-k_{21}(A)]$ which is constant for first-order initiation. The rate of monomer consumption is then given by

$$\lim_{t\to\infty}\frac{1}{N_l}\frac{dN_l}{dt}=-\frac{k_{2l}(A)I_1}{k_{31}(A)},\quad l=1, 2.$$

The limiting over-all rate follows the same order as the rate of initiation of the slower species. This result is exactly analogous to the one obtained in simple polymerization reactions where it holds throughout the reaction.[6,7] The rate factor depends only upon the constants characteristic for active ends formed by the slower reacting species. This is not unexpected since this type end is the only one formed during the final stages. Equation (4b) can now be specialized to give copolymer systems equivalent to those defined by Jenckel.[3] Case 1: Each species polymerizes independently; expressed by $k_{22}(A)=k_{21}(B)=0$, $k_{32}(A)=k_{31}(B)=0$. The over-all rate is:

$$\frac{d\ln z}{dt}=\frac{I_2k_{22}(B)}{k_{32}(B)}-\frac{I_1k_{21}(A)}{k_{31}(A)}.$$

This shows, as one expected, that the result of the copolymerization is the same as that obtained by separate polymerization and subsequent mixing. The first term on the right equals $-(1/N_2)(dN_2/dt)$ and the second $(1/N_1)(dN_1/dt)$. The same type of result was obtained by Wall.[4] Case 2: In the other extreme, each species adds on to active ends formed by the other type; $k_{21}(A)=k_{22}(B)=0$, $k_{31}(A)$

$=k_{32}(B)=0$. The result is a checker board polymer. One obtains:

$$\frac{d\ln z}{dt}=\frac{(I_1z+I_2)(z-1)}{k_{32}(A)[k_{22}(A)]^{-1}+k_{31}(B)[k_{21}(B)]^{-1}}\frac{1}{z}.$$

Case 3: $-A-A$, $-B-B$, $-B-A$, and $-A-B$ additions occur with equal probability; $k_{21}=k_{22}$, $k_{31}=k_{32}$ for A and B. Equation (4) with constant values for the R_i yields:

$$d\ln z/dt=I_2-I_1.$$

This is a result of the same type as that holding for case 1; furthermore, if the velocities of initiation are also equal, no change of monomer composition results during the whole process and it remains equal to the composition of polymer formed.

Equation (6a) holds also for radical termination. However, the solution (6a) contains the quantities $\sum n_{rs}(A)$ and $\sum n_{rs}(B)$ explicitly, as can be seen from the definition (5) of the α's. In order to determine the sums, we revert to (7), which represents in this case implicit equations for the desired quantities in terms of rate constants and monomer concentrations. On substituting for the ω's in (7) a set of simultaneous cubic equations for $\sum n_{rs}(A)$ and $\sum n_{rs}(B)$ results. The linear term is negligible in comparison with the constant and quadratic terms because of the magnitudes of the different rates. The cubic term is also negligible until N_1 becomes vanishingly small. The solution obtained with these approximations is:

$$\sum n_{rs}(A)=\beta(B)/\gamma(A)\sum n_{rs}(B)$$
$$=\beta(B)\left\{\frac{I_1N_1+I_2N_2}{\beta(B)[k_3(A,A)\beta(B)+k_3(A,B)\gamma(A)]+\gamma(A)[k_3(A,B)\beta(B)+k_3(B,B)\gamma(A)]}\right\}^{\frac{1}{3}}. \quad (7')$$

This expression may be used to determine the average values of the rates. Introduction of the values into (4') and use of the definitions of the β's and γ's yields for the over-all rate for radical termination:

$$\frac{d\ln z}{dt}=I_2-I_1+\frac{N_2^{\frac{1}{3}}(I_1z+I_2)^{\frac{1}{3}}\{k_{21}(B)[k_{22}(A)-k_{21}(A)]z+k_{22}(A)[k_{22}(B)-k_{21}(B)]}{\{k_3(A,A)k_{21}^2(B)z^2+2k_3(A,B)k_{21}(B)k_{22}(A)z+k_3(B,B)k_{22}^2(A)\}^{\frac{1}{3}}}. \quad (4b')$$

If the initiation is first order, (4b') and (4b) show that the distinction between radical and monomer termination lies in the explicit dependence of the over-all rate upon the concentration N_2 in the former case.

If the kinetic distinction between the two types of growing ends is dropped as was done in the derivation of (6) for the distribution of active radical, (4b) and (4b') become

$$\frac{d\ln z}{dt}=(I_1z+I_2)\frac{k_{22}-k_{21}}{k_{31}z+k_{32}} \quad (4c)$$

and

$$\frac{d\ln z}{dt}=(I_2-I_1)+\left(\frac{I_1z+I_2}{k_3}\right)^{\frac{1}{3}}N_2^{\frac{1}{3}}(k_{22}-k_{21}), \quad (4c')$$

where all the k's represent true rates, not average rates as in (4a) and (4') which have the same form.

Unless experimental data are very accurate, it will be difficult to distinguish between the type of behavior described by (4b) and that of (4c); for the ratio of a quadratic to a cubic function of z in (4b) is replaced by the ratio of a constant to a linear term in (4c). Analogous reasoning applies to a comparison of (4b') and (4c'). As far as the dependence of growth and termination upon individual chain composition is concerned, the form of (6) seems to preclude our deriving information from

measurements of over-all rate and from size distribution data. We shall, therefore, make (4c) and (4c') the basis for our further considerations.

Equation (4c) or the full equation (4) with constant coefficients R_i can immediately be integrated. Equation (4c) and the first equation in (4) yield for a first-order initiation process (I_1, I_2 constant):

$$k_{32}I_1 \ln\frac{z}{z_0}+(k_{31}I_2-k_{32}I_1)\ln\frac{I_1z+I_2}{I_1z_0+I_2}=I_1I_2(k_{22}-k_{21})t,$$

$$\ln\frac{N_2}{N_2(0)}=\frac{R_4}{R_2-R_4}\ln z/z_0+\left(\frac{R_4}{R_4-R_2}-\frac{R_3}{R_3-R_1}\right)\ln\frac{(R_1-R_3)z+(R_2-R_4)}{(R_1-R_3)z_0+(R_2-R_4)}\doteq-\frac{k_{22}}{k_{22}-k_{21}}\ln z/z_0, \tag{4d}$$

where $N_2(0)$ and z_0 are the initial mole fraction for the second species and mole ratio, respectively. The approximate equation is valid since rates of growth are large with respect to rates of initiation and termination, and since k_{22}/k_{21} is of the same order of magnitude as k_{32}/k_{31}. This procedure is not acceptable if the rates are very nearly equal, but this has already been considered as case 3 in this section.

The rate constants are best determined from the graph of $d \ln z/dt$ *versus* z. That is, one would find experimentally the $\ln z-t$ curve, calculate the slope and plot it *versus* the corresponding values of z. Figure 1[8] is such a curve for selected values of the rate constants and for different ratios of the two termination rates. Equal velocities of initiation are assumed. Inequality of initiations would not change the general shape of the curves, except for a possible change of sign of the slope. Differences in the growth rates merely shift the curves vertically. Jenckel's[3] and Wall's[4] equations yield the horizontal line.

The experimental data of Marvel and co-workers[9] seem to deviate from the horizontal line. It is difficult to judge from these data whether the deviations follow this theory. For very large values of z the slope is zero since both species are reacting independently. The ratio of the two growth rates can easily be found from (4d).

Equations (2') for radical termination yield as intermediate integral a relation between N_1, N_2, and t, which can be written as follows, if the initiations are first order:

$$\ln\frac{N_2}{N_2(0)}=-\frac{k_{22}}{k_{22}-k_{21}}\ln\frac{z}{z_0}+\frac{k_{22}k_{21}}{k_{22}-k_{21}}\left(\frac{I_2}{k_{22}}-\frac{I_1}{k_{21}}\right)t. \tag{4d'}$$

Equation (4c') then gives for the over-all rate:

$$\frac{d\ln z}{dt}=(I_2-I_1)+[N_2(0)]^{\frac{1}{2}}\frac{(k_{22}-k_{21})}{k_3^{\frac{1}{2}}}\left(\frac{z_0}{z}\right)^{k_{22}/2(k_{22}-k_{21})}(I_1z+I_2)^{\frac{1}{2}}\exp\left\{\frac{k_{22}k_{21}}{2(k_{22}-k_{21})}\left(\frac{I_2}{k_{22}}-\frac{I_1}{k_{21}}\right)t\right\}. \tag{4c''}$$

Unless the two rates of propagation are very nearly equal, the coefficient of t in (4d') and (4c'') will be sufficiently small to make the t factor negligible over a wide interval of the reaction. Under these conditions, (4d') becomes identical with the approximate form of (4d). The slope of the $\ln z-t$ curve depends also upon the initial monomer concentrations, while monomer termination gives a dependence upon the instantaneous ratio z only (4c). Extrapolation of the slope of the $\ln z-t$ curve to zero time yields a straight line according to (4c''), if plotted *versus* the square root of the initial mole fraction $N_2(0)$. Its intercept equals I_2-I_1.

---

[8] We are indebted to Mr. Charles P. Powell for his aid in carrying out the numerical computations.

[9] C. S. Marvel, G. D. Jones, T. W. Mastin, and G. L. Schertz, J. Am. Chem. Soc. **64**, 2356 (1942).

IV. COPOLYMER COMPOSITION AND SIZE DISTRIBUTION

The mole fraction of stable polymer N_{rs} is given by the following equations according to scheme (1), for the stable copolymer formed in a time element dt (hereafter called instantaneous copolymer distribution):

$$\frac{dN_{rs}}{dt}=k_{31}N_1n_{r-1s}+k_{32}N_2n_{rs-1};$$

Monomer termination. (8)

$$\frac{dN_{rs}}{dt}=\frac{k_3}{2}\sum_{i,\,j=0}^{r,\,s}n_{r-is-j}n_{ij};\qquad \frac{dN_{rs}}{dt}=k_3n_{rs}\sum_{i,\,j}n_{ij};$$

Radical termination. (8′)

n_{rs} is derived from (6) for rates independent of r and s:

$$n_{rs}=\omega^r(\omega')^s\left[I_1/k_{21}\binom{r+s-1}{s}+\frac{I_2}{k_{22}}\binom{r+s-1}{r}\right], \quad (6a)$$

$$\sum_{i,\,j}n_{ij}=(I_1N_1+I_2N_2)(\alpha-\beta-\gamma)^{-1},$$

where

$\omega=\omega_{ij}$ and $\omega'=\omega'_{ij}$ are independent of i, j.

Equation (6a) is valid for radical termination if the α's in ω and ω' are defined:

$$\alpha=k_{21}N_1+k_{22}N_2+k_3N_2^{\frac{1}{2}}\left(\frac{I_1z+I_2}{k_3}\right)^{\frac{1}{2}}.$$

Elimination of t in (8) leads by means of relations (4c), (4d), and (6a) to the following expressions valid for first-order initiation and monomer termination:

$$\frac{dN_{rs}}{dz}=\frac{N_2(0)}{z_0(k_{22}-k_{21})}\left(\frac{z_0}{z}\right)^{1+k_{22}/k_{22}-k_{21}}\times\frac{k_{31}z+k_{32}}{I_1z+I_2}f(r,s)\omega^r(\omega')^{s-1},$$

with

$$f(r,s)=\frac{I_1k_{22}k_{31}}{k_{21}^2}\binom{r+s-2}{s}+\frac{I_2k_{32}}{k_{22}}\binom{r+s-2}{s-2}+\left(\frac{I_2k_{31}}{k_{21}}+\frac{I_1k_{32}}{k_{21}}\right)\binom{r+s-2}{s-1}. \quad (8a)$$

Unfortunately it is not possible to integrate this expression in closed form and find in this manner the distribution of stable polymer corresponding to a monomer composition z. Numerical integration is required after the rate constants have been determined from kinetic data. The distribution of stable polymer first formed may be obtained as:

$$N_{rs}(z\to z_0)=\left[\frac{dN_{rs}}{dz}\right]_{z=z_0}(z-z_0).$$

If the monomer ratio z_0 is maintained, this gives the distribution at any instant. The total number of molecules of a certain total chain length p can be determined by means of the equation derived from (8):

$$\frac{d}{dz}\sum_{r+s=p}N_{rs}=N_2\frac{dt}{dz}(\omega+\omega')^{p-2}\left[I_1\frac{k_{22}k_{31}}{k_{21}^2}\frac{\omega^2}{\omega'}+\frac{(I_2k_{31}+I_1k_{32})}{k_{21}}\omega+\frac{I_2k_{32}}{k_{22}}\omega'\right].$$

For the total number of polymer molecules we obtain:

$$\frac{d}{dz}\sum_{r+s=2}^{\infty}N_{rs}=N_2(I_1z+I_2)\frac{dt}{dz},$$

a result which can be written down directly in view of the steady state condition. Integration of the last expression using (4c) and (4d) gives:

$$\sum_{r+s=2}^{\infty}N_{rs}=\frac{k_{31}}{k_{21}}N_1(0)\left[1-\left(\frac{z_0}{z}\right)^{k_{21}/k_{22}-k_{21}}\right]+\frac{k_{32}}{k_{22}}N_2(0)\left[1-\left(\frac{z_0}{z}\right)^{k_{21}/k_{22}-k_{21}}\right].$$

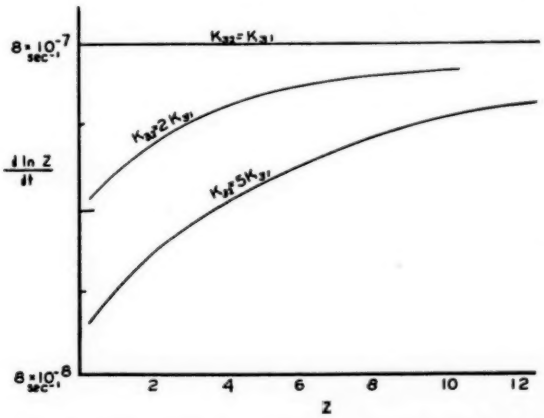

FIG. 1. Slope of $\ln z-t$ curve as a function of z, (4c), for various ratios k_{31}/k_{32}. $I_1=I_2=10^{-9}$ sec.$^{-1}$; $k_{21}=2.10^{-3}$ mole^{-1} liter sec.$^{-1}$; $k_{22}=5k_{21}$; $k_{31}=10^{-5}$ mole^{-1} liter sec.$^{-1}$.

The number average molecular weight of the polymerized material is given by

$$\bar{M}_n(z)=\frac{M_1[N_1(0)-N_1(z)-n_{10}]+M_2[N_2(0)-N_2(z)-n_{01}]}{\sum_{r+s=2}^{\infty} N_{rs}+\sum_{r,s} n_{rs}-n_{10}-n_{01}}. \tag{9}$$

M_1 and M_2 denote the molecular weights of the two monomer species. All mole fractions can be expressed as functions of z by means of relations (3), (4d), and (6a). For the final number average molecular weight we find in this manner, if the small amount of monomer radical is neglected:

$$\bar{M}_n(\infty)=\frac{M_1 z_0+M_2}{\frac{k_{31}}{k_{21}}z_0+\frac{k_{32}}{k_{22}}}. \tag{9a}$$

For a one-component polymerization one has in place of (9a) the familiar result:

$$\bar{M}_n(\infty)=M_1 k_{21}/k_{31}.$$

As is to be expected, the result (9a) depends upon the initial monomer composition which appears here as a weight factor in the average formed over the contribution of the two species to the total. One may guess that the weight average molecular weights of copolymer and pure polymer will be similarly related. The quotient of the two terms in (9) equals the weight ratio w of the two species in the polymerized material:

$$w(z)=\frac{M_1}{M_2}z_0\frac{1-(z_0/z)^{k_{21}/(k_{22}-k_{21})}}{1-(z_0/z)^{k_{22}/k_{22}-k_{21}}}. \tag{10}$$

For $z\to\infty$, the polymer composition naturally becomes equal to the initial monomer composition $(M_1/M_2)z_0$. The result (10) can be valid only beyond the induction period, when the concentration of activated chains n_{rs} is stationary and when n_{10} and n_{01}, whose initial values cannot be determined by the method used here, are negligible in comparison with the terms retained in the numerator and denominator of (10). On extrapolating, however, the composition curve to zero time, $z=z_0$, (10) reduces to:

$$w(z_0)=\frac{M_1}{M_2}z_0\frac{k_{21}}{k_{22}}.$$

Hence the intercept of the polymer composition curve gives the ratio of the rates of growth for the two components. Equation (10) may easily be expressed in terms of weight percentage composition of monomer which gives a more accurate graph for large values of z. Because of the identity of (4d′) and (4d) previously discussed, (10) holds approximately also in the case of radical termination. The instantaneous distribution by weight, $(d/dz)[(M_1r+M_2s)N_{rs}]$ according to (8a), is plotted in Figs. 2 and 3 *versus* the total chain length for constant chain composition $\delta=s/r$ and

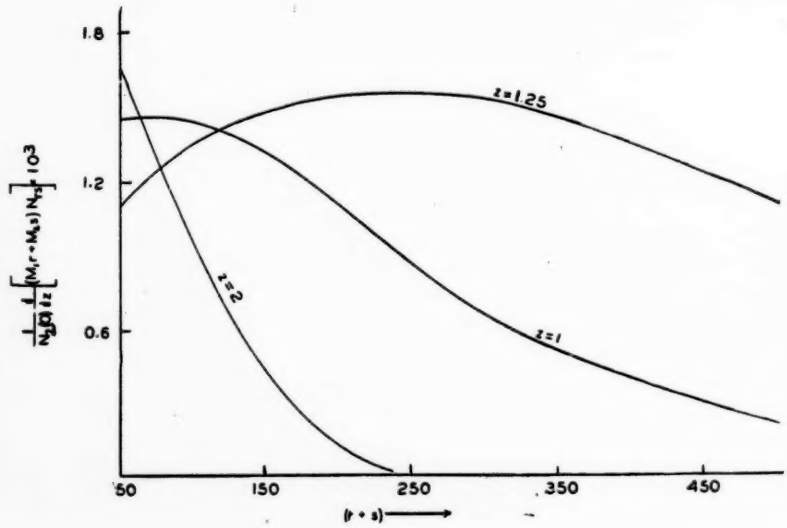

FIG. 2. Instantaneous weight distribution (9) at constant chain composition $\delta=s/r=4$ as a function of chain length $r+s$, at various stages of the reaction. Rates identical with those in Fig. 1 with $k_{32}=2k_{31}$, $z_0=0.4$. Vertical scale should be divided by ten for $z=2$.

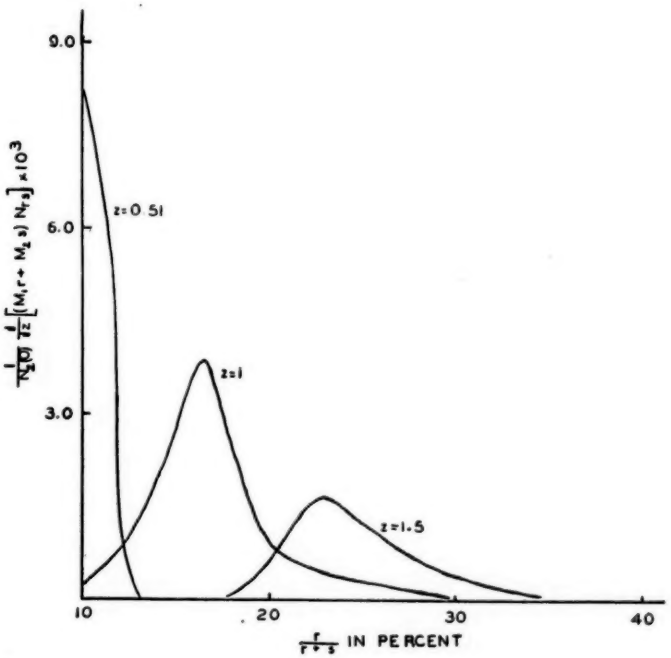

FIG. 3. Instantaneous weight distribution (9) at constant chain length $r+s=200$ as a function of chain composition $r/r+s$ at various stages of the reaction. Numerical values of constants identical with those in Fig. 2. Ordinate scale for curve $z=0.51$ should be multiplied by two.

versus the composition $r/r+s$ for constant chain length, respectively, at various stages z of the reaction. Some of the values chosen were suggested by Reinhardt's[10] data on the vinyl chloride (species 1) vinylidene chloride (species 2) system. Stirling's formula can be used to replace the factorials for most of the values of r and s shown in the graphs. In the plots at constant δ, (8a) leads to:

$$(M_1r+M_2s)\frac{dN_{rs}}{dz}=A(z)r!\left\{\frac{(\delta+1)^{\delta+1}}{\delta^{\delta}}\times\frac{k_{22}^{\delta}k_{21}z}{[(k_{21}+k_{31})z+(k_{22}+k_{32})]^{\delta+1}}\right\}^{r}. \quad (9)$$

The maximum of the distribution is at

$$(r+s)_{\max}=r_{\max}(1+\delta)=\left(\frac{1+\delta}{2}\right)\times\left[\ln\left(\frac{\delta^{\delta}}{(\delta+1)^{\delta+1}}\frac{[(k_{21}+k_{31})z+k_{22}+k_{32}]^{\delta+1}}{k^{\delta}\,k_{22}^{21}z}\right)\right]^{-1}.$$

It may be seen that both for very large and very small values of z, the maximum shifts to very small values of r. If the composition of the monomer residue is such that (depending essentially upon the growth rates) the mean composition of polymer just formed deviates pronouncedly from the desired one (δ), then the latter will, because of statistical reasons, occur only in very small chains. Accordingly one may expect the maximum in Fig. 2 to be farthest to the right, when the monomer composition z(max) obeys the relation

$$\delta=\frac{k_{22}+k_{32}}{k_{21}+k_{31}}\frac{1}{z\,(\max)}. \quad (10)$$

Setting $d(r+s)_{\max}/dz$ equal to zero actually leads to this result. The corresponding value of the molecular weight is found from the above equa-

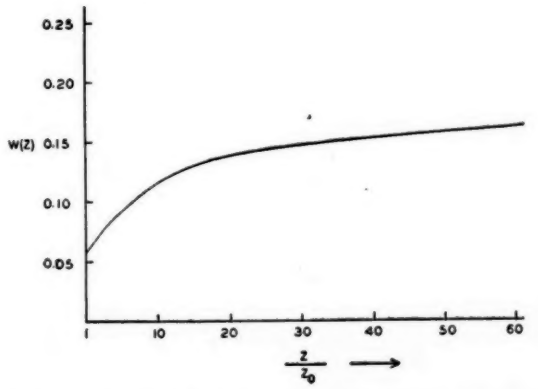

FIG. 4. Weight ratio $w(z)$ of reactants in copolymer as a function of mole ratio z of monomer (10). Numerical values of constants are the same as those in Fig. 2.

[10] R. C. Reinhardt, Ind. Eng. Chem. **35**, 422 (1943).

tion for $(r+s)_{\max}$ after insertion of the value for $z(\max)$. Expansion of the logarithm gives the following equation for the largest obtainable molecular weight corresponding to a maximum in the composition distribution curve:

$$\frac{1}{2}\frac{M_1\frac{1}{\delta}+M_2}{\frac{k_{31}}{k_{21}}\frac{1}{\delta}+\frac{k_{32}}{k_{22}}}. \tag{11}$$

Comparison of this equation with relation (9a) shows that this maximum molecular weight is exactly one-half the final number average molecular weight obtained if the initial monomer ratio z_0 equals the desired ratio $1/\delta$ in the chains. If one wishes to maintain throughout the polymerization a given ratio δ in long chains, the initial composition z_0 must be chosen equal to $z(\max)$ and z maintained at this value by suitable monomer addition. In Fig. 3 the maximum shifts to larger contents of type one monomer with progressing copolymerization, as is to be expected. The instantaneous distributions of polymer formed by the interaction of two activated chains are given by the following equations, derived from (8′) and (6a) in the Appendix III:

$$\frac{dN_{rs}}{dt}=\frac{k_3}{2}\omega^r(\omega')^s\left\{\left(\frac{I_1}{k_{21}}\right)^2\binom{r+s-1}{s+1}(s-1)+\frac{I_1I_2}{k_{21}k_{22}}\left[\binom{r+s-1}{s}(s-1)+\binom{r+s-1}{r}(r-1)\right]+\left(\frac{I_2}{k_{22}}\right)^2\binom{r+s-1}{r+1}(r-1)\right\};$$

$r, s>0$, Combination; (8a′)

$$\frac{dN_{r0}}{dt}=\frac{k_3}{2}(r-1)\omega^r(I_1/k_{21})^2;$$

$$\frac{dN_{0s}}{dt}=\frac{k_3}{2}(s-1)(\omega')^s\left(\frac{I_2}{k_{22}}\right)^2;$$

$$\frac{dN_{rs}}{dt}=k_3^{\frac{1}{2}}N_2^{\frac{1}{2}}(I_1z+I_2)^{\frac{1}{2}}\omega^r(\omega')^s\left[\frac{I_1}{k_{21}}\binom{r+s-1}{s}+\frac{I_2}{k_{22}}\binom{r+s-1}{r}\right].$$ Disproportionation.

By means of (4c″), (8a′) may again be formulated in terms of z through elimination of the time variable. It may be noted from (8a) and (8a′) that the distribution by number, N_{rs}, will exhibit a maximum in the case of combination, while curves for polymer terminated by means of monomer or by a disproportionation mechanism shows a maximum only if plotted as weight distribution, similarly as in the case of one-component systems.[7] Equation (8a[1]) gives at once the distribution $\lim_{z\to z_0} N_{rs}$ of stable polymer formed initially, if t is eliminated by means of z in analogy to the case previously discussed. Plots at constant composition and chain length, respectively, lead to the same conclusions as before. No analytical expression for the maximum chain length obtainable with a desired composition δ can be found because of the complications arising from the definition of ω and ω' in this case. If the factor containing k_3 in ω and ω' can be neglected, Eq. (10) with omission of k_{31} and k_{32} is again obtained.

Relations for the size and composition distribution developed here or found by similar methods for other polymerization mechanisms should permit at least an estimation of the homogeneity of a copolymer with respect to size and composition at various stages of the reaction, once the kinetics of the process is established and the velocity constants for the elementary steps are known. In the case of insoluble or nearly insoluble cross-linked polymers of the vinyl-divinyl type the only thermodynamic method available at present for an analysis of the product formed is a study of the swelling isotherms.[11] This allows a determination of the average chain length between two cross links. Kinetic investigations enable one to supplement this information with distribution data. Jenckel[3] has carried out fractionations on four soluble copolymer systems, namely, styrene and methacrylic acid ester, methyl methacrylate and vinyl acetate, respectively, and vinyl pyrrolidine-vinyl carbazole. He furthermore attempted to draw conclusions as to the kinetics of the process on this basis. However, in his analysis the inhomogeneity in respect to size was neglected. In general, chain

[11] P. J. Flory and J. Rehner, Jr., J. Chem. Phys. **11**, 521 (1943).

composition as well as chain length[12] determine the thermodynamic equilibrium at a given temperature.[13] It is evident for instance, that the shorter chains precipitated from a solution contain more of that component which, as a pure polymer, is less soluble in the same solvent.

Finally, considerations of this type will play a role in the application of Flory's[14] and Stockmayer's[15] theory of gel formation to cross-linked polymers, by determining the relative probabilities with which mono- and divinyl enter the chains, and therefore the average number of cross bonds per chain. The intramolecular distribution of cross bonds can then be calculated in terms of the extent of reaction. The number P_i of groups of monovinyl units containing i members in N_{rs} cross-linked chains of length $(r+s)$ which have been formed in an interval dz, is given by:[16]

$$P_i = N_{rs}(r+s)(1-\omega)^2\omega^i;$$

for $i \ll r+s$, with

$$\omega = \frac{k_{21}z}{k_{21}z+k_{22}}.$$

k_{22} designates the rate of cross-bond formation, k_{21} that of addition of monovinyl units. If the chain length is not sufficiently large, the effect of the two ends and their mode of formation must be taken into account by the introduction of parameters for initiation and termination and modification of the above formula.[16]

We should like to acknowledge our indebtedness to Dr. R. F. Boyer and Dr. R. C. Reinhardt of The Dow Chemical Company for many helpful discussions.

APPENDIX

I. Solution of the Difference Equations (5a)

The result for n_{r0} and n_{0s} is easily found. Direct substitution in (5a) for low values of r and s leads to the following typical equations:

$$\alpha_{12}n_{12} = \beta_{02}n_{02} + \gamma_{11}n_{11};$$

$$\alpha_{32}n_{32} = \frac{\beta_{02}\beta_{12}\beta_{22}n_{02} + \gamma_{11}\beta_{12}\beta_{22}n_{11}}{\alpha_{12}\alpha_{22}} + \frac{\gamma_{21}\beta_{22}}{\alpha_{22}}n_{21} + \gamma_{31}n_{21};$$

or

$$\alpha_{r2}n_{r2} = \alpha_{02}\prod_{l=0}^{r-1}\left(\frac{\beta_{l2}}{\alpha_{l2}}\right)n_{02} + \sum_{j=1}^{r} n_{j1}\gamma_{j1}\prod_{l=j}^{r-1}\frac{\beta_{l2}}{\alpha_{l2}}.$$

The first term on the right expresses that an n_{r2} may be built from an n_{02} by adding on r units of the first kind; the second term that n_{r2} may be built from $n_{11}, n_{21}\cdots n_{r1}$ by joining a unit of the second kind and then completing the structure by adding a sufficient number of the first species. This may be generalized to

$$\alpha_{rs}n_{rs} = \alpha_{0s}\prod_{l=0}^{r-1}\left(\frac{\beta_{ls}}{\alpha_{ls}}\right)n_{0s} + \sum_{j=1}^{r} n_{j\,s-1}\gamma_{j\,s-1}\prod_{l=j}^{r-1}\left(\frac{\beta_{ls}}{\alpha_{ls}}\right)$$

which can be explained as before. It is equivalent to the intermediate result presented in the text. On substituting n_{0s} and ω's from the text this becomes:

$$\alpha_{rs}n_{rs} = I_2N_2\prod_{l=0}^{r-1}\omega_{ls}\prod_{l=1}^{s-1}\omega_{0l}' + \sum_{j_1=1}^{r}\gamma_{j_1\,s-1}n_{j_1\,s-1}\prod_{l=j_1}^{r-1}\omega_{ls}.$$

This expression can be utilized to establish a recurrence formula between n_{j_1s-1} and n_{j_2s-2} with $1 \leqq j_2 \leqq j_1$. n_{j_2s-2} may be expressed in terms of n_{j_3s-1} with $1 \leqq j_3 \leqq j_2$. Continued substitution and rearrangement leads to (6).

II. Solution of Difference Equations (5b)

Equations (5b) gives for the pure radical species:

$$n_{r0} = \frac{I_1N_1}{\beta(A)}[\omega(A)]^r; \quad n_{0s} = \frac{I_2N_2}{\gamma(B)}[\omega'(B)]^s.$$

Examining a $n_{rs}(A)$ for low values of r, s, for example, $n_{22}(A)$:

$$n_{22}(A) = \frac{I_1N_1}{\alpha(A)}\omega'(A)\omega'(B)\omega(B) + \frac{I_2N_2}{\alpha(B)}[\omega(B)\omega'(A)\omega(B) + \omega'(B)\omega(B)\omega(A)].$$

We see that there will be in all cases two expressions, one

---

[12] See, for instance, H. Staudinger and J. Schneiders, Ann. **541**, 151 (1939).

[13] This can be expressed roughly by an extension of the theory of P. J. Flory, J. Chem. Phys. **10**, 51 (1942) and M. L. Huggins, Ann. N. Y. Acad. Sci. **43**, 1 (1942). Let the heat of mixing depend solely upon the polymer composition and be independent of the intramolecular arrangement, which is reasonable. Applying G. Scatchard's [Chem. Rev. **8**, 321 (1931)] expression for the heat of mixing to the ternary system, the parameter K (in Flory's notation), a ratio between cohesional and thermal energy, assumes the following form:

$$K = 2v_1/RT[A_{12}\kappa + A_{13}(1-\kappa) - A_{23}\kappa(1-\kappa)].$$

κ is the chain composition $r/r+s$ in the notation adopted, v_1 the molar volume of the solvent. The indices 2 and 3 refer to the two monomer species. The A coefficients depend upon the nature of the respective components only and monomers 2 and 3 are assumed to be approximately equal in size. The relations for the partial molal entropies will in general depend upon the intramolecular arrangement of the two species which determines the internal flexibility of the polymer molecule, unless they are chemically similar enough. Disregarding this factor, the above authors' results give at once a relation between chain length and composition at the critical point of formation of a two-phase system at a given temperature. Furthermore, the slope of the plot of reduced osmotic pressure *versus* concentration (in weight per volume) for small concentrations is proportional to $(1-K)$ and is therefore a function of the chain composition. Osmotic data on copolymers are very desirable in this connection.

[14] P. J. Flory, J. Am. Chem. Soc. **63**, 3096 (1941).

[15] W. H. Stockmayer, J. Chem. Phys. **11**, 45 (1943); W. H. Stockmayer and H. Jacobson, *ibid.* **11**, 393 (1943).

[16] F. T. Wall, J. Am. Chem. Soc. **62**, 803 (1940); **63**, 821 (1941). R. Simha, *ibid.* **63**, 1479 (1941).

corresponding to initiation by the first species, the other by the second. The terms in the ω's again express the manner of growth of the active nuclei. From the meaning of the ω's we can interpret for this example the first product in the I_2 term as growth in the following order: $B-A-B-A-$, and the second: $B-B-A-A$. The I_1 term represents: $A-B-B-A$. The total number of terms in the expression for $n_{rs}(A)$ will evidently be equal to the number of ways of arranging the structural units within the chain with specified ends:

$$\underbrace{\frac{(r+s-2)!}{(r-2)!s!}}_{\text{Initiated by } A}+\underbrace{\frac{(r+s-2)!}{(r-1)(s-1)}}_{\text{Initiated by } B.}=\binom{r+s-1}{s}$$

Likewise for $n_{rs}(B)$:

$$\binom{r+s-1}{r}.$$

Let us now characterize a possible intramolecular configuration by i, the number of $A-A$, j, the number of $B-A$, k, the number of $A-B$, and by l, the number of $B-B$ linkages. Each configuration gives rise to a term $\omega(A)^i\omega(B)^j\omega'(A)^k\omega'(B)^l$ multiplied by a statistical weight factor. To determine this factor we consider first the $n_{rs}(A)$ initiated by B. The conditions to be fulfilled by i, j, k, and l are: $i+j=r$, since an A must follow an A or a B; $j=k+i$, since all the groups formed by B except the first are preceded by an A ($A-B$ linkage) and all are succeeded by an A including the first ($B-A$ bond); $j+l=s$, since a B must be followed by an A or by a B. Let m_t be the number of groups formed by t structural units of type A, whence $\Sigma m_t=j$, $\Sigma tm_t=r$. Let m_t' have the same meaning for type B and $\Sigma m_t'=j$, $\Sigma tm_t'=s$. The weight factor for the specified configuration i, j, k, l is

$$\sum_{m_t'}\frac{(\Sigma m_t')!}{\Pi(m_t')!}\sum_{m_t}\frac{(\Sigma m_t)!}{\Pi(m_t)!}=\sum_{m_t'}\frac{j!}{\Pi(m_t')!}\sum_{m_t}\frac{j!}{\Pi(m_t)!}\quad(A-1),$$

to be summed over all values of m_t and m_t' compatible with the auxiliary conditions. The sum over m_t' gives the independent configurations resulting from a permutation of the B groups, that over m_t of the A groups. The product therefore gives the total number of independent configurations. Using the multinomial theorem to evaluate one of these sums we find:

$$(\Sigma_t x_t{}^t z^t)^j=j!\sum_{m_t}\prod_t\frac{(x_t{}^t z^{tm_t})}{m_t!}=j!\sum_m z^{\Sigma tm_t}\prod_t\frac{x_t{}^{tm_t}}{m_t!}\quad(\Sigma m_t=j),$$

whence:

$$\sum_{m_t}\frac{j!}{\prod_t m_t!}=\lim_{x_t\to 1}\{\text{coeff. of } z^r \text{ in } (\Sigma_t x_t{}^t z^t)^j\}$$

$$=\text{coeff. of } z^r \text{ in } \frac{z^j}{(1-z)^j}=\binom{r-1}{j-1}.$$

Replacing r by s gives the sum over m_t'. The final weight factor is:

$$\binom{r-1}{j-1}\binom{s-1}{j-1}.$$

For $m_{rs}(A)$ initiated by A, the conditions for i, j, k, and l are $\Sigma m_t=j+1$, $\Sigma m_t'=j$, $i+j+1=r$, $j=k$, $j+l=s$. Substituting these values for the sums into $(A-1)$ and using the multinomial theorem, we obtain for the weight factor

$$\binom{r-1}{j}\binom{s-1}{j-1}.$$

For $n_{rs}(B)$ initiated by A, the analysis is the same as for $n_{rs}(A)$ initiated by B with $\Sigma m_t'=\Sigma m_t=k$, $i+k=r$, $j=k-1$, $k+l=s$, hence the weight factor:

$$\binom{r-1}{k-1}\binom{s-1}{k-1}.$$

$n_{rs}(B)$ initiated by B carries the conditions $\Sigma m_t'=k+1$, $\Sigma m_t=k=j$, $i+k=r$, $k+l+1=s$. The weight factor is:

$$\binom{r-1}{k-1}\binom{s-1}{k}.$$

Introducing the weight factors as coefficients of the ω's and substituting the values of the exponents in terms of r and s, we find:

$$n_{rs}(A)=\frac{I_1N_1}{\alpha(A)}\sum_{j=1}^{s}\binom{r-1}{j}\binom{s-1}{j-1}\times[\omega'(A)]^j[\omega'(B)]^{s-j}[\omega(B)]^j[\omega(A)]^{r-j-1}$$

$$+\frac{I_2N_2}{\alpha(B)}\sum_{j=1}^{s}\binom{r-1}{j-1}\binom{s-1}{j-1}\times[\omega'(A)]^{j-1}[\omega'(B)]^{s-j}[\omega(B)]^j[\omega(A)]^{r-j};$$

$$n_{rs}(B)=\frac{I_1N_1}{\alpha(A)}\sum_{k=1}^{r}\binom{r-1}{k-1}\binom{s-1}{k-1}\times[\omega'(A)]^k[\omega'(B)]^{s-k}[\omega(B)]^{k-1}[\omega(A)]^{r-k}$$

$$+\frac{I_2N_2}{\alpha(B)}\sum_{k=1}^{r}\binom{r-1}{k-1}\binom{s-1}{k}\times[\omega'(A)]^k[\omega'(B)]^{s-k-1}[\omega(B)]^k[\omega(A)]^{r-k}.$$

The first expression on the right for $n_{rs}(A)$ may be written as:

$$I=\frac{I_1N_1}{\alpha(A)}[\omega(A)]^{r-1}[\omega'(B)]^s\sum_{j=1}^{s}\binom{r-1}{j}\binom{s-1}{j-1}\left[\frac{\omega'(A)\omega(B)}{\omega(A)\omega'(B)}\right]^j.$$

Now

$$\binom{r-1}{j}\binom{s-1}{j-1}=\binom{r-1}{j}\binom{s}{j}-\binom{r-1}{j}\binom{s-1}{j}.$$

$$\sum_{j=1}^{s}\binom{r-1}{j}\binom{s}{j}x^j=(r-1)sx+\frac{(r-1)(r-2)}{1\cdot 2}\frac{s(s-1)}{1\cdot 2}x^2+\cdots$$

$$=F(1-r,-s,1,x)-1,$$

where $F(a,b,c,x)$ is the hypergeometric function[17]

$$F(a,b,c,x)=1+\frac{ab}{c}x+\frac{a(a+1)}{1\cdot 2}\frac{b(b+1)}{c(c+1)}x^2+\cdots.$$

Likewise:

$$\sum_{j=1}^{s}\binom{r-1}{j}\binom{s-1}{j}x^j=-F(1-r,1-s,1,x)+1$$

and

$$I=\frac{I_1N_1}{\alpha(A)}[\omega(A)]^{r-1}[\omega'(B)]^s\times[F(1-r,-s,1,x)-F(1-r,1-s,1,x)].$$

[17] E. T. Whittaker and G. N. Watson, *Modern Analysis* (The Cambridge University Press, 1940).

Application of this procedure to the other summations gives (6a).

In computing the sums over $n_{rs}(A)$ and $n_{rs}(B)$, the sums over the pure polymer species are easily evaluated. In the copolymer $n_{rs}(A)$ we have for the first term, substituting $i=j-1$.

$$\frac{I_1N_1}{\alpha(A)}\frac{1}{\omega(A)}\sum_{j=1}^{s}\sum_{r,s\geqq 1}^{\infty}[\omega(A)]^r[\omega'(B)]^s\binom{r-1}{j}\binom{s-1}{j-1}x^j$$

$$=x\frac{I_1N_1}{\alpha(A)\omega(A)}\sum_{i=0}^{\infty}x^i\sum_{s=i+1}^{\infty}[\omega'(B)]^s\binom{s-1}{i}\times\sum_{r=i+2}^{\infty}[\omega(A)]^r\binom{r-1}{i+1}$$

$$=x\frac{I_1N_1}{\alpha(A)\omega(A)}\sum_{i=0}^{\infty}x^i\left[\frac{\omega'(B)}{1-\omega'(B)}\right]^{i+1}\left[\frac{\omega(A)}{1-\omega(A)}\right]^{i+2}$$

$$=\frac{I_1N_1}{\alpha(A)[1-\omega(A)]}\frac{\omega(A)\omega'(B)x}{[1-\omega(A)][1-\omega'(B)]-x\omega(A)\omega'(B)}.$$

The second term gives

$$\frac{I_2N_2x}{\alpha(B)\omega'(A)}\sum_i x^i\sum_{r,s\geqq 1}[\omega(A)]^r[\omega'(B)]^s\binom{r-1}{i}\binom{s-1}{i}$$

$$=\frac{I_2N_2}{\alpha(B)\omega'(A)}\frac{x\omega(A)\omega'(B)}{[1-\omega(A)][1-\omega'(A)]-x\omega(A)\omega'(B)}.$$

Combination of these terms gives the sums in (7). $\Sigma n_{rs}(B)$ is determined in the same manner.

III. Derivation of (8a′)

Introducing the values for n_{ij} and $n_{r-i\ s-j}$ from (6a) into (8′) one is led to four sums. The first is:

$$\left(\frac{I_1}{k_{21}}\right)^2\frac{k_3}{2}\omega^r(\omega')^s\sum_{i,j}\binom{r-i+s-j-1}{s-j}\binom{i+j-1}{j}$$

$$=\left(\frac{I_1}{k_{21}}\right)^2\frac{k_3}{2}\omega^r(\omega')^s\sum_{\lambda=2}^{r+s-2}S_\lambda=\left(\frac{I_1}{k_{21}}\right)^2\frac{k_3}{2}\omega^r(\omega')^sS_I,$$

where

$$S_\lambda=\sum_{j=1}^{s-1}\binom{r+s-1-\lambda}{s-j}\binom{\lambda-1}{j}$$

$$=\sum_{j=0}^{s}\binom{r+s-1-\lambda}{s-j}\binom{\lambda-1}{j}-\binom{r+s-\lambda-1}{s}-\binom{\lambda-1}{s}.$$

Now

$$\binom{m+n}{p}=\sum_{j=0}^{p}\binom{m}{p-j}\binom{n}{j};\quad\binom{m+1}{p+1}=\sum_{j=0}^{m-p}\binom{m-j}{j}.$$

Consequently:

$$S_\lambda=\binom{r+s-2}{s}-\binom{r+s-\lambda-1}{s}-\binom{\lambda-1}{s}$$

and

$$S_I=\binom{r+s-2}{s}(r+s-3)-\sum_{\lambda=2}^{r+s-2}\binom{r+s-\lambda-1}{s}-\sum_{\lambda=2}^{r+s-2}\binom{\lambda-1}{s}.$$

The first summation on the right gives with $\delta=\lambda-2$:

$$\sum_{\delta=0}^{r+s-4}\binom{r+s-3-\delta}{s}=\sum_{\delta=0}^{r-3}\binom{r+s-3-\delta}{s}=\binom{r+s-2}{s+1},$$

since the binomial coefficient is zero when the bottom term exceeds the top. The second summation in S_I may be written with $\delta=r+s-2-\lambda$:

$$\sum_{\lambda=s+1}^{r+s-2}\binom{\lambda-1}{s}=\sum_{\delta=0}^{r-3}\binom{r+s-3-\delta}{s}=\binom{r+s-2}{s+1}.$$

Finally:

$$S_I=\binom{r+s-2}{s}(r+s-1)-2\binom{r+s-2}{s+1}=\binom{r+s-1}{s+1}(s-1).$$

The second sum is

$$\left(\frac{I_1}{k_{21}}\right)\left(\frac{I_2}{k_{22}}\right)\frac{k_3}{2}\omega^r(\omega')^s\sum_{i,j}\binom{i+j-1}{j}\binom{r+s-i-j-1}{r-i}.$$

Since

$$\binom{r+s-i-j-1}{s-j-1}=\binom{r+s-i-j}{s-j}-\binom{r+s-i-j-1}{s-j},$$

$$S_{II}=\sum_{i,j}\binom{i+j-1}{j}\binom{r+s-i-j}{s-j}-S_I.$$

The first term above on the right may be obtained from S_I by replacing r by $r+1$:

$$S_{II}=(s-1)\binom{r+s-1}{s}.$$

The third and fourth terms are

$$\left(\frac{I_1}{k_{21}}\right)\left(\frac{I_2}{k_{22}}\right)\frac{k_3}{2}\omega^r(\omega')^s\sum_{i,j}\binom{i+j-1}{i}\binom{r+s-i-j-1}{s-j}$$

and

$$\left(\frac{I_2}{k_{22}}\right)^2\frac{k_3}{2}\omega^r(\omega')^s\sum_{i,j}\binom{i+j-1}{i}\binom{r+s-i-j-1}{r-i}.$$

The sums become identical with the second and first upon interchange of r and s, i and j. Substitution of the values found in this manner gives (8a′).

Polymer Spectra of a Cyanine Dye

RICHARD W. MATTOON
Ryerson Physical Laboratory, University of Chicago, Chicago, Illinois

(Received February 21, 1944)

In dilute aqueous solutions the dye 1,1′-diethyl-2,2′-cyanine chloride, a photographic sensitizer, has two broad molecular absorption bands with maxima at 4900 and 5230A. For a 10^{-2} molar water solution at room temperature, which is a gel, a new, intense, and exceedingly narrow absorption and fluorescence band has been found at 5730A by G. Scheibe, and by E. Jelley by other methods. The electric polarization of this band in both absorption and fluorescence is parallel to the long dye polymers formed in the gel. In the present investigation the occurrence and behavior of this "P band" were studied for thin dye films deposited on glass from solutions containing water. The P band shifts about 50A to greater wave-length, becomes broader and weaker, and finally disappears as the water is removed by pumping and/or by increasing the temperature. This behavior is reversible if water vapor is readmitted. The position of the P band enables a measurement of the humidity of the atmosphere surrounding the film. The effect of temperature from -195 to $+100$°C is described. The P band can be made to appear starting with water solutions as dilute as 10^{-5} M by freezing the water, locally concentrating the solution. For dye films, there is observed a second, weaker absorption band (called the P_{M1} band) at 5430A similar to the P band in structure and behavior but polarized perpendicular to the polymer chains and requiring a higher dye concentration before appearing. Reasons discussed in the paper indicate that the P band is due to single dye polymer chains while the P_{M1} band should belong to a system of coupled chains lying mutually parallel and forming threads. These threads were observed microscopically. A dehydrated film may contain a fraction of the dye molecules in monomeric form, another fraction (showing only the molecular bands much broadened) in an array anchored to the supporting surface such that the mere addition of water *vapor* immediately produces the polymer chains with the P and P_{M1} bands, and the remainder in crystalline form with a broad absorption band at 5650 and a broad fluorescence band at 6200A. Experiments undertaken to determine the number of water molecules per dye molecule necessary for polymerization were only sufficient to determine that the order of magnitude of the ratio is from 1 : 2 to 10 : 1. An attempt is made to interpret the absorption and fluorescence bands of the polymer chains by the hypothesis of exciton migration.

1. INTRODUCTION

THE dye 1,1′-diethyl-2,2′-cyanine chloride is one of a class used for sensitizing photographic emulsions for longer wave-lengths when adsorbed on the surface of the silver halide grains.[1] This red dye shows two normal molecular absorption bands each several hundred angstroms wide with maxima[2] at 4900 and 5230A, characteristic of the molecules when dissolved in polar solvents such as alcohol.

However, if the solvent is water some unusual phenomena occur. As the concentration of the dye is increased, the 5230A molecular absorption band becomes weaker, a new absorption band begins to appear (E. E. Jelley[3] and G. Scheibe[4]), and at the same time the viscosity of the solution increases.[5] [A "saturated solution" at room temperature[6] is about $3(10)^{-2}$ mole/liter.] At a concentration of about 10^{-2} M the viscosity is so high that the solution is a gel[4] while the new absorption band with its maximum at about 5730A is intense and unusually narrow as compared with normal absorption bands of polyatomic molecules. It actually resembles a broadened atomic absorption line. Diluting or heating the gel causes the new band and the gel state to disappear,[5–8] and these effects are indefinitely reversible. They are explained[8] as the result of a reversible polymerization in which the dye molecules are coupled together through the medium of the water molecules to form long

[1] For the average areal density distribution of the adsorbed dye see, for instance, S. E. Sheppard, R. H. Lambert, and R. D. Walker, J. Chem. Phys. **7**, 265 (1939). For the spectral region where the iodide of this dye sensitizes emulsions see C. E. Kenneth Mees, *The Theory of the Photographic Process* (The Macmillan Company, New York, 1942), p. 980.

[2] L. G. S. Brooker and G. H. Keyes, J. Am. Chem. Soc. **58**, 659 (1936). This reference is for the iodide compound the molecular spectrum of which is essentially identical to that of the chloride compound.

[3] E. E. Jelley, Nature **138**, 1009 (1936).

[4] G. Scheibe, Zeits. f. angew. Chemie **50**, 51 (1937).

[5] G. Scheibe, Kolloid Zeits. **82**, 1 (1938).

[6] H. Ecker, Kolloid Zeits. **92**, 35 (1940).

[7] G. Scheibe, L. Kandler, and H. Ecker, Naturwiss. **25**, 75 (1937).

[8] G. Scheibe, A. Mareis, and H. Ecker, Naturwiss. **25**, 474 (1937).

polymer chains. The presence of H_2O (or D_2O) mixed in other solvents is sufficient to bring out this polymer band, but without water it is absent.[6] The gel state has been called a "nematic phase",[9] or a "*Z* state",[10] or a "mesophase",[11] and the band characteristic of this polymerized state has been called a "*P* band",[6] or a "*Z* band",[10] or a "*J* band".[11] The terms "gel" and "*P* band" (*P* for polymer) will be used in this report, and "gel" will mean about a 10^{-2} *M* solution of dye in water at room temperature.

The structure of the dye molecule is shown in Fig. 1.[12–14] The dimethyl iodide compound was first synthesized many years ago by O. Fischer and G. Scheibe;[15] subsequently improvements in synthesis have been made on the diethyl chloride compound by F. M. Hamer,[16] and by L. G. S. Brooker and collaborators.[17]

The dye in a dilute aqueous solution at room temperature does not fluoresce. However, irradiation of the *gel* with light of the same wave-length as the polymer absorption band (5730A) causes fluorescence in this *P* band[3,18,19] (*P* for polymer), analogous to the resonance fluorescence of atoms. Irradiation of the gel with light of the wave-lengths of one of the two molecular absorption bands (5230 or 4900A), or with shorter wave-lengths, does not produce fluorescence in these molecular bands, but again causes fluorescence only in the *P* band.

If the amount of water in the gel is further reduced, new optical and mechanical properties are observed. Scheibe and L. Kandler[13] state that under these conditions both molecular bands shift their positions to longer wave-lengths. Jelley[9] finds that comparable dye concentrations give a thread-like but non-crystalline structure (third phase*). Further, when all the water is removed it is possible to obtain dye crystals

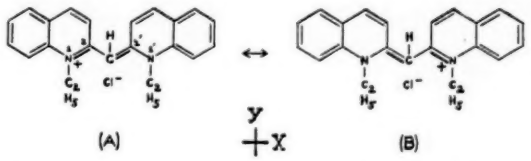

FIG. 1. The dye 1,1′-diethyl-2,2′-cyanine chloride, $C_{23}H_{23}N_2Cl$, shows resonance between several configurations. One of these combinations (A↔B) is shown above. (The identical dye is called *N,N′*-Diäthyl-Pseudo-Isocyanin-Chlorid in the German literature, and 1:1′-diethyl-ψ-cyanine chloride in the British literature. Eastman Kodak Company's designation is Dye V a. The notation used here in the text seems the least ambiguous.) The electric polarization of the 4900A molecular absorption band is along the *y* direction; that of the 5230A molecular absorption band is along *x*. The single polymer consists of dye molecules piled one on top of the other, like a pack of cards, extending in the *z* direction. The electric polarization of the 5730A polymer absorption and fluorescence band is along *z*, determined by aligning the single polymer chains of the gel by streaming orientation.

(fourth phase), which do not show the narrow *P* band but do show a different absorption and fluorescence spectrum.

J. Franck and E. Teller[20] have presented a theory in which the shape and behavior of the polymer band, the resonance fluorescence, and other spectroscopic and photochemical properties are explained. This *P* band has all the properties expected from an electronic transition in a giant polymer in which the single resonators are so strongly coupled in the excited state that the energy remains in one molecule of the polymer a very short time compared with an oscillation period of that molecule (exciton[21] migration).

Scheibe and co-workers[13,18] have suggested that the dye molecules are coupled together by the inductive forces of the *p* electrons of the dye molecules, and also that the water molecules and conjugation play a role in forming the polymer. On the other hand, Sheppard[10,11,22] has proposed that the intermolecular coupling is due to the linkage of two water molecules with the two pairs of corresponding nitrogen atoms of any two adjacent dye molecules along the polymer.

Many more observations have been enumerated in a survey by Sheppard.[11] The present investigation is devoted to a further experimental study of the dye polymerization.

[9] E. E. Jelley, Nature **139**, 631 (1937).
[10] S. E. Sheppard, Science **93**, 42 (1941).
[11] S. E. Sheppard, Rev. Mod. Phys. **14**, 303 (1942).
[12] G. Scheibe, Zeits. f. angew. Chemie **52**, 631 (1939).
[13] G. Scheibe and L. Kandler, Naturwiss. **26**, 412 (1938).
[14] G. Scheibe, A. Schöntag, and F. Katheder, Naturwiss. **27**, 499 (1939).
[15] O. Fischer and G. Scheibe, J. prakt. Chemie **100**, 86 (1920).
[16] Frances M. Hamer, J. Chem. Soc., p. 206 (1928).
[17] L. G. S. Brooker and G. H. Keyes, J. Am. Chem. Soc. **57**, 2488 (1935).
[18] G. Scheibe, Zeits. f. angew. Chemie **50**, 212 (1937).
[19] G. Scheibe, Naturwiss. **25**, 795 (1937).
* The first phase is a molecularly dispersed solution; the second corresponds to the gel with primary polymerization.

[20] J. Franck and E. Teller, J. Chem. Phys. **6**, 861 (1938).
[21] J. Frenkel, Physik. Zeits. Sowjetunion **9**, 158 (1936).
[22] C. E. Kenneth Mees, *The Theory of the Photographic Process* (The Macmillan Company, New York, 1942), p. 1076.

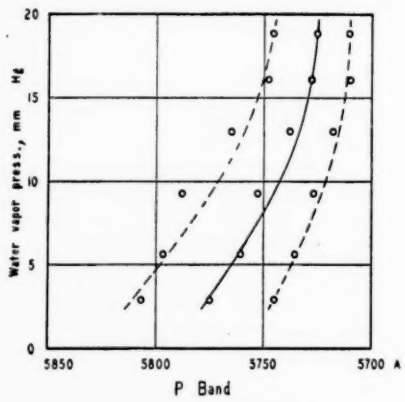

FIG. 2. —— position of maximum absorption. – – – position of the edges at estimated half-maximum absorption. With increasing water vapor pressure in the environment of a dye film at room temperature (21.4°C for the above data, and using Method 1 mentioned in the text), the wave-length of the maximum absorption of the *P* band continuously decreases, the width at half-maximum decreases, and the intensity of the maximum increases. Any new position is attained rapidly and reproducibly.

2. DEPENDENCE OF THE *P* BAND AT ROOM TEMPERATURE ON WATER VAPOR PRESSURE

For dye films made by the evaporation of a solvent from a solution, Scheibe and coworkers[13,23] have shown that the *P*-absorption band becomes weaker and broader and shifts to somewhat longer wave-lengths as water is removed from the film by pumping. Jelley[9] has also noticed such a shift with aging. In the present work this observation has been studied by several methods.

Most of the experiments were done with thin films of dye on glass; in a few cases polished metal surfaces were used. To make these films a dye solution of 1 mg per cc of solvent, or 2.76 $(10)^{-3}$ *M*, is placed on clean glass and the solvent is allowed to evaporate. Water is a poor solvent for this purpose because it does not evaporate uniformly and quickly, but the lower alcohols and chloroform in humid air behave more satisfactorily. Ethyl alcohol (95 percent) is preferable. The best thickness for observing the *P* band is about 5 $(10)^{-6}$ g of dye per cm^2. A thinner film shows the *P* band too weakly; a thicker film acts as a red filter with a fairly sharp cut-off at about 5850A.

[23] G. Scheibe, A. Schöntag, J. Kopske, and K. Henle, Zeits. f. wiss. Photographie, Photophysik, u. Photochem. **38**, 1 (1939).

Even if absolute ethyl alcohol, used as the solvent, evaporates from the glass in ordinary air, the *P* band appears since water vapor from the atmosphere immediately enters the alcohol and also condenses on the film due to cooling by evaporation. When the gel state is reached the *P* band appears suddenly, intense, and narrow at 5730A. The gel film appears red by reflected light. Further drying reduces the intensity of the *P* band, broadens it, and shifts it continuously to longer wave-lengths (depending upon the humidity of the environment). The film now looks solid and appears golden by reflected light.

Such dye films on glass show the *P*-absorption band nicely when placed before the slit of a spectroscope with a white light continuous background. The instrument used was a direct vision Schmidt and Haensch (three-prism) spectroscope with a resolving power which permitted estimation of the position of the maximum absorption of the *P* band with an accuracy of about ±3A.

Measurements of the dependence of the *P* band at room temperature on water vapor pressure were made by many methods, three examples of which follow:

1. In a closed box with glass windows the films were mounted over large flat trays in which was spread out a slushy mixture of water saturated with various salts, with an excess of salt. The air in the box was circulated. Each salt maintains its own characteristic constant water vapor pressure (depending upon temperature), and the values used were taken from the data of the U. S. Bureau of Standards.

2. The dye films were put in a closed glass vessel which was connected by a large tube to a remote reservoir of liquid water kept at various temperatures. In this way the water vapor pressure of the environment of the films could be controlled.

3. Water-saturated air at room temperature and dehydrated air were mixed in various proportions at various total pressures for the environment of the films.

These methods gave the same behavior of the *P* band; the presence or absence of dehydrated air made no difference.

The results are shown in Fig. 2. The total shift of the *P* band from the lowest water vapor pressure at which it is observable to saturation is about 50A. The position of the *P* band at all water vapor pressures remains distinct from that of each of the two molecular bands. The *P*-band behavior is understandable if one assumes that the polymer chains become longer as more water

is taken up (see, for instance, the discussion by Franck and Teller[20]).

The position of the *P*-absorption band of such dye films on glass can be used to measure water vapor pressure. This is a hygrometer* based on a new principle.

After remaining a long time in ordinary air (where water vapor is always available), films of dye often develop a "permanent" disappearance of the *P* band. This disappearance can usually be attained quickly by heating normal polymerized films to about 100°C in an environment of very low water vapor pressure. These films when cooled to room temperature in ordinary air usually do not show the *P* band, but instead show a weak absorption band with its maximum at about 5650A and an estimated full width at half-maximum of about 200A. Placing these films in water-saturated air at room temperature, or even at temperatures as high as 100°C where the water vapor pressure is one atmosphere, usually does not cause the *P* band to reappear. Only if *liquid* water is condensed on the surface of the film (for instance, by strong exhalation), so that for a time the dye is dissolved in water, does the 5650A band disappear and the *P* band reappear. After the surplus water has evaporated the dye film shows the normal reversibly polymerized *P*-band phenomena. It has been concluded, therefore, that another solid modification[24] of the dye is possible (Jelley's[9] fourth phase). As will be shown, this is a crystalline state of the dye which must be distinguished from the polymerized state. Consequently, dye molecules deposited on glass in a way which excludes water molecules during the formation of the film should give this crystalline state, which cannot be converted into the polymerized state by the mere presence of water *vapor* if liquid water is excluded.

To prove this, the following arrangement was used. A gas-tight glass box was fitted with sealed-on rubber gloves for manipulation. The box contained an atmosphere of CO_2 kept free from water vapor by the use of P_2O_5. The dye was deposited on the surface of glass in the manner described above, but great care was taken that the solvent, absolute ethyl alcohol or chloroform, was free from water. The evaporation of the solvent from the surface of the glass took place inside the dry box. In this way films were made which did not show the *P* band in the dry box nor after transfer to normal humid air. However, these films did show the 5650A crystal absorption band. Scheibe and collaborators[23] have used anhydrous amyl alcohol to get solid films not showing the *P* band.

The same effect was obtained in experiments originally carried out to study the formation of monomolecular films of dye on the surface of mercury. Inside the dry box mentioned above glass slides were dipped through the dye film on mercury, in the manner of the Langmuir and Blodgett[25] built-up film technique. These films, which were non-uniform after about 50 dips, again did not show the *P* band in the dry box nor after transfer to normal humid air. However, both these films and those mentioned in the previous paragraph showed the normal reversibly polymerized *P*-band phenomena when droplets of water dissolved the dye and the excess water evaporated.

Macroscopic crystals of the dye obtained by standard crystallization methods do not show the *P* band even when put in a water-saturated atmosphere at room temperature, but do show the 5650A crystal absorption band.

These results do not contradict the observation that dye films deposited in normal humid air, or from a solution containing water, or both, can be dehydrated and rehumidified reversibly and repeatedly at room temperature in the manner previously described. The removal of the water links permits the molecular planes to acquire new positions with respect to each other (probably a perfect disorder) but not to change the positions of their anchor points on the supporting surface; these molecules are therefore prevented from grouping themselves into the crystalline state but remain in the right array to be aligned again into polymer chains as soon as water vapor is admitted. A dehydrated film may contain a fraction of the dye molecules in dispersed

* To make a practical instrument the temperature must be accounted for and the dye sample has to be replaced after several months. The design of such a practical instrument was not completed, but its feasibility was demonstrated.

[24] J. A. Leermakers, B. H. Carroll, and C. J. Staud, J. Chem. Phys. **5**, 878 (1937).

[25] Katharine B. Blodgett and Irving Langmuir, Phys. Rev. **51**, 964 (1937).

TABLE I. Effect of low temperature on the *P* band. 2.76 $(10)^{-4}$ *M* dye in water, 3 mm thick.

Temp.	$\lambda_{max.\ abs.}$	Estimated full width at half-max.
20°C	no band	
−10	5730A	50A
−20	5720	40
−78	5712	30
−183	5700	25
−195	5685	20

The intensity of the maximum absorption increases with decreasing temperature. With liquid oxygen (−183°C) or aged liquid air the *P* band must be distinguished from the broader molecular absorption band of liquid oxygen from 5740 to 5800 with its maximum at about 5780A.

monomeric form, another fraction in this particular array ready to be polymerized by water vapor, and the remainder in crystalline form.

3. DEPENDENCE OF THE *P* BAND AT VARIOUS TEMPERATURES ON WATER VAPOR PRESSURE

Warming the gel to about 60°C causes the gel state and the associated *P* band to disappear.[5, 6] From such observations one can conclude that even at room temperature the lengths of the polymer chains are reduced by heat movement. Consequently the formation of still longer chains was studied by lowering the temperature as far as −195°C (liquid nitrogen). Since it was desired to have sufficient water present at all temperatures the following procedure was adopted. A glass absorption cell about 3 mm thick was filled with a dilute solution of dye in water (about 10^{-4} *M* which is too dilute for the *P* band to appear at room temperature). As the temperature is lowered to about −10°C pure ice crystals (free of dye) form; between them there is a concentrated dye solution. As soon as the ice starts to form the *P* band appears. If the temperature is lowered further the chains lengthen, since the heat motion does not break them as frequently. Table I gives an example of the continuous change of the *P* band with lower temperatures.

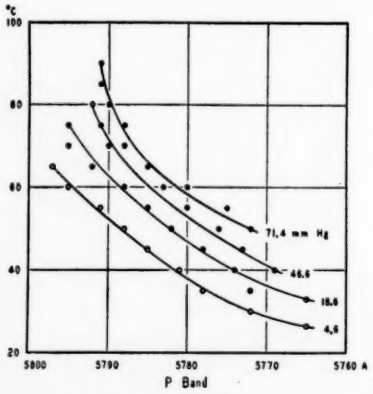

FIG. 3. The position of the maximum absorption of the *P* band depends upon both the temperature of the film and the water vapor pressure indicated for each curve. The *P* band disappeared just above the highest temperature shown for each curve.

Even a 10^{-5} *M* solution of dye in water, which has only a faint pink color, shows the *P* band when frozen. At low temperatures polymerized dye films on glass show spectroscopic behavior of the *P* band similar to that of frozen water solutions (Table I).

Increasing the temperature of dye films causes the *P* band to shift continuously to *longer* wave-lengths and finally to disappear; increasing the water vapor pressure of the environment of the films causes the *P* band to shift continuously to *shorter* wave-lengths and to become more intense. The simultaneous application of these two opposing effects was studied. The water vapor pressure was kept constant while the temperature of the film was increased until the *P* band disappeared. Then the film was restored to its original condition, a different water vapor pressure was established, the experiment was repeated, and so forth. The results are shown in Fig. 3. The spectroscopic behavior is in accord with the concept that a thermodynamic equilibrium exists between formation and destruction of chains so that the chain length increases with increase of water concentration relative to the dye (in this region), and decreases with increasing temperature.

4. POLARIZED ABSORPTION AND FLUORESCENCE OF THE *P* BAND

With films of dye prepared in the manner described in Section 2, as the solvent evaporates one can follow the development of the polymerized state by the fluorescence excited with the near ultraviolet light of a mercury arc passing through a Wood filter. If evaporation occurs in relatively dry air, the yellow fluorescence appears as the concentration becomes high enough to initiate gel formation and reaches its maximum intensity when the gel state is attained. The fluorescence of the film then becomes weaker

corresponding to the less polymerized state which occurs in equilibrium with the relatively dry air. Placing the film in moist air, or breathing on it, causes the *P*-band fluorescence to flash up again. These observations are in accord with the data published by F. Katheder.[26] When the film is dried out entirely and irreversibly, the weak red fluorescence of crystals appears. This is a broad band with its maximum at about 6200A.

The experiments of Scheibe[12] in which the electric polarization of the *P* band was determined by aligning the polymer chains with streaming orientation were repeated. The gel was squeezed between two glass plates, one of which was moved linearly with respect to the other one. Polaroids were used as polarizer and analyzer. It was confirmed that the electric polarization of the *P* band both in absorption and in fluorescence is along the polymer axis, that is, parallel to the direction of relative motion of the two glass plates.

5. INFLUENCE OF POLYMERIZATION ON THE MOLECULAR BANDS

The molecular bands shift their positions but slightly as the concentration of the dye becomes great enough to form the gel, for which the *P* band is most highly developed, but the absorption coefficient of the 5230 A molecular band decreases until it becomes roughly half as great when the *P* band shows its greatest strength.[5,23] The 4900A molecular band is affected to a smaller extent. However, if the concentration of the dye becomes so great that the polymer band already starts to fade from lack of water, according to Scheibe and Kandler[13] the 5230 molecular band shifts to 5430 (described as 5300 to 5425 by them) and the 4900 molecular band shifts to 5100A, due to "neighborhood action of adjoining polymer chains." In the present investigation during the depletion of water a continuous shift of the 5230 molecular band to 5430 was not visually observed. The 5430 band appeared just when the *P* band started to fade, broaden, and shift continuously to longer wave-lengths. Meanwhile the two molecular bands became less distinct without appreciably changing their positions and finally blurred out to a general broad absorption band without distinct maxima

[26] F. Katheder, Kolloid Zeits. **92**, 299 (1940); **93**, 28 (1940).

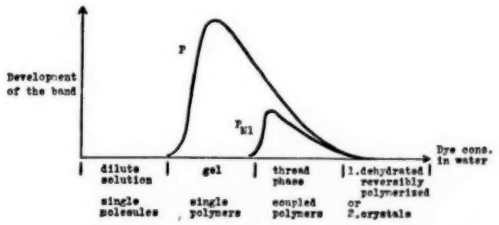

FIG. 4. A qualitative representation of the dependence of the *P*- and P_{M1}-band relationship on dye concentration in water. By a higher development of the band is meant more absorption at the maximum, a narrower band, and the maximum shifted to shorter wave-lengths.

when the water was entirely removed. After the 5430 band had appeared, it also faded, broadened, and shifted continuously to longer wave-lengths simultaneously with the *P* band. It seemed obvious to interpret the neighborhood action as a secondary polymerization of many chains all parallel to each other forming threads and coupled together in the *x*-*y* plane of Fig. 1. The hypothesis which is introduced to explain the spectroscopic behavior gains support from the fact that Sheppard had to assume (for other reasons) that there exist not only molecular chains called "nematoids" but also aggregates of sideways coupled chains termed "smectoids".[11]

To study this behavior, films slightly thicker than those described in Section 2 were used. Figure 4 qualitatively describes the development of this second polymer band in relation to the

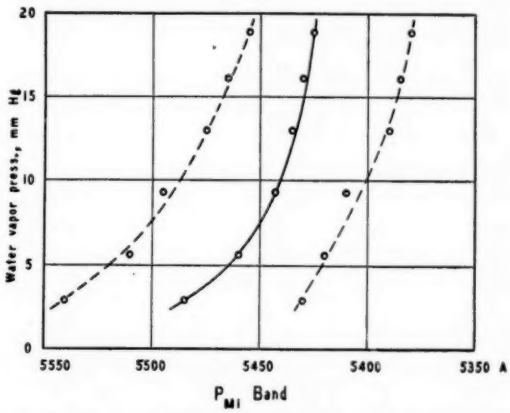

FIG. 5. —— position of maximum absorption. – – – position of the edges at estimated half-maximum absorption. The above data were taken simultaneously with those shown in Fig. 2 where the conditions and behavior are described. The P_{M1} band behaves very similarly to the *P* band. The P_{M1} band is only about 1.5 times the *P*-band width. The displacement between the bands remains nearly constant at 300A, for various water vapor pressures. The P_{M1} band is always weaker and broader than the *P* band under the same conditions.

P band as the dye concentration in water changes. This second polymer band at 5430A will be called the P_{M1} band (polymer band due to modified molecular band). The P_{M1} band needs higher dye concentration to appear than does the P band, but from there on both bands respond in much the same way to water depletion.

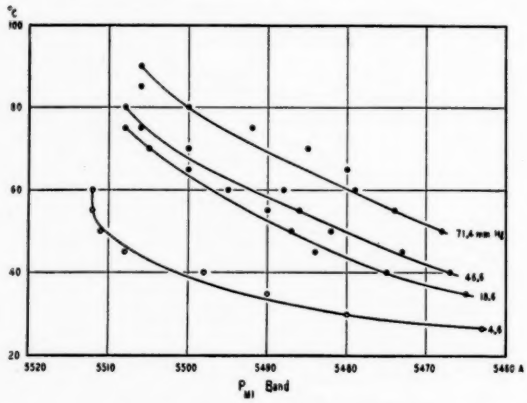

FIG. 6. The position of the maximum absorption of the P_{M1} band depends upon both the temperature of the film and the water vapor pressure indicated for each curve, analogous to the behavior of the P band shown in Fig. 3. The above data were taken simultaneously with those shown in Fig. 3. The curves for both bands run nearly parallel and both bands disappear at nearly the same high temperature. The distortion of the lowest curve may be due to the beginning of crystal formation, for which the conditions are favorable.

Figure 5 shows the measurements of position and breadth of the P_{M1} band as a function of the water vapor pressure. Figure 6 gives the position of the P_{M1} band as a function of temperature and water vapor pressure combined. Figure 7 is a spectrogram of all three bands—the P band and both modified molecular bands.

The polarization of the P_{M1} band in absorption is not in the same direction as that of the P band. Oriented dye films on glass in moist air were obtained by sliding one glass plate off the other one and quickly drying the remaining oriented gel (which was between the plates). The electric polarization of the P_{M1} band in absorption is perpendicular to the single polymer chains, that is, in the plane of the molecules, in accordance with the hypothesis that it is the 5230A molecular band modified by the coupling between polymer chains. The fact that the P_{M1} band appears at a higher dye concentration than that necessary for the P band and the fact that the P_{M1} band absorption is weaker than that of the P band indicate that the coupling between polymer chains is weaker than the coupling between the molecules of a single polymer chain.

6. EVIDENCE FOR DYE THREAD FORMATION

If NaCl (or, for instance, KCl, $HgCl_2$, $SrCl_2$) is added in excess to a dilute solution of the dye in water (10^{-4} M), the common negative ion (Cl^-) salting-out effect causes the dye molecules to coagulate into visible threads, which eventually coalesce to form a thick suspension (showing P-band fluorescence), leaving the supernatant liquid colorless.

The dye was spread on a clean mercury surface in *air*, using 95 percent ethyl alcohol as the solvent for a dilute spreading solution. If now the dye film is compressed to a small area by a mica barrier, visible threads of dye are formed. When the barrier is moved back, making more area available, the film does not re-expand and the threads remain.

Films of dye obtained in the manner described at the beginning of Section 2 show, in air, under a binocular microscope, threads of dye from about 10 to 100 microns long, confirming Jelley's observation.[9] Furthermore, these threads do not change their appearance (length) when the film is put in a water-saturated atmosphere (breathed onto), in spite of the fact that the P band shifts according to Fig. 2. This is further evidence that the dye molecules, when deposited on a surface in a polymerized configuration, do not move their anchor points with respect to that surface as the water vapor pressure is changed.

7. WATER:DYE MOLECULAR RATIO FOR POLYMERS

Sheppard[10,11,22] has proposed a special model with two water molecules linking each dye molecule to each neighbor along the polymer chain. Attempts were made in the present investigation to measure the amount of water taken up by the dye to attain a certain stage of polymerization. The following figures indicate the orders of magnitude of the effects to be expected.

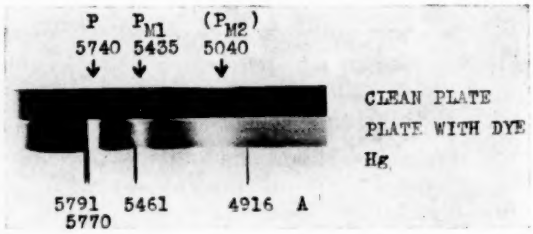

FIG. 7. Spectrogram of the dye on glass in ordinary air made in the manner described at the beginning of Section 2, using a Zeiss constant deviation prism spectrograph and Eastman 103 D plate.

One may cover, for instance, 100 cm^2 of glass (or metal) surface with 8.3 $(10)^{17}$ dye molecules $[5(10)^{-6}\ g/cm^2]$ with a film in which the dye is dehydrated but polymerizable by water vapor. If now as many water molecules are taken up to achieve the polymerization as there are dye molecules present, the hygroscopicity of the dye should be great enough to reduce the water content of 20 cc of saturated air at 20°C from 100 percent to 92.7 percent relative humidity. It is not possible to weigh this mass of water $[25\ (10)^{-6}\ g]$ with a normal balance, but it is possible to measure the change of the humidity in the gaseous state by using the position of the *P*-absorption band (Fig. 2) of dye films on small glass test plates as indicating hygrometers.

Many different experimental arrangements were used, but in principle they were all based on the idea that a certain amount of water-saturated air was admitted to a vessel containing the glass plates clean and then the glass plates covered with the dye; the differences in relative humidity were measured. The amount of water taken up by the walls of the vessel and the clean glass plates was always greater than the amount taken up by the dye itself. To minimize the amount of water adsorbed on the vessel walls many different surfaces were tried. The best results were obtained with glass covered with silver or with polystyrene. But it was only possible to determine that a vessel containing several plates covered with the dye films always took up 5 or 10 percent more water to attain a certain high relative humidity than when the plates were without the dye.

These results were not very reproducible and one may conclude only that for films polymerized to the maximum extent the amount of water taken up by originally dehydrated dye is of the order of magnitude of $\frac{1}{2}$ to 10 water molecules per dye molecule.*

8. DISCUSSION

All authors agree that the 5730A polymer band (the *P* band) belongs to a polymer chain of 1,1′-diethyl-2,2′-cyanine chloride molecules lined up in a direction perpendicular to the planes of the molecules which are coupled together by water molecules. The question is an open one of how the water accomplishes the coupling and whether an intercoupled system of conjugated double bonds or a system of coupled optical resonators furnishes a more adequate description. The first picture is analogous to an electron migration along the polymer chains; the second to an exciton migration. The optical properties of the *P* band (width, transition probability, resonance fluorescence) fit both pictures equally well, but it seems difficult if not impossible to write a valence structure for the conjugated system along the whole polymer chain.

One conceivable structure supporting the hypothesis of exciton migration, but different from that proposed by Sheppard,[10,11,22] is suggested here. This structure is offered *only* as an example of other similar configurations, all of which may actually contribute to the resonance coupling.

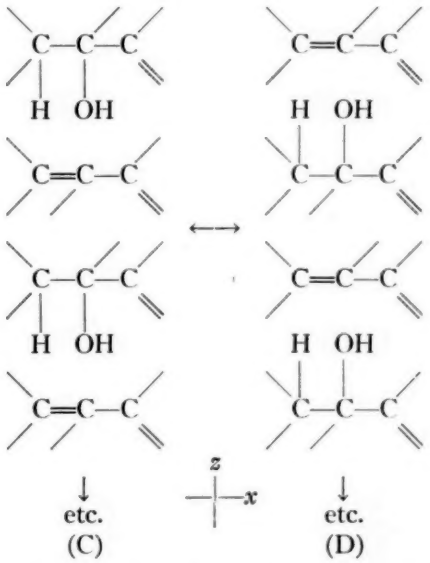

In this picture the plane of the paper is the *x*-*z* plane of Fig. 1; in other words, the planes of the dye molecules are perpendicular to the paper and the polymer axis is in the *z* direction. The groups of three C atoms represent the three central C atoms of the dye molecule (Fig. 1). A water molecule, placed midway between a pair of dye molecules and probably coplanar with them, is attached first to one of the pair (configuration C) and then to the other of the pair (configuration D) by opening the double bond

* In the gel $(10^{-2}\ M)$ there are about 5500 water molecules per dye molecule.

between two C atoms. The positions of the H and OH nuclei do not change during this "resonance." In this polymer the ratio of water molecules to dye molecules would be 1:2. The introduction of a water molecule between two dye molecules modifies the resonance along the x direction and may be the reason why the absorption coefficient of the 5230A molecular band decreases with polymerization.[5,23]. The second molecular band at 4900A (polarized along y of Fig. 1) may not be influenced in the same way, since cases are known in which the transition from a dye to the leukodye influences only one of the absorption bands. The new "resonance" along the polymer axis (z) could account for the polarization of the absorption and fluorescence of the new main polymer band at 5730A and the coupling of the electronic transition in the molecular bands with this P band (as indicated by the fluorescence excitation). The fact that the polymerization is *ad libitum* reversible by admission or removal of water vapor, once part of the molecules are anchored to the surface with the right spacing,* is independent of the special assumption introduced for the coupling by water molecules. The same is true for the irreversibility of polymerization by water vapor once the dye molecules are permitted to form the crystalline state.

The P_{M1} band, which appears when secondary polymerization joins polymer chains to form threads, depends upon the presence of water in a manner very similar to that of the P band. The question arises, therefore, whether a second hydration occurs coupling the ends of the dye molecules together. Such an hypothesis seems improbable, however, since the special steric conditions necessary for such interaction are hardly fulfilled at two different places of the dye molecules. The following assumption is much more plausible. The water molecules are necessary for lining up the dye molecules to form polymer chains, but by this process all planes of the dye molecules are forced into parallel positions. If now polymer chains join together to form threads, the molecules in all adjacent chains also become coplanar. This coplanarity corresponds to a lining up of the optical resonators in the molecules and is therefore favorable for an exciton migration. If the water is partially or entirely removed, the coplanarity will be correspondingly partially or entirely destroyed; this in turn de-couples the adjacent dye molecules. As mentioned in Section 5, the removal of the water does not restore the structure of the normal molecular bands, but produces only a visibly structureless general absorption in the spectral region of the molecular bands, and causes the disappearance of the P and P_{M1} bands. This is understandable since dye molecules adsorbed on glass in such an array are supposed to give an absorption spectrum broadened and blurred by the adsorption forces and by the non-coplanarity of the dye molecules.

Irradiation with light of wave-length in the P_{M1} band (electrically polarized perpendicular to the axis of the polymer chains) causes no fluorescence in the P_{M1} band but produces fluorescence in the P band only (electrically polarized parallel to the axis of the chains).[27] This indicates an interaction between the two different excited states such that the energy absorbed in the resonator system of the coupled molecules is transferred to the excitation along the polymer chains. The transition probability of the P band is so much higher than that of the P_{M1} band that the energy once transferred will be emitted before it has a chance to flow back into the molecular resonators.

The author is highly indebted to Professor J. Franck who suggested this problem and continually guided its progress. Grateful acknowledgment is made to Drs. S. E. Sheppard, L. G. S. Brooker, and E. E. Jelley of the Eastman Kodak Company not only for supplying the dye samples but also for helpful discussion. The author also wishes to thank the General Electric Company for awarding the Charles A. Coffin Fellowship during part of this investigation.

* This fraction of the dye molecules will not readily form the crystalline state when dehydrated. To transform them into the crystalline state the adsorption forces must be overcome (heat of desorption). It is possible to get such a transformation at room temperature after a sufficiently long waiting period (perhaps months).

[27] G. Scheibe, Zeits. f. Electrochemie u. angew. physik. Chemie **47**, 73 (1941).